Towards a Theory of Quantum Gravity Through Geometrization of Quantum Mechanics

Thesis by
ChunJun Cao

In Partial Fulfillment of the Requirements for the
degree of
Doctor of Philosophy

Caltech

CALIFORNIA INSTITUTE OF TECHNOLOGY
Pasadena, California

2018
(Defended May 1, 2018)

ChunJun Cao
ORCID: 0000-0002-5761-5474

ACKNOWLEDGEMENTS

Before I start my long list of appreciations, I think it is worth reminding myself that the greatest lesson I have learned in my past few years is that no accomplishment of mine is that of a single person; rather, it is insignificant in comparison to all the people who have made me the person I am today.

I would like to begin by thanking my wonderful advisor, Sean Carroll, for his invaluable support and wisdom in physics as well as in life. I am immensely grateful for all the guidance and encouragement Sean has offered over the years. My academic life at Caltech has been fruitful and exhilarating thanks to Sean's dedication to physics as well as the well-being of students. I am thankful to the members of my thesis committee, Clifford Cheung, David Hsieh, Anton Kapustin, and John Preskill, for offering their valuable insights and expertise.

I also thank my collaborators, Ning Bao, Aidan Chatwin-Davies, Sebastian Fischetti, Nick Hunter-Jones, Cindy Keeler, Junyu Liu, Shaun Maguire, Liam McAllister, Spiros, Michalakis, Jason Pollack, Grant Remmen, Ashmeet Singh, Eugene Tang, Michael Walter, Zitao Wang, Zhao Yang, Yuan Yao, Ariel Zhitnitsky, and Claire Zukowski, with whom I have had a wonderful time exploring the realm of physics. I am especially thankful for Ning Bao and Ariel Zhitnitsky, who are wonderful collaborators and great mentors. I also thank my friend Aidan Chatwin-Davies, who is always considerate, vibrant and full of optimism throughout our five years at Caltech. I very much enjoyed my conversations with Zitao Wang, who has been patient in entertaining my wildest questions and speculations. I am indebted to Tony Bartolotta, Bartek Czech, Dan Harlow, Matthew Heydeman, Alex Kubica, Jenia Mozgunov, Ingmar Saberi, Brian Swingle, Xiao-Liang Qi, Gunther Uhlmann, Mark van Raamsdonk, Guifre Vidal, Tian Wang, Mark Wise,Yi-zhuang You, and many others for the interesting physics discussions.

I also thank Caltech, for fostering an intellectually stimulating environment and for support its students. It truly has been a humbling experience to learn and walk among some of the giants of our time.

My deepest appreciation to all my friends, who made my PhD years warm and full of life: Bob Briton, Alice Chik, Steven Dong, Frank Hong, Voonhui Lai, Jonas Lippuner, James Liu, John Pang, Alvin Phua, Jamie Rankin, Bekah Silva, Yong Sheng Soh, Zhan Su, Alex Tseng, Becky Wang, Dan Wu, and Lucie Xiang. My

special thanks to John Pang, for his generousity and hospitality for letting me sleep on the couch and using his car when necessary. We had a lot of good times at Bridges, too. I am immensely grateful for my fellow group mates, Ashmeet Singh, Alec Ridgeway, and James St. Germaine-Fuller, for the consistent social and emotional support as well as wonderful physics interactions. I also thank the Dungeons and Dragons and our PC gaming crew: Aidan Chatwin-Davies, Mike Grudic,David Guszejnov, Florian Hoffmann, Seva Ivanov, Anna Komar, Alex Kubica, Clare Lahey, and Jenia Mozgunov. My thanks to the Caltech Ultimate Frisbee pickup group, and Caltech Concert Band and Chamber Music, which helped maintain my mental sanity during the initial years of graduate school.

I recall some of the memory-making restaurants like Sansai for giving us cheap but mostly reliable food when I am too lazy to cook. I also very muched enjoyed my visits to the Counter and Abricott. I still think the Top Restaurant at Allen and Colorado makes the best chicken katsu, disagree with me all you want. Thanks to Sam Woo's for the interesting food making; it has certainly made an indelible impression on me during my last year.

Lastly, I would like to thank my parents, who have been supportive in whatever goal I pursue, and for caring and guiding me throughout the past five years. I am grateful to my girlfriend who has been supportive even in my worse days. And thanks to God who sustains me by His grace and mercy.

I would like to acknowledge the Natural Sciences and Engineering Research Council of Canada (NSERC) which help support my research. The research is funded in part by the Walter Burke Institute for Theoretical Physics at Caltech, by DOE grant DE-SC0011632, by the Foundational Questions Institute, by the Gordon and Betty Moore Foundation through Grant 776 to the Caltech Moore Center for Theoretical Cosmology and Physics, and by the Natural Sciences and Engineering Research Council of Canada (NSERC).

ABSTRACT

In this thesis, we adapt an approach by assuming quantum mechanics as a fundamental theory of nature and attempt to recover familiar concepts such as space-time geometry and gravity from quantum wavefunctions and their unitary evolutions. More specifically, we explore a number of approaches in "geometrizing" quantum systems using techniques such as tensor networks and manifold learning. We find that consistency conditions in quantum gravity can be used to put constraints on tensor network models that approximate the anti-de Sitter/Conformal Field Theory correspondence. Furthermore, quantum circuits and tensor networks can also be used to describe cosmological models and reproduce important features of space-time configurations such as de Sitter space. We find that a generic framework using quantum circuit to describe cosmology puts an upper bound on the number of e-folds during the inflationary phase of the Universe's expansion. In addition to tensor network models, we also propose a Bulk Entanglement Gravity framework that analyzes the entanglement data of a quantum state in a Hilbert space without any *a priori* assumptions on geometry, such as the likes of a boundary conformal field theory. We find that from an amorphous configuration, one can directly recover geometry of bulk space-time from a generic class of wavefunctions that is fully characterized in this thesis via quantum entropy cone techniques. We find that under a number of assumptions, it is possible to derive linearized Einstein's equation from a version of Jacobson's entanglement equilibrium conditions for an emergent spacetime geometry in the weak field limit near Minkowski space. We show that non-local entanglement perturbations display features of wormhole-like configurations. We also clarify connections between Bulk Entanglement Gravity and highly generic features in quantum error correction codes that can be used to derive gravity.

PUBLISHED CONTENT AND CONTRIBUTIONS

[1] Ning Bao, ChunJun Cao, Sean M. Carroll, Aidan Chatwin-Davies, Nicholas Hunter-Jones, Jason Pollack, and Grant N. Remmen. "Consistency conditions for an AdS multiscale entanglement renormalization ansatz correspondence". In: *Phys. Rev.* D91.12 (2015), p. 125036. DOI: 10.1103/PhysRevD.91.125036. arXiv: 1504.06632 [hep-th].
C. C participated in the conception of the project as well as the formulation of the main arguments, performed mathematical analysis of the entanglement bounds, and helped write the manuscript.

[2] Ning Bao, ChunJun Cao, Sean M. Carroll, and Aidan Chatwin-Davies. "De Sitter Space as a Tensor Network: Cosmic No-Hair, Complementarity, and Complexity". In: *Phys. Rev.* D96.12 (2017), p. 123536. DOI: 10.1103/PhysRevD.96.123536. arXiv: 1709.03513 [hep-th].
C. C participated in the conception of the project, drafted and performed mathematical analysis of the arguments, and helped write the manuscript.

[3] Ning Bao, ChunJun Cao, Sean M. Carroll, and Liam McAllister. "Quantum Circuit Cosmology: The Expansion of the Universe Since the First Qubit". In: (2017). arXiv: 1702.06959 [hep-th].
C. C participated in the conception of the project as well as the formulation of the main arguments, performed mathematical analysis, and helped write the manuscript.

[4] Ning Bao, ChunJun Cao, Michael Walter, and Zitao Wang. "Holographic entropy inequalities and gapped phases of matter". In: *JHEP* 09 (2015), p. 203. DOI: 10.1007/JHEP09(2015)203. arXiv: 1507.05650 [hep-th].
C. C participated in the conception of the project, performed analytical and numerical analysis that led to the theorems and their proofs, and helped write the manuscript.

[5] ChunJun Cao, Sean M. Carroll, and Spyridon Michalakis. "Space from Hilbert Space: Recovering Geometry from Bulk Entanglement". In: *Phys. Rev.* D95.2 (2017), p. 024031. DOI: 10.1103/PhysRevD.95.024031. arXiv: 1606.08444 [hep-th].
C. C participated in the conception of the project, drafted and performed mathematical analysis of the arguments, and helped write the manuscript.

[6] ChunJun Cao and Sean M. Carroll. "Bulk entanglement gravity without a boundary: Towards finding Einstein's equation in Hilbert space". In: *Phys. Rev.* D97.8 (2018), p. 086003. DOI: 10.1103/PhysRevD.97.086003. arXiv: 1712.02803 [hep-th].
C. C participated in the conception of the project, drafted and performed mathematical analysis of the arguments, and helped write the manuscript.

TABLE OF CONTENTS

LIST OF ILLUSTRATIONS

LIST OF TABLES

Chapter 1

INTRODUCTION

Since the early twentieth century, general relativity and quantum mechanics has transformed and continue to reshape our understanding of the Universe. Both theories are highly successful in their respective domains, and are verified by a large number of experiments.

On one hand, the theory of general relativity[1, 2, 3] has provided a framework that combined space and time, which we had previously thought to be immutable. It is, in a way, a geometrization of gravity: it turns what Sir Isaac Newton calls the "invisible hand" of gravitational attraction into a fantastic landscape of distortions and curvatures of spacetime geometry. In all appearances, it is a highly powerful and consistent theory on a large scale. From black holes to gravitational waves, from the Big Bang to the near future of our Universe, hints of general relativity echoes through out the cosmos.

Quantum mechanics[4, 5], on the other hand, has its appeals on a microscopic scale. The micro-world, after all, seems to be puzzled with quantum weirdness and uncertainty. Despite many of the open questions surrounding it, quantum mechanics has revolutionized our understanding of the small. Thus far, it has yielded a number of breakthroughs from semi-conductors to exotic materials and to quantum computation.

Following the development and triumphs of quantum field theory[6, 7] by combining special relativity and quantum mechanics, a natural question, therefore, is how does general relativity, which has been quite successful in the macroscopic, relate to quantum mechanics, which thus far has been ruling a predominantly complementary realm? What is the intermediary that interpolates the two seemingly disparate theories? Are they two sides of the same coin or does one supersede the other? One supposition is that gravity and spacetime geometry, like hydrogen atoms, also has quantum mechanical features. Such a school of thought, also known as quantum gravity, has been a long-sought-after price since the inception of quantum mechanics and general relativity. Several approaches such as string theory[8, 9], loop quantum gravity[10], causal set[11], canonical quantum gravity[12, 13], quantum graphity [14] have offered various insights into understanding many aspects of a possible theory of quantum gravity.

Although from the outset, quantum gravity seems to position itself by taking quantum mechanics as a more fundamental theory, it can seem counter-intuitive that many of the common approaches to a generate quantum theory often start by "quantizing" a classical theory[6, 7]. Nevertheless, many have made tremendous progress using a semiclassical approach[2], yielding important clues for quantum gravity such as blackhole thermodynamics[15, 16, 17] and holographic bounds [18, 19, 20].

However, if one were to treat quantum mechanics truly as *the* fundamental theory of nature, then it is crucial that our existing physical constructs should be derivable from the inner workings of a purely quantum mechanical theory. Such is a motivation behind an it-from-qubit program, where anything ("it") can emerge from the more fundamental quantum information constituents ("qubit"). As a proper subset of those problems, one has to, therefore, also find gravity inside quantum mechanics.

In other words, instead of quantizing gravity by taking the form of general relativity as is, we would like to "gravitize" quantum mechanics by finding general relativity in it.

For instance, given a complex manybody quantum mechanical system, the approach aims to define spacetime geometry from an amorphous but complex quantum configuration. In particular, if the aforementioned hypothesis has any validity, we should also find features of gravity emerging naturally from the fundamental properties of quantum mechanics in some of those geometries.

In this thesis, I will focus primarily on the different methods in obtaining spatial geometries from quantum information or related data. The first approach focuses on tensor networks, which are complex networks with additional structures that can effectively encode entanglement information of a quantum state. Intuitively, the network connectivity often reflects the structure of quantum entanglement in different parts of the state. Certain types of tensor networks can also have connectivities that can be recognizable as spatial or spacetime geometries. Indeed, we will examine a particular network construction which mimics the spatial geometry of a timeslice of anti-de Sitter (AdS) space, a spacetime geometry with a negative cosmological constant. The same network also has a natural interpretation as de Sitter space, which is a spacetime with a positive cosmological constant and a better description of our own Universe.

More specifically, we will study the proposal that tensor network can be used to capture features of the Anti-de Sitter/Conformal Field Theory (AdS/CFT) correspondence. The AdS/CFT correspondence was first discovered in the context of Superstring Theory by Juan Maldacena [21], although traces of its existence can also be found in earlier works [22]. The theory can be understood as a concrete realization of the holographic principle, where a gravitational theory of N-dimensions can be described by an equivalent theory of $N-1$-dimensions. In this specific instance, the bulk theory, which is a theory of quantum gravity, lives in an N-dimensional anti-de Sitter space, while its dual, the conformal field theory (CFT), is living on the conformal boundary of AdS: an $N-1$ dimensional spacetime with flat geometry.

Interestingly, it was proposed by Shinsei Ryu and Tadashi Takayanagi [23] that for a CFT with holographic dual, the entanglement entropy of a subregion in the boundary CFT is, to leading order, equal to the area of a minimal surface in the AdS bulk which anchors on the boundary of the subregion. Therefore, by treating the CFT as a fundamental quantum mechanical theory, a theory of quantum gravity in the bulk can emerge from the quantum information encoded on the boundary. Given the powerful and more concrete construction of AdS/CFT, most of the interesting progress in the recent it-from-qubit program are examined in this particular context, which includes the reconstruction of spatial geometry[24, 25, 26, 27], emergence of linearized gravity[28, 29], black holes[30, 31], bulk action and complexity [32, 33, 34, 35], and many more[36, 37, 38]. It has also become a fertile testing ground for other general guidelines and insights for understanding quantum gravity.

Nevertheless, ideally one wish to understand the theory of quantum gravity beyond AdS/CFT, because it does not naïvely describe our physical Universe. Furthermore, in a fully quantum approach, a minimal set of information also should not include a background geometry of, for instance, the boundary CFT. Hence it is interesting to extend the lessons from AdS/CFT to a more general setting by cutting down some of the assumptions that were freely available in the form of a CFT. To this end, we will also consider a more general scenario of finding geometry from quantum mechanics. In particular, we assume that only a quantum state and a preferred factorization are given. Using entanglement data, I show that a flat spatial geometry can be obtained using certain methods in machine learning. We will see that features of gravity naturally emerge from entanglement properties such as monotonicity of mutual information or monogamy of entanglement. Under a list of assumptions, it is also possible to derive the linearized Einstein's equation directly in the a bulk spacetime in the weak field regime using quantum entanglement or mutual information, without relying on holography or the various structures of a boundary geometry or conformal field theory such as the case of AdS/CFT.

In Chapter 2, I will examine a tensor network representation of AdS/CFT correspondence. It is first discussed by [37] that a particular type of tensor network known as the Multiscale Entanglement Renormalization Ansatz (MERA) [39] captures simple features of the correspondence. We will review the concept of tensor network as well as MERA networks. We find that the MERA network describes the proposed bulk geometry only on super-AdS scales. It also needs to satisfy a number of constraints in order to be consistent with a theory of gravity in the bulk. It is found that MERA as it stands is inconsistent as a toy model of AdS/CFT without modifications.

In Chapter 3, we will discuss the proposal where the same MERA network can be interpreted as de Sitter space, a spacetime geometry that has a positive cosmological constant. We confirm the earlier proposal that MERA carries causal structures, such as cosmological horizons, consistent with those of de Sitter space on the Hubble scale or greater. The tensor network description also naturally produces a version of the cosmic no-hair theorem, such that any perturbations or inhomogeneities are "washed out" by the expansion of the universe over time. The network most naturally describes a global picture of de Sitter space, however a local description is also possible with modifications. Finally we derive a bound on the quantum complexity of states generated by the MERA network and show that it is consistent with a version of the complex equals action/volume proposal in the bulk of de Sitter spacetime.

In Chapter 4, a proposal of constructing cosmological models with quantum circuits is discussed. Although a concrete model is still lacking, we find that coupled with the usual assumptions of de Sitter entropy and holography, the framework in its most general form upper bounds the maximum number of e-folds during the inflationary expansion phase of the Universe. Interestingly, the number is just large enough to resolve the horizon problem.

In Chapter 5, we characterize the so-called quantum entropy cone of a class of low energy quantum states in many condensed matter systems that satisfy the area law. More explicitly, for any subsystem of the quantum state that corresponds to a subregion, for instance, of a spatial lattice, the entanglement entropy of the quantum state associated with the subregion scales as the surface area of the same subregion. To leading order, where the entropy is exactly the area, we provide a complete set of (in)equalities of entanglement entropies that fully characterize the allowed entanglement structure of such states. The allowed configurations of entanglement entropies form a quantum entropy cone, whose super-cone overlaps with the quantum entropy cone of states which have a holographic dual. We also propose a generic 4-party quantum inequality which to the best of our knowledge has not been proposed or ruled out by previous literature.

In Chapter 6, we will examine an algorithm to derive geometry from a quantum state given a state and its Hilbert space factorization. Making use of some of the results in chapter 4, we find that it is possible to recover the geometric information encoded in the form of quantum mutual information. We use a machine learning technique to recover the best-fit dimensionality of the "emergent" spatial manifold. Then we show that entanglement properties of any quantum state can give rise to features akin to those of gravity by deriving a spatial analog of the Einstein's equation. Furthermore, non-local entanglement perturbations also give rise to a configuration that is wormhole-like, reminiscent to the ER=EPR proposal [30] where entanglement is conjectured to gives rise to wormholes.

Finally in Chapter 7, we further refine the proposal in 6 by considering entanglement perturbations on a flat spacetime background, which can be derived from the techniques introduced in the previous chapter. We use tensor Radon transform to show that the spatial metric tensor can be uniquely reconstructed up to a gauge transformation. Similarly, we show that the linearized Hamiltonian constraint is equivalent to a version of Jacobson's entanglement equilibrium [40]. With additional assumptions, it is possible to show that such systems satisfy linearized Einstein's equation. We make the observation that a highly generic class of quantum error correction codes also have the natural structure needed to derive such relations.

The works in this thesis demonstrate a glimpse of the power of combining quantum information theory, high energy physics, gravity and cosmology. It shows promise that an approach to quantum gravity by geometrization of quantum mechanics can provide insights that are previously not apparent in the other quantization approaches. The generality of such emergent phenomena also open doors for connections with complex behaviours in manybody quantum systems, complex networks, and machine learning. On a broader level, the work also connects with foundations of quantum mechanics and quantum to classical transition. By understanding how the perceived classical spacetime geometry can be derived from information encoded in a wavefunction, this thesis also points toward a great number of interesting future works and questions.

Chapter 2

CONSISTENCY CONDITIONS FOR AN ADS/MERA CORRESPONDENCE

The Multi-scale Entanglement Renormalization Ansatz (MERA) is a tensor network that provides an efficient way of variationally estimating the ground state of a critical quantum system. The network geometry resembles a discretization of spatial slices of an AdS spacetime and "geodesics" in the MERA reproduce the Ryu–Takayanagi formula for the entanglement entropy of a boundary region in terms of bulk properties. It has therefore been suggested that there could be an AdS/MERA correspondence, relating states in the Hilbert space of the boundary quantum system to ones defined on the bulk lattice. Here we investigate this proposal and derive necessary conditions for it to apply, using geometric features and entropy inequalities that we expect to hold in the bulk. We show that, perhaps unsurprisingly, the MERA lattice can only describe physics on length scales larger than the AdS radius. Further, using the covariant entropy bound in the bulk, we show that there are no conventional MERA parameters that completely reproduce bulk physics even on super-AdS scales. We suggest modifications or generalizations of this kind of tensor network that may be able to provide a more robust correspondence.

This chapter is based on the Ref:
Ning Bao, ChunJun Cao, Sean M. Carroll, Aidan Chatwin-Davies, Nicholas Hunter-Jones, Jason Pollack, and Grant N. Remmen. "Consistency conditions for an AdS multiscale entanglement renormalization ansatz correspondence". In: Phys. Rev. *D91.12 (2015), p. 125036.* DOI: `10.1103/PhysRevD.91.125036`. *arXiv:* `1504.06632 [hep-th]`.

2.1 Introduction

The idea that spacetime might emerge from more fundamental degrees of freedom has long fascinated physicists. The holographic principle suggests that a $(D + 1)$-dimensional spacetime might emerge from degrees of freedom in a D-dimensional theory without gravity [42, 43]. While a completely general implementation of this idea is still lacking, the AdS/CFT correspondence provides a specific example in which to probe the holographic emergence of spacetime. AdS/CFT is a conjectured correspondence between D-dimensional conformal field theories (CFTs) in Minkowski space and $(D + 1)$-dimensional asymptotically anti-de Sitter (AdS) spacetimes [21, 44, 45]. An intriguing aspect of this duality is the Ryu–Takayanagi formula [23, 46], according to which the entanglement entropy of a region B on the boundary is proportional to the area of a codimension-two extremal surface $\tilde{B}$ embedded in the bulk curved spacetime whose boundary is B:

$$S(B) = \frac{\text{area}(\tilde{B})}{4G} + \text{corrections}. \tag{2.1}$$

In other words, given a CFT state, one may think of bulk distance and geometry (at least near the boundary) as being charted out by the entanglement properties of the CFT state.

A central question in this picture of spacetime emerging from entanglement is: What is the precise relationship between bulk degrees of freedom and boundary degrees of freedom? Expressed in a different way, what is the full map between states and operators in the boundary Hilbert space and those in the bulk? While investigations of AdS/CFT have thrown a great deal of light on this question, explicit simple models are still very helpful for studying it in more detail.

Meanwhile, from a very different perspective, tensor networks have arisen as a useful way to calculate quantum states in strongly-interacting many-body systems [47]. One significant example is the Multi-scale Entanglement Renormalization Ansatz (MERA) [39], which is relevant for critical (gapless) systems, *i.e.*, CFTs. Starting from a simple state in a low-dimensional Hilbert space, acting repeatedly with fixed tensors living on a network lattice produces an entangled wave function for the quantum system of interest; varying with respect to the tensor parameters efficiently computes the system's ground state.

Working "backwards" in the MERA, starting with the ground state and gradually removing entanglement, produces a set of consecutively renormalized quantum states. This process reveals a renormalization direction along the graph, which may be thought of as an emergent radial direction of space. As pointed out by Swingle [37], the MERA graph can serve as a lattice discretization of spatial slices of AdS. Furthermore, one can use the MERA to calculate the entanglement entropy of regions of the original (boundary) critical system; this calculation amounts to tracing over bonds in the tensor network that cross the causal cone of the boundary region. The causal cone is a sort of extremal surface for the MERA, motivating comparison to the Ryu–Takayanagi formula.

It is therefore natural to conjecture that the MERA provides a concrete implementation of the emergence of spacetime, in the form of a correspondence between boundary and bulk regions reminiscent of AdS/CFT [37]. Such an AdS/MERA correspondence would be extremely useful, since the basic building blocks of the MERA are discrete quantum degrees of freedom from which quantities of physical interest may be directly calculated. Some specific ideas along these lines have recently been investigated [48, 49, 50, 51].

In this paper, we take a step back and investigate what it would mean for such a correspondence to exist and the constraints it must satisfy in order to recover properties we expect of physics in a bulk emergent spacetime. After reviewing the MERA itself and possible construals of the AdS/MERA correspondence in the next section, in Sec. 2.3 we then derive relationships between the MERA lattice and the geometry of AdS. We find that the MERA is unable to describe physics on scales shorter than the AdS radius. In Sec. 2.4 we explore constraints from calculating the entanglement entropy of regions on the boundary, in which we are able to relate MERA parameters to the central charge of the CFT. Finally, in Sec. 2.5 we apply the covariant entropy (Bousso) bound to regions of the bulk lattice. In the most naïve version of the AdS/MERA correspondence, we find that no combination of parameters is consistent with this bound, but we suggest that generalizations of the tensor network may be able to provide a useful correspondence.

2.2 AdS/MERA

Let us begin by recalling the definition and construction of the MERA. We will then introduce the AdS/MERA correspondence and discuss the motivation for and consequences of this proposal.

2.2.1 Review of the MERA

The MERA is a particular type of tensor network that provides a computationally efficient way of finding the ground states of critical quantum many-body systems, *i.e.*, CFTs, in D dimensions. (For a recent review of tensor networks in general, see Ref. [47]. Detailed analyses of the MERA are given in [39, 52, 53] and references therein.) In this work, we restrict our attention to the case $D = 1 + 1$.

The MERA tensor network is shown in Fig. 2.1. The quantum system being modeled by the MERA lives at the bottom of the diagram, henceforth "the boundary" in anticipation of the AdS/MERA connection to be explored later. We can think of the tensor network as a quantum circuit that either runs from the top down, starting

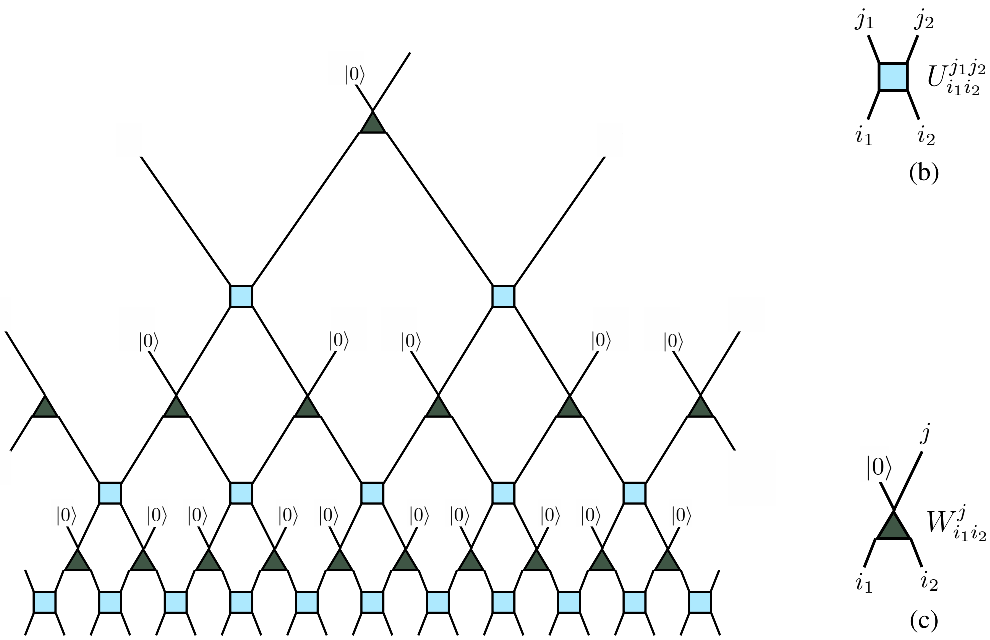

(a)

Figure 2.1: (a) Basic construction of a $k = 2$ MERA (2 sites renormalized to 1). (b) The squares represent disentanglers: unitary maps that, from the moving-upward perspective, remove entanglement between two adjacent sites. (c) The triangles represent isometries: linear maps that, again from the moving-upward perspective, coarse-grain two sites into one. Moving downward, we may think of isometries as unitary operators that, in the MERA, map a state in $V \otimes |0\rangle$ into $V \otimes V$. The i and j labels in (b) and (c) represent the tensor indices of the disentangler and isometry.

with a simple input state and constructing the boundary state, or from the bottom up, renormalizing a boundary state via coarse-graining. One defining parameter of the MERA is the rescaling factor k, defining the number of sites in a block to be coarse-grained; in Fig. 2.1 we have portrayed the case $k = 2$. The squares and triangles are the tensors: multilinear maps between direct products of vector spaces. Each line represents an index i of the corresponding tensor, ranging over values from 1 to the "bond dimension" χ. The boundary Hilbert space $\mathcal{H}_{\text{boundary}} = V^{\otimes \mathcal{N}_{\text{boundary}}}$ is given by a tensor product of $\mathcal{N}_{\text{boundary}}$ individual spaces V, each of dimension χ. (In principle the dimension of the factors in the boundary could be different from the bond dimension of the MERA, and indeed the bond dimensions could vary over the different tensors. We will assume these are all equal.)

As its name promises, the MERA serves to renormalize the initial boundary state via coarse-graining. If we were to implement the MERA for only a few levels, we would end up with a quantum state in a smaller Hilbert space (defined on a fixed level of the tensor network), retaining some features of the original state but with some of the entanglement removed. However, we can also run the MERA backwards, to obtain a boundary state from a simple initial input. By varying the parameters in the individual tensors, we can look for an approximation of the ground state of the CFT on the boundary. Numerical evidence indicates that this process provides a computationally efficient method of constructing such ground states [53, 54].

The tensors, or gates, of the MERA come in two types. The first type are the disentanglers, represented by squares in Fig. 2.1. These are unitary maps $U : V \otimes V \longrightarrow V \otimes V$, as in Fig. 2.1b. The name comes from thinking of moving upward through the network, in the direction of coarse-graining, where the disentanglers serve to remove local entanglement; as we move downward, of course, they take product states and entangle them. The second type of tensors are the isometries, represented by triangles. From the moving-downward perspective these are linear maps $W : V \longrightarrow V \otimes V$; moving upward, they implement the coarse-graining, see Fig. 2.1c. The isometries are subject to the further requirement that $W^\dagger W = I_V$, where I_V is the identity map on V, and $WW^\dagger = P_A$, where P_A is a projector onto some subspace $A \subset V \otimes V$. From the top-down perspective, we can also think of the isometries as bijective unitary operators $W_U : V \otimes V \longrightarrow V \otimes V$, for which a fixed "ancilla" state (typically the ground state $|0\rangle$) is inserted in one of the input factors, as shown in Fig. 2.1c. More generally, isometries could map $q < k$ sites onto k sites, $W : V^{\otimes q} \longrightarrow V^{\otimes k}$.

The MERA is not the simplest tensor network which implements coarse-graining. For instance, the tree tensor network [55] (also considered in a holographic context in Ref. [48]), similar to MERA but without any disentanglers, also implements coarse-graining. However, tensor networks without disentanglers fail to capture the physics of systems without exponentially-decaying correlations, and consequently cannot reproduce a CFT ground state.

An example that invites analysis with a MERA is the transverse-field Ising model [56]. In $1+1$ dimensions, the model describes a chain of spins with nearest-neighbor interactions subject to a transverse magnetic field. Its Hamiltonian is

$$\hat{H} = -J \sum_i \hat{\sigma}_i^z \hat{\sigma}_{i+1}^z - h \sum_i \hat{\sigma}_i^x \,, \tag{2.2}$$

where $\hat{\sigma}_i^z$ and $\hat{\sigma}_i^x$ are Pauli operators and where J and h set the strength of the nearest-neighbor interactions and the magnetic field, respectively. Notably, the system achieves criticality at $J = h$, where a quantum phase transition occurs between ordered ($J > h$) and disordered ($J < h$) phases. In this example, the open legs at the bottom of the MERA describe the state of the one-dimensional lattice of spins. A single application of disentanglers and isometries can be thought of as a true real-space renormalization, producing a lattice of spins that is less dense than the preceding lattice by a factor of q/k.

In general, much information is required to describe an arbitrary MERA. In principle, the Hilbert spaces, the disentanglers, and the isometries could all be different. Also, for $k > 2$, there is no canonical way of laying out the disentanglers and isometries; the circuit itself must be specified. We will restrict ourselves to the case $q = 1$, so that isometries have 1 upward-going leg and k downward-going legs. Further, without loss of generality, we take the same vector spaces, disentanglers, and isometries everywhere in the MERA, a simplification that is enforced by the symmetries of the boundary ground state. These symmetries — namely, translation- and scale-invariance — dictate that the MERA parameters and structure be homogeneous across the whole tensor network.

For geometric considerations, it is useful to abstract away all of the information about unitary operators and to draw a MERA as a graph as shown in Fig. 2.2. In such a graph, we only indicate the connectivity of sites at any given level of coarse-graining as well as the connectivity of sites under renormalization group flow.

2.2.2 An AdS/MERA Correspondence?

The possibility of a correspondence between AdS and the MERA was first proposed by Swingle in Ref. [37], where it was noted that the MERA seems to capture certain key geometric features of AdS. At the most basic level, when viewed as a graph with legs of fixed length, a MERA may be thought of as a discretization of the hyperbolic plane, which is a spatial slice of AdS_3. In this discretization, the base of the MERA tree lies on the boundary of the AdS slice and the MERA lattice sites fill out the bulk of the slice [37, 31].

Interestingly, the structure of a MERA is such that it seems to go beyond a simple discretization of the hyperbolic plane. Certain discrete paths in the MERA naturally reproduce geodesics of the hyperbolic plane [37, 57]. Moreover, this phenomenon makes it possible to understand the computation of CFT entanglement entropy using a MERA as a discrete realization of the Ryu–Takayanagi formula [58]. These and

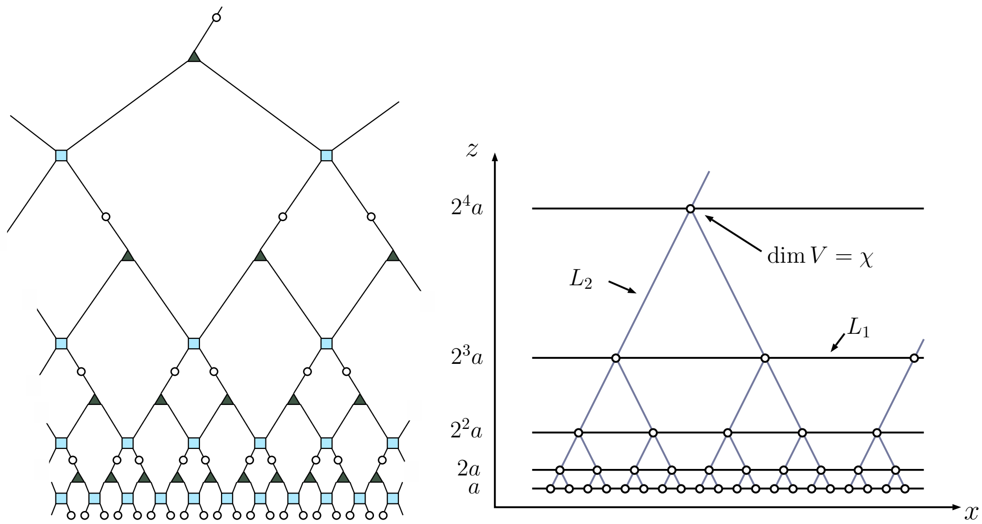

(a)

(b)

Figure 2.2: (a) A $k = 2$ MERA, and (b) the same MERA with its disentanglers and isometries suppressed. The horizontal lines in the graph on the right indicate lattice connectivity at different renormalization depths, and the vertical lines indicate which sites at different depths are related via coarse-graining due to the isometries. Each site, represented by a circle, is associated with a Hilbert space V with bond dimension χ. In the simplest case, a copy of the same Hilbert space is located at each site. When assigning a metric to the graph on the right, translation and scale invariance dictate that there are only two possible length scales: a horizontal proper length L_1 and a vertical proper length L_2.

other examples [37, 57] seem to suggest that a MERA may in fact be elucidating the structural relationship between physics on the boundary of AdS and its bulk.

In this work we take the term “AdS/MERA correspondence" to mean more than simply a matching of graph geometry and continuous geometry. In the spirit of the AdS/CFT correspondence, we suppose that (at least some aspects of) both boundary and bulk physics are described by appropriate Hilbert spaces $\mathcal{H}_{\text{boundary}}$ and $\mathcal{H}_{\text{bulk}}$ respectively, which must have equal dimensions. A full AdS/MERA correspondence would then be a specification of these Hilbert spaces, as well as a prescription which makes use of the MERA to holographically map states and operators in $\mathcal{H}_{\text{boundary}}$ to corresponding states and operators in $\mathcal{H}_{\text{bulk}}$ and vice-versa. To preserve locality in the bulk and the symmetries of AdS, it is natural to identify $\mathcal{H}_{\text{bulk}}$ with the tensor product of individual spaces V_{bulk}, each located at one site of the MERA. If it exists, this correspondence provides a formulation of bulk calculations in terms of the MERA. An AdS/MERA correspondence should allow us to, for example, calculate bulk correlation functions, or bulk entanglement entropies using tools from or the structure of the MERA.

There is one straightforward way to construct such a map $\mathcal{H}_{\text{boundary}} \leftrightarrow \mathcal{H}_{\text{bulk}}$. We have noted that the isometries $W : V \to V \otimes V$ can be thought of as unitaries $W_U : V \otimes V \to V \otimes V$ by imagining that a fixed ancillary state $|0\rangle$ is inserted in the first factor; for a k-to-one MERA, one would insert $k-1$ copies of the $|0\rangle$ ancilla at each site to unitarize the isometries. From that perspective, running upwards in the tensor network provides a map from the MERA ground state on the boundary to a state $|0\rangle^{\otimes(k-1)\mathcal{N}_{\text{bulk}}} \in V^{\otimes(k-1)\mathcal{N}_{\text{bulk}}}$, where at each isometry there is a copy of $V^{\otimes(k-1)}$ and $\mathcal{N}_{\text{bulk}}$ denotes the number of bulk lattice sites, excluding the boundary layer. As we ultimately show in Sec. 2.5, one has $\mathcal{N}_{\text{boundary}} = (k-1)\mathcal{N}_{\text{bulk}}$. We can then identify $\mathcal{H}_{\text{boundary}} = \mathcal{H}_{\text{bulk}} = V^{\otimes \mathcal{N}_{\text{boundary}}}$ and think of the tensor network as a quantum circuit providing a map between arbitrary states $\mathcal{H}_{\text{boundary}} \to \mathcal{H}_{\text{bulk}}$. In this construction, the MERA ground state on the boundary gets mapped to the factorized bulk state $|0\rangle^{\otimes(k-1)\mathcal{N}_{\text{bulk}}}$, but other boundary states will in general produce entangled states in the bulk (keeping the tensors themselves fixed).

Something very much like this construction was proposed by Qi [48], under the name “Exact Holographic Mapping" (EHM). That work examined a tensor network that was not quite a MERA, as no disentanglers were included, only isometries. As a result, while there is a map $\mathcal{H}_{\text{boundary}} \to \mathcal{H}_{\text{bulk}}$, the boundary state constructed by the tensor network does not have the entanglement structure of a CFT ground state. In particular, it does not seem to reproduce the Ryu–Takayanagi formula in a robust way. Alternatively, we can depart from Qi by keeping a true MERA with the disentanglers left in, in which case the bulk state constructed by the quantum circuit has no entanglement: it is a completely factorized product of the ancilla states. Such a state doesn’t precisely match our expectation for what a bulk ground state should look like, since there should be at least some entanglement between nearby regions of space.

Therefore, while it is relatively simple to imagine constructing a bulk Hilbert space and a map between it and the boundary Hilbert space, it is not straightforward to construct such a map that has all of the properties we desire. It might very well be possible to find such a construction, either by starting with a slightly different boundary state, or by adding some additional structure to the MERA.

For the purposes of this paper we will be noncommittal. That is, we will imagine that there is a bulk Hilbert space constructed as the tensor product of smaller spaces at each MERA site, and that there exists a map $\mathcal{H}_{\text{boundary}} \to \mathcal{H}_{\text{bulk}}$ that can be constructed from the MERA, but we will not specify precisely what that map might be. We will see that we are able to derive bounds simply from the requirements that the hypothetical correspondence should allow us to recover the properties we expect of bulk physics, including the background AdS geometry and features of semiclassical quantum gravity such as the Bousso bound on bulk entropy.

2.3 MERA and Geometry

If a MERA is a truly geometrical object that describes a slice of AdS, then the graph geometry of a MERA should give the same answers to geometric questions as the continuous geometry of a slice of AdS. Here, we reconsider the observation by Swingle [37, 57] that certain trajectories on the MERA coincide with trajectories in AdS and we investigate the constraints that this correspondence places on the graph metric of the MERA. We find that a MERA necessarily describes geometry on super-AdS length scales, and moreover, there is no redefinition of the MERA coordinates that results in the proper distance between MERA sites mapping to any sub-AdS length scale.

2.3.1 Consistency conditions from matching trajectories

In order to speak of graph geometry, one must put a metric on the MERA graph, *i.e.*, one must assign a proper length to each bond in the graph of Fig. 2.2. Presumably, the metric should originate from correlations between the sites in the MERA. In the absence of an explicit identification of the origin of the graph metric, however, at least in the case of a MERA describing the ground state of a CFT, it is sensible to identify two length scales. Explicitly, we must assign a proper length L_1 to horizontal bonds and a proper length L_2 to vertical bonds. Indeed, translational and conformal invariance guarantee that these are the only two length scales in any graph metric one can assign to a MERA for which an AdS/MERA correspondence exists. In particular, the ground state of a CFT is translation invariant, so each horizontal bond in the finest (UV-most) lattice should have the same proper length so as to respect this symmetry. Self-similarity at all scales then requires that any horizontal bond at any level of renormalization have this same proper length. There is no *a priori* reason why the vertical bonds should share the proper length of the horizontal bonds and indeed we will see that their proper length will be different. However, again by self-similarity and translation invariance, all vertical bonds must be assigned the same proper length.

The observation in Ref. [37] that certain paths in the MERA graph coincide with corresponding paths in slices of AdS is what established the possibility of an AdS/MERA correspondence. Here we will carefully examine these paths and determine what constraints the requirements that they match place on MERA parameters, *i.e.*, on the bond lengths L_1 and L_2 and on the rescaling factor k.

Consider a constant-time slice of AdS_3 with the following metric:

$$\mathrm{d}s^2 = \frac{L^2}{z^2}(\mathrm{d}z^2 + \mathrm{d}x^2). \tag{2.3}$$

We will compare the proper lengths of straight horizontal lines and geodesics in the AdS slice to the proper lengths of the corresponding paths in the MERA graph. In the AdS slice, let γ_1 be a straight horizontal line ($\mathrm{d}z = 0$) sitting at $z = z_0$ with coordinate length x_0. Let γ_2 be a geodesic whose endpoints lie near the boundary $z = 0$ and are separated by a coordinate distance x_0 at the boundary. In this choice of coordinates, such a geodesic looks like a semicircle (see Fig. 2.3). It is a straightforward computation to show that the proper lengths of these curves are

$$|\gamma_1|_{\mathrm{AdS}} = \frac{L}{z_0}x_0 \qquad \text{and} \qquad |\gamma_2|_{\mathrm{AdS}} = 2L\ln\left(\frac{x_0}{a}\right). \tag{2.4}$$

Note that there is a UV cutoff at $z = a \ll x_0$ and that we have neglected terms of order a/x_0.

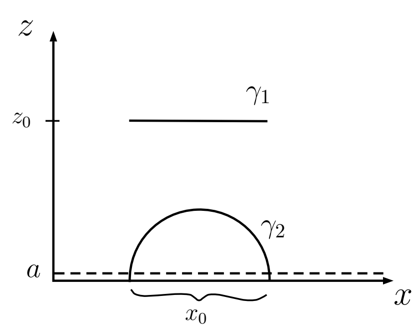

Figure 2.3: A horizontal line (γ_1) and a geodesic (γ_2) in a spatial slice of AdS_3.

We fix L_1 and L_2 by comparing γ_1 and γ_2 to horizontal lines and “geodesics" in the MERA, respectively. Consider two sites in a horizontal lattice at depth m (*i.e.*, m renormalizations of the UV-most lattice) and separated by a coordinate distance x_0 in the coordinate system shown in Fig. 2.2. By fiat, this lattice sits at $z_0 = k^m a$. The number of bonds between the two sites at depth m is $x_0/(k^m a)$ (see Fig. 2.2 for the case $k = 2$). It follows that the proper length of the line connecting the two points is just

$$\begin{aligned} |\gamma_1|_{\text{MERA}} &= L_1 \cdot (\text{number of bonds between endpoints}) \\ &= L_1 \left. \frac{x_0}{z_0} \right|_{z_0 = k^m a} . \end{aligned} \tag{2.5}$$

To have $|\gamma_1|_{\text{AdS}} = |\gamma_1|_{\text{MERA}}$, we should therefore set $L_1 = L$.

Similarly, consider two lattice sites on the UV-most lattice separated by a coordinate distance x_0. If we assume that $x_0 \gg a$, then the shortest path (geodesic) in the MERA connecting the two lattice sites is the path that goes up in the renormalization direction and then back down again. The two sites are separated by x_0/a bonds on the UV-most lattice, so $\log_k(x_0/a)$ renormalization steps are needed to make the sites either adjacent or superimposed. This means that the geodesic that connects the endpoints is made up of $2\log_k(x_0/a)$ bonds (as we have to go up and then back down again, giving the factor of 2). It follows that the proper length of the geodesic is

$$\begin{aligned} |\gamma_2|_{\text{MERA}} &= L_2 \cdot (\text{number of bonds in the geodesic}) \\ &= 2L_2 \log_k \left(\frac{x_0}{a} \right) . \end{aligned} \tag{2.6}$$

To have $|\gamma_2|_{\text{AdS}} = |\gamma_2|_{\text{MERA}}$, we should therefore set $L_2 = L \ln k$.

2.3.2 Limits on sub-AdS scale physics

One aspect of the matching of geodesics that is immediately apparent is that the MERA scales L_1 and L_2 that parametrize the proper distance between lattice sites are of order the AdS scale L or larger, as was also noted in Refs. [37, 31]. This runs counter to the typical expectation that, in a discretization of spacetime, one expects the granularity to be apparent on the UV, rather than the IR, scale. That is, sub-AdS scale locality is not manifested in the MERA construction and must be encoded within each tensor factor [57].

One could try to evade this difficulty by attempting to redefine the MERA coordinates $(x, z)^{\text{MERA}}$ (those of Fig. 2.2) as functions of the AdS coordinates $(x, z)^{\text{AdS}}$ (those of Fig. 2.3) and taking a continuum limit; above, we assumed that the two sets of coordinates were simply identified. That is, suppose $x^{\text{MERA}} = f(x^{\text{AdS}})$ and $z^{\text{MERA}} = g(z^{\text{AdS}})$. (For example, one could consider $f(x) = \varepsilon x$ for small ε and imagine taking the continuum limit, with the aim of making L_1 much smaller than the AdS scale.) If a is still the UV cutoff on the AdS side, then in the MERA we have $f(a)$ as the UV-most lattice spacing and $g(a)$ as the UV cutoff in the holographic direction. Consider the computation of $|\gamma_1|$. From the AdS side, we have $|\gamma_1|_{\text{AdS}} = Lx_0^{\text{AdS}}/z_0^{\text{AdS}}$. On the MERA side, the number of sites spanned by $x_0^{\text{MERA}} = f(x_0^{\text{AdS}})$ is $x_0^{\text{MERA}}/k^m f(a)$, while the holographic coordinate is $z_0^{\text{MERA}} = k^m g(a)$. Hence,

$$|\gamma_1|_{\text{MERA}} = L_1 \frac{f(x_0^{\text{AdS}})}{f(a)} \frac{g(a)}{g(z_0^{\text{AdS}})}. \tag{2.7}$$

Equating $|\gamma_1|_{\text{AdS}} = |\gamma_1|_{\text{MERA}} \equiv |\gamma_1|$, we have

$$g(z_0^{\text{AdS}}) \frac{\partial}{\partial x_0^{\text{AdS}}} |\gamma_1| = L_1 \frac{f'(x_0^{\text{AdS}})}{f(a)} g(a) = L \frac{g(z_0^{\text{AdS}})}{z_0^{\text{AdS}}}. \tag{2.8}$$

Since the right side of the first equality only depends on x_0^{AdS} and the second equality only depends on z_0^{AdS}, but we can vary both parameters independently, both expressions must be independent of both AdS coordinates. Hence, we must have $f(x) = \varepsilon_x x$ and $g(z) = \varepsilon_z z$ for some constants ε_x and ε_z. Plugging everything back into Eq. (2.7) and comparing with $|\gamma_1|_{\text{AdS}}$, we again find that $L_1 = L$, so no continuum limit is possible. Similarly, in computing $|\gamma_2|$, we note that the number of bonds between the endpoints on the UV-most lattice level is $x_0^{\text{MERA}}/f(a)$, so the geodesic connecting the endpoints has $2\log_k(x_0^{\text{MERA}}/\varepsilon_x a)$ bonds. On the other hand, we have $|\gamma_2|_{\text{AdS}} = 2L\ln(x_0^{\text{AdS}}/a) = 2L\ln(x_0^{\text{MERA}}/\varepsilon_x a)$. That is, in equating $|\gamma_2|_{\text{AdS}}$ and $|\gamma_2|_{\text{MERA}}$, we must again set $L_2 = L\ln k$. We thus also find that no continuum limit is possible in the holographic direction. That is, we have shown that there is a constant normalization freedom in the definition of each of the coordinate distances on the AdS and MERA sides of any AdS/MERA duality, but such a coordinate ambiguity is unphysical and does not allow one to take a continuum limit. One still finds that the physical MERA parameters L_1 and L_2 are AdS scale. This means that there truly is no sense in which a discrete MERA can directly describe sub-AdS scale physics without the addition of supplemental structure to replace the individual tensors. This fact limits the ability of the MERA to be a complete description of the gravity theory without such additional structure. It might be the case that one needs a field theoretic generalization of the MERA, such as continuous MERA (cMERA) [59, 60, 61] or some local expansion of the individual tensors into discrete tensor networks with a different graph structure to describe sub-AdS physics, but such a significant generalization of the tensor network is beyond the scope of this work and in any case would no longer correspond to a MERA proper.

2.4 Constraints from Boundary Entanglement Entropy

Because the MERA can efficiently describe critical systems on a lattice, quantities computed in the MERA on scales much larger than the lattice spacing should agree with CFT results. In this section, we will compute the entanglement entropy of ℓ_0 contiguous sites in the MERA and exploit known CFT results to obtain constraints on the properties of the MERA. In particular, we will find an inequality relating the MERA rescaling factor k and bond dimension χ to the CFT central charge c. This constraint is interesting in its own right, but it will prove critical in the next section when we begin to compute bulk properties.

2.4.1 MERA and CFT Entanglement Entropy

For a $(1+1)$-dimensional CFT in a pure state, the von Neumann entropy of a finite interval B, which is typically referred to as the entanglement entropy, is known to be [62, 63]

$$S(B) = \frac{c}{3} \ln \ell_0 , \tag{2.9}$$

where the length of the interval is much smaller than the system size. Here, ℓ_0 is the length of the interval in units of the UV cutoff. In the notation of the last section, we have $\ell_0 = x_0/a$. In the special case that the CFT is dual to AdS in $2+1$ dimensions, the central charge is set by the Brown–Henneaux formula [22],

$$c = \frac{3L}{2G}. \tag{2.10}$$

Also note that the length of the geodesic that connects the two ends of B (the curve γ_2 in Fig. 2.3) is given in Eq. (2.4) by $|\gamma_2| = 2L \ln \ell_0$. The Brown–Henneaux relation allows us to reproduce the Ryu–Takayanagi formula [23, 64] from the entanglement entropy,

$$S(B) = \frac{\text{area}(\tilde{B})}{4G}, \tag{2.11}$$

where $\tilde{B} = \gamma_2$ is the extremal bulk surface with the same boundary as B. For a boundary with one spatial dimension and a bulk with two spatial dimensions, any simply-connected region B is an interval, the extremal bulk surface is a geodesic, area$(\tilde{B})$ is a length, and G has mass dimension -1.

The MERA calculation of the entanglement entropy of ℓ_0 sites in the CFT has an analogous geometric interpretation. Suppose one is given the MERA representation of a lattice CFT ground state, *i.e.*, one uses a MERA to generate the CFT state. Denote by $S_{\text{MERA}}(\ell_0)$ the entanglement entropy of the resulting state restricted to ℓ_0 sites. In Ref. [58], it is shown that for a specific, optimal choice of ℓ_0 sites, for ℓ_0 parametrically large, the following bound is placed on $S_{\text{MERA}}(\ell_0)$ for a MERA with $k = 2$:

$$S_{\text{MERA}}(\ell_0) \leq 2 \log_2 \ell_0 \ln \chi. \tag{2.12}$$

Parsing the equation above, this bound essentially counts the number of bonds that the *causal cone* of the ℓ_0 sites in question crosses ($\sim 2\log_2 \ell_0$) and $\ln \chi$ is the maximum entanglement entropy that a single bond can possess when the rest of the MERA is traced out.

The causal cone of a region B consisting of ℓ_0 contiguous UV sites in a MERA resembles a bulk extremal surface for the boundary region B. Given ℓ_0 sites in the UV, their causal cone is defined as the part of the MERA on which the reduced density matrix (or in other words, the state) of B depends. An example of a causal cone is illustrated in Fig. 2.4.

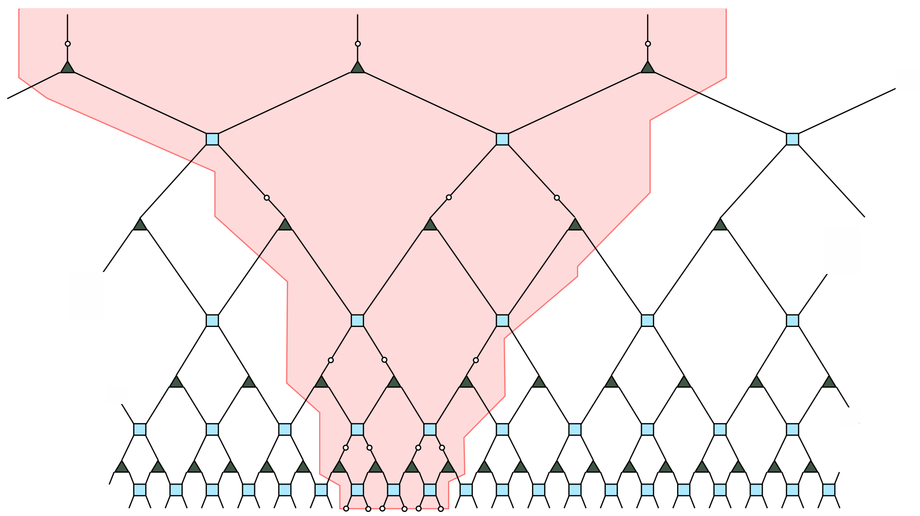

Figure 2.4: Causal cone (shaded) for a set of $\ell_0 = 6$ sites in a MERA with $k = 2$. The width ℓ_m of the causal cone at depth m is $\ell_1 = 4$, $\ell_2 = 3$, $\ell_3 = 3$, $\ell_4 = 3$, etc. The crossover scale for this causal cone occurs at $\bar{m} = 2$. Between the zeroth and first layer, $n_1^{\text{tr}} = 2$ bonds are cut by the causal cone. Similarly, $n_2^{\text{tr}} = 2$, $n_3^{\text{tr}} = 3$, etc.

In particular, note that the number of bonds that a causal cone crosses up to any fixed layer scales like the length of the boundary of the causal cone up to that layer. It is in this sense that Eq. (2.12) is a MERA version of Ryu–Takayanagi. Also note that the width of the causal cone shrinks by a factor of $\sim 1/k$ after every renormalization step until its width is comparable to k. As such, if one denotes the width of the causal cone at a layer m by ℓ_m, then ℓ_m is roughly constant for all m greater than some $\bar{m}$ (see Fig. 2.4). The scale $\bar{m}$ is called the *crossover scale*.

For general k, it is also possible to formulate a bound similar to Eq. (2.12) for the entanglement entropy of ℓ_0 sites. For parametrically large ℓ_0, we find that

$$S_{\text{MERA}}(\ell_0; B) \leq 4(k-1)\log_k \ell_0 \ln \chi \,. \tag{2.13}$$

We demonstrate this bound in App. 2.A using techniques that are similar to those developed in Ref. [58]. In particular, note that we do not allow ourselves to choose the location of the ℓ_0 sites in question. As such, we remind ourselves that S_{MERA} can depend on the location of the region B (and not only its size) by including it in the argument of S_{MERA}. This is also the reason why our Eq. (2.13) is more conservative than the optimal bound given in Eq. (2.12).

2.4.2 Constraining S_{MERA}

Let us examine Eq. (2.13) a bit more closely. As discussed in App. 2.A, $4(k-1)$ is an upper bound on the number of bonds that the causal cone could cut at any given depth m below the crossover scale $\bar{m}$. (The crossover scale $\bar{m}$ is attained after roughly $\log_k \ell_0$ renormalization steps.) For a given causal cone, *i.e.*, for ℓ_0 sites at a given location with respect to the MERA, let us parametrize our ignorance by writing

$$S_{\mathrm{MERA}}(\ell_0; B) \leq 4 f_B(k) \log_k \ell_0 \ln \chi \,, \tag{2.14}$$

where $f_B(k)$ grows no faster than $(k-1)$ and counts the (average) number of bonds cut by the causal cone at any depth up to the crossover scale. Explicitly,

$$f_B(k) \equiv \frac{1}{4\bar{m}} \sum_{m=0}^{\bar{m}-1} n_m^{\mathrm{tr}} \,, \tag{2.15}$$

where n_m^{tr} denotes the number of bonds that the causal cone cuts at the m^{th} level.

Each cut bond contributes at most $\ln \chi$ to the entropy (the case of maximal entanglement). As such, it is instructive to introduce a parameter $\eta_B \in [0,1]$ that describes the degree of entanglement of the sites in the causal cone. In doing so we may rewrite the inequality (2.14) as an equality:

$$S_{\mathrm{MERA}}(\ell_0; B) = 4 f_B(k) \log_k \ell_0 \cdot \eta_B \ln \chi . \tag{2.16}$$

The quantity $\eta_B \ln \chi$ is the average entanglement entropy per cut bond in the causal cone of B. Equivalently, Eq. (2.16) may be taken as the definition of η_B.

This definition of η_B of course depends on the location of B and only applies to bonds that are cut by the causal cone of B. In what follows, it will be advantageous to have a notion of average entanglement entropy per bond that applies to *all* bonds in the MERA. To this end, start with a lattice consisting of ℓ_{tot} sites in total and consider the limit in which the size of a region B is unbounded but where the ratio $\ell_0/\ell_{\mathrm{tot}}$ is held constant (so that B does not grow to encompass the whole domain of the CFT). In this limit, $S_{\mathrm{MERA}}(\ell_0; B) \to S_{\mathrm{MERA}}(\ell_0)$ and $f_B(k) \to f(k)$ should be independent of the exact location of B, *i.e.*, S_{MERA} should exactly agree with Eq. (2.9). Let us consequently define the average entanglement entropy per bond in the MERA:

$$\eta \ln \chi = \lim_{\ell_0 \to \infty} \frac{S_{\mathrm{MERA}}(\ell_0)}{4 f(k) \log_k(\ell_0)}, \tag{2.17}$$

The quantity η is then a property of the MERA itself.

Intuitively, one would not expect each individual bond in the MERA to be maximally entangled and so it should be possible to constrain η more tightly than $\eta \leq 1$. This expectation is made more precise via the following considerations. To begin, consider a MERA with $k = 2$ and examine a pair of isometries at a fixed depth m. As indicated in Fig. 2.5a, let ρ_2 denote the density matrix of the bonds and ancillae emanating from the two isometries and let ρ_1 denote the density matrix of the four highlighted bonds below the isometries. We again assume that the ancillae are initialized to the pure product state composed of factors of $|0\rangle$. Taking into account the ancillae, or in other words promoting the isometries to unitaries, we see that ρ_1 and ρ_2 are related by a unitary transformation, so $S(\rho_1) = S(\rho_2)$. By assumption, the state of each ancilla is $|0\rangle$, so $\rho_2 = \tilde{\rho}_2 \otimes |0\rangle\langle 0| \otimes |0\rangle\langle 0|$ for some density matrix $\tilde{\rho}_2$. This in turn implies that $S(\rho_2) = S(\tilde{\rho}_2) \leq 2 \ln \chi$. From the definition of η above, the entanglement entropy of a single bond is asymptotically given by $\eta \ln \chi$, so $S(\rho_1) \simeq 4\eta \ln \chi$. It therefore follows that $\eta \leq 1/2$.

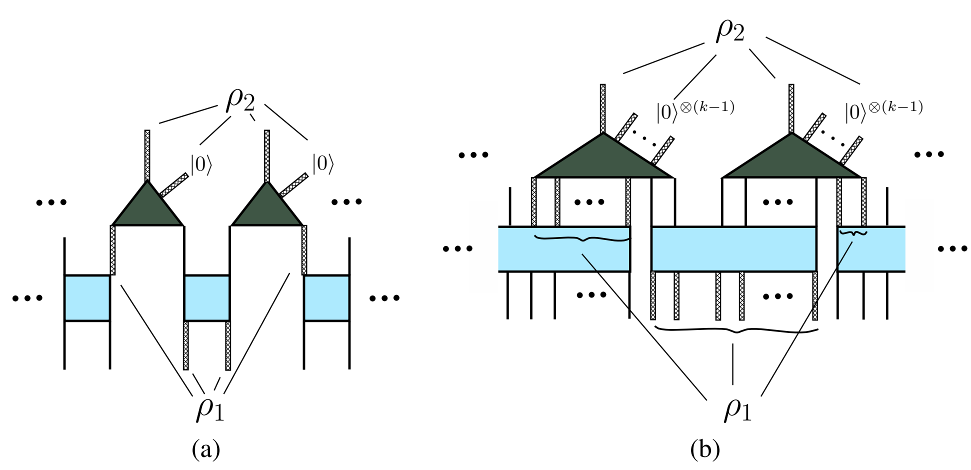

Figure 2.5: A pair of isometries with their ancillae explicitly indicated for a MERA with (a) $k = 2$ and (b) general k. The thick bonds below the isometries, the state of which is denoted by ρ_1, are unitarily related to the bonds that exit the isometries and the ancillae, the state of which is denoted by ρ_2.

For general k, the argument is nearly identical. We again begin by considering a pair of isometries at a given level m (see Fig. 2.5b). Analogously with the $k = 2$ case, let ρ_2 denote the density matrix of the two bonds and $2k-2$ ancillae emanating from the two isometries and let ρ_1 denote the density matrix of the $2k$ highlighted bonds below the isometries. There is only one disentangler that straddles both of the isometries in question for any layout of the MERA. As such, at most k of the lower bonds enter a disentangler from below and the rest directly enter the isometries. Here as well ρ_1 and ρ_2 are related by a unitary transformation so that $S(\rho_1) = S(\rho_2)$. Similarly, $\rho_2 = \tilde{\rho}_2 \otimes (|0\rangle\langle 0|)^{\otimes 2k-2}$ for some density matrix $\tilde{\rho}_2$, so $S(\rho_2) = S(\tilde{\rho}_2) \leq 2 \ln \chi$. The region described by ρ_1 always consists of $2k$ bonds, so we may again asymptotically write $S(\rho_1) \simeq 2k\eta \ln \chi$. It therefore follows that $k\eta \leq 1$, and since $f(k) \leq (k-1)$, we may write

$$\eta f(k) \leq \frac{k-1}{k} \,. \tag{2.18}$$

We note that, in computational practice, one typically does not use the "worst-case scenario" construction explored in App. 2.A; a more conventional construction would result in a tighter bound on $f(k)$ and hence a stricter inequality than Eq. (2.18). For our purposes, however, we will remain as conservative as possible and therefore use the inequality (2.18) in our subsequent bounds.

2.4.3 Matching to the CFT

Finally, we obtain a constraint on k, χ, and η in terms of the central charge c by collecting the results of this section. Let us work in the limit where the interval is much larger than the lattice spacing, $\log_k \ell_0 \gg 1$. We have seen that this is precisely the regime in which η and $f(k)$ are well-defined quantities independent of the choice of B. It is also the regime in which we can equate the CFT entropy $S(\ell_0) = (c/3) \ln \ell_0$ with the MERA entropy (2.16). Doing so, the central charge is given by

$$c = \frac{3L}{2G} = 12\eta\, f(k) \frac{\ln \chi}{\ln k} \,. \tag{2.19}$$

Then in light of Eq. (2.18), we find that

$$c \leq 12 \left(\frac{k-1}{k \ln k} \right) \ln \chi \,. \tag{2.20}$$

To recapitulate, given a CFT with central charge c and a MERA representation of its ground state, a necessary condition for a consistent AdS/MERA correspondence is that the MERA parameters k and χ satisfy the constraint (2.20). Importantly, this implies that, for a well-defined semiclassical spacetime (for which $c \gg 1$), the bond dimension χ must be exponentially large in the size of the AdS scale compared to the Planck scale.

Let us also note that we can still obtain a bound from Eq. (2.19), albeit a weaker one, without using the result of Eq. (2.18). Recall that this latter result relies on having unentangled ancillae in the MERA. This is not necessarily the case for other tensor network bulk constructions, as we will subsequently discuss. As such, if we disregard the result of Eq. (2.18), we still have by virtue of their definitions that $f(k) \le k-1$ and $\eta \le 1$. The following weaker but more general bound on the central charge therefore follows from Eq. (2.19) for such generalized tensor networks:

$$c \le 12\left(\frac{k-1}{\ln k}\right)\ln\chi. \tag{2.21}$$

2.5 Constraints from Bulk Entanglement Entropy

In addition to the compatibility conditions from geodesic matching and boundary entanglement entropy, it is well-motivated to seek out any other possible quantities that can be computed in both the MERA and AdS/CFT frameworks, so as to place further constraints on any AdS/MERA correspondence. One important example of such a quantity is the entropy associated with regions in the bulk, as opposed to on the boundary.

2.5.1 The Bousso Bound

The notion of placing bounds on the entropy of regions of spacetime in a quantum gravity theory has been explored for many years, first in the context of black hole thermodynamics [65] and the Bekenstein bound [66] and later in more general holographic contexts, culminating in the covariant entropy bound, *i.e.*, the Bousso bound [18, 20].

The statement of the Bousso bound is the following: given a spacelike surface $\mathcal{B}$ of area A, draw the orthogonal null congruence on the surface and choose a direction in which the null generators have non-positive expansion. Let the null geodesics terminate at caustics, singularities, or whenever the expansion becomes positive. The null hypersurface swept out by these null geodesics is called the *lightsheet*. Then the entropy S going through the lightsheet is less than $A/4G$.

Let our spacelike surface $\mathcal{B}$ be a 2-ball of area A on a spacelike slice of AdS and choose as the lightsheet the ingoing future-directed null congruence. This lightsheet will sweep out the entire interior of $\mathcal{B}$ and will terminate at a caustic at the center of $\mathcal{B}$. Since the system is static, the entropy S passing through this lightsheet is the entropy of the system on $\mathcal{B}$, which by the Bousso bound satisfies

$$S(\mathcal{B}) \leq \frac{A}{4G}\,. \tag{2.22}$$

It is natural to cast the Bousso bound as a constraint on the dimension of the bulk Hilbert space. As argued in Ref. [67], the thermodynamic entropy of a system about which we only know the boundary area A is just the logarithm of the dimension of the true Hilbert space of the bulk region in question (as opposed to the naïve Hilbert space in quantum field theory), which the Bousso bound implies is less than $A/4G$.[1] As such, if we denote the Hilbert space of $\mathcal{B}$ by $\mathcal{H}_{\mathcal{B}}$, let us replace Eq. (2.22) with the slightly more concrete statement

$$\ln \dim \mathcal{H}_{\mathcal{B}} \leq \frac{A}{4G}. \tag{2.23}$$

2.5.2 A MERA version of the Bousso Bound

Our aim is to compute both sides of the inequality (2.23) using the MERA. For this calculation, it is instructive to change our parametrization of the hyperbolic plane from coordinates (x, z), which take values in the half-plane $z > 0$, to coordinates (ρ, θ), which take values in a disk $0 \leq \rho < 1$, $0 \leq \theta < 2\pi$. Embeddings of the MERA in a disk are often depicted in the literature, *e.g.*, [71]; here we make this coordinate transformation explicit, since we wish to carefully study the geometric properties of the MERA.

To begin, consider a MERA consisting of a single tree that contains a finite number of layers m. This situation is illustrated in Fig. 2.6a for $k = 2$ and $m = 4$. Note that such a MERA begins with a top-level tensor at the m^{th} level that seeds the rest of the MERA in the IR.

The base of the MERA is made up of k^m sites. Without loss of generality, let us locate the leftmost site of the base of the MERA at $x = 0$, so that the UV-most sites sit at coordinates $(x, z) = (na, a)$, where $n = 0, 1, 2, \ldots, (k^m - 1)$ as shown in Fig. 2.6b. Let us also assume periodic boundary conditions for this MERA and hence identify $x = 0$ and $x = k^m a$.

[1] Moreover, it is known that there exists an asymptotically-AdS bulk configuration that saturates the Bousso bound, namely, the BTZ black hole [68, 69], which further implies that $\ln \dim \mathcal{H}_{\mathcal{B}}$ in fact equals $A/4G$. However, we will not need this stronger assertion in what follows. A similar but unrelated result equating the area of a region with its entanglement entropy in vacuum was obtained in Ref. [70].

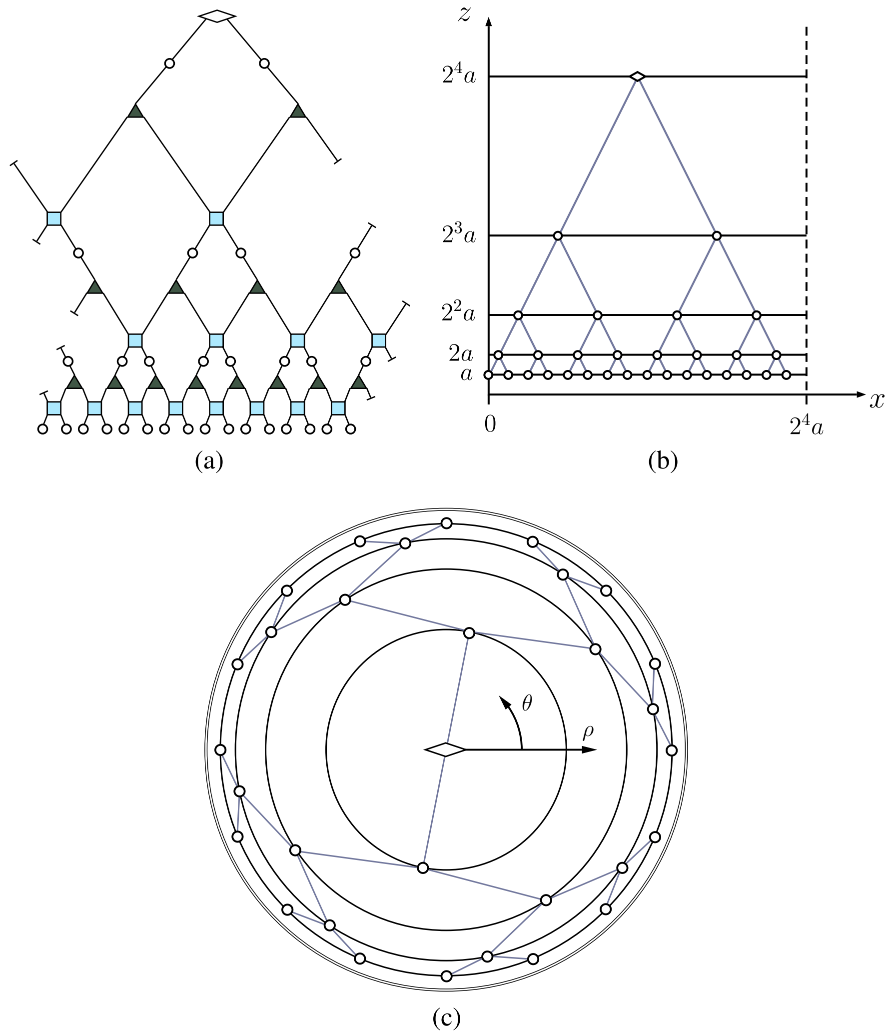

Figure 2.6: (a) A $k = 2$ MERA consisting of $m = 4$ layers and with periodic boundary conditions, (b) the corresponding embedding in (x, z) coordinates, and (c) the embedding in (ρ, θ) coordinates.

Next, define the coordinates (ρ, θ) as follows:

$$\begin{aligned} \rho &= \frac{k^m a - z}{k^m a}, \\ \theta &= 2\pi \frac{x}{k^m a}. \end{aligned} \tag{2.24}$$

In these coordinates, the metric reads

$$\mathrm{d}s^2 = \frac{L^2}{(1-\rho)^2}\left[\mathrm{d}\rho^2 + \left(\frac{\mathrm{d}\theta}{2\pi}\right)^2\right], \tag{2.25}$$

cf. Eq. (2.3). This embedding of the MERA is shown in Fig. 2.6c; the top-level tensor always sits at $\rho = 0$ and the lower layers of the MERA are equally spaced on circles of radii $1/2$, $3/4$, $7/8$, ... that are centered at $\rho = 0$.

More generally, one could construct a top-level tensor that has T legs, each of which begets a tree of sites. In this case, $x = 0$ and $x = Tk^{m-1}a$ are identified, so one should define the angular variable as $\theta \equiv 2\pi x/(Tk^{m-1}a)$. The metric (2.25) is correspondingly modified and reads

$$\mathrm{d}s^2 = \frac{L^2}{(1-\rho)^2}\left[\mathrm{d}\rho^2 + \frac{T^2}{k^2}\left(\frac{\mathrm{d}\theta}{2\pi}\right)^2\right]. \tag{2.26}$$

This situation is depicted in Fig. 2.7. (If $T = k$, however, then it is not necessary to introduce any new structure in addition to the disentanglers and isometries that were already discussed, *i.e.*, one may take the top-level tensor to be one of the isometries.)

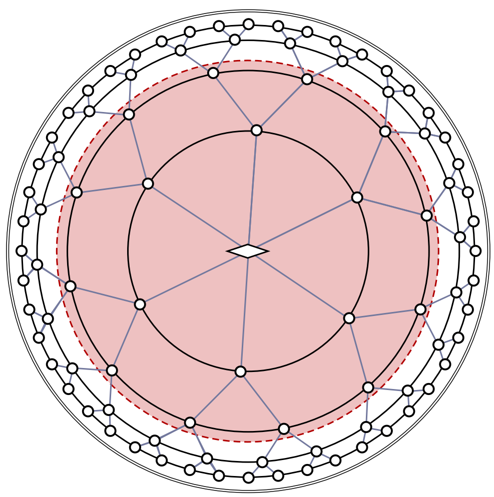

Figure 2.7: Disk parametrization of the Poincaré patch of AdS in which a MERA has been embedded. The top tensor of the MERA shown has $T = 6$. The shaded region is a ball $\mathcal{B}$, which is this case contains $N_{\mathcal{B}} = 1$ generation.

We may immediately compute the right-hand side of Eq. (2.23). Let the ball $\mathcal{B}$ be centered about $\rho = 0$, and suppose $\mathcal{B}$ contains the top-level tensor, the sites at the top tensor's legs, and then the first $N_{\mathcal{B}}$ generations of the MERA emanating from these sites, as indicated in Fig. 2.7. The boundary of $\mathcal{B}$ is a circle at constant ρ, so its circumference according to the MERA is $A = Tk^{N_{\mathcal{B}}}L$. As such, we may write

$$\frac{A}{4G} = \frac{Tk^{N_{\mathcal{B}}}L}{4G} = \frac{Tk^{N_{\mathcal{B}}}c}{6}, \tag{2.27}$$

where in the second equality we used the Brown-Henneaux relation, Eq. (2.10).

How one evaluates the left-hand side of Eq. (2.23) using the MERA is not as immediate. Recall that $\mathcal{H}_{\mathcal{B}}$ is the Hilbert space of *bulk states*. The MERA, however, does not directly prescribe the quantum-gravitational state in the bulk; it is not by itself a bulk-boundary dictionary. As we mentioned in Sec. 2.2.2, the minimal assumption that one can make is to posit the existence of a bulk Hilbert space factor V_{bulk} associated with each MERA site that is not located at the top tensor. To keep the assignment general, we assign a factor V_{T} to the top tensor. The dimensionality of each V_{bulk} factor should be the same in order to be consistent with the symmetries of the hyperbolic plane. The assumption of a Hilbert space factor at every MERA site is minimal in the sense that it introduces no new structure into the MERA. A true AdS/MERA correspondence should dictate how states in the bulk Hilbert space are related to boundary states. However, for our analysis, it is enough to simply postulate the existence of the bulk Hilbert space factors V_{bulk} and V_{T}, each of which may be thought of as localized to an AdS-scale patch corresponding to the associated MERA site.

In addition to the site at the top tensor, the number of regular MERA sites that the ball $\mathcal{B}$ contains is given by

$$\mathcal{N}_{\mathcal{B}} = T \sum_{i=0}^{N_{\mathcal{B}}} k^i = T \left(\frac{k^{N_{\mathcal{B}}+1} - 1}{k - 1} \right) . \tag{2.28}$$

As such, the Hilbert space of bulk states restricted to $\mathcal{B}$ is $\mathcal{H}_{\mathcal{B}} = (V_{\text{bulk}})^{\otimes \mathcal{N}_{\mathcal{B}}} \otimes V_{\text{T}}$. Next, suppose that $\dim V_{\text{bulk}} = \tilde{\chi}$ and that $\dim V_{\text{T}} = \tilde{\chi}_{\text{T}}$, where, like χ, $\tilde{\chi}$ and $\tilde{\chi}_{\text{T}}$ are some fixed, $N_{\mathcal{B}}$-independent numbers. Then $\dim \mathcal{H}_{\mathcal{B}} = \tilde{\chi}_{\text{T}}(\tilde{\chi}^{\mathcal{N}_{\mathcal{B}}})$. Note that one would expect χ and $\tilde{\chi}$ to have a very specific relationship in a true bulk/boundary correspondence, the nature of which will be explored later in this section. Combining Eqs. (2.27) and (2.28), the dimensionality of $\mathcal{H}_{\mathcal{B}}$ is upper bounded as follows:

$$\ln \dim \mathcal{H}_{\mathcal{B}} \leq \frac{A}{4G} \qquad \Longrightarrow \qquad T \left(\frac{k^{N_{\mathcal{B}}+1} - 1}{k - 1} \right) \ln \tilde{\chi} + \ln \tilde{\chi}_{\text{T}} \leq \frac{T k_{\mathcal{B}}^{N} c}{6} . \tag{2.29}$$

After isolating c in Eq. (2.29) and using the result of Eq. (2.19), we find that

$$c = 12 \eta f(k) \frac{\ln \chi}{\ln k} \geq 6 \left(\frac{k^{N_{\mathcal{B}}+1} - 1}{k^{N_{\mathcal{B}}}(k - 1)} \ln \tilde{\chi} + \frac{1}{T k^{N_{\mathcal{B}}}} \ln \tilde{\chi}_{\text{T}} \right) . \tag{2.30}$$

Next, let us consider this inequality in the limit of large $N_{\mathcal{B}}$. A motivation for this limit is the fact that the natural scale of validity of an AdS/MERA correspondence is super-AdS, as was established in Sec. 2.3. Moreover, by virtue of its definition, there is always an ambiguity of order the AdS scale in the radius of the ball $\mathcal{B}$. That is, the region in AdS denoted by $\mathcal{B}$ is only well-defined in the MERA if $\mathcal{B}$ is large compared to the AdS scale L. Taking the limit of large $N_{\mathcal{B}}$, Eq. (2.30) reduces to

$$\eta f(k) \geq \frac{k \ln k}{2(k - 1)} \left(\frac{\ln \tilde{\chi}}{\ln \chi} \right) . \tag{2.31}$$

By using the bound on $\eta f(k)$ given by Eq. (2.18), we arrive at a constraint on k, χ, and $\tilde{\chi}$:

$$\frac{k^2 \ln k}{2(k-1)^2} \left(\frac{\ln \tilde{\chi}}{\ln \chi}\right) \leq 1. \tag{2.32}$$

In principle, the above inequality could be satisfied for any k, provided that the dimension $\tilde{\chi}$ of the factors V_{bulk} can be arbitrarily chosen with respect to the bond dimension χ. However, the essence of holography, that the bulk and boundary are dual descriptions of the same degrees of freedom and therefore have isomorphic Hilbert spaces [45], implies a relation between χ and $\tilde{\chi}$. Namely, for a MERA with a total of N levels of sites in the bulk strictly between the UV-most level and the top-level tensor, the number of bulk sites $\mathcal{N}_{\text{bulk}}$ that are not located at the top tensor is given by Eq. (2.28) with $N_{\mathcal{B}} = N$, and the number of sites in the boundary description is $\mathcal{N}_{\text{boundary}} \equiv Tk^{N+1}$. The bulk Hilbert space thus has dimension $\tilde{\chi}^{\mathcal{N}_{\text{bulk}}} \tilde{\chi}_{\text{T}}$ and the boundary Hilbert space has dimension $\chi^{\mathcal{N}_{\text{boundary}}}$. Equating[2] the dimension of the bulk and boundary Hilbert spaces then yields

$$\frac{\ln \tilde{\chi}}{\ln \chi} = \frac{1}{\mathcal{N}_{\text{bulk}}} \left(Tk^{N+1} - \frac{\ln \tilde{\chi}_{\text{T}}}{\ln \chi}\right) \overset{N \text{ large}}{\longrightarrow} k - 1, \tag{2.33}$$

where we took the limit of N large, consistent with Eq. (2.31) and in keeping with the expectation that the UV cutoff be parametrically close to the boundary at $\rho = 1$. Putting together Eqs. (2.32) and (2.33), we obtain a constraint on k alone:

$$\frac{k^2 \ln k}{2(k-1)} \leq 1. \tag{2.34}$$

This constraint cannot be satisfied for any allowed value of the rescaling factor k, which must be an integer greater than or equal to 2. We thus learn that a conventional MERA cannot yield a consistent AdS/MERA correspondence. The MERA cannot simultaneously reproduce AdS geodesics, respect the Ryu–Takayanagi relation, and (using the only construction for the bulk Hilbert space available to the MERA by itself) satisfy the Bousso bound. That is, there exists no choice of MERA parameters that can faithfully reproduce geometry, holographic properties, and bulk physics.

If we relax this bound and, instead of Eq. (2.18), only observe the weaker, natural bounds $\eta \leq 1$ and $f(k) \leq k - 1$ as discussed at the end of Sec. 2.4.3, the constraint (2.34) is correspondingly modified:

$$\frac{k \ln k}{2(k-1)} \leq 1. \tag{2.35}$$

[2] We recognize that there are other proposals [49, 72] that do not require an exact equivalence between the bulk and boundary Hilbert spaces, but, even in these cases, there is the requirement of an exact equivalence between the logical qubits on the boundary with the Hilbert space of the bulk.

In contrast to Eq. (2.34), this latter bound can be satisfied, but only for $k = 2$, 3, or 4. As such, other AdS/tensor network correspondences, in which the ancillae are perhaps entangled and therefore do not describe a conventional MERA, are not ruled out. Note that we never needed to compute bulk entanglement entropy explicitly — and therefore did not need to treat separately the possibility of entanglement among ancillae — because we cast the Bousso bound as a constraint on the size of the bulk Hilbert space itself. The appearance of η in Eq. (2.31) corresponds to entanglement in the boundary theory as computed by the tensor network; Eqs. (2.31) and (2.33) still apply.

2.6 Conclusion

The notion of emergence of spacetime based on a correspondence between AdS and a tensor network akin to AdS/CFT is a tantalizing one. A necessary step in such a program is the evaluation and comparison of calculable quantities on both sides of the duality. In this work, we have subjected the proposed AdS/MERA correspondence to such scrutiny. To summarize, let us restate our three main findings:

1. In matching the discrete graph geometry of the MERA to the continuous geometry of a spatial slice of AdS, we demonstrated that the MERA describes geometry only on scales larger than the AdS radius. Concretely, as shown in Sec. 2.3, the proper length assigned to the spacing between adjacent sites in the MERA lattice must be the AdS scale.

2. By requiring that the entropy of a set of boundary sites in the MERA — whose computation is a discrete realization of the Ryu–Takayanagi formula — be equal to the CFT ground state entropy of the same boundary region in the thermodynamic limit, we obtained a constraint on the parameters that describe a MERA in terms of the CFT central charge [Eqs. (2.20) and (2.21)], which implies that the bond dimension χ must be exponentially large in the ratio of the AdS scale to the Planck scale.

3. In the natural construction of a bulk Hilbert space ($\mathcal{H}_{\text{bulk}}$) using the MERA, we used the Bousso bound to constrain the dimension of $\mathcal{H}_{\text{bulk}}$. When combined with our previous results, we found that any strict AdS/MERA correspondence cannot satisfy the resulting constraint, Eq. (2.34). Upon relaxing the definition of the MERA or allowing for additional structure, however, we obtained a looser constraint, Eq. (2.35), which may not rule out some other AdS/tensor network correspondences.

In particular, more general correspondences between AdS and MERA-like tensor networks, in which we allow the ancillae to be entangled when reproducing the CFT ground state [and for which Eq. (2.35) applies in place of Eq. (2.34)] are not ruled out by our bounds, provided that the rescaling factor $k = 2$, 3, or 4. Further, it is interesting to note that our bounds extend to states other than the vacuum that are described by a MERA. One such example, namely, states at finite temperature dual to black holes in AdS, is discussed in App. 2.B below.

While the consistency conditions that we found are specific to the MERA tensor network, many of the ideas and techniques that we used apply equally well to other tensor networks. In the EHM, for instance, the type of bulk Hilbert space dimensionality arguments that we made based on the covariant entropy bound may be directly transferred to the EHM. The same stringent final constraints that we derived do not apply to the EHM, however, since it is unclear to what extent the EHM reproduces the Ryu–Takayanagi formula (which renders the results of Sec. 2.4 inapplicable). Our bulk Hilbert space arguments similarly apply to the holographic error-correcting code proposal in Ref. [49], which furthermore purports to reproduce a version of the Ryu–Takayanagi formula. It is presently unknown, however, whether the boundary state of a holographic code can represent the ground state of a CFT, so an identification of entropies similar to the identification $S_{\mathrm{MERA}} = S_{\mathrm{CFT}}$, upon which our boundary entropy constraints so crucially depend, cannot yet be made.

In closing, we have found several consistency conditions that any AdS/MERA correspondence must satisfy. The totality of these constraints rules out the most straightforward construal of an AdS/MERA correspondence. Other interesting holographic correspondences that are described by tensor networks more general than the MERA and that respect all of our bounds may indeed be possible. Our consistency conditions are nice validity checks for these correspondences when applicable and in other cases they may inspire similar consistency conditions. The program of identifying the emergence of spacetime from the building blocks of quantum information is an ambitious one; stringent consistency conditions, such as those presented in this paper, are important for elucidating the subtleties in this quest and in providing guidance along the way.

2.A Entropy bound for general MERAs

Following the method presented in Ref. [58], let us compute an upper bound for the entanglement entropy of a region B consisting of ℓ_0 sites in a MERA with rescaling factor k. We will use the notation of Ref. [58] throughout.

First, recall the result from Ref. [58] that the entanglement entropy of a region consisting of ℓ_0 sites is bounded by

$$S_{\mathrm{MERA}}(\ell_0; B) \leq (\ell_{m'} + N^{\mathrm{tr}}_{m'}) \ln \chi. \tag{2.36}$$

The quantity $\ell_{m'}$ is the width of the causal cone at depth m' and $N^{\mathrm{tr}}_{m'} = \sum_{m=0}^{m'-1} n^{\mathrm{tr}}_m$ is the total number of sites that are traced out along the boundary of the causal cone. In other words, $N^{\mathrm{tr}}_{m'}$ is the number of bonds that are cut by the causal cone up to a depth m' (*cf.* Fig. 2.4). The quantity $\ln \chi$ is the maximum entanglement entropy that each site that is traced out could contribute to $S_{\mathrm{MERA}}(\ell_0; B)$. Note that Eq. (2.36) holds for all $m' \geq 0$.

The width of the causal cone for a given m' depends sensitively on the structure of the MERA. In particular, the number of sites that are traced out at each renormalization step depends on the choice of disentanglers, as well as how they are connected to the isometries. For instance, in a MERA with a rescaling factor k, any given disentangler could have anywhere from 2 up to k incoming and outgoing legs. (It should be reasonable to require that any disentangler can have no more than k incoming and k outgoing legs so that it straddles no more than two isometries.) It is thus clear that the number of bonds that one cuts when drawing a causal cone, and hence the entanglement entropy of the region subtended by that causal cone, depends on the choice of disentanglers and connectivity.

Nevertheless, we can compute an upper bound for $S_{\mathrm{MERA}}(\ell_0; B)$ by considering a worst-case scenario for the number of bonds cut by the causal cone. We begin by asking: What is the largest number of bonds that a causal cone could cut in one renormalization step at a depth m'? The layout of disentanglers and isometries that produces this situation is shown at one side of a causal cone in Fig. 2.8. If the causal cone at the bottom of the renormalization step incorporates a single bond that goes into a disentangler accepting k bonds, then the causal cone must cut the other $k-1$ bonds entering the disentangler. Then if this disentangler is arranged so that its leftmost outgoing bond is the first bond to enter an isometry from the right, the causal cone must cut the other $k-1$ bonds entering the isometry. If this arrangement is mirrored on the other side of the causal cone, we see that $4(k-1)$ bonds are cut by the causal cone in this renormalization step, *i.e.*, $n^{\mathrm{tr}}_{m'} = 4(k-1)$.

Recall that for any finite ℓ_0, after a fixed number of renormalization steps, the width of the causal cone remains constant for any further coarse-grainings. The depth at

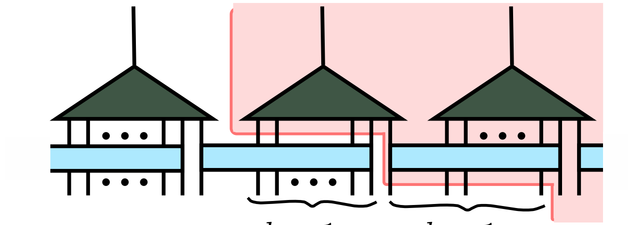

Figure 2.8: Left side of a causal cone that cuts the maximum possible number of bonds over the course of one renormalization step. The rectangles are disentanglers that accept k bonds as input and the triangles are isometries that coarse-grain k bonds into one. The causal cone is the shaded region. If this situation is mirrored on the right side of the causal cone, then $4(k-1)$ bonds are cut in this renormalization step.

which this occurs is called the crossover scale and is denoted by $\bar{m}$. Therefore, the causal cone will cut the largest possible number of bonds when the arrangement described above and depicted in Fig. 2.8 occurs at every step up until the crossover scale. Then, by Eq. (2.36), the entropy bound is given by

$$S_{\mathrm{MERA}}(\ell_0; B) \leq (\ell_{\bar{m}} + 4(k-1)\bar{m}) \ln \chi, \tag{2.37}$$

where $\ell_{\bar{m}}$ is the width of the causal cone at the crossover scale.

For any given causal cone in a MERA with scale factor $k \geq 2$, the maximum number of additional sites the causal cone can pick up at some level m' is $4(k-1)$. Therefore, for a causal cone that contains $\ell_{m'}$ sites at depth m', the number of sites in the causal cone after one renormalization step $\ell_{m'+1} \leq \lceil(\ell_{m'} + 4(k-1))/k\rceil \leq \ell_{m'}/k + 5$. Applying the relation recursively, we find that the number of sites $\ell_{m'}$ at any layer $m' < \bar{m}$ is bounded,

$$\ell_{m'} \leq \frac{\ell_0}{k^{m'}} + 5\sum_{m=1}^{m'} \frac{1}{k^m} \leq \frac{\ell_0}{k^{m'}} + 5\,. \tag{2.38}$$

Setting $m' = \bar{m}$, it trivially follows that the crossover scale obeys $\bar{m} \leq \log_k \ell_0$. Furthermore, we notice that this is the scale at which the entanglement entropy is minimized if we trace over the remaining sites. In other words, the number of bonds cut by going deeper into the renormalization direction is no less than the bonds cut horizontally, so $4(k-1) \geq \ell_{\bar{m}}$ [3]. Applying the bounds for $\bar{m}$ and $\ell_{\bar{m}}$ on Eq. (2.37),

[3] Alternatively, we can see this from a heuristic argument by noting that the crossover scale is the scale at which the causal cone has a constant width for further coarse-grainings, *i.e.*, $(\ell_{\bar{m}}+4(k-1))/k \approx \ell_{\bar{m}}$. Therefore, $\ell_{\bar{m}} \lesssim 4 \leq 4(k-1)$.

we arrive at an upper bound on $S_{\text{MERA}}(\ell_0; B)$ for a k-to-one MERA,

$$S_{\text{MERA}}(\ell_0; B) \leq 4(k-1)(1+\log_k \ell_0)\ln\chi. \tag{2.39}$$

When ℓ_0 is parametrically large, we neglect the $O(1)$ contribution to the bound on $S_{\text{MERA}}(\ell_0; B)$, which yields Eq. (2.13).

2.B BTZ Black Holes and Thermal States in AdS/MERA

Thus far, we have found constraints on the structure of a MERA that can describe CFT states dual to the AdS_3 vacuum. One might ask whether these results extend to other constructions that exist in three-dimensional gravity. Although pure gravity in AdS_3 has no local or propagating degrees of freedom, there exist interesting non-perturbative objects, namely, BTZ black holes [68]. In this appendix, we extend our constraints on boundary entanglement entropy to these objects.

The non-rotating, uncharged BTZ black hole solution is given in Schwarzschild coordinates by

$$\mathrm{d}s^2 = -\frac{(r^2-r_+^2)}{L^2}\mathrm{d}t^2 + \frac{L^2}{(r^2-r_+^2)}\mathrm{d}r^2 + r^2\mathrm{d}\phi^2, \tag{2.40}$$

with a horizon at $r = r_+$. Noting that Euclidean time is compactified by identifying $\tau \sim \tau + 2\pi L^2/r_+$, the horizon temperature of the black hole is given by $T = r_+/2\pi L^2$. Additionally, the Bekenstein–Hawking entropy of the black hole is

$$S_{\text{BH}} = \frac{\text{Area}}{4G} = \frac{\pi r_+}{2G}. \tag{2.41}$$

Let us now consider applying a MERA with rescaling factor k and bond dimension χ to a CFT at a finite temperature, where instead of minimizing the energy of the boundary state, one minimizes the free energy. In the CFT, turning on a temperature introduces a scale, going as the inverse temperature, which screens long-range correlations. Thus, the state will have classical correlations in addition to entanglement and the effect of a finite temperature on the entanglement entropy is the appearance of an extensive contribution. As one runs the MERA and coarse-grains, the thermal correlations that cannot be removed become more relevant. The MERA, which is unable to remove the extensive contribution, truncates at a level with multiple sites. The schematic entanglement renormalization process is illustrated in Fig. 2.9. The state at the top level effectively factorizes, where each factor appears maximally mixed [37, 57]. A tractable realization of this

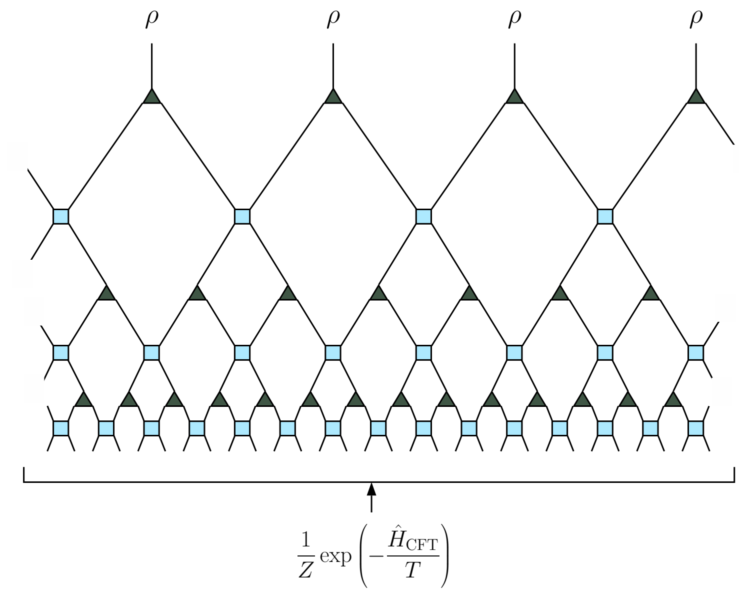

Figure 2.9: The MERA, when applied to a thermal CFT state $Z^{-1}\exp(-\hat{H}_{\mathrm{CFT}}/T)$, where $Z = \mathrm{tr}(\exp(-\hat{H}_{\mathrm{CFT}}/T))$, truncates after a finite number of layers. The boundary state at the top of the truncated MERA effectively factorizes into a product of maximally mixed states $\rho = I/\chi$.

tensor network structure recently appeared in Ref. [73], which found a MERA representation of a thermal state.

Keeping in mind that the holographic dual of a finite-temperature state in the CFT is a black hole in AdS, where the temperature of the CFT corresponds to the Hawking temperature of the black hole, we note that the truncated MERA is suggestive of a black hole horizon [37]. If the MERA is to be interpreted as a discretization of the geometry, then the geometry has ended at some scale. Also, as we approach the horizon, the amount of Hawking radiation that we see increases and the temperature measured by an observer at the horizon diverges. The density matrix of some system in the infinite-temperature limit is given by the product of a maximally mixed state at each site, just like the state at the top of the MERA. It is important to note that, as was pointed out in Ref. [73], in order to reproduce the correct thermal spectrum of eigenvalues, a small amount of entanglement must be present between the sites at the horizon. If the bond dimension were taken to be infinite, then the sites at the horizon truly would factorize. But for a finite bond dimension, one should really think of the horizon as a high-temperature state, with sites effectively factorized.

For small regions on the boundary, the length of the subtending bulk geodesic is subextensive and so the Ryu–Takayanagi formula maintains that the boundary region's entanglement entropy is subextensive as well. However, if we consider a large enough region on the boundary, the geodesic will begin to probe the horizon of the black hole. The geodesic will run along the black hole horizon and pick up an extensive contribution to the entropy. We consider a boundary theory living on a lattice consisting of n_{b} sites, with total system coordinate length $x_{\mathrm{sys}} = n_{\mathrm{b}}a$. In the limit as r approaches the boundary in the metric (2.40), we see that $Tx_{\mathrm{sys}} = r_+/L$, as was pointed out in Refs. [23, 64]. We further note that this implies that the system coordinate size is of order AdS radius, $x_{\mathrm{sys}} = 2\pi L$.

Let us now view the MERA of Fig. 2.9 as a discretization of a BTZ spacetime and repeat the analysis of Sec. 2.3. In this discretization, the layers of the MERA lie along circles of fixed radius r in the coordinates of Eq. (2.40). Again, we ask what proper length L_1 separates sites in any given layer of the MERA.

First, note that a path at fixed r_0 that subtends an angle ϕ_0 has proper length $r_0\phi_0$. At the boundary of the MERA, we consider a region defined by $0 \leq \phi \leq \phi_0 = 2\pi x_0/x_{\mathrm{sys}}$, where x_0 is the coordinate length of the interval, consisting of ℓ_0 lattice sites. The boundary of the MERA is at a fixed radius $r = r_{\mathrm{b}}$. Naturally, the boundary radius r_{b} can be interpreted as a UV cutoff and is related to the lattice spacing a by $r_{\mathrm{b}} = L^2/a$ [23]. By equating the proper distance of the region in the MERA, $\ell_0 L_1$, with that at the boundary of the BTZ spacetime, $r_{\mathrm{b}}\phi_0$, we find the proper length between horizontal bonds to be $L_1 = L$.

With the foresight that the top of the MERA is suggestive of a black hole horizon with proper length $2\pi r_+$, the number of sites at the final layer is therefore $n_{\mathrm{h}} = 2\pi r_+/L$. This further tells us that the MERA truncates after a finite number of layers m, given by

$$m = \log_k \left(\frac{n_{\mathrm{b}}}{n_{\mathrm{h}}}\right) = \log_k \frac{1}{2\pi T a}\,. \tag{2.42}$$

This coincides with the conclusion in Refs. [73, 74] that the MERA representation of a thermal state is obtained after $O(\log_k(1/T))$ iterations of coarse-graining.

Now consider a region B on the boundary consisting of ℓ_0 sites and for which the corresponding geodesic contains a segment running along the BTZ horizon. The subextensive contribution to the entropy in the MERA is exactly as before, in which we pick up at most $\ln \chi$ from each bond we cut with the causal cone of the region B. Furthermore, we will now pick up an extensive contribution from the horizon, where the number of horizon sites within the causal cone is ℓ_{h} and each such site in the product state on the horizon contributes maximally to the entropy by an amount

$\ln \chi$. Combining the contributions, we find

$$S_{\text{MERA}}(B) = 4\eta_B f_B(k) \log_k \left(\frac{\ell_0}{\ell_\text{h}}\right) \ln \chi + \ell_\text{h} \ln \chi\,. \tag{2.43}$$

Recall that the entanglement entropy of a single interval B of coordinate length x_0 in a CFT at finite temperature [63] is given, up to a non-universal constant, by

$$S_{\text{CFT}}(B) = \frac{c}{3} \ln \left(\frac{1}{\pi a T} \sinh \pi x_0 T\right)\,, \tag{2.44}$$

where x_0 is much smaller than the total system size x_{sys}. The standard field-theoretic derivation of the above entropy is done by computing the Euclidean path integral on an n-sheeted Riemann surface and analytically continuing to find the von Neumann entropy. The same result can be derived by computing geodesic lengths on spatial slices of BTZ spacetimes and making use of the Ryu–Takayanagi formula.

When $T \to 0$ in Eq. (2.44), we recover the usual result (2.9). In the $T \to \infty$ limit, the von Neumann entropy gives the usual thermal entropy as entanglement vanishes. Taking $Tx_0 \gg 1$, the leading and subleading contributions to the entanglement entropy are

$$S_{\text{CFT}} = \frac{c}{3}\pi x_0 T + \frac{c}{3} \ln \frac{1}{2\pi a T}\,, \tag{2.45}$$

where the first term is the thermal entropy for the region B.

Now let us consider a finite-temperature CFT that is dual to a BTZ black hole with horizon temperature $T = r_+/2\pi L^2$. In terms of geometric MERA parameters, we find that Eq. (2.45) becomes

$$S_{\text{CFT}} = \frac{c}{6}\,\ell_\text{h} + \frac{c}{3} m \ln k\,. \tag{2.46}$$

Here we used the fact that $\ell_\text{h} = x_0 r_+/L^2$ as well as Eq. (2.42), where we note that m can also be written as $\log_k(\ell_\text{b}/\ell_\text{h})$. The result (2.46) coincides precisely with the extensive and subextensive contributions calculated using the MERA in Eq. (2.43) provided that $c/\ln \chi \sim \mathcal{O}(1)$. Therefore, we find that the truncated MERA correctly captures the entanglement structure of thermal CFT states and their dual BTZ spacetimes. These conclusions are in agreement with those in Refs. [31, 74].

As a check of the claim that c and $\ln \chi$ should be of the same order, we can compare the horizon entropy given by the contribution from the sites at the final layer with the Bekenstein–Hawking entropy (2.41) of a BTZ black hole. There are n_h sites comprising the horizon, each with Hilbert space dimension χ. The system is in the infinite-temperature limit — and hence described by a maximally mixed density matrix, with entropy contribution $\ln \chi$ from each site — so

$$S_{\text{horizon}} = n_{\text{h}} \ln \chi \,. \tag{2.47}$$

Making use of the Brown–Henneaux relation and requiring that the entropy (2.47) coincide with the Beckenstein-Hawking entropy, we again find that $c/\ln \chi \sim O(1)$. More specifically, taking the counting to be precise, we find that

$$c/\ln \chi = 6\,, \tag{2.48}$$

which is qualitatively in agreement with the previous conclusion (2.20) that the Hilbert space dimension must be exponentially large in c.

With this relation, the extensive terms in Eqs. (2.43) and (2.46) agree precisely. Further identifying the subextensive terms, we find $\eta_B f_B(k) = (\ln k)/2$. If we then impose the constraint (2.18), we find that

$$\frac{k \ln k}{2(k-1)} \leq 1\,. \tag{2.49}$$

This last inequality exactly reproduces Eq. (2.35) and thus constrains k to be 2, 3, or 4. Interestingly, we have found the weaker of the two bounds derived in Sec. 2.5, without needing to consider the Bousso bound.

As desired, the truncated MERA computation of entanglement entropy agrees with the expected entanglement entropy given by the application of the Ryu–Takayanagi formula to the length of the minimal surface in a BTZ spacetime. The fact that the results of matching boundary entanglement entropy given in Sec. 2.4 further hold in BTZ spacetimes might not be too surprising given that such spacetimes are quotients of pure AdS_3.

Chapter 3

DS-MERA CORRESPONDENCE

We investigate the proposed connection between de Sitter spacetime and the MERA (Multiscale Entanglement Renormalization Ansatz) tensor network, and ask what can be learned via such a construction. We show that the quantum state obeys a cosmic no-hair theorem: the reduced density operator describing a causal patch of the MERA asymptotes to a fixed point of a quantum channel, just as spacetimes with a positive cosmological constant asymptote to de Sitter. The MERA is potentially compatible with a weak form of complementarity (local physics only describes single patches at a time, but the overall Hilbert space is infinite-dimensional) or, with certain specific modifications to the tensor structure, a strong form (the entire theory describes only a single patch plus its horizon, in a finite-dimensional Hilbert space). We also suggest that de Sitter evolution has an interpretation in terms of circuit complexity, as has been conjectured for anti-de Sitter space.

This chapter is based on the Ref:
Ning Bao, ChunJun Cao, Sean M. Carroll, and Aidan Chatwin-Davies. "De Sitter Space as a Tensor Network: Cosmic No-Hair, Complementarity, and Complexity". In: Phys. Rev. *D96.12 (2017), p. 123536. DOI:* `10.1103/PhysRevD.96.123536`*. arXiv:* `1709.03513 [hep-th]`*.*

3.1 Introduction

Even in the absence of a completely-formulated theory of quantum gravity, a great deal can be learned by combining insights from classical gravity, semiclassical entropy bounds, the principles of holography and complementarity, and the general structure of quantum mechanics. A natural testing ground for such ideas is de Sitter space, a maximally symmetric spacetime featuring static causal patches with a finite entropy. De Sitter is also of obvious phenomenological relevance, given the positive value of the cosmological constant in the real world. In this paper we apply ideas from quantum circuits and tensor networks to investigate quantum properties of de Sitter on super-horizon scales.

The Multiscale Entanglement Renormalization Ansatz (MERA) is a well-studied tensor network that was originally developed to find ground states of 1+1 dimensional condensed matter theories [39]. In recent years, an interesting connection has been drawn between the MERA and AdS_3/CFT_2, by way of using the MERA to discretize the AdS space [37, 57]. The argument was made that this could be seen as a way of emerging AdS space from the boundary CFT, thus establishing AdS/CFT as a theory in which bulk spacetime emerges from entanglement properties on the boundary. Further work exploring this direction and generalizing it to other types of tensor networks has been done by [48, 49, 76], and a p-adic approach to AdS/CFT using trees is explored by [77, 78]. However, the AdS/MERA correspondence seems to have tensions with other known results in holography. For example, it is puzzling that AdS/MERA appears to suggest a "bulk geometry" in the form of a tensor network even for a CFT with a small central charge. Additionally, it needs to satisfy a set of stringent constraints, brought on by the fact that it is supposed to duplicate the established results of AdS/CFT [21, 23]. It appears that AdS/MERA in its simplest form is not able to satisfy all of the constraints imposed by holography with AdS geometry [41, 79, 80], although extensions may be able circumvent this difficulty [81].

There is also considerable interest in studying a more general notion of geometry from entanglement beyond the context of AdS/CFT [82], where geometries are related to our physical universe [83, 84]. A connection between the MERA and de Sitter spacetime has been suggested, where we think of the tensors as describing time evolution, rather than as relating different spatial regions [51, 79, 85]. In the case of 1+1 dimensions, it is also claimed [79] that the MERA can be thought of as a discretization of a slice in the "kinematic space" [50, 26], which corresponds to the space of geodesics in the hyperbolic plane in the particular case of AdS_3/CFT_2. This beautifully illustrates a correspondence between regions in the dual kinematic space, which take on information-theoretic interpretations, and the individual tensors localized in the MERA. More tentatively, quantum circuits have been proposed as a way of studying realistic cosmological evolution from inflation to the present epoch and beyond [86].

In this paper we investigate this proposed connection between the MERA and de Sitter, under the assumption that a MERA-like circuit is able to simulate effective quantum gravitational dynamics on super-Hubble scales for some subset of quantum states in a theory of quantum gravity. We show that the structure of the MERA is able to reproduce some desirable features of evolution in a de Sitter background. In particular, we identify a scale invariant past causal cone as the static patch where an analogous light-like surface functions as the cosmic horizon. Then we show that a version of the cosmic no-hair theorem can be derived from the fixed point of the quantum channel, whereby any state will asymptote to the channel fixed point at future infinity. We next examine the issue of horizon complementarity in the MERA context, and argue that the global and local descriptions of de Sitter [87, 88] can be equivalent up to a unitary change of basis. We observe similarities between a strong version of local de Sitter and the implementation of a quantum error correcting code. Lastly, we derive a bound on the quantum complexity of the MERA circuit, and show that the complexity scales in a manner that is consistent with the "complexity equals action" conjecture [32].

3.2 The MERA and the de Sitter causal patch

In Fig. 3.1 we illustrate the MERA tensor network. In its original conception as an ansatz for constructing ground states of 1-d spin systems, one starts with a simple quantum state at the top of the diagram, and propagates it downward through a series of gates to a final state at the bottom. Each line represents a factor of Hilbert space, which might be quite high-dimensional. Moving downward is the "fine-graining" direction, and upward is "coarse-graining." The square gates are "disentanglers" (although they create entanglement as we flow downward), which take two factors in and output another two factors. The triangular gates are "isometries," which can be thought of as taking in a single factor and outputting two factors; alternatively, we can imagine inputting two factors, one of which is a fixed state $|0\rangle$, and outputting another two, so that the total dimensionality entering and exiting each tensor is equal. We will adopt the latter perspective in this paper. It is often convenient to consider generalizations where $k > 2$ factors enter and exit each tensor.

In the AdS/MERA correspondence, tensors are taken to represent factors of Hilbert space, and the two-dimensional geometry of the graph is mapped to the hyperbolic plane. Here, where we are interested in studying a dS/MERA correspondence, flow through the circuit represents evolution through time. Note that, while it is common in general relativity to draw spacetime diagrams with the future at the top, the convention in quantum circuits for MERA is to start with one or more "top tensors" and evolve downward. Here we will stick to the conventions of the respective communities; time flows downward in MERA circuit diagrams, and upward in spacetime diagrams.[1]

[1]We will occasionally draw circuit diagrams in which time flows from left to right, just to keep things lively.

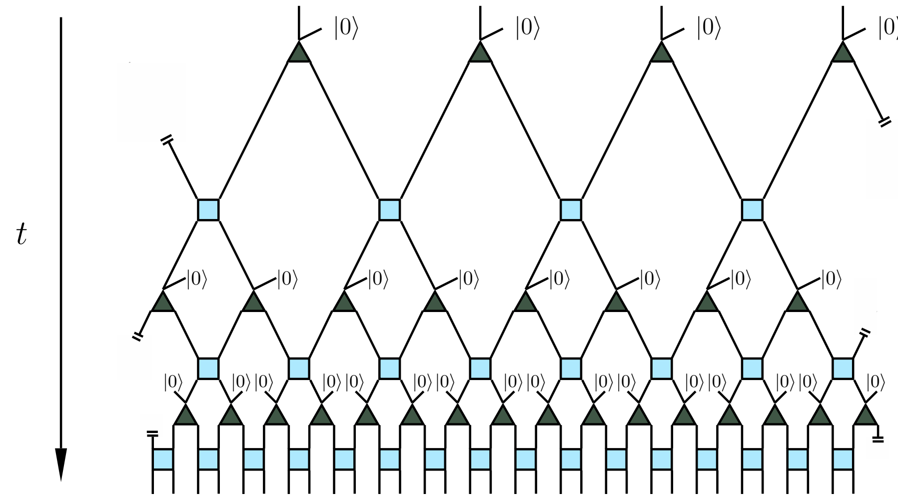

Figure 3.1: A periodic binary MERA. The green triangles denote the isometries and the blue squares denote the disentanglers. The kets labeled $|0\rangle$ are ancilla states inserted into each isometry. The action of the circuit is to take a state at the top and evolve it downward. In anticipation of the connection to de Sitter, the fine-graining direction is labelled as the direction of increasing t.

In this work, we will mostly be concerned with MERAs that are scale and translationally invariant (the same disentanglers and isometries appear everywhere in the network). We use the term "site" in the MERA to refer to a Hilbert space factor that lives on a leg that exits a disentangler (or equivalently, that enters an isometry). When the MERA is used as a variational ansatz for a physical system like a spin chain, the collection of sites at any given layer corresponds to the state of the physical lattice at that renormalization scale. For more extensive reviews of tensor networks and the MERA see [52, 71, 41].

Viewed as a circuit in which the fine-graining direction corresponds to the future or past direction (away from the de Sitter throat), the MERA reproduces the causal structure of de Sitter spacetime [51, 79, 85]. Recently, as a part of their studies of kinematic space, Czech *et al.* further pointed out that there is a natural way of associating the MERA with half of the 1+1-dimensional de Sitter manifold [79]. Here we briefly explain how this works.

Let $\mathcal{M}$ be 1+1-dimensional de Sitter spacetime with the usual global coordinatization:

$$ds^2 = \ell_{\text{dS}}^2(-dt^2 + \cosh^2 t \, d\theta^2). \tag{3.1}$$

The timelike coordinate t takes all real values, and θ is an angular coordinate that is 2π-periodic. In these coordinates, $\mathcal{M}$ looks like a hyperboloid whose constant-t

sections are circles that attain a minimum radius at $t = 0$ and that grow in either direction away from $t = 0$. The proper radius at $t = 0$ is equal to ℓ_{dS}, which is called the de Sitter radius. A convenient coordinate transformation is to set $\cosh t = \sec \alpha$, under which the metric becomes conformally flat:

$$ds^2 = \frac{\ell_{\mathrm{dS}}^2}{\cos^2 \alpha} \left(-d\alpha^2 + d\theta^2\right) . \tag{3.2}$$

Because of this, the full de Sitter manifold is often represented by a rectangle in the θ-α plane with $-\pi/2 < \alpha < \pi/2$ and $0 < \theta < 2\pi$, as in the Penrose diagram of de Sitter, Fig. 3.2.

Consider now the top half of the de Sitter manifold with $t \geq 0$ (or $0 \leq \alpha < \pi/2$). Starting at $t_0 \equiv 0$, the length of the constant-t_n slice doubles at every subsequent time $t_n = \operatorname{arccosh} 2^n$ with $n = 1, 2, \ldots$ This suggests identifying the top of a translationally invariant binary MERA with the $t_0 = 0$ slice, and subsequent layers of the MERA with the subsequent t_n slices, so that the MERA describes the top half of the de Sitter hyperboloid. This identification is illustrated in Fig. 3.3, in which the sites of the n^{th} layer of the MERA have been chosen to lie at the angles

$$\theta_j^{(n)} = \frac{\pi}{2^{n+1}} \left(j + \frac{1}{2}\right) \qquad j = 0, \ \ldots, 2^{n+2} - 1 . \tag{3.3}$$

The fact that the top of the MERA was chosen to have four sites was no coincidence. With this choice, the *future domain of dependence* of any two adjacent sites at the top of the MERA precisely coincides with (the top half of) a single static patch of de Sitter. Or, to use terminology that is more familiar in the MERA literature, each

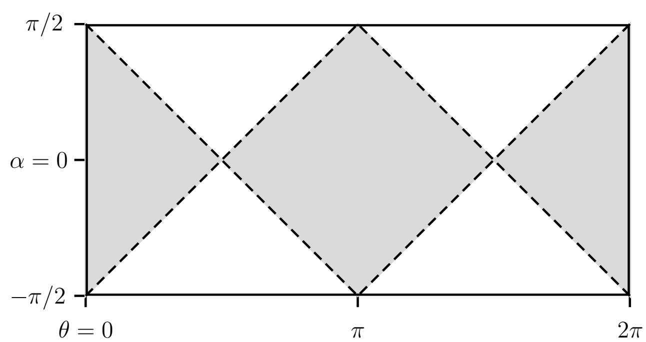

Figure 3.2: The Penrose diagram of global (1+1)-dimensional de Sitter spacetime. As this is a spacetime diagram, time now runs from bottom to top. The boundaries of two complete disjoint causal patches, one centered at $\theta = 0$ and the other centered at $\theta = \pi$, are drawn with a dashed line, and the interiors of the patches are shaded. Light rays travel along 45° lines in this diagram.

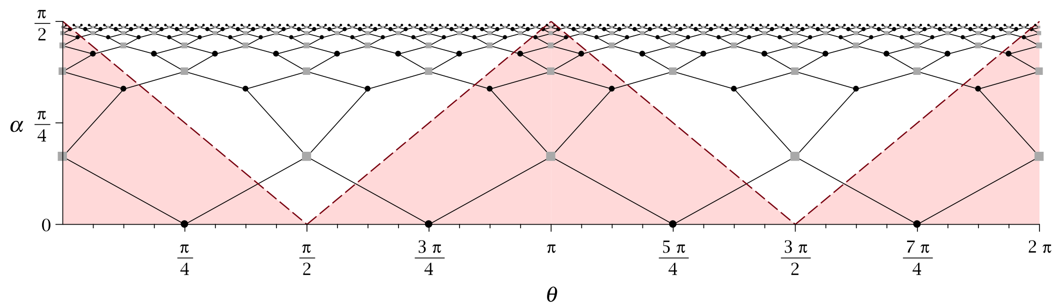

Figure 3.3: A geometric de Sitter-MERA correspondence, mapping the MERA circuit to the top half of the de Sitter geometry. Note that the fine-graining direction of the MERA in this diagram points upward to match the future direction in the Penrose diagram. The domain of dependence of any pair of adjacent sites in the initial layer of the MERA is entirely contained within a single static patch in de Sitter. Two of the four possible static patch interiors are shaded in red. (The other two static patches are centered at $\theta = \pi/2$ and $\theta = 3\pi/2$.)

static patch of de Sitter that is centered at $\theta = 0$, $\pi/2$, π, or $3\pi/2$ coincides with a causal cone [58] in the MERA such that every layer of the causal cone contains precisely two sites of the MERA (i.e., the causal cone is stationary).

Let us elaborate a bit on the terminology above. First, recall how a domain of dependence is defined on a smooth manifold:

Definition 3.2.1. *Let $S \subset \mathcal{M}$ be a subset of a smooth Lorentzian manifold $\mathcal{M}$. The future (resp. past) domain of dependence of S is the set of all points $p \in \mathcal{M}$ such that every past (resp. future) inextensible causal curve through p intersects S.*

This suggests the following analogous definition for a domain of dependence in a MERA:

Definition 3.2.2. *Let S be a collection of sites in a MERA. The future (resp. past) domain of dependence of S is the set of all MERA sites p such that starting at p and moving only in the past, or coarse-graining direction (resp future, or fine-graining direction), one inevitably arrives at a site in S.*

In de Sitter space, the proper radius of the cosmological horizon is constant. Given an inextendible timelike geodesic, a static patch is defined as the set of all points connected to that geodesic by both past- and future-oriented causal curves, and its size is given by the horizon radius. In particular, in 1+1 dimensions the horizon radius is $\pi\ell_{\text{dS}}/2$. Within a constant-t slice, a horizon volume is an interval of proper length $\pi\ell_{\text{dS}}$, and static patches are diamonds in the Penrose diagram (cf. Fig. 3.2).

In line with [79], we here adopt a correspondence between the MERA and half of the full 1+1-dimensional de Sitter manifold in which stationary causal cones in the MERA are in correspondence with static patches of de Sitter. In the spirit of tensor-network/spacetime correspondences, one should think of the MERA and the state that it describes as some state of quantum gravity describing quantum fields evolving in a semiclassical de Sitter background. In other words, despite lacking an explicit theory of quantum gravity, we suggest that some aspects of the effective dynamics for a quantum gravity state that describes classical de Sitter spacetime can be described and organized at a fundamental level by a suitably-chosen MERA.

In this picture, each site of the MERA carries a Hilbert space $\mathcal{H}_*$, and the Hilbert space that corresponds to a given horizon volume, call it $\mathcal{H}_{\text{static}}$, is the tensor product of the Hilbert spaces of the sites that lie within the horizon. We do not count the Hilbert spaces that correspond to unentangled ancillae as part of the static patch Hilbert space, since we only attach a spacetime interpretation to entangled degrees of freedom in the MERA proper. To be consistent with the Gibbons-Hawking entropy of de Sitter spacetime [89], it should be that $\ln \dim \mathcal{H}_{\text{static}} \sim S_{\text{dS}}$, where S_{dS} is the de Sitter entropy. Hence, for our Universe, where $S_{\text{dS}} \sim 10^{122}$, the corresponding bond dimension (*i.e.*, the dimensionality of $\mathcal{H}_*$) is of order $\dim \mathcal{H}_* \sim \exp(10^{122})$ per site.

This is a very coarse-grained description of de Sitter spacetime. For a binary MERA, there are only two sites per horizon volume, and layers of the MERA within a static patch are separated by cosmological timescales. Furthermore, a binary MERA only accommodates 4 distinct static patches (Fig. 3.2). We imagine, however, that it should be possible to refine this horizon-scale description via, *e.g.*, local gadget expansions, in which the large Hilbert space $\mathcal{H}_*$ could be factorized according to sub-horizon locality. This perhaps can be achieved by some version of cMERA [59, 60, 90].

One might wonder whether it is possible to pack more MERA sites into a single slice of the static patch by starting with more sites at the top of the MERA, or by considering a MERA with a larger branching factor. The number of sites at the top of the MERA is fixed by the number of sites per layer in the stationary causal cone, however. If the stationary causal cone has m sites per layer, then the $t = 0$ slice contains $2m$ sites. The reason is simply because the $t = 0$ slice of de Sitter

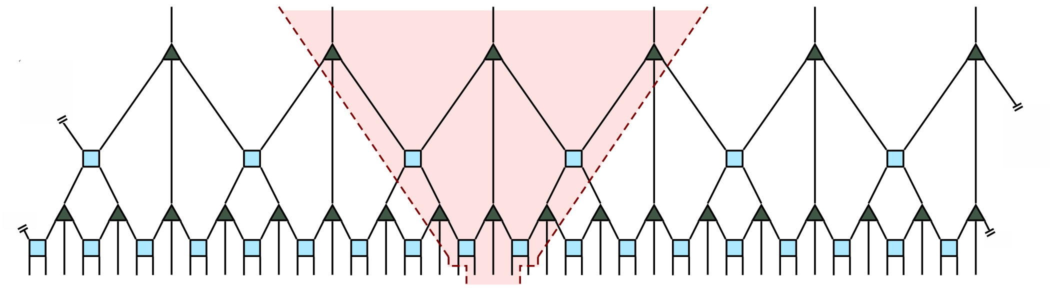

Figure 3.4: A ternary MERA. Ancillae are suppressed in this diagram. A stationary causal cone with three sites per layer is indicated by the shaded region.

contains exactly two disjoint horizon volumes. The quantity m in turn is fixed by the branching factor and the structure of the MERA. For a binary MERA, a stationary causal cone always has $m = 2$ sites per layer. A ternary MERA has $m = 3$ sites per layer in a stationary causal cone (Fig. 3.4). However, in general for a k-nary MERA, in which the number of sites increases k-fold in each layer of the MERA, there can only ever be $m = 2$ or 3 sites per layer in a stationary causal cone. Further details of stationary causal cones and a proof of this last fact are given in App. 3.A.

Unfortunately, the global de Sitter-MERA correspondence as formulated on a (hyper)cubic lattice does not easily generalize to higher dimensions due to discretization artifacts. The possibility of a de Sitter-MERA correspondence in higher dimensions is discussed in App. 3.B.

3.3 Cosmic No-Hair as a channel property

Via the correspondence described above, each constant-t slice of a de Sitter static patch is assigned a Hilbert space

$$\mathcal{H}_{\text{static}} = \mathcal{H}_* \otimes \mathcal{H}_*, \tag{3.4}$$

where $\mathcal{H}_*$ is the Hilbert space of a single MERA site. If we restrict our attention to a single static patch, then the MERA also defines a superoperator, $\mathcal{E}$, which maps a state in $\mathcal{H}_{\text{static}}$ forward by one Hubble time to a state on the next slice. With the disentanglers and isometries held fixed and uniform across the MERA, the action of $\mathcal{E}$ may be written explicitly as

$$\mathcal{E}(\rho) = U_{BC}\ \mathrm{Tr}_{AD}\left[V_{AB} \otimes V_{CD}(|0\rangle\langle 0|_A \otimes \rho_{BC} \otimes |0\rangle\langle 0|_D)V_{AB}^\dagger \otimes V_{CD}^\dagger\right] U_{BC}^\dagger. \tag{3.5}$$

The labels A, B, C, and D indicate on which Hilbert space factors operators act, but we may subsequently omit them when it does not cause confusion. The ancillae are labelled by A and D, and $\mathcal{H}_{\text{static}}$ is labelled by B and C, cf. Fig. 3.5.

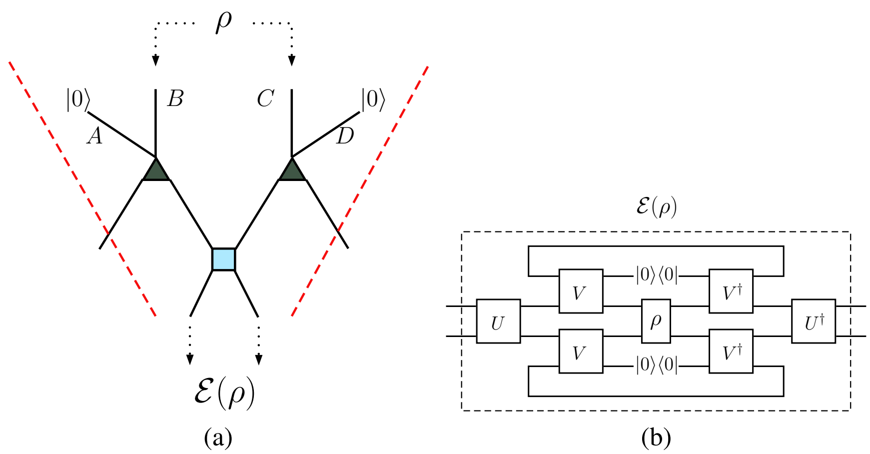

Figure 3.5: (a) A single step of the MERA within the causal patch, viewed as a channel $\mathcal{E}$, and (b) the equivalent circuit diagram. Time runs in the downward direction in (a).

In the MERA literature, $\mathcal{E}$ is known as the *descending superoperator* [52, 53]. It is a quantum channel by construction, i.e., it is completely positive and trace-preserving on the set of states (density operators), which for future reference we will denote by $\mathcal{S}(\mathcal{H}_{\text{static}})$. In precise language, given a Hilbert space $\mathcal{H}$, if $\mathscr{H}(\mathcal{H})$ denotes the space of Hermitian operators on $\mathcal{H}$, then the set of states is

$$\mathcal{S}(\mathcal{H}) \equiv \{\rho \in \mathscr{H}(\mathcal{H}) \mid \operatorname{Tr} \rho = 1,\ \langle\psi|\rho|\psi\rangle \geq 0 \ \ \forall\, |\psi\rangle \in \mathcal{H}\}\,. \tag{3.6}$$

Consider now starting at some given layer with a state $\rho_0 \in \mathcal{S}(\mathcal{H}_{\text{static}})$ and repeatedly applying the map $\mathcal{E}$. Intuitively, every application of $\mathcal{E}$ dilutes the original state ρ_0 by entangling it with the same ancillary state $|00\rangle\langle 00|_{AD}$ before taking a partial trace, at which point information about ρ_0 flows out of the static patch. It is therefore natural (and correct) to expect that the state on the static patch should settle down to a future asymptotic steady state, regardless of the initial state ρ_0.

We will make this expectation rigorous below, but first we note that this observation suggests a sort of *cosmic no-hair theorem* for the de Sitter-MERA correspondence. In classical general relativity, a cosmic no-hair theorem is roughly the statement that a positive cosmological constant causes a spacetime to asymptotically tend to a de Sitter state in the future. The following theorem of Wald pertaining to Bianchi spacetimes, which are homogeneous but anisotropic cosmological models, is perhaps the most precise statement of a cosmic no-hair theorem [91]:

Theorem 3.3.1 (Wald)**.** *All Bianchi spacetimes (with the exception of certain strongly-curved Bianchi IX spacetimes) that are initially expanding, that have a* *positive cosmological constant, and whose matter content obeys the strong and dominant energy conditions asymptote to de Sitter in the future.*

Various generalizations and variations of this theorem exist in the literature [92, 93, 94, 95, 96, 97, 98, 99, 100, 101]. In particular, quantum cosmic no-hair theorems show that the quantum states of fields tend to their respective vacuum states on an asymptotically de Sitter background [102, 103, 104]. The MERA results here are reminiscent of these quantum cosmic no-hair theorems.

Let us now add some rigor to the above observations. When $\mathcal{H}$ is finite-dimensional, quantum channels are necessarily contractions on $\mathcal{S}(\mathcal{H})$ [105]. Recall that a linear map $T : X \to X$ on a Banach space X is a *contraction* if there exists $0 < \kappa \leq 1$ such that $d(T(x_1), T(x_2)) \leq \kappa\, d(x_1, x_2)$ for all $x_1, x_2 \in X$, where d is the metric on X. For $\mathcal{S}(\mathcal{H})$, the metric is most commonly defined using the 1-norm,

$$d(\rho, \sigma) \equiv ||\rho - \sigma||_1, \tag{3.7}$$

where $||A||_1 = \mathrm{Tr}\sqrt{A^\dagger A}$ for any linear operator A.[2] A contraction is *strict* when $0 < \kappa < 1$, in which case the contraction mapping principle guarantees that there is a unique fixed point $x_\star \in X$ such that $T(x_\star) = x_\star$. Furthermore, the sequence $\{T^n(x_0)\}_{n=1}^{\infty}$ converges to the fixed point $x_\star$ for any choice of the starting point x_0.

Quantum channels need not be strict contractions in general; however, it is certainly easy to write down channels that are strict contractions [105]. Returning to the de Sitter-MERA correspondence, we may simply suppose that the disentanglers U and isometries V are chosen such that the superoperator $\mathcal{E}$ is a strict contraction. Moreover, numerical assays seem to indicate that this is generally the case for random U and V [53, 52]. Our intuition that the state in a causal patch should tend to some asymptotic fixed state in the future is therefore warranted.

Regardless of the channel's contractive properties, it is easy to see that $\mathcal{E}$ has at least one fixed point by examining its adjoint. To define the adjoint, take the domain of $\mathcal{E}$ to be the space of Hermitian operators, $\mathscr{H}(\mathcal{H})$, which is closed under addition and multiplication by real numbers. The space $\mathscr{H}(\mathcal{H})$ with the Frobenius inner product

$$\langle T, S \rangle \equiv \mathrm{Tr}\left(S^\dagger T\right) \tag{3.8}$$

is then a Hilbert space over the real numbers. As usual, the adjoint operator is defined by the relation $\langle \mathcal{E}(T), S \rangle = \langle T, \mathcal{E}^\dagger(S) \rangle$. Using this definition, it is straightforward to

[2] All norms are equivalent in finite dimensions, i.e., for any two norms $\|\cdot\|_a$ and $\|\cdot\|_b$, there exist constants $m > 0$ and $M > 0$ such that $m\|v\|_a \leq \|v\|_b \leq M\|v\|_a$ for all v in the normed space.

show that the action of $\mathcal{E}^\dagger$ is

$$\mathcal{E}^\dagger(S) = {}_{AD}\langle 00| V^\dagger_{AB} V^\dagger_{CD} \left[I_{AD} \otimes (U^\dagger S U)_{BC} \right] V_{AB} V_{CD} |00\rangle_{AD} \,. \tag{3.9}$$

In the MERA literature, $\mathcal{E}^\dagger$ is known as the *ascending superoperator*. In this form, it is clear that the identity operator is an eigenvector of $\mathcal{E}^\dagger$ with eigenvalue $\lambda = 1$. Therefore, $\bar{\lambda} = \lambda = 1$ is also in the spectrum of $\mathcal{E}$, or in other words, $\mathcal{E}$ necessarily has a fixed point.

That $\lambda = 1$ is an eigenvalue of $\mathcal{E}$ is well-known [52, 53]; however, we exhibited $\mathcal{E}^\dagger$ because it clearly shows that, in general, $\mathcal{E}$ is not self-adjoint. In particular, this means that the eigenvector of $\mathcal{E}$ to the eigenvalue 1, call it $\rho_\star$, is not trivially the identity operator. An interesting question is how much freedom is possible in choosing $\rho_\star$ by specifying the disentanglers and isometries U and V. Clearly there are families fixed points. For example, if $\rho_\star$ is such that $\mathcal{E}(\rho_\star) = \rho_\star$ for a given choice of U and V, then $\tilde{\rho}_\star \equiv (W^\dagger \otimes W^\dagger)\rho_\star(W \otimes W)$ is the fixed point of the channel $\tilde{\mathcal{E}}$ with $\tilde{U} = W^\dagger U$ and $\tilde{V} = (I \otimes W)V$ for any unitary operator W on $\mathcal{H}_*$. From exactly what subset of $\mathcal{S}(\mathcal{H})$ the fixed point $\rho_\star$ may be chosen is an open problem.

3.4 Global de Sitter and Complementarity

In classical general relativity, there are no barriers to describing de Sitter spacetime in a global way. However, in light of complementarity [106], an interesting question is whether quantum gravity also accommodates a global description of de Sitter, or whether a fully quantum theory only exists on a single causal patch. We will suggest that a local picture (describing only a single patch) is possible via the MERA if the Hamiltonian is essentially time-dependent; as a result, this perspective also avoids Poincaré recurrences.

Complementarity, as it was originally envisioned for black holes, asserts that the ability of an observer to describe the region around them in terms of local quantum field theory on a smooth spacetime background does not extend into the unobservable region behind a horizon. For example, when describing physics outside of the black hole in a black hole spacetime, one should think of all of the black hole's degrees of freedom as residing just above its apparent horizon on a stretched horizon [107]. Nevertheless (and neglecting possible issues regarding firewalls [108]), there should also exist a complementary description of the black hole that is appropriate to, e.g., an observer who crosses the horizon, where the black hole interior is very much a real place. Any possible discrepancies in these two descriptions are then purportedly resolved by the fact that an observer who crosses the horizon becomes causally disconnected from the black hole exterior, and so information about these discrepancies cannot be communicated to the exterior. Applied to de Sitter cosmology, horizon complementarity suggests that a single observer can only describe physics using local quantum field theory in a region that stretches out to the horizon, but no farther. To this observer, the only sign of the rest of the universe is encoded on a stretched horizon. If one considers two observers that have overlapping horizon volumes, then there is presumably some partial mapping between their respective local descriptions of physics.

The question then arises as to whether an infinitely big spacetime outside the de Sitter horizon actually exists in this picture. A weak version of complementarity might posit that it does, but that its existence cannot be described by any one observer; the underlying quantum theory would nevertheless still describe states in an infinite-dimensional Hilbert space. A stronger version would postulate that the entire quantum theory has a finite-dimensional Hilbert space (with dimension of order $e^{S_{\rm dS}}$), and all that exists can be described by a single Hubble patch and its horizon [109, 110, 111, 112, 113, 114, 115, 87, 88]. The descriptions of physics in different horizon volumes contained in different causal patches are then related by a global unitary transformation. The distinction might seem academic, but is actually crucial: unitary evolution with a time-independent Hamiltonian in a finite-dimensional Hilbert space leads to Poincaré recurrences and Boltzmann brains [114, 116, 117], which can be avoided if Hilbert space is infinite-dimensional [118].

Let us refer to the weak complementarity perspective as the "global" view (different regions of the classical de Sitter spacetime have an independent existence, and Hilbert space is infinite-dimensional), and the strong complementarity perspective as the "local" view (there is only one patch worth of information, and Hilbert space is finite-dimensional). The MERA tensor network, we will argue, can accommodate the local description, and with a bit of modification, the global description as well. We find that there is a natural sense in which the information associated with any single static patch can be localized on the static patch and its horizon. We then propose a modified network that we call SCMERA ("Strong Complementarity MERA") that could, in principle, capture the local strong complementarity view. In order to have consistent time-evolution in the SCMERA, we will see that it is effectively generated by a time-dependent Hamiltonian, i.e., the unitary operator that maps a layer in the SCMERA to the next layer changes as a function of depth in the network. While such evolution is in tension with our expectations in cosmology, where the Hamiltonian evolution should be time-independent, it does avoid certain undesirable phenomena like Poincaré recurrences. Given how little we know about quantum cosmology, it seems worth keeping different perspectives in mind.

3.4.1 Slicing, weak complementarity, and pseudo-holography

A notable feature of the MERA is that it naturally provides a way to both define different Cauchy slices and relate the states defined on them. Up until now, we have thought of states in global de Sitter as being defined on constant time slices, or in other words, on a single layer at constant depth in the MERA. However, given such a state that we label by $|\Psi\rangle_{\mathrm{dS}}$, by picking some collection of sites on which it is defined, one can define a new state $|\tilde{\Psi}\rangle_{\mathrm{dS}}$ (which is in a tensor product with some collection of n ancillae) and a new Cauchy slice by pushing the state on the chosen sites back up (i.e., backwards in time) through the MERA. In other words, $|\Psi\rangle_{\mathrm{dS}}$ and $|\tilde{\Psi}\rangle_{\mathrm{dS}} \otimes |0\rangle^{\otimes n}$ are related by partial unitary evolution, and the horizontal cut through the MERA on which $|\tilde{\Psi}\rangle_{\mathrm{dS}} \otimes |0\rangle^{\otimes n}$ is defined constitutes a new Cauchy slice. In particular, given a static patch, the state $|\Psi\rangle_{\mathrm{dS}}$ can be pushed back up through the MERA in this way so that the resulting state is supported entirely on the sites that comprise $\mathcal{H}_{\mathrm{static}}$ and sites that are on the lightlike horizon, as illustrated in Fig. 3.6. Note that this wouldn't be possible for a generic state living on a constant $t = T$ slice in the Hilbert space of the complete theory, but can be done for the specific states that arise via the MERA from the initial state at $t = 0$ (the top tensors).

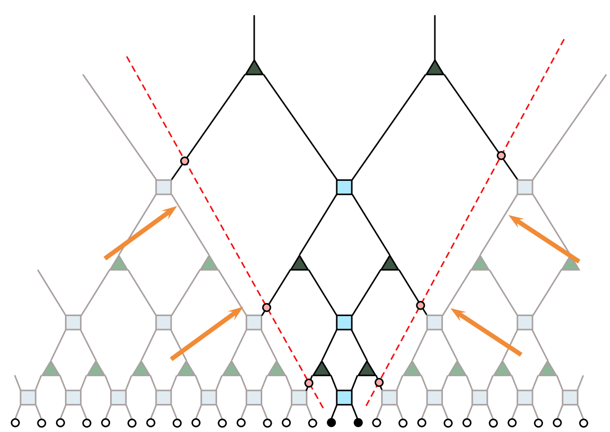

Figure 3.6: Sites outside the horizon at any given layer (indicated by white dots) are unitarily related, via the MERA, to a state on the horizon (indicated by red dots) and a collection of ancillae (not shown), $|\tilde{\Psi}\rangle_{\mathrm{dS}} \otimes |0\rangle^{\otimes n}$. A state $|\Psi\rangle_{\mathrm{dS}}$ corresponding to the de Sitter spatial slice is prepared at the bottom layer. The sites inside the static patch are indicated by the filled black dots.

The observation above suggests a toy model for weak complementarity as well as a sort of "pseudo-holography." The network clearly admits a global de Sitter description on constant time slices, but a more observer-centric view of the local patch consists of the state defined on $\mathcal{H}_{\text{static}}$ and a collection of horizon sites, as discussed above and shown in Figure 3.6. For a stationary observer O_A who travels along a timelike geodesic at the center of the static patch, all information relevant to O_A's local description of physics is given by the degrees of freedom in the static patch interior. The information about the exterior is encoded in the degrees of freedom that reside on the horizon. However, for another observer O_B who travels away from O_A and leaves the patch, their surrounding spacetime geometry and description of the quantum state can be "manufactured" by propagating O_A's horizon degrees of freedom down through the MERA. In this way, the region that is accessible to O_B is realized by decompressing [79] the information that is contained on O_A's horizon. The information that was previously understood to have localized on the horizon for O_A is, up to inclusion of ancillae, unitarily transformed to a state defined on spacetime that is to the exterior of O_A's static patch. This map between the local descriptions of different observers is a realization of weak complementarity, with information about spacetime to the exterior of an observer's cosmic horizon being encoded on the horizon in a way that seems holographic.

This picture of weak complementarity is not really holographic, however, because the number of apparent degrees of freedom associated with the horizon increases toward the future in the MERA, i.e., the number of horizon sites grows with every subsequent layer. In a true holographic model, the size of the boundary Hilbert space should remain constant. We investigate this possibility, or in other words, the possibility of strong complementarity, in the next section.

3.4.2 Strong Complementarity, recoverability, and quantum error correction

In the local, strong complementarity picture, the degrees of freedom represented by the static patch of a single observer, plus those on the corresponding horizon, together describe a closed system constituting the entirety of Hilbert space, which is correspondingly finite-dimensional. Ordinarily, assuming a time-independent Hamiltonian, such a setup would lead to recurrences and Boltzmann brains. What we will find, however, is that it is more natural from the MERA perspective to imagine evolution inside the patch that is equivalent to a time-dependent Hamiltonian. (Cosmological evolution with a time-dependent Hamiltonian also plays a role in Banks and Fischler's approach to holographic spacetime [119, 120, 121].)

A local picture is possible in the MERA because of its particular circuit construction that begins with a finite number of inputs (4 for a binary MERA), where only two non-overlapping static patches at $t = 0$ are present. Consequently, the total number of quantum degrees of freedom for the input is limited to that of two non-overlapping patches and is, of course, finite. Let $\chi_* \equiv \dim \mathcal{H}_*$ denote the dimension of the Hilbert space of a single MERA site (the bond dimension). Then, even though the number of sites in the MERA grows as a function of depth, the global state at any given subsequent layer of the MERA only resides in a subspace of dimension χ_*^4. Because $\dim \mathcal{H}_{\text{static}} = \chi_*^2$ remains the same at every step in the MERA within the static patch, there always exists a purification of the state $\rho_{\text{static}} \in \mathcal{S}(\mathcal{H}_{\text{static}})$ in a Hilbert space with dimension χ_*^2. Therefore, simply by counting Hilbert space dimensions, we could imagine that such a purifying Hilbert space, call it $\mathcal{H}_{\text{horizon}}$, resides on the horizon of the static patch. The horizon state would have to be unitarily related to the global state of the MERA outside the static patch (which is a preferred purification of ρ_{static}).

To turn the network into a description of a single-patch universe, we propose modifying the MERA circuit as follows. First, choose any single static patch in the MERA (cf. Fig. 3.3). At $t = 0$, we identify the degrees of freedom inside a static patch as interior degrees of freedom living in the Hilbert space $\mathcal{H}_{\text{static}}$. The remaining exterior degrees of freedom in the other patch can now be identified with the horizon within the Hilbert space $\mathcal{H}_{\text{horizon}}$, with $\dim \mathcal{H}_{\text{static}} = \dim \mathcal{H}_{\text{horizon}} < \infty$. For a local picture, we preserve the circuit structure for the static patch interior, but now we introduce separate circuit dynamics for $\mathcal{H}_{\text{horizon}}$, as shown in Fig. 3.7. In particular, a recovery tensor (indicated by the ellipse) acts to extract ancilla states at the horizon. Because the interior network is unchanged, the previous cosmic no-hair result about the interior state continues to hold.

This circuit structure constrains the action of the recovery tensor that acts on $\mathcal{H}_{\text{horizon}}$ in Fig. 3.7 if we demand unitary evolution. At each time step, new ancillae are mixed with the interior via the action of the isometries (triangular tensors), and then some information will flow to the horizon and become inaccessible to any interior observer via the action of the disentanglers (square tensors). To be consistent with the literature, label the Hilbert space of the ancillae by S, the static patch Hilbert space by E (i.e., $\mathcal{H}_{\text{static}} \equiv E$), and the horizon Hilbert space by A (i.e. $\mathcal{H}_{\text{horizon}} \equiv A$). If it is always the same ancillary state σ_S (which we have simply taken to be $\sigma_S = |0\rangle\langle 0|_S$ throughout) that gets mixed in via the isometries, then in order to have consistent

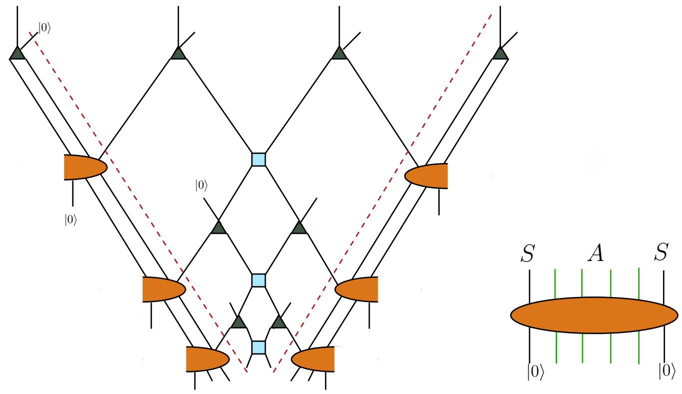

Figure 3.7: The strong complementarian version of MERA that describes a static patch for a local observer with horizon degrees of freedom. The future direction points downward in the fine-graining direction. Dashed red lines demarcate the interior of the de Sitter static patch. The combined system, including a constant number of ancillae, evolves unitarily. The horizon degrees of freedom at each time step are acted upon by a single recovery tensor (orange ellipse), which serves as a map that distills the same ancillary state (represented by $|0\rangle$ in the figure) that is entangled in the interior at the horizon. (Half-ellipses on opposite sides of the tensor network are identified.) The ancillary system is denoted by S while the horizon degrees of freedom are denoted by A.

unitary evolution, it must be that the recovery tensor, which acts on AS, must spit out a state of the form $\rho''_A \otimes \sigma_S$. Put another way, if at every time step we re-introduce a fresh "copy" of the ancillary state σ_S, then unitarity in each time step demands that σ_S be restored after evolving forward in time. (Alternatively we could drop the requirement of unitary evolution; we will return to this possibility at the end of this section.) We call such a circuit for the local picture the Strong Complementarity MERA (SCMERA). The usual global picture can be easily restored by allowing ourselves more ancillary degrees of freedom and replacing the horizon tensors with the usual MERA circuit. As a result, the local and global pictures are related by some global unitary transformation that act on the extended set of ancillae.

Let us ask whether it is possible to have a circuit with the tensor structure in Fig. 3.7 that spits out the state σ_S at every time step. To answer this question, it is useful to analyze the SCMERA circuit from the perspective of recovery maps. At each time step of SCMERA, we can describe the quantum process by

$$\rho_{AES} = \rho_{AE} \otimes \sigma_S \xrightarrow{U_{SE} \otimes I_A} \rho'_{AES} \xrightarrow{U_{SA} \otimes I_E} \rho''_{AES} = \rho''_{AE} \otimes \sigma_S, \tag{3.10}$$

as shown in the quantum circuit diagram in Fig. 3.8. U_{SE} corresponds to the isometries that entangle the ancillae and the interior degrees of freedom, as well as

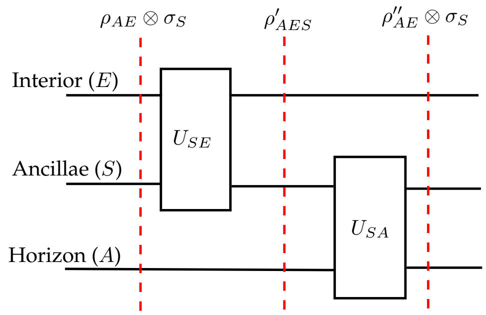

Figure 3.8: Each time step of SCMERA can be condensed into a circuit diagram. The dashed lines mark the resulting quantum state at the end of a subprocess. In the case where the MERA global state is pure, which is the case we consider here, it follows that ρ_{SEA}, ρ'_{SEA}, and ρ''_{SEA} are all pure states.

the disentanglers, while U_{SA} acts on the horizon. Since U_{SA}, which corresponds to the elliptical orange tensor in Figure 3.7, must recover the state σ_S, we call it the recovery tensor.

Although the existence of such a recovery tensor is not always guaranteed, we can examine the necessary conditions that these tensors and states must satisfy to allow such a recovery operation. For instance, if the ancillary qudit is always initialized in a fixed vector, e.g., $|0\rangle_S$, or more generally is always chosen from some fixed subspace of S, then one can derive necessary conditions for recoverability by appealing to results from quantum error correction.

To understand the recoverability of the ancillary state, we first consider the action of U_{SE} as a quantum channel on S, $\mathcal{N}_{\rho_{SE}} : S(\mathcal{H}_S) \to S(\mathcal{H}_S)$. This is always possible because the initial state is uncorrelated across S and E. However, because the state in E is in principle arbitrary (and certainly will change at each time step if the mapping is not at a fixed point), the channel can depend on the input ρ_{SE}. Likewise, the recovery tensor will not remain fixed at every time step. This is what we mean when we say that the SCMERA describes evolution that is generated by a time-dependent Hamiltonian; the recovery tensor will change at every time step if it must recover σ_S exactly.

Given such a channel and knowledge of the fixed ancillary state σ, there always exists a process in the reduced system S that recovers σ. Let $\sigma \geq 0$ be the known state in which the ancillary system is initialized. In general, there exists a completely positive trace preserving (CPTP) recovery map R such that $R \circ \mathcal{N}_{\rho_{SE}}(\sigma') = \sigma'$ for all σ' if and only if the monotonicity condition is saturated [122, 123, 124, 125]:

$$D(\sigma'\|\sigma) = D(\mathcal{N}_{\rho_{SE}}(\sigma')\|\mathcal{N}_{\rho_{SE}}(\sigma)), \tag{3.11}$$

where $D(\sigma'\|\sigma)$ is the relative entropy between σ' and σ. In particular, σ is always recoverable because the monotonicity condition is trivially saturated when $\sigma' = \sigma$. For the finite-dimensional case, one can construct an explicit Petz recovery map P that will always recover σ':

$$P_{\sigma,\mathcal{N}_{\rho_{SE}}} : X \mapsto \sigma^{1/2}\mathcal{N}^{\dagger}_{\rho_{SE}}(\mathcal{N}_{\rho_{SE}}(\sigma)^{-1/2}X\mathcal{N}_{\rho_{SE}}(\sigma)^{-1/2})\sigma^{1/2}. \tag{3.12}$$

Since we here consider the trivial case where $\sigma' = \sigma$, the Petz map can always recover σ.

Unfortunately, in the case of interest here the existence of a Petz recovery map does not lead us to the sought-after unitary U_{SA}, since the Petz map doesn't necessarily take the form of a partial trace $\mathrm{Tr}_A(U_{SA}\,\rho'_{SA}\,U^{\dagger}_{SA})$. Indeed, we can in fact argue that the Petz map *cannot* identically be the map $\mathrm{Tr}_A(U_{SA}\,\rho'_{SA}\,U^{\dagger}_{SA})$. This latter recovery map cannot be CP over the set of all density operators if A, S, E are in an entangled state, which will generally be the case[3], whereas the Petz map is CP by construction. So while U_{SA} may exist, it cannot be found in this way.

In light of this difficulty, a different line of attack is to use the given unitary structure of the SCMERA as a starting point and see whether recovery can be engineered. This amounts to interpreting recovery as an instance of quantum error correction that protects against deletion of E. Think of the state σ_S that the ancillae are initialized in as an encoded message. At any given time step, the message is encoded into the combined SEA system by entangling it with EA. A part of the system, E, subsequently becomes inaccessible to us. We then wish to recover the encoded message by acting on the reduced SA system only with U_{SA}. If this is to be possible, then the allowed interactions U_{SE} are constrained. (This picture is reminiscent of quantum secret sharing.)

Since σ_S is the message that we want to recover and since we discard E, here $\mathcal{N}_{\rho_{SE}}$ is essentially a noisy channel, which we suppose takes on a particular Kraus form,

$$\mathcal{N}_{\rho_{SE}} : X \mapsto \sum_{\mu} N_{\mu}XN^{\dagger}_{\mu}, \tag{3.13}$$

[3]Even if one fixes a particular input at $t = 0$ to be a product state, entanglement will still be generated at a later time. This is because S, E generically become entangled after the isometry.

for a given initial state ρ_{SE}[4]. In this context, in order for a recovery map R to exist, the Kraus operators N_μ must obey the following necessary and sufficient condition [127]. For the sake of generality, suppose that instead of wanting to recover a fixed state $|0\rangle_S$, the encoded message was chosen from a fixed subspace of S that has an orthonormal basis $\{|\phi_i\rangle_S\}$ (the specific case for SCMERA corresponds to there only being one basis vector, namely, $|0\rangle_S$). Then, the Kraus operators must obey the Knill-Laflamme condition,

$$\langle\phi_i|N_\mu^\dagger N_\nu|\phi_j\rangle = C_{\mu\nu}\delta_{ij}\,, \tag{3.14}$$

where $C_{\mu\nu}$ is a Hermitian matrix. This condition places a constraint on what U_{SE} are allowed.

In the case of a single fixed state $|0\rangle_S$, the condition above is trivially satisfied, and so recovery is always possible. However, here as well it is not guaranteed whether there is a quantum error correcting code (QECC) on the whole SEA system that is consistent with SCMERA such that the ancillary state can always be recovered on the SA subsystem on the horizon. We do not know whether such a code exists, but it would have to satisfy certain requirements that we now explore.

In the case where the ancillary qudit is fixed to be a particular state, the code subspace is 1-dimensional. An implementation that allows one to decode the message may be possible to realize with the help of a $k = 0$ code[5]. (See [127] for a detailed review.) For a binary MERA, in which the interior, horizon, and ancillary Hilbert spaces are altogether comprised of 8 qudits, a satisfactory encoding would require a $[\![8, k, d]\!]$ code, where $k = 0$ if the ancillary states are always fixed to be $|0\rangle_S$. Because 2 qudits are effectively erased in discarding the interior (i.e., a known erasure location), the distance of the code must satisfy $d \geq t + 1$ with $t = 2$. As a zeroth order check, we see that this requirement is consistent with the quantum Singleton bound

$$n - k \geq 2(d - 1) \tag{3.15}$$

for $3 \leq d \leq 5$ with $k = 0$. Also note that, while we mainly consider the case where $k = 0$, larger code spaces with $k > 0$ (i.e., a situation where the ancillary state is chosen among several options at each step) are not ruled out. For example,

[4] Recall that any trace-preserving channel on a reduced system can be written using a (potentially input-dependent) set of Kraus operators $\{N_\mu\}$, where $\sum_\mu N_\mu^\dagger N_\mu = I$ [126].

[5] The properties of a quantum error correcting code on qudits of dimension χ are often abbreviated by the notation $[\![n, k, d]\!]$ where n is the block size, k is the number of encoded qudits, and d the code distance. For $k = 0$, the χ^k-dimensional code subspace is precisely one-dimensional.

a hypothetical tensor network that encodes $k = 2$ qudits worth of information could realize a QECC with $d = 3, 4$. We note that there exist binary codes that are compatible with our requirements on n, k, and d, for example, the $[[8, 3, 3]]$ code (see section 7.12.3 in [128]), and presumably there also exist codes for qudit systems; however, we are unaware of their specific forms, and much less whether or not they are compatible with the tensor structure of SCMERA.

In summary, by interpreting SCMERA as a recovery operation or an error correcting code, we identify several necessary but generally insufficient criteria that the SCMERA circuit must meet. Note, however, that failure to meet these criteria cannot rule out strong complementarity, but it can rule out SCMERA as a model.

Finally, we elaborate a bit more on the unitarity of the proposed SCMERA circuit. The overall SCMERA tensor network can be understood as a circuit by including the ancillary degrees of freedom, S. In the case of perfect recovery of the ancillary state on the horizon, the ancillary state that was added in the interior can be discarded from the horizon at the end of the computation in each time step so that the total size of Hilbert space remains constant throughout. Alternatively, we can also understand the adding-and-discarding process as recycling the ancillary degrees of freedom at each step. It is clear in this sense that we have a unitary process on the same finite-dimensional Hilbert space. However, note that the unitary recovery mapping on the horizon need not recover the ancillary state perfectly. In fact, a universal (i.e., constant in time) unitary recovery map applied to every time step cannot in general achieve perfect recovery. In this case, recycling of the approximately recovered ancillary qudit will lead to information backflow into the static patch interior, which in turn leads to Poincaré recurrences. Discarding such ancillary qudits on the horizon avoids recurrences even when using a universal recovery map, but breaks unitarity. If we demand perfect recovery of the ancillary qudit, then the unitary evolution is necessarily time-dependent. It is, however, unclear if such time-dependence is only limited to swapping operations on the horizon.

3.5 Circuit Complexity and de Sitter Action

In AdS/CFT, the "complexity equals action" proposal [32] suggests that the complexity of a CFT thermofield double state as it evolves in time is proportional to the Einstein-Hilbert (EH) action of a region of the bulk known as the Wheeler-De Witt patch. Explicitly, $C = qS_{\text{EH}}$, where the proportionality constant is calculated to be $q = 1/\pi\hbar$. Similarly, here we can show that complexity, calculated using the MERA circuit, scales in the same way as the corresponding spacetime action in de Sitter space.

For a given MERA-like circuit that is translationally and scale invariant, it is possible to estimate its complexity by choosing a reference state and gate set. It is natural to choose the reference state to be the initial state of dS/MERA, which we write as $|\Psi(t=0)\rangle = |\psi\rangle \otimes |\phi\rangle^{\otimes N}$. $|\Psi\rangle$ consists of the initial entangled component $|\psi\rangle$ which encodes the entanglement information needed to reconstruct the de Sitter spatial geometry at $t = 0$, and $|\phi\rangle^{\otimes N}$ denotes all the ancillary degrees of freedom that will later get entangled up to some time $t = T$. Here, because we only consider bounds on complexity, the estimate won't depend on the particular form of $|\psi\rangle$; we can take it to be an arbitrary state that lives on the initial few sites of the MERA at $t = 0$.

We obtain a straightforward estimate of complexity if we choose a reference gate set that corresponds to the exact disentanglers and isometries, $\{U, V\}$, that were used to build the MERA circuit. For a k-nary MERA, suppose that U, V are k-local and denote the total number of ancillae that get entangled up to time $t \leq T$ by

$$N(T) = \sum_{j=0}^{T} k^j. \tag{3.16}$$

It then follows that for any non-trivially entangled state $|\Psi(T)\rangle$, where none of the qudits in $|\Psi(T)\rangle$ can be written as a product state between the qudit and its complement[6], a lower bound on its complexity $C(T)$ is proportional to $N(T)$. This is because, even using an optimal circuit that could potentially be more efficient than the MERA, it takes at least $N(T)/k$ k-local gates to even minimally entangle all of the product ancillae. The actual complexity to create the state with the correct entanglement structure at $t = T$ is therefore strictly lower-bounded. In addition, the MERA circuit itself that constructs the state $|\Psi(T)\rangle$ constitutes a trivial complexity upper bound. Hence, for generic scale and translationally invariant MERA in arbitrary dimensions with k-local disentanglers and isometries, the complexity satisfies

$$C_0 N(T) \leq C(T) \leq C_1 N(T), \tag{3.17}$$

where $C_1 > C_0$ are order-unity numbers that depend on the specific circuit construction. For the (1+1)-dimensional binary MERA shown, $C_0 = 4$ and $C_1 = 8$.

[6]For example, this is expected for a CFT vacuum state.

Choosing a different reference gate set would give different coefficients C_0 and C_1, but the exponential dependence on T would remain unchanged.

An important distinction from the usual holographic complexity proposal [32] is the lack of a boundary theory, and hence a notion of bulk-boundary duality. Similarly, the proposal also differs from [129], where the complexity of the state on the de Sitter boundary is compared to the action or volume of a holographic asymptotically anti-de Sitter bulk. Because only the de Sitter bulk is present, we test a bulk complexity-action (volume) proposal by directly comparing the circuit complexity of MERA, which is conjectured to describe de Sitter spacetime, to the Einstein-Hilbert action (spacetime volume) of the same region in de Sitter.

The Einstein-Hilbert action of the portion of de Sitter spacetime covered by the global time interval $0 \le t \le T$ in D dimensions is given by

$$\begin{aligned} S_{\mathrm{EH}} &= \frac{1}{16\pi G}\int_0^T dt \int d\Omega_{D-1}\sqrt{-g}R \\ &= \frac{R\ell_{\mathrm{dS}}^D \mathcal{S}_{D-1}}{16\pi G}\int_0^T dt\, \cosh^{D-1} t \\ &= \frac{R\ell_{\mathrm{dS}}^D \mathcal{S}_{D-1}}{16\pi G}\frac{1}{(D-1)2^{D-1}} e^{(D-1)T} \; + \; \text{subleading}, \end{aligned}$$

where $R = D(D-1)/\ell_{\mathrm{dS}}^2 = 2D\Lambda/(D-2)$ is the Ricci curvature for de Sitter space with cosmological constant Λ and $\mathcal{S}_{D-1}$ is the volume of the $(D-1)$-sphere. We see that the scaling behavior is indeed consistent with the circuit complexity computed above, and the action satisfies the complexity bound for some appropriate choice of constant q. Note that each tensor in the MERA is mapped to a proper volume in de Sitter [79]. Therefore, comparison of other spacetime regions would yield a similar conclusion. It cannot differentiate the complexity = volume versus complexity = action proposal, because the constant Ricci curvature in de Sitter space only changes q by a constant factor.

The proportionality constant between complexity and action depends on the choice of gate set, and differs from $q = 1/\pi\hbar$ in the original proposal. See [34, 35] for similar conclusions from more detailed studies in the context of quantum field theory. Interestingly, assuming the validity of the conjecture, the $(\ell_{\mathrm{dS}}/\ell_{\mathrm{pl}})^{D-2}$ scaling behavior in the action may suggest that the complexity of a correct circuit with sub-Hubble features should approximately scale as the horizon area (recall that R scales like ℓ_{dS}^{-2}). In the case of the MERA, this is encoded in the otherwise arbitrary choice of q, because the network structure is not sensitive to $\ell_{\mathrm{dS}}/\ell_{\mathrm{pl}}$.

3.6 Discussion

Discretizing de Sitter spacetime using the MERA seems to provide some interesting interpretations, in particular in terms of giving a natural information-theoretic reason for cosmic no-hair, constraining de Sitter complementarity, and giving the de Sitter action an information-theoretic interpretation. It would be interesting to ask what other consequences thinking of de Sitter spacetime in a tensor network/information-theoretic way could provide. For example, would a different tensor network discretization be more natural for answering other questions, or is the choice of tensor network discretization fixed by the spacetime metric one is attempting to duplicate? If so, are there other natural spacetimes (Lorentzian or Euclidean), for which different tensor networks might provide insights into open problems?

The MERA is naturally suited to describing de Sitter spacetime on super-Hubble scales, since structure within a horizon volume is not resolved. The state within a patch can nevertheless be encoded in the tensors inside the horizon, and perturbations of such a state in the de Sitter background can be initialized in the MERA input state. The cosmic no-hair result is then the fact that such perturbations flow to a fixed-point of the evolution superoperator within a patch.

Another limitation of this de Sitter-MERA correspondence is that it clearly breaks the rotational symmetry of spacelike sections of de Sitter; a binary MERA that corresponds to (1+1)-dimensional de Sitter spacetime picks out four preferred causal patches, or equivalently, fixes the cardinal directions on the circle. It also breaks boost symmetry in that the MERA fixes a preferred global $t = 0$ slice. To this end, hyperinvariant tensor networks may be an interesting improvement on the MERA [81]. Hyperinvariant tensor networks were introduced to address, among other issues, a similar problem for AdS-MERA correspondences that the MERA picks out a preferred center point of the hyperbolic plane. In a hyperinvariant tensor network, any node in the tensor network can be taken to be the "center" of the hyperbolic plane, thus restoring a significant amount of symmetry. Since the radial direction in AdS corresponds to the renormalization direction of the MERA, which here corresponds to the timelike direction of de Sitter, a hyperinvariant tensor-network/de Sitter correspondence would likely no longer fix a preferred global $t = 0$ slice. Instead, the effective causal cone of any pair of adjacent nodes could be used to define a de Sitter static patch.

It would be interesting to push the present analysis beyond a strict de Sitter background. For example, it should be possible to adapt the tensor network to allow for bubble nucleation and eternal inflation. A classical variant of this was already considered in [130], and it would be useful to further investigate the evolution of quantum states using the kind of methods explored here.

This material is based upon work supported by the U.S. Department of Energy, Office of Science, Office of High Energy Physics, under Award Number DE-SC0011632, as well as by the Walter Burke Institute for Theoretical Physics at Caltech and the Foundational Questions Institute.

3.A Stationary causal cones of the MERA

Given a k-nary MERA, in which the number of sites in each layer increases k-fold with every fine-graining step, what is the number of sites per layer of a stationary causal cone?

Example 3.A.1. Consider a binary MERA as in Fig. 3.1. Within the MERA, consider a set of sites at some layer and draw their causal cone in the coarse-graining direction. If the smallest simply-connected region that contains all of the initial sites is made up of L sites, then after $\sim \log_2 L$ steps in the coarse-graining direction, the causal cone will contain 2 or 3 sites [58]. Once the cone at some layer contains 2 or 3 sites, Fig. 3.9 illustrates how the width of the causal cone can evolve under further coarse-graining. Notice that if the cone contains 2 sites at some layer, then it is possible for the next layer to have either 2 or 3 sites, but if a given layer contains 3 sites, then all subsequent layers will contain 3 sites. Therefore, a stationary causal cone having the same width at every layer can only have 2 sites per layer or 3 sites per layer. In particular, only the stationary causal cone with 2 sites per layer is left/right-symmetric in a binary MERA.

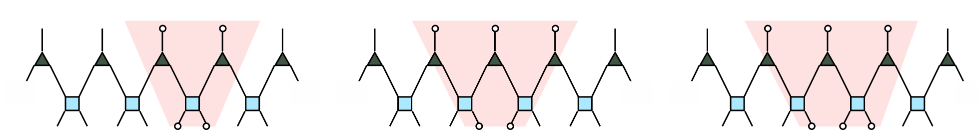

(a) (b) (c)

Figure 3.9: Ways in which a minimal-width causal cone can propagate between layers in a binary MERA. (a) $2 \to 2$, (b) $2 \to 3$, (c) $3 \to 3$.

Example 3.A.2. Consider a ternary MERA as in Fig. 3.4. Similarly, the causal cone of any given collection of sites will contain 2 or 3 sites after $\sim \log_3 L$ steps in the coarse-graining direction. If the cone contains 3 sites at some layer, then it is possible for the next layer to have either 2 or 3 sites, but if a given layer contains 2 sites, then all subsequent layers will contain 2 sites (Fig. 3.10). Therefore, a stationary causal cone having the same width at every layer can only have 2 sites per layer or 3 sites per layer. Here, only the stationary causal cone with 3 sites per layer is left/right-symmetric in a ternary MERA.

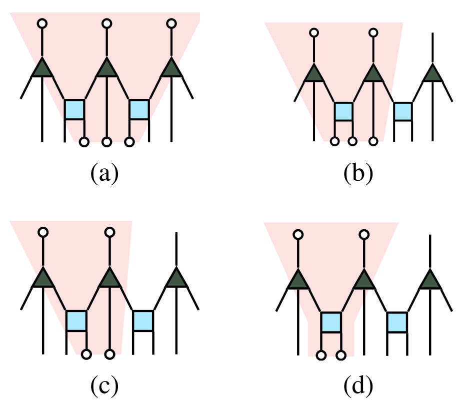

Figure 3.10: Ways in which a minimal-width causal cone can propagate between layers in a ternary MERA. (a) $3 \to 3$, (b) $3 \to 2$, (c) $2 \to 2$, first instance, (d) $2 \to 2$, second instance.

The case of a general k-nary MERA follows straightforwardly from the two examples above:

Proposition 3.A.3. *A stationary causal cone having the same width at every layer in a homogeneous k-nary MERA has 2 or 3 sites per layer.*

Proof: Given some homogeneous k-nary MERA with any arrangement of disentanglers and isometries, all of the legs in the tensor network can be blocked together to form composite legs so that the network takes the form of a binary or ternary MERA, as illustrated in Fig. 3.11, whence the proposition follows from the examples above. $\square$

3.B Higher-dimensional generalizations

Consider a d-dimensional MERA, where each layer is a hypercubic d-dimensional lattice. Here, the MERA is k-nary when each site in one layer gives rise to k^d sites

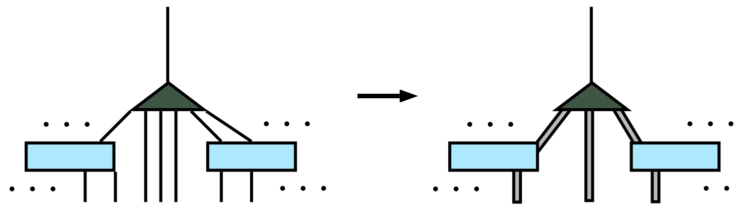

Figure 3.11: Legs in an arbitrary MERA can be blocked together. In this way, that the causal structure matches that of a binary or ternary MERA becomes apparent.

in the next layer (see Fig. 3.12). The global MERA-de Sitter correspondence does not carry through in this case, simply because, on the de Sitter side, there is no way to latticize the d-sphere using a regular hypercubic lattice that is self-similar under fine-graining (although see [131] for a generalization to 2 dimensions).

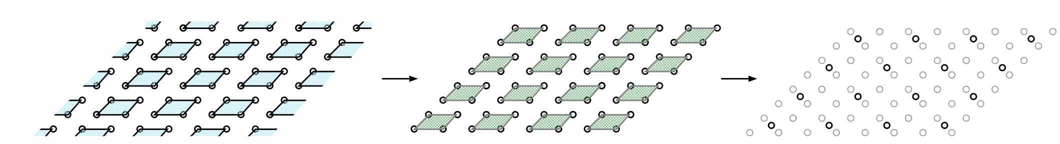

Figure 3.12: A 2D MERA. In a single coarse-graining step, blocks of 4 sites are acted on by a disentangler (blue); then blocks of 4 sites that are displaced from the last set of blocks are acted on by an isometry (green), reducing the number of sites by a factor of 4.

This is not to say that a generalization to higher dimension is impossible. One could consider a different tiling of global de Sitter that preserves uniformity and is self-similar under some refinement operation. For example, on a 2-sphere, regular or semi-regular tilings are possible using triangularizations, but these different tilings would necessarily require some sort of variation on the MERA tensor network. To the best of our knowledge, such generalizations are still unexplored.

On the other hand, one could still study the correspondence between de Sitter and a hypercubic MERA by restricting one's attention to only a single static patch. In this scenario, it is consistent to think of the MERA as defining a superoperator which maps the state on m^d sites of a given slice of a single static patch to the next slice. (Remember, the number of sites per horizon volume, i.e., per slice of the static patch, remains constant.) Therefore, the usual unmodified MERA may still be useful for understanding local aspects of de Sitter quantum gravity in higher dimensions.

Chapter 4

QUANTUM CIRCUIT COSMOLOGY

In this chapter, we consider cosmological evolution from the perspective of quantum information. We present a quantum circuit model for the expansion of a comoving region of space, in which initially-unentangled ancilla qubits become entangled as expansion proceeds. We apply this model to the comoving region that now coincides with our Hubble volume, taking the number of entangled degrees of freedom in this region to be proportional to the de Sitter entropy. The quantum circuit model is applicable for at most 140 e-folds of inflationary and post-inflationary expansion: we argue that no geometric description was possible before the time t_1 when our comoving region was one Planck length across, and contained one pair of entangled degrees of freedom. This approach could provide a framework for modeling the initial state of inflationary perturbations.

This chapter is based on the Ref:
Ning Bao, ChunJun Cao, Sean M. Carroll, and Liam McAllister. "Quantum Circuit Cosmology: The Expansion of the Universe Since the First Qubit". In: (2017). arXiv: `1702.06959 [hep-th]`.

4.1 Introduction

Predictions of inflationary cosmology [132, 133, 134] are generally derived in the framework of quantum fields evolving in a classical background spacetime. While this approach has had empirical success, it raises an important conceptual problem: degrees of freedom are represented as modes of fixed comoving wavelength, and as space expands, modes with wavelengths less than the Planck length are stretched to be super-Planckian, and so become visible in a long-wavelength effective description. One manifestation of this issue is the trans-Planckian problem (see e.g. [135, 136, 137, 138, 139, 140, 141]), which asks whether newly-appearing modes are in a state other than the usual Bunch-Davies vacuum [142], and if so, how this affects the predictions of inflation.

Our concern in this paper is with a deeper problem: not the quantum state of modes that are initially trans-Planckian, but the very nature and existence of such modes. In the context of quantum field theory in curved spacetime, where the dimensionality of Hilbert space is infinite, it is possible in principle to imagine a limitless store of zero-energy modes initially frozen into their vacuum states, which become dynamical when their wavelengths grow longer than the Planck length. But is this infinite supply of degrees of freedom physically meaningful? In this note we confront this problem from the perspective of the emergence of spacetime from quantum entanglement [23, 143, 31, 28, 65, 144, 120, 121, 82].

We suggest that each finite-sized comoving region of space is described by a finite number of quantum degrees of freedom, so the supply of new modes is not limitless. Concretely, we posit that a finite comoving region of space can be described by a density matrix associated with a Hilbert space $\mathcal{H}$ of fixed, finite dimension D. A convenient, though logically inessential, representation takes $\mathcal{H}$ to be the tensor product of n qubit degrees of freedom, so that $D = 2^n$. These degrees of freedom include both those describing space itself, and the modes of an emergent field theory on wavelengths much larger than the Planck scale.

As a toy model for the evolution of a fixed comoving region C, we propose a simple quantum circuit. (Our approach thus bears a family resemblance to the proposal that the universe can be thought of as a quantum computer [145, 146].) A quantum circuit consists of a network of quantum gates, each of which performs a unitary transformation on the basic factors of the Hilbert space of a quantum system, which we have taken to be qubits. This yields a convenient representation of the evolution of the system. At any time t, we can divide the n degrees of freedom in $\mathcal{H}$ into a number $n_e(t)$ that are entangled with each other (and whose entanglements are responsible for the spacetime structure), and a number $n_u(t)$ that are not entangled with anything:

$$n = n_e(t) + n_u(t)\,. \tag{4.1}$$

The unentangled degrees of freedom can be thought of as "ancilla" qubits. These are initially not entangled with each other, nor with the degrees of freedom describing other regions. In our model, as space expands and the physical size of C increases, no new degrees of freedom are brought into existence. Instead, more and more of the ancilla qubits become entangled with those that are already part of the spacetime structure. The fundamental gate in our quantum circuit entangles an ancilla qubit with the rest of the circuit; this is interpreted as a small amount of expansion. See Fig. 4.1.

We will apply this picture to the history of our comoving patch, i.e. the comoving volume that now coincides with our Hubble volume. For a Hubble volume in de Sitter

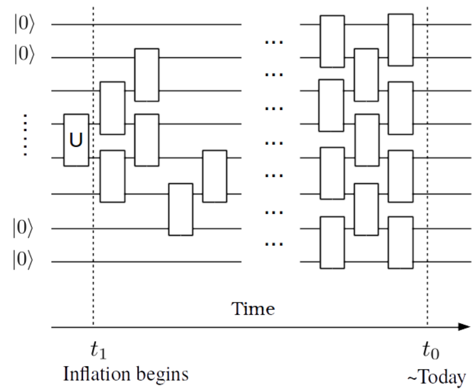

Figure 4.1: A schematic for a cosmological quantum circuit. The ancillary qubits are initialized in $|0\rangle$ states, and the boxes are unspecified unitary gates.

space we argue that $D \approx e^S$, with S the de Sitter entropy, so that $n \approx n_e \approx S/\ln 2$. Our own comoving patch therefore contains $n \approx 10^{122}$ entangled degrees of freedom today. In our past, when our comoving region was smaller, many of these degrees of freedom were not yet entangled.

This picture provides a candidate description of the quantum state of our comoving region at very early times. If inflation lasted for just the minimal number of e-folds necessary to solve the horizon problem, then at the start of inflation our comoving region was approximately a Hubble volume. However, if inflation lasted slightly longer than this (as quantified below), then sufficiently early in inflation the diameter of our comoving region was the Planck length ℓ_p. A semiclassical description of quantum fields in this region is problematic, because the wavelengths of such modes are $< \ell_p$. In most approaches to the trans-Planckian problem, the underlying spacetime is taken to be smooth, and ambiguities associated to modes on this background are addressed by imposing a cutoff prescription.

In our picture, in contrast, even the notion of a classical metric ceases to make sense for a region of Planckian size: we will argue that for such a small region, there is insufficient entanglement for a description in terms of a smooth emergent spacetime to be valid. Correspondingly, we will find that the time evolution in our quantum circuit is trivial before the time t_1, the "time of one e-bit", when our comoving patch contained just one pair of entangled degrees of freedom, and had size $\approx \ell_p$. Before this time, the space corresponding to our comoving patch had not yet emerged.

We will argue that the total number of e-folds of inflationary and post-inflationary expansion since the time t_1 is bounded,

$$N_{\text{tot}} \leq 140\,. \tag{4.2}$$

This implies an upper bound on the total number of e-folds of inflation between the time t_1 and the time of reheating, which is close to (but safely above) the number needed to provide a resolution to the horizon problem [132, 147, 148, 149]. (The upper bound (4.2) is related to other bounds that rely on the finite dimensionality of Hilbert space [150, 151, 152, 153, 154], as we explain in the Discussion.)

One aim of this note is to initiate a new approach to the trans-Planckian problem. The time t_1 entering the bound (4.2) is the time when our comoving region was one Planck length across, and correspondingly when modes that are horizon-sized today had Planckian wavelengths. Although our quantum circuit has trivial time evolution before this point, it provides a simple quantum-mechanical model for the time *shortly after* t_1, when a geometric description of our comoving region was not yet valid, but ancilla qubits were beginning to become entangled, as a precursor to the emergence of a smooth geometry. One might therefore adapt our setup to examine the quantum state of the curvature perturbations for $t \approx t_1$. More broadly, our approach provides a speculative but relatively concrete framework for answering certain questions about the very early history of our universe: what happened when our region was Planckian in size? Does cosmological expansion proceed continuously or in quantized steps?

4.2 The Trans-Planckian Problem

We will first briefly recall some well-known aspects of the trans-Planckian problem in inflationary cosmology (see [141] for a review).

We consider a flat Friedmann-Robertson-Walker universe with metric

$$ds^2 = -dt^2 + a(t)^2 d\vec{x}^2\,. \tag{4.3}$$

A comoving volume C is one that has fixed coordinates $\vec{x}$ over time, while a Hubble volume at a given time t is a ball of physical radius $H^{-1}(t)$, where $H = \dot{a}/a$. We write $R(t)$ for the physical radius of C. The number of e-folds between two times t_1 and $t_2 > t_1$, denoted $N(t_1, t_2)$, is defined as

$$e^{N(t_1,t_2)} = \frac{R(t_2)}{R(t_1)}. \tag{4.4}$$

The region of primary interest is the comoving volume that coincides now with our Hubble volume, i.e. the region such that $R(t_0) = H^{-1}(t_0)$, with t_0 the present time.

We refer to this region as "our comoving patch" or "our comoving volume", and denote it by $C^H(t)$.

The trans-Planckian problem is a potential ambiguity that arises if the total amount of expansion that our comoving patch experienced exceeds the minimum number of e-folds needed to solve the horizon problem. The underlying issue is that semiclassical methods may not be valid for describing modes with wavelengths shorter than the Planck length ℓ_p. In cosmologies with considerably more than 60 e-folds of inflation, some of the modes visible in the Cosmic Microwave Background (CMB) and Large Scale Structure had such sub-Planckian wavelengths at the beginning of inflation [1]. To see this, recall that in an inflationary scenario involving just enough e-folds to solve the horizon problem, the large-angle modes of the CMB exited the horizon at the very beginning of inflation. Because these modes now have wavelengths of order $H_0^{-1} \approx e^{140}\ell_p$, with H_0 the present-day Hubble parameter, they were sub-Planckian at the beginning of inflation if the total number N_{tot} of e-folds of inflationary and post-inflationary expansion exceeds 140. The critical number $N_{\text{tot}} = 140$ does not depend on the equation of state during or after inflation, nor on the reheat temperature T_{RH}. However, the division of N_{tot} into N_I e-folds of inflationary expansion and N_P e-folds of post-inflationary expansion does depend on T_{RH}. (For example, with Standard Model particle content and $T_{RH} = 10^{15}$ GeV, the critical value of N_I is 75.)

Thus, in cosmologies with

$$N_{\text{tot}} = 140 + \Delta N \tag{4.5}$$

total e-folds of expansion between the beginning of inflation and the present, all modes of present wavelength $\leq H_0^{-1}e^{\Delta N}$ were sub-Planckian at the beginning of inflation. While it may be that such a cosmology can be described semiclassically, with modes in the Bunch-Davies vacuum or in another well-behaved vacuum state, the trans-Planckian question consists of taking seriously the issue of modes with sub-Planckian wavelengths.

Requiring that modes of current wavelength H_0^{-1} had wavelengths longer than ℓ_p at the start of inflation is equivalent to requiring that our comoving region, of current size H_0^{-1}, had size greater than ℓ_p at the start of inflation. However, in most reasoning about trans-Planckian issues, the physical origin of the ambiguity is the problem of specifying the quantum state of modes with sub-Planckian wavelengths, not the

[1] This trans-Planckian problem, which concerns perturbations with wavelength $\ll \ell_p$, should not be confused with the problem of controlling super-Planckian field displacements $\Delta\phi \gg M_p$. The former can occur in inflationary models with $\Delta\phi \ll M_p$.

problem of describing a comoving region of sub-Planckian size. After all, in classical gravity a comoving region is just some chosen subset of a spacelike hypersurface, and at the level of a classical, homogeneous FRW cosmology there is no obvious problem when the size of this subset becomes sub-Planckian. Correspondingly, the trans-Planckian problem is usually understood as a question about the initial state of currently-observable modes, rather than as a hard upper bound on the total amount of expansion in our history. The condition $N_{\text{tot}} \leq 140$ is then a bound only to the extent that one insists on making predictions for the CMB without providing a description of modes of sub-Planckian wavelengths.

Here we will derive a superficially identical upper limit, $N_{\text{tot}} \leq 140$, from rather different assumptions. Importantly, in our treatment $N_{\text{tot}} = 140$ turns out to be a limit beyond which our description of the *background*, not just of the inflationary perturbations, fails. Specifically, we will find that for $N_{\text{tot}} > 140$, a description of our comoving region as emerging from entanglement is inapplicable at sufficiently early times. Thus, inflationary cosmologies with $N_{\text{tot}} > 140$ necessarily violate one or more of our assumptions, which we enumerate below. Although we believe these assumptions are all plausible, any of them may reasonably be questioned. Our main point is to explore the consequences of assuming their validity.

4.3 Counting Entangled Degrees of Freedom

Our analysis rests on counting entangled degrees of freedom in de Sitter space, so we will first recall the relevant definitions in a quantum-mechanical toy model without gravity. Consider N spins in some subsystem A, and N' spins in A^C, the complement of A. (By specifying "spins" we imagine that the factorization of Hilbert space into fundamental qubits is fixed, so that the amount of entanglement between any particular degrees of freedom is uniquely defined.) The entanglement entropy of A across the bipartition is defined as $S_A = -\operatorname{Tr} \rho_A \ln \rho_A$, where ρ_A is the reduced density matrix of A. The *number of entangled degrees of freedom* in A, $n_e(A)$, is defined as the number of qubits in the A subsystem that are nontrivially entangled with at least one other qubit, either inside or outside A. For bipartite entanglement, the number of entangled degrees of freedom is (up to factor of 2) a quantity known as the distillable entanglement. There are multipartite generalizations of this quantity as well, though computing them becomes more challenging.

The amount of entanglement in A can also be expressed in terms of e-bits. An e-bit is a unit of entanglement that corresponds to the entanglement entropy of one half of a Bell pair. The number of e-bits is equal to the total amount of entanglement (in the form of Bell pairs or other fundamental units of multipartite entanglement, such as GHZ or W states for tripartite information) that can be extracted from a quantum state through a theoretically optimal distillation protocol. Said colloquially, the number of e-bits is the amount of entanglement inherent in a quantum state. Because each degree of freedom can share at most one e-bit of entanglement with the entire remainder of the system, the number of e-bits in the spins in A is bounded above by $n_e(A)$.

For a fixed tensor product decomposition of the Hilbert space into a set of qubits, the number of entangled degrees of freedom is a well-defined property of a quantum state, whereas the entanglement entropy of a subregion depends on how that subregion is defined [2]. For example, simply by considering a bipartition where all of the entangled degrees of freedom reside on one side of a bipartition, one makes the entanglement across that bipartition zero, while this choice has no effect on the number of entangled degrees of freedom in the state as a whole.

Suppose the Hilbert space of the spins in $A + A^C$ has dimension $D = D_A \times D_{A^C} = 2^N \times 2^{N'}$, with D_A and D_{A^C} the dimensions of the subspaces describing A and A^C, respectively. Assume, without loss of generality, $D_A \leq D_{A^C}$. We say that A is maximally entangled with A^C if every spin in A is maximally entangled with one or more spins in A^C. In such a case the entanglement entropy of A across the bipartition is maximized, so that

$$S_A = \ln D_A = n_e(A) \ln 2 = N \ln 2 \,. \tag{4.6}$$

That is, in maximally entangled configurations, the number of entangled degrees of freedom determines the dimension of the entangled subsector of the Hilbert space. (In the case where the joint A, A^C system is a thermal system, the entanglement entropy is nearly maximized and (4.6) is approximately satisfied.) More generally, however, n_e can be much greater than the entropy. Take, for example, the N-party GHZ state, where $n_e = N$ but $S = 1$ for any non-trivial bipartition.

[2] The number of entangled degrees of freedom is not necessarily invariant under a global change of basis implemented by some unitary transformation that can change the notion of a "fundamental qubit." For example, in the AdS/CFT correspondence the entangled boundary degrees of freedom are mapped nonlocally to the bulk. In more specific examples, such as those illustrated by Exact Holographic Mapping [48] or MERA as a unitary quantum circuit [52], a change of basis turns a highly entangled set of qudits into a set that has little or no entanglement. However, for our purposes, n_e should be understood as being defined with respect to a fixed set of qubits.

4.4 Framework and Assumptions

We now consider the number of entangled degrees of freedom in the context of cosmology. Our assumptions are as follows:

1. The evolution of an approximately homogeneous comoving region of space can be described as that of a density matrix associated with a factor of Hilbert space of fixed, finite dimension D.

2. At any time t, to a given comoving region C there is associated a number $n_e(t)$ of entangled degrees of freedom describing the spacetime (and matter) structure of C. There are also $n_u(t) = n - n_e(t)$ unentangled degrees of freedom, with $n = \log_2 D$, which play no role in the emergent semiclassical geometry or matter configuration.

3. For a Hubble volume in de Sitter space with cosmological constant Λ and Hubble constant $H_\Lambda = \sqrt{\Lambda/3}$, the total number of entangled degrees of freedom is approximately the de Sitter entropy,

$$n_e(\mathrm{dS}) \approx \frac{S_{\mathrm{dS}}}{\ln 2}. \tag{4.7}$$

   We assume that (4.7) holds to good approximation as long as the expansion is very close to de Sitter, as it is in inflation and in the present epoch.

4. The number of entangled degrees of freedom $n_e(t)$ in the comoving volume C^H that now coincides with our Hubble volume can never be less than one.

Let us briefly discuss the motivation for these assumptions.

The first assumption, that the quantum state of our comoving region of space is described by a fixed factor of Hilbert space, is a well-justified approximation in a universe that is nearly homogeneous on large scales. In a general curved spacetime, it would be hard to think of a given region of space as describing a fixed quantum system for all times, as there is no preferred way to evolve it into the future. (Equivalently, there is no preferred timelike vector field along which to associate a spatial region at one time with one at other times.) But the large-scale homogeneity of our observed universe allows us to define comoving coordinates, and to use these to divide the universe into well-defined regions. (There is now a preferred vector field, orthogonal to the hypersurfaces of homogeneity.) This is not to say that our comoving patch evolves as a causally closed system; individual photons, for example, certainly enter and leave such a region. But a photon entering our comoving patch does not represent a new degree of freedom; it is described by previously unexcited degrees of freedom (the vacuum of the electromagnetic field) now becoming excited. Information is entering our region, in other words, but not new qubits, much like a wave traveling through the ocean is not made of a fixed set of water molecules. In our picture, the entangling of qubits causes space to expand, but the qubits themselves were always part of the Hilbert space factor describing our observable patch, and were simply unentangled initially. Unentangled "ancilla" qubits of this sort are commonplace in quantum circuits and tensor networks, including in the description of emergent holographic spaces [155, 39, 37, 47, 41, 79, 49, 76].

A crucial feature in our analysis is that the dimension D of the Hilbert space of our comoving region is finite. There are well-known obstacles to imagining that regions of spacetime are described by finite-dimensional Hilbert spaces, including the fact that the Lorentz group does not admit nontrivial finite-dimensional unitary representations. On the other hand, there is suggestive evidence — for example, the Bekenstein/holographic bounds [156, 18, 157] — that in quantum gravity the Hilbert space of a finite region is indeed finite, and for our purposes we will accept this as a working assumption. Note also that reasoning about complementarity leads to similar conclusions [114], although our work does not rely on the validity of complementarity.

The second assumption is inspired by the program of relating spacetime geometry to quantum entanglement (for a review, see [158]). While geometry from entanglement was originally motivated from examples in AdS/CFT, more general constructions of emergent spacetime are possible [30, 82], including tensor network descriptions in which the entanglement of finitely many quantum degrees of freedom creates connectivity that reflects the geometry [37, 71]. It has also been argued that MERA [39] can be interpreted as de Sitter space [51, 79, 85]. Entanglement is crucial for such models of emergent space, where smoothness and connectedness of space usually corresponds to a large number of degrees of freedom being entangled in an organized manner. In the case where there is little or no entanglement among the quantum degrees of freedom associated with spatial regions, the spatial geometry becomes disconnected, and in certain contexts a firewall can form.

The third assumption captures the idea that a horizon-sized patch of de Sitter space is an equilibrium system, with a maximum entropy. The Gibbons-Hawking entropy of a Hubble volume is proportional to the area [159],

$$S_{\mathrm{dS}} = \frac{A_{\mathrm{dS}}}{4\ell_p^2} = \frac{\pi}{\ell_p^2 H_\Lambda^2}, \tag{4.8}$$

and can be interpreted as the entanglement entropy across the horizon. The approximate equality (4.7) is then a conjectured property motivated by the near-equilibrium character of an approximately de Sitter phase.

The final assumption, that $n_e(t) \geq 1$ for our comoving patch, is crucial to our argument. This assumption may be less familiar and less plausible than the others, so let us explain the justification. The statement is that for t such that $n_e(t) < 1$, the degrees of freedom in our comoving patch were not entangled with anything. Because our region of space literally *is* that collection of entangled qubits, there is a sense in which our space did not exist before t_1. Said more carefully, our semiclassical region of space had not yet emerged at such early times: the factor of Hilbert space that would eventually describe our comoving region did not contain even a single e-bit, and there was no geometric interpretation of the degrees of freedom that we find around us today. Nonzero entanglement is necessary for smooth spacetime.

The quantum circuit of Fig. 4.1 provides a useful perspective on assumption (iv). In this setting, time evolution is described via the discretization of the Hamiltonian evolution into smaller unitaries in the form of quantum gates. When no gates are being applied to the quantum degrees of freedom in the comoving patch, these degrees of freedom are evolving trivially. However, it is always conceivable that space is infinite in extent, and that the total dimension of Hilbert space (once we include regions outside our observable patch) is infinite. Our comoving patch is then a subset of a larger circuit that allows other patches or observers to evolve further back in time, to times before t_1. As far as the degrees of freedom in our comoving patch are concerned, the larger "super-circuit," whose degrees of freedom are detached from our own, has no effect whatsoever on our comoving patch, as long as no nontrivial gate acts on the degrees of freedom in our comoving patch. This is indeed consistent with a crude model that uses MERA to model the initial inflationary phase. After the last entangled degree of freedom of our comoving patch is disentangled from the rest of the network, evolving time further backwards on the remaining circuit will not apply any more gates on the qubits describing our region. If instead our comoving patch is not a part of a larger circuit, the initial state is necessarily pure and there is no further time evolution backwards to times $t < t_1$.

4.5 Upper Bound on Total Expansion

We will now derive a bound on the amount of inflation that can be described in our quantum circuit model. Denote by $n_e(C^H, t_I)$ the number of entangled degrees of freedom at time t_I in our comoving volume C^H. We are interested in finding the critical time t_1 ("the time of one e-bit") when this number barely exceeds 1,

$$n_e(C^H, t_1) \approx 1 . \tag{4.9}$$

We denote the physical size $R(C^H)$ at $t = t_1$ by $R(t_1)$.

Reasoning based on holography and black hole physics strongly suggests that $R(t_1) \gtrsim \ell_p$, corresponding to at most of order one entangled degree of freedom per Planckian-sized region. To see this, consider a black hole with radius of order the Planck scale. It is widely believed that a black hole provides the densest packing of information into a region of a given size, and is also maximally entangled with the remainder of the universe it resides in. A system that is maximally entangled with its purifying region has $S = n_e \ln 2$, as previously discussed. Moreover, the entropy of the black hole is given by the Bekenstein-Hawking formula [156], $S = A/(4\ell_p^2)$, which the Gibbons-Hawking formula closely parallels. This suggests that the number of entangled degrees of freedom inside a Planck-sized black hole is also of order unity. Taking a region of space to have a number of entangled degrees of freedom less than or equal to that of a black hole of comparable size, we conclude that the number of entangled degrees of freedom in a Planckian-sized region C obeys

$$n_e(C) \lesssim 1 . \tag{4.10}$$

Indeed, it has been suggested that the black hole bound, at least for entanglement entropy, is saturated in de Sitter space [157].

We will take (4.10) to be approximately saturated, corresponding to $R(t_1) \approx \ell_p$, which leads to the loosest bound on the total duration of inflation: the quantum circuit picture then becomes valid once $R(C^H) \gtrsim \ell_p$. (We have not excluded the possibility that $R(t_1) \gg \ell_p$, in which case our description becomes valid only when $R(C^H) \gg \ell_p$, but this would lead to a tighter bound on the duration of inflation.) We thus find that

$$N(t_1, t_0) \lesssim -\ln(H_0\ell_p) \approx 140. \tag{4.11}$$

Our argument for this result has been fairly general; in the Appendix we discuss more specific assumptions about de Sitter entanglement that lead to tighter bounds.

Note that (4.11) bounds the total amount of inflationary and non-inflationary expansion between the time t_1, defined by the property that our comoving volume contains a single e-bit at $t = t_1$, and the present time t_0, with $n_e(t_0) \sim 10^{122}$. It does not directly limit expansion occurring before t_1 or after t_0, but as we discuss further below, our logic does lead to suggestive statements about these times.

Our bound on the total number of e-folds of expansion can be converted into one on the number of e-folds of inflation using standard cosmology. If reheating to a temperature $T_{\rm RH}$ is approximated as instantaneous, and occurs at a time $t_{\rm RH}$, the number of e-folds since reheating is

$$N_{\rm post} = \ln \frac{a(t_0)}{a(t_{\rm RH})} \,. \tag{4.12}$$

The scale factor is related to the temperature and the effective number of relativistic degrees of freedom g_{*S} via $a \propto g_{*S}^{-1/3} T^{-1}$. In the Standard Model, g_{*S} is of order 4 today, and of order 100 above the electroweak scale. We therefore have

$$N_{\rm post} \approx \ln \left(3 \frac{T_{\rm RH}}{T_0} \right) \tag{4.13}$$

$$= 65 + \ln(T_{\rm RH}/10^{15}\ {\rm GeV}) \,. \tag{4.14}$$

This expression only depends on the current CMB temperature, $T_0 = 2.25 \times 10^{-4}$ eV, and the expected entropy production in the Standard Model; it is independent of the equation of state of the universe since inflation. If inflation ends near the GUT scale, $T_{\rm RH} \sim 10^{15}$ GeV, our limit (4.11) implies that the total number of effective inflationary e-folds is bounded by

$$N_I = N_{\rm tot} - N_{\rm post} \lesssim 75 \,. \tag{4.15}$$

Lower reheating temperatures lead to weaker bounds on N_I, e.g. for $T_{\rm RH} \sim 10^5$ GeV we have $N_I \lesssim 98$.

In a model with a given reheating temperature $T_{\rm RH}$, solving the horizon problem requires

$$N_I \geq N_{\rm post} - \frac{1}{2} \ln(1 + z_{eq}) \approx N_{\rm post} - 4 \,, \tag{4.16}$$

with z_{eq} the redshift of matter-radiation equality. Thus, according to our bound (4.11), the number of inflationary e-folds since the time t_1 can exceed the number needed to solve the horizon problem by at most

$$N_{\rm extra} = 14 - 2\ \ln(T_{\rm RH}/10^{15}\ {\rm GeV}) \,. \tag{4.17}$$

The bound (4.11) is therefore compatible with solving the horizon problem via inflation occurring after the time t_1, but does not allow for much "unnecessary" inflation after t_1.

4.6 Details of the Quantum Circuit

A few features of our proposed quantum circuit deserve additional explanation. First of all, in our setup the initial state contains no entanglement. This is a highly non-generic situation, but is perfectly compatible with the empirical fact that our universe began in a state of very low entropy [160] – the von Neumann entropy of any subregion described by the initial state of the circuit will vanish. We do not attempt here to provide an explanation for this well-known cosmological fine-tuning, merely to model it.

Second, the circuit in Fig. 4.1 is constructed to describe our comoving region $C^H(t)$, but causal influences have entered $C^H(t)$ at various times in cosmic history. Such influences should be represented by the action of gates that entangle the qubits shown in Fig. 4.1 with qubits describing different degrees of freedom elsewhere: for example, an atom outside C^H might emit a photon that we detect. A more rigorously complete quantum circuit representing cosmological evolution would include gates describing such processes, which we are neglecting here. As discussed above, the entry of a a photon into our region does not change the dimensionality of our Hilbert space, though it does change the quantum state of our region.

What matters for our analysis is that the spacetime structure of our comoving region comes into being (interpreted semiclassically as "the universe expands") by entangling existing degrees of freedom within our Hilbert space, rather than by attaching additional degrees of freedom from outside. This is our answer to the questions posed in the introduction about the appearance of new modes as the universe expands. For cosmological evolution described by a finite-dimensional Hilbert space, the total number of degrees of freedom is always fixed. In essence, the quantum circuit picture presents a natural framework for the newly "created" modes to become entangled with the rest when they are no longer trans-Planckian, by modeling the process as ancillary qubits becoming entangled as time evolves.

The circuit picture provides a concrete, operational sense in which the condition that there should be at least one entangled degree of freedom can be made precise. Namely, no information about the spacetime is imparted by gates acting on qubits in our comoving region at times $t < t_1$. All entanglement that sources such information must be injected by unitaries that appear later in the circuit, i.e. at a time after the "beginning" of the universe.

We can ask how the quantum circuit picture applies to the future evolution of the universe. One the one hand, it is conceivable that we live in a universe near a late time de Sitter vacuum in which almost all of the $n = S/\ln 2$ degrees of freedom in the entire Hilbert space of our region are entangled, and all further time evolution simply increases the circuit complexity. It may then be possible to adopt the complexity picture where time evolution is directly defined by the growth of complexity [33].

On the other hand, it is also plausible that the current de Sitter phase is metastable, and can decay into a vacuum with a smaller (positive) cosmological constant, and so a larger entropy $S' > S$. We will not give a quantum circuit description of the associated tunneling process in this work. However, we remark that $(S' - S)/\ln 2$ additional ancilla qubits are required, and the gates that entangle them with the degrees of freedom of the false vacuum are different from those that describe exponential expansion within the false vacuum.

4.7 Discussion

We have proposed a quantum circuit picture for cosmological expansion. Our fundamental assumption was that expansion corresponds to the progressive entanglement of degrees of freedom that were initially unentangled. Time evolution corresponds to the application of quantum gates that create entanglement, and the amount of cosmic time elapsed since the unentangled initial state is determined by the circuit complexity. We posited that the total number of degrees of freedom in our Hubble volume is a finite number related to the area of the de Sitter horizon, and that the number of entangled degrees of freedom in a region with a geometric description can never be less than one.

This picture differs markedly from the conventional intuition based on quantum field theory in curved spacetime. In that context, the number of degrees of freedom (and hence the dimensionality of Hilbert space) is potentially infinite. In an effective description with a Planck-scale cutoff, new degrees of freedom are continually appearing as they expand from sub-Planckian to safely super-Planckian wavelengths. Our picture seems more compatible with the principles of unitary evolution (new degrees of freedom are never created) and holography (the total number of degrees of freedom is finite in a de Sitter universe).

In our approach, there is a general upper bound on the number of e-folds of cosmological expansion since the time t_1 when there was a single pair of entangled degrees of freedom in the comoving region that now coincides with our Hubble volume. The number of inflationary e-folds consistent with this bound is comfortably, but not parametrically, larger than what is needed to solve the horizon problem.

Our bound limits the total number of e-folds of expansion within our comoving patch, but our ignorance about the underlying theory of quantum gravity allows for potentially different global scenarios. If we take seriously the de Sitter entropy as telling us the dimensionality of the Hilbert space corresponding to our observable patch of spacetime, there are two possibilities. One is that this Hilbert space represents the entire universe; there is no larger multiverse described by additional degrees of freedom, and only the degrees of freedom in the bulk and on the boundary of de Sitter exist [112, 113, 115, 88]. In that case our bound is a straightforward limit on the total amount of expansion space can undergo before reaching its de Sitter equilibrium state.

The other possibility is that our observable patch represents only part of the universe, and its Hilbert space is just one part of a larger Hilbert space. In that case, the classical universe is much larger than what we observe. It follows that there could be many more e-folds of total expansion than what our bound indicates. However, even in that case our bound applies to the number of physically meaningful e-folds of expansion of our own space. Any additional expansion occurring before t_1 did not involve any of the degrees of freedom that currently constitute the spacetime geometry in our observable universe: at that early stage our degrees of freedom were completely unentangled, and the space that was then expanding now corresponds to regions outside our comoving volume. In this sense, our bound applies to the universe we see, even if the full theory describes additional degrees of freedom as well.

Our upper bound on inflationary e-folds is similar to a bound derived by Banks and Fischler [150]; see also [151, 152, 154]. Like ours, their bound comes from assuming that physics in a de Sitter patch is described by a finite-dimensional Hilbert space. Unlike us, they require that the quantum state be pure rather than mixed and that the de Sitter phase be absolutely stable, and their early-time constraint comes from insisting that physics be described by an effective quantum field theory, rather than insisting that the entangled spacetime structure contain at least one qubit. Our bounds are also numerically different, both because we do not invoke any assumptions about the equation of state at early times, and because we find a different scaling of the entropy with the number of e-folds. The bound due to Kaloper, Kleban, and Sorbo [151] is based on what an observer in de Sitter can conceivably measure, rather than on unitary quantum evolution by itself. That of Phillips, Scacco, and Albrecht [154] is derived within the framework of a de Sitter equilibrium picture [161], which again involves a slightly different set of fundamental assumptions. The spirit behind these various bounds is certainly similar; we believe that the one presented here is based on a simple set of explicit assumptions, and is unique in making direct reference to ancilla degrees of freedom gradually becoming entangled as space expands, but our logic is not incompatible with that of previous bounds.

There is also related work by Arkani-Hamed *et al.*, which proceeds from weaker assumptions than those we have invoked, and finds bounds exponentially weaker than our own [153]. Their analysis is different: they rely on the slow increase of entropy during slow-roll inflation, which follows from the gradual reduction of the energy density during that phase. They then obtain a bound involving the de Sitter entropy at the end of non-eternal inflation, which we may denote $S_{\mathrm{dS}}^{\mathrm{early}}$. Their logic is to place an upper bound on the number of modes detectable by a hypothetical future observer in a late-time phase with negligible cosmological constant, e.g. Minkowski space. We have instead considered an observer in a cosmology that has entered, or is entering, a late-time de Sitter phase (possibly but not necessarily metastable) with finite cosmological constant $\Lambda > 0$, and finite de Sitter entropy $S_{\mathrm{dS}}^{\mathrm{late}}$. Notice that our analysis allows $N_{\mathrm{tot}} \to \infty$ in the limit $\Lambda \to 0$. The bound of [153] (see also [162]) is

$$N_{\mathrm{tot}} \leq \frac{1}{12} S_{\mathrm{dS}}^{\mathrm{early}}, \tag{4.18}$$

while ours is

$$N_{\mathrm{tot}} \leq \ln\left(S_{\mathrm{dS}}^{\mathrm{late}}/\pi\right) . \tag{4.19}$$

Thus, our bound is compatible with, but quite different from, that of [153].

In closing, let us point out some possible applications of our picture. One advantage of describing time evolution through a quantum circuit is that one can in principle reverse the computation. As the quantum circuit we outlined in this work is a unitary circuit, one can imagine simply running it in reverse, with generic data about the quantum state today, to gain intuition about what generic states in the early universe could have looked like. This could be done either via Monte Carlo generation of the state of the current universe, or through some ansatz for the current entanglement. (Our circuit is meant to describe the full quantum state of the universe, not only the branch of the wave function we find ourselves on; details of the actual state are therefore unobservable to us.) This computation would of course require knowledge of the specific gates in the circuit. Performing the evolution backward in time by inverting each gate separately is in principle much simpler than inverting a generic unitary operator acting on the Hilbert space.

We stress that although the spacetime picture breaks down when the number of entangled qubits is not large, the circuit as a unitary picture does not. By an appropriate modification of the quantum circuit presented here one could aim to explore the initial state of inflationary perturbations, by characterizing how the degree of entanglement of the state evolves as a function of time. More ambitiously, entanglement in a phase where $n_e(t)$ is not large (but $n_e(t) > 1$) might provide a model for the chaotic conditions at nearly-Planckian densities, and for the emergence of inflating regions in this era. However, realizing these applications would require the development of a more detailed dictionary between entanglement and (quasi) de Sitter spacetimes.

The assumptions leading to our proposal are not secure beyond reasonable doubt, although they do seem to follow from plausible conjectures about holography and unitarity. Perhaps the most important lesson from this analysis is that phenomena in quantum gravity can be very different from our semiclassical intuition, in ways that can have important consequences for cosmology.

4.A Appendix

We arrived at the bound $N(t_1, t_0) \leq 140$ by means of relatively general assumptions. In this appendix we comment on how specific models for the emergence of de Sitter space from entanglement could lead to more restrictive bounds. These speculations are largely based on [82].

Two persistent difficulties in understanding de Sitter space from entanglement are the absence of a spatial boundary and the presence of de Sitter entropy. This entropy, and hence the number of entangled degrees of freedom (since de Sitter is supposed to be an equilibrium state), scales as the horizon area, whereas local bulk quantities naively scale as volumes. It therefore appears that one cannot assign quantum degrees of freedom locally to each subregion in de Sitter space, as many of these degrees of freedom would have to be shared non-locally to account for the sub-extensive scaling.

On the other hand, in order to be consistent with the picture presented in [82, 28, 65, 144], the entanglement entropy will also need to satisfy an approximate area law for local regions in order for Einstein gravity to emerge. This constrains the kind of structure we are allowed to consider in order to build up de Sitter space. For small regions, the entanglement has to be predominantly short-ranged, and satisfy an area law. However, on longer scales comparable to the Hubble radius, the dominant entanglement will be long-ranged, so that some of the quantum degrees of freedom that encode the geometry of such regions are shared non-locally. This picture of entanglement is similar to that presented in [163].

To start, we assume that the state from which de Sitter emerges allows us to define subregions of the emergent geometry. Consider a subregion A of linear size R in a Hubble patch of a de Sitter phase with Hubble constant H. We assume that the number $n_e(A)$ of quantum degrees of freedom that encode the geometric information of A is well-defined (even if one cannot necessarily localize all $n_e(A)$ degrees of freedom to the subregion), and that

$$n_e(A) \approx f_R(x) n_e(\mathrm{dS})\,. \tag{4.20}$$

Here we have some function $0 \leq f_R(x) \leq 1$, where $0 \leq (x = RH) \leq 1$ parametrizes the dimensionless ratio between the size of the subregion and that of the Hubble patch. The R-dependent functional form captures the transition of the scaling behaviour for the number of quantum degrees of freedom, which changes from volume law scaling to area law scaling when considering larger and larger regions. Correspondingly, the dominant form of entanglement in these regions transitions from short-ranged to long-ranged.

As such, it is reasonable to conjecture that

$$x^3 \leq f_R(x) \leq x^2, \tag{4.21}$$

which captures the area-to-volume transition. Now we can derive a bound on the duration of inflation. Let $x = R(t_1)/R(t_I)$, where t_1 marks the beginning of inflation, t_I is any time during the inflationary phase, and t_0 is the present. Then we have

$$n_e(t_1) \approx f_{R(t_1)}(x) \frac{\pi R(t_I)^2}{\ell_p^2 \ln(2)} \leq x^2 \frac{\pi R(t_I)^2}{\ell_p^2 \ln(2)} = \frac{\pi R(t_0)^2 e^{-2N(t_1,t_0)}}{\ell_p^2 \ln 2}, \tag{4.22}$$

where we have used $R(t_I) \sim H(t_I)^{-1} = H(t_1)^{-1}$. Combining (4.22) and assumption (iv), we have

$$N(t_1, t_0) \leq \frac{1}{2} \log \frac{\pi R(t_0)^2}{\ell_p^2 \ln(2)} \approx 140. \tag{4.23}$$

However, if the form of $f_R(x)$ were known, e.g. from a model of a de Sitter tensor network, the transition function could be explicitly evaluated. For instance, suppose we obtained $f_R(x) = x^{q(R)}$ for some $q(R)$ such that (4.21) is satisfied. Then we could write

$$N(t_1, t_0) \leq \frac{2-q}{q} \ln \frac{R(t_I)}{\ell_p} + \ln \frac{R(t_0)}{\ell_p} + \frac{1}{q} \ln \frac{\pi}{\ln 2} \approx 140 - \frac{q-2}{q} \ln \frac{R(t_I)}{\ell_p}, \quad (4.24)$$

which is sensitive to the inflationary scale and to the entanglement structure of de Sitter. Because $R(t_I) \geq \ell_p$ by (iii) and (iv), we see that for $q(R)$ between 2 and 3, (4.24) yields a potentially tighter bound.

For instance, following the arguments in [163], let us assume a $q = 3$ relation. Then we find that

$$N(t_1, t_0) \approx -\ln(H_0 \ell_p) + \frac{1}{3} \ln(H(t_1)\ell_p) + \frac{1}{3} \ln\left(\frac{\pi}{\ln 2}\right). \quad (4.25)$$

Observational upper limits on primordial tensor modes [164] give an upper bound $H(t_{CMB})\ell_p \leq 5 \times 10^{-6}$ on the Hubble scale at the time t_{CMB} when the modes visible at large angular scales in the CMB exited the inflationary horizon. Because $t_1 < t_{CMB}$ in general, we cannot directly bound $H(t_1)$ from observations: the inflationary energy could have diminished noticeably between t_1 and t_{CMB}. But if we could exclude a rapid decrease in energy over that interval — perhaps through limits on the scale-dependence of the scalar and tensor power spectra — and so have $H(t_1) \sim H(t_{CMB})$, the bound (4.25) would read

$$N(t_1, t_0) \lesssim 140 + \frac{1}{3} \ln(5 \times 10^{-6}) = 136\,. \quad (4.26)$$

For inflation that ends near the GUT scale, $T_{\text{RH}} \sim 10^{15}$GeV, we would have $N_I \lesssim 71$. Lower reheating temperatures lead to weaker bounds on N_I, e.g. for $T_{\text{RH}} \sim 10^5$GeV we have $N_I \lesssim 98$.

Chapter 5

ENTROPY INEQUALITIES FOR AREA-LAW SYSTEMS

For gapped phases of many local Hamiltonians, the low energy states of the system satisfy an area law scaling of entanglement entropy. To characterize the entanglement structure of such systems, we determine the linear entropy inequalities satisfied by systems for an arbitrary number of subsystems. To leading order, where the entropy satisfies an exact area law, we fully characterize the entanglement entropy cone of any number of systems. In particular, we find that all holographic entropy inequalities found in [165] are also valid in such systems. In gapped systems with topological order, the "cyclic inequalities" derived recently for the holographic entanglement entropy generalize the Kitaev-Preskill formula for the topological entanglement entropy. Finally, we propose a candidate linear inequality

$$\begin{aligned} &S(ABD) + S(ABC) + S(BCD) - 2S(BD) - 2S(BC) + S(CD) - S(AD) \\ &- S(AC) - S(AB) + 2S(B) + S(A) \le 0 \end{aligned}$$

for general 4-party quantum states.

This chapter is based on the Ref:
Ning Bao, ChunJun Cao, Michael Walter, and Zitao Wang. "Holographic entropy inequalities and gapped phases of matter". In: JHEP *09 (2015), p. 203.* DOI: `10.1007/JHEP09(2015)203`. *arXiv:* `1507.05650 [hep-th]`.

5.1 Introduction

In recent years, the study of quantum entanglement and quantum information in general has produced a myriad of applications in high energy physics and condensed matter physics. A key tool for the quantification of entanglement is, in particular, the entanglement entropy. For general quantum systems, the von Neumann entanglement entropies of subsystems are known to obey subadditivity, the Araki-Lieb inequalities, weak monotonicity, and strong subadditivity, respectively:

Subadditivity:

$$S(A) + S(B) - S(AB) \ge 0. \tag{5.1}$$

Araki-Lieb:

$$S(C) + S(ABC) - S(AB) \geq 0. \tag{5.2}$$

Weak Monotonicity:

$$S(AB) + S(AC) - S(B) - S(C) \geq 0. \tag{5.3}$$

Strong Subadditivity:

$$S(AB) + S(AC) - S(A) - S(ABC) \geq 0. \tag{5.4}$$

Such inequalities are important, as they constrain the phase space of entanglement in quantum systems and can in turn be translated into other physical quantities. In particular, in condensed matter physics there exists a conjectured relationship [167, 168] between the existence of a gap in a system and whether or not the entanglement entropy in that system obeys an area law [169]. It therefore seems a fruitful direction to explore and better characterize the properties of the entanglement entropy in quantum-mechanical systems.

It should be noted, however, that entropy inequalites for general quantum states are relatively rare; indeed, (5.1)–(5.4) are the only unconditional entropy inequalities known to date. Luckily, there exist classes of quantum systems for which the entanglement entropy is easier to characterize.

5.1.1 Entropy inequalities from holography

In holography, it has been shown that entanglement entropies of regions on the boundary are equal to the areas of the minimal surfaces subtending the boundary region, or in terms of the celebrated Ryu-Takayanagi formula [23, 64]:

$$S(A) = \frac{\text{Area}}{4G}. \tag{5.5}$$

The Ryu-Takayanagi formula gives us a powerful new tool for computing entanglement entropies in regimes where such calculations are usually intractible. In higher dimensions, for example, it turns what would be a difficult (if not impossible) conformal field theory calculation into a straightforward minimization of area in a classical metric.

Interestingly, these holographic entenglement entropies obey a larger set of inequalities than those obeyed by the generic quantum mechanical systems. In [170], it was discovered that, indeed, there is a new entanglement entropy inequality which is true for all systems with semi-classical holographic duals, i.e., the conditional mutual information is monogamous, or

$$S(AB) + S(AC) + S(BC) \geq S(A) + S(B) + S(C) + S(ABC). \tag{5.6}$$

This was done using a method known as inclusion/exclusion, in which minimal surfaces corresponding to the (positively signed) entropic terms on the left hand side are repartitioned into non-minimal surfaces corresponding to the terms on the right hand side. As non-minimal surfaces have more area than minimal surfaces, if such a partitioning can be done, then the inequality is true. A more detailed description of the methodology is available in [170]. Recently, this has also been generalized to higher numbers of regions in [171] by converting the geometric procedure described above to a combinatoric set of contraction mappings from points on a hypercube, which corresponds to the left hand side entanglement entropies, to points on another hypercube, which corresponds to the right hand side entropies. This new method has yielded a new, infinite family of inequalities that has been proven for holographic systems. These so-called "cyclic" inequalities for $n = 2k + 1$ subsystems take the form

$$\begin{aligned} \mathrm{CYC} &= \sum_{l=1}^{k-1} I(A_1 ... A_l : A_{k+l+1} : A_{k+l+2} ... A_{2k+1}) - \sum_{j=1}^{k} I(A_1 ... A_j : A_{j+1} ... A_{j+k} : A_{j+k+1}) \\ &= \sum_{i=1}^{n} S(A_i | A_{i+1} \dots A_{i+k}) - S(A_1 \dots A_n) \geq 0, \end{aligned} \tag{5.7}$$

where $I(A : B : C) = S(A) + S(B) + S(C) - S(AB) - S(AC) - S(BC) + S(ABC)$ and $S(X|Y) = S(XY) - S(Y)$ is the conditional entropy. This new generalization has also led to the discovery of several further holographic entropy inequalities [171].

Holographic systems are not the only class of quantum systems that obey a more restrictive set of entanglement entropy inequalities. The set of stabilizer states in quantum error correction does so, as well [172, 173, 174]. It is interesting, however, that the known stablizer inequalities are implied by (weaker than) the holographic inequalities, thus suggesting a nontrivial relationship between these two types of states.

It is important to note that the utilization of holography in the inclusion-exclusion proof technique is actually quite minimal. Instead, holographic entropy inequalities are reduced to linear inequalities between the areas of boundaries of certain bulk regions. However, these inequalities are then proved for arbitrary bulk regions, not only for those that minimize the Ryu-Takayanagi entropy. As suggested in [171], it is therefore natural to expect that they hold likewise in condensed matter systems that satisfy an area law. The exploration of this idea, and the applicability of the resulting inequalities for other condensed matter systems, will be the focus of the remainder of this work. As any system with an exact area law entropy scaling necessarily satisfies these entropy inequalities, they may also provide further indication, particularly in the direction of falsification, as to whether a gapped system indeed implies area law scaling for entanglement entropy.

Another potentially interesting relationship here is to the field of AdS/CMT [175, 176]; as we will see, the entanglement entropies for gapped phases of matter with an exact area scaling obey the constraints of general holographic systems, which is suggestive of possibly nontrivial holographic duals of condensed matter systems.

5.1.2 Organization

In this work we extend and characterize the realm of applicability of the holographic entanglement entropy inequalities to condensed matter systems. The organization of the paper will be as follows: In section 5.2, we formally prove the validity of the cyclic inequalities for systems that obey an exact area law. In section 5.3, we show that these inequalities have a valid interpretation as the topological entanglement entropy in two spatial dimensions. In section 5.4, we fully characterize the entanglement entropy in systems satisfying an exact area law, and we give a minimal and complete set of entropy inequalities and equalities for any fixed number of regions. We comment about the analogous problem for general quantum system and propose a candidate inequality for four-partite quantum systems. Finally, we conclude in section 6.6.

5.2 Gapped systems with trivial topological order

Here we consider gapped systems with trivial topological order in d+1 dimensions. The entanglement entropy $S(A)$ of a subsystem A, which measures the entanglement between A and its complement A^c, is defined to be the von Neumann entropy

$$S(A) \equiv -\operatorname{tr} \rho_A \log \rho_A, \tag{5.8}$$

where ρ_A is the reduced density operator for A obtained by tracing out all degrees of freedom outside of A in the many-body ground state of the gapped system.

Note that for a bipartite system in a pure state, the reduced density operators obtained by tracing out either part have the same set of eigenvalues, hence the same von

Neumann entropy, which can be seen via a Schmidt decomposition [128] of the pure state that we started with. This implies that for any division of the system into subsystems A and its complement A^c,

$$S(A) = S(A^c) \tag{5.9}$$

is satisfied.

For gapped systems with trivial topological order, we assume that the entanglement entropy $S(A)$ of a subsystem A scales as the area of its boundary and neglect any sub-area scaling for the moment. Namely,

$$S(A) \sim \partial A. \tag{5.10}$$

Note that for any two regions A and B in d spatial dimensions that are non-overlapping except possibly at their boundaries, the entanglement entropy of the combined region AB satisfies

$$S(AB) \sim \partial(AB) = \partial A + \partial B - 2A \cap B. \tag{5.11}$$

Here $A \cap B$ denotes the area of the codimension 1 hypersurface where regions A and B intersect. The above follows from (5.10) because for any d-dimensional regions A, B, and C, the triple intersection $A \cap B \cap C$ is of measure zero.

We claim that the cyclic inequality (5.7) for $n = 2k + 1$ regions is satisfied as a strict equality in this system, namely

$$\sum_{i=1}^{n} S(A_i | A_{i+1} \dots A_{i+k}) = S(A_1 \dots A_n), \tag{5.12}$$

where the sum is cyclic and all indices are taken modulo n. To prove (5.12), we compute:

$$\begin{aligned}
\text{LHS} \sim & \sum_{i=1}^{n} \partial(A_i \dots A_{i+k}) - \partial(A_{i+1} \dots A_{i+k}) \\
= & \sum_{i=1}^{n} \left\{ \partial A_i - \sum_{\substack{\{j_1, j_2\} \\ j_1, j_2 \in Q_0}} 2A_{j_1} \cap A_{j_2} - \sum_{\substack{\{j_1, j_2\} \\ j_1, j_2 \in Q_1}} 2A_{j_1} \cap A_{j_2} \right\} \\
= & \partial A_1 + \dots + \partial A_n - \sum_{i=1}^{n} \sum_{j \in Q_0} 2A_i \cap A_j, \\
\text{RHS} \sim & \partial(A_1 \dots A_n) \\
= & \partial A_1 + \dots + \partial A_n - \sum_{\substack{\{j_1, j_2\} \\ j_1, j_2 \in \mathcal{N}}} 2A_{j_1} \cap A_{j_2},
\end{aligned}$$

where $Q_l = \{i + l, \ldots, i + k\}$, $\mathcal{N} = \{1, \ldots, n\}$ and $\{j_1, j_2\}$ are unordered pairs that take on the indicated values. Hence to prove that LHS = RHS, we need to show that

$$\sum_{\substack{\{j_1,j_2\} \\ j_1,j_2 \in \mathcal{N}}} A_{j_1} \cap A_{j_2} = \sum_{i=1}^{n} \sum_{j \in Q_0} A_i \cap A_j. \tag{5.13}$$

The LHS sums over $n(n+1)/2 = (k+1)(2k+1)$ distinct unordered pairs of indices $\{j_1, j_2\}$, so it contains $(k+1)(2k+1)$ distinct terms. The summation on the RHS also contains $(k+1)(2k+1)$ terms. So in order to prove that LHS = RHS, it suffices to prove that any term appearing in the summation on the LHS also appears in the summation on the RHS. This is equivalent to proving that for any unordered pair $\{j_1, j_2\}$, $j_1, j_2 \in \{1, \ldots, n\}$, there exists $i \in \{1, \ldots, n\}, j \in \{i, \ldots, i + k\}$, such that $\{j_1, j_2\} = \{i, j\}$.

We have the following two cases:

1. $j_2 \in \{j_1, \ldots, j_1 + k\}$. In this case, we just take $i = j_1, j = j_2$.

2. $j_2 \notin \{j_1, \ldots, j_1 + k\}$. In this case, if $j_1 \notin \{j_2, \ldots, j_2 + k\}$, then $\{j_1, \ldots, j_1 + k\} \cap \{j_2, \ldots, j_2 + k\} = \emptyset$, otherwise $j_1 + h_1 = j_2 + h_2$, for some $h_1, h_2 \in \{1, \ldots, k\}$. Therefore, either $j_1 = j_2 + h_2 - h_1$, or $j_2 = j_1 + h_1 - h_2$. Since either $h_1 - h_2 \in \{1, \ldots, k\}$, or $h_2 - h_1 \in \{1, \ldots, k\}$, we are forced to conclude that either $j_2 \in \{j_1, \ldots, j_1 + k\}$, or $j_1 \in \{j_2, \ldots, j_2 + k\}$. Both lead to contradictions. So if $j_2 \notin \{j_1, \ldots, j_1 + k\}$, and if $j_1 \notin \{j_2, \ldots, j_2 + k\}$, then $\{j_1, \ldots, j_1 + k\} \cap \{j_2, \ldots, j_2 + k\} = \emptyset$. Since each set contains $k + 1$ distinct numbers, and if their intersection is empty, their union would contain $2k + 2$ distinct numbers, contradicting $n = 2k + 1$. Thus we finally arrive at the conclusion that $j_2 \notin \{j_1, \ldots, j_1 + k\} \implies j_1 \in \{j_2, \ldots, j_2 + k\}$. In this case, we just take $i = j_2, j = j_1$.

Combining cases 1 and 2, we conclude that for any unordered pair $\{j_1, j_2\}$, $j_1, j_2 \in \{1, \ldots, n\}$, there exists $i \in \{1, \ldots, n\}, j \in \{i, \ldots, i + k\}$, such that $\{j_1, j_2\} = \{i, j\}$. Hence (5.13) indeed holds and (5.12) is exactly satisfied by such systems.

In section 5.4 below, we will generalize this result and identify *all* entropy inequalities and equalities that are obeyed in systems with an exact area-law scaling. We will find that any holographic entropy inequality is valid for systems with an exact area law.

5.3 Topological entanglement entropy

5.3.1 Construction and validity

Here we consider general gapped systems in 2 + 1 dimensions. It is shown in [177, 178, 179] that the entanglement entropy of a region A with smooth boundary has the form

$$S_A = \alpha L - b_0 \gamma \tag{5.14}$$

in the limit $L/a \to \infty$ where a is the correlation length. Here b_0 denotes the number of connected components of ∂A, the boundary of region A. The topological entanglement entropy $-\gamma$ is a universal constant characterizing the topological state and α is a non-universal and ultraviolet divergent coefficient dependent on the short wavelength modes near the boundary of region A. In particular, $\gamma = \log \mathcal{D}$ captures the far-IR behaviour of entanglement and the total quantum dimension, $\mathcal{D}$, which can be obtained from topological quantum field theory computations, is related to the number of superselection sectors of the system[177].

We divide the plane into $2k + 2$ regions, labeled by $A_0, A_1, A_2, \ldots, A_{2k+1}$, where A_0 labels the complement of $A_1 A_2 \ldots A_{2k+1}$, i.e., $A_0 \equiv (A_1 A_2 \ldots A_{2k+1})^c$. In order for the topological entropy S_{topo} defined in (5.16) to be a topological invariant, we require the division of the plane to satisfy

$$\bigcap_{i \in I} A_i = \emptyset, \text{ for all } I \subset \{0, 1, 2, \cdots, 2k+1\}, \text{such that } 0 \in I, \text{and } |I| > 3. \tag{5.15}$$

In other words, there is no point on the plane that is shared by A_0 and more than two other regions. We define the topological entropy S_{topo} for $2k + 2$ regions as

$$S_{\text{topo}} \equiv \sum_{i=1}^{2k+1} S(A_i | A_{i+1} \ldots A_{i+k}) - S(A_1 \ldots A_{2k+1}), \tag{5.16}$$

where all indices are taken modulo $(2k+1)$. Note that our definition of the topological entropy reduces to the Kitaev-Preskill one [177] when $k = 1$ (i.e., a division of the plane into 4 regions). Also note that our calculation in section 5.2 implies that for gapped systems with trivial topological order, $S_{\text{topo}} = 0$, that is, the dependence of S_{topo} on the length of the boundaries cancels out.

To see that S_{topo} is a topological invariant, consider deforming the boundary between regions labeled by the index set $J \subset \{0, 1, 2, \ldots, 2k+1\}$, i.e., points in the set

$$S \equiv \bigcap_{j \in J} A_j .$$

We note the following properties of the entanglement entropy before proceeding to the main arguments:

- Under general deformations of the plane, the change in the entanglement entropy of any region A, $\Delta S(A)$, is equal to the change in the entanglement entropy of the complement of A, $\Delta S(A^c)$. This follows as a consequence of (5.9).
- For any $k \notin J$, points of deformation (points in S) are far from A_k. Therefore, we expect $\Delta S(A_k) = 0$, provided that all regions are large compared to the correlation length. In the same spirit, $\Delta S(A) = 0$ for any region A that is a union of such A_k's. It then follows if A is appended to any region B, the change in entanglement of that region is unaffected, namely, $\Delta S(B \cup A) = \Delta S(B)$.

Now we argue for the topological invariance of S_{topo}. Possible deformations of the regions are classified into the following two cases:

1. $0 \notin J$. In this case,

$$\begin{aligned}
\Delta S_{\text{topo}} &= \sum_{i=1}^{2k+1} [\Delta S(A_i A_{i+1} \dots A_{i+k}) - \Delta S(A_{i+1} \dots A_{i+k})] - \Delta S(A_1 \dots A_{2k+1}) \\
&= \sum_{i=1}^{2k+1} [\Delta S((A_i A_{i+1} \dots A_{i+k})^c) - \Delta S(A_{i+1} \dots A_{i+k})] - \Delta S((A_1 \dots A_{2k+1})^c) \\
&= \sum_{i=1}^{2k+1} [\Delta S(A_0 A_{i+1+k} A_{i+2+k} \dots A_{i+2k}) - \Delta S(A_{i+1} \dots A_{i+k})] - \Delta S(A_0) \\
&= \sum_{i=1}^{2k+1} \Delta S(A_{i+1+k} A_{i+2+k} \dots A_{i+2k}) - \sum_{i=1}^{2k+1} \Delta S(A_{i+1} \dots A_{i+k}) \\
&= \sum_{i=1}^{2k+1} \Delta S(A_{i+1} A_{i+2} \dots A_{i+k}) - \sum_{i=1}^{2k+1} \Delta S(A_{i+1} \dots A_{i+k}) = 0,
\end{aligned}$$

   where in the last step, we cyclically left permute the summands in the first summation by k steps, which leaves the summation invariant.

2. $0 \in J$. In this case, by condition(5.15), we can either have $|J| = 2$ or $|J| = 3$.

a) $|J| = 2$. Denote the only nonzero element in J as j. In this case,

$$\begin{aligned}\Delta S_{\text{topo}} =& \Delta S(A_j A_{j+1} \dots A_{j+k}) + \Delta S(A_{j-1} A_j \dots A_{j+k-1}) + \cdots \\ &+ \Delta S(A_{j-k} A_{j-k+1} \dots A_j) - \Delta S(A_j A_{j+1} \dots A_{j+k-1}) \\ &- \Delta S(A_{j-1} A_j \dots A_{j+k-2}) - \cdots - \Delta S(A_{j-k+1} A_{j-k+2} \dots A_j) \\ &- \Delta S(A_1 A_2 \dots A_{2k+1}) \\ =&(k+1)\Delta S(A_j) - k\Delta S(A_j) - \Delta S(A_j) = 0.\end{aligned}$$

b) $|J| = 3$. Denote the nonzero elements in J as j_1 and j_2. Moreover, since $j_1, j_2 \in \{1, 2, \cdots, 2k+1\}$, $|j_1 - j_2| \leq k$, i.e., they are separated by a distance of at most k (note j_1, j_2 are mod $(2k+1)$ integers). Without loss of generality, we assume $j_2 = j_1 + l$, for some $0 < l \leq k$. We further write j_1 as j for simplicity. In this case,

$$\begin{aligned}\Delta S_{\text{topo}} =& \Delta S(A_j \dots A_{j+l} \dots A_{j+k}) + \cdots + \Delta S(A_{j+l-k} \dots A_j \dots A_{j+l}) \\ &+ \Delta S(A_{j+l-k-1} \dots A_j \dots A_{j+l-1}) + \cdots + \Delta S(A_{j-k} A_{j-k+1} \dots A_j) \\ &+ \Delta S(A_{j+l} A_{j+l+1} \dots A_{j+l+k}) + \cdots + \Delta S(A_{j+1} \dots A_{j+l} \dots A_{j+k+1}) \\ &- \Delta S(A_j \dots A_{j+l} \dots A_{j+k-1}) - \cdots - \Delta S(A_{j+l-k+1} \dots A_j \dots A_{j+l}) \\ &- \Delta S(A_{j+l-k} \dots A_j \dots A_{j+l-1}) - \cdots - \Delta S(A_{j-k+1} A_{j-k+2} \dots A_j) \\ &- \Delta S(A_{j+l} A_{j+l+1} \dots A_{j+l+k-1}) - \cdots - \Delta S(A_{j+1} \dots A_{j+l} \dots A_{j+k}) \\ &- \Delta S(A_1 A_2 \dots A_{2k+1}) \\ =&(k-l+1)\Delta S(A_j A_{j+l}) + l\Delta S(A_j) + l\Delta S(A_{j+l}) \\ &- (k-l)\Delta S(A_j A_{j+l}) - l\Delta S(A_j) - l\Delta S(A_{j+l}) - \Delta S(A_j A_{j+l}) = 0.\end{aligned}$$

To see that S_{topo} is a universal quantity, we consider the same argument in [177], where a smooth deformation of the local Hamiltonian during which no quantum critical points are encountered. Since the Hamiltonian is local, any smooth deformations of the Hamiltonian can be written as a sum of smooth deformations of local terms. Moreover, by utilizing the topological invariance of S_{topo}, we may deform the regions in the following ways while keeping S_{topo} invariant:

- Stretch the boundaries of the regions so that $L \to \infty$, and the entanglement entropy of a region takes the form of (5.14).
- Deform the boundaries of the regions so that all deformation of the Hamiltonian happens locally in the bulk of the regions.

We further assume that the correlation length remains small compared to the size of the regions throughout the deformation. Hence any local deformations of the Hamiltonian in the bulk only has miniscule effects for the ground state near the boundary. As a result, the entanglement entropies of the deformed regions (and hence S_{topo}) should not be affected by such local deformations of the Hamiltonian.

Thus we conclude that the topological entropy we defined in (5.16) is both a topological invariant (invariant under deformations of the boundary of the regions that keep the topology of the regions unchanged) and a universal quantity (invariant under smooth deformations of the Hamiltonian during which no quantum critical points are encountered).

For a general division of the plane into $2k+2$ regions that satisfies condition (5.15), we can compute the topological entropy:

$$S_{\text{topo}} = -\gamma\Big\{\sum_{i=1}^{2k+1}\Big(b_0[\partial(A_i \ldots A_{i+k})] - b_0[\partial(A_{i+1} \ldots A_{i+k})]\Big) + b_0[\partial(A_1 \ldots A_{2k+1})]\Big\}, \tag{5.17}$$

where all indices are taken modulo $(2k + 1)$, and $b_0[\partial A]$ denotes the zeroth Betti number (the number of connected components) of the boundary of a region A.

Hence S_{topo} is proportional to the topological entanglement entropy $-\gamma$, with the proportionality constant determined by the topology of the regions. This implies that we can extract the topological entanglement entropy of a $2 + 1$ dimensional topologically ordered system with a mass gap by suitably divide the system into $2k + 2$ regions, and compute the topological entropy S_{topo}.

5.3.2 Examples

Here we consider a few examples which elucidate some of the general constructions in section 5.3.1. Figures 5.1 and 5.2 illustrate two possible divisions of the plane into $2k + 2$ regions that satisfy condition (5.15).

There are three types of deformations to the regions for both divisions. We consider the change in S_{topo} under such deformations.

First, consider deforming the boundary between two regions in figures 5.1 and 5.2. This can either be the boundary between two slices of the pie, say A_1 and A_2, or the boundary between a slice of the pie and the complement of the pie, say A_1 and A_0. In the former case, region A_0 is not involved in the deformation, so case 1 of our general analysis for the topological invariance of S_{topo} implies that $\Delta S_{\text{topo}} = 0$.

In the latter case, there is one more region (A_1) besides A_0 that are involved in the deformation, so case 2a of our general analysis implies $\Delta S_{\text{topo}} = 0$.

Next, consider deforming a triple point where three regions meet. Without loss of generality, consider the three regions A_1, A_2 and A_0. There are two more regions (A_1 and A_2) besides A_0 that are involved in the deformation, so case 2b of our general analysis implies that $\Delta S_{\text{topo}} = 0$.

Note that for the division in figure 5.1, one could also deform the center of the pie chart, which is seemingly different from other points in the plane. All $2k+1$ regions but A_0 are involved in the deformation. However, since A_0 is not involved, case 1 of our general analysis still applies in this case, and $\Delta S_{\text{topo}} = 0$.

To compute the topological entropy S_{topo} for these two divisions, we apply the general formula (5.17). For pie-chart divisions in figures 5.1 and 5.2,

$$b_0[\partial(A_i \dots A_{i+k})] = b_0[\partial(A_{i+1} \dots A_{i+k})] = 1;$$

therefore the summation in (5.17) gives zero, and one simply counts b_0 for the boundary of the union of all $2k+1$ regions, which yields $-\gamma$ and -2γ respectively.

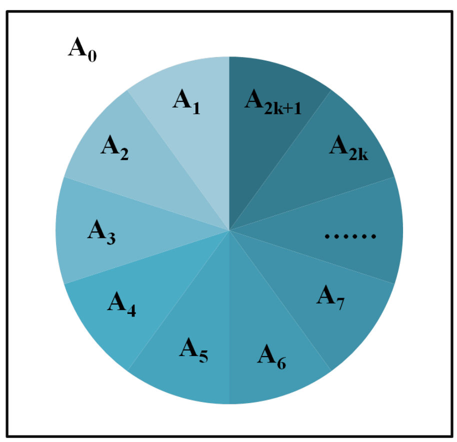

Figure 5.1: A pie-chart division of the plane into $2k+2$ regions, labeled by $A_0, A_1, \dots, A_{2k+1}$.

5.3.3 Beyond area-law scaling

In the above sections, we have considered systems where the entanglement entropy is in the form of (5.14). In general, (5.14) will be supplemented with various corrections. We here consider a few examples and examine the behavior of the topological entropy (5.16) as a function of k in systems that deviate from exact area-law scaling.

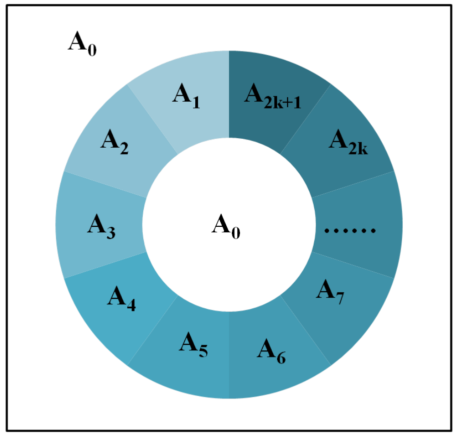

Figure 5.2: A pie-chart division of the plane into $2k + 2$ regions, with a hole in the middle, labeled by $A_0, A_1, \ldots, A_{2k+1}$.

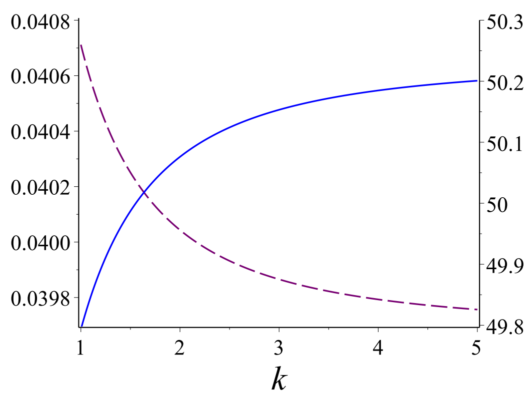

Figure 5.3: For systems that deviate from exact area law, the general behaviors of corrections to S_{topo} in the forms of $1/\ell$ and $\ell \log \ell$ are sketched in purple and blue respectively (color online) for $R = 10$. The numerical values are up to some unknown constant of order ϵ or β.

Since the correction leads to imperfect cancellation of the local contributions to entanglement entropy, (5.16) thus yields the topological entropy up to some local correction factors. For the following examples, we restrict ourselves to the pie-chart division in 2 + 1 dimensions in figure 5.1 with radius R in units of the lattice size a. For the sake of simplicity, the $2k + 1$ slices are divided evenly.

For a generic 2 + 1 dimensional gapped system with non-trivial topological order, the entanglement entropy of some region A with perimeter L large compared to the correlation length is given by

$$S_A = \alpha L - b_0 \gamma + \frac{\beta_1}{L} + \frac{\beta_3}{L^3} + \cdots, \tag{5.18}$$

where the correction from (5.14) assumes the form of β_p / L^p, for all odd integers p.

The $\mathcal{O}(L^{-p})$ correction to the topological entropy (5.16) is given by

$$\Delta S^{p}_{\text{topo}} = \frac{\beta_p}{(2\pi R)^p}\Big\{(2k+1)^{p+1}\Big(\frac{1}{(x+1)^p} - \frac{1}{x^p}\Big) - 1\Big\}, \tag{5.19}$$

where $x = (1+2/\pi)k + 1/\pi$. For $k \geq 1$, $(\partial|\Delta S^{p}_{\text{topo}}|/\partial k) < 0$ for each p. The higher k expressions are therefore slightly less sensitive to deviations of the local piece from perfect area-law scaling.

More generally, we may consider entropy scaling $S_A = \alpha L - \gamma + \epsilon f(L/a)$ where we recast other small deviations in the local piece of entanglement entropy into the form of $f(L/a)$. Let $\ell = L/a$ for a lattice with spacing a, we here briefly sketch the behaviors for corrections $f(\ell) = \log(\ell)$ and $f(\ell) = \ell\log(\ell)$ [180, 181]. Note that near criticality[181], $\ell\log(\ell)$ scaling becomes dominant in the local piece of entanglement entropy. For systems sufficiently far from a phase transition, we can treat them as an order ϵ correction in the area-law systems.

For $f(\ell) = \log(\ell)$,

$$\Delta S_{\text{topo}} = \epsilon \log\Big\{\frac{1}{2\pi R}\Big(1 + \frac{1}{x}\Big)^{2k+1}\Big\}, \tag{5.20}$$

where $x = (1+2/\pi)k + 1/\pi$.

And for $f(\ell) = \ell\log(\ell)$,

$$\Delta S_{\text{topo}} = \epsilon \log\Big\{\frac{1}{(2\pi R)^{2\pi R}}\Big(\frac{(2R + \frac{2\pi}{2k+1}(k+1)R)^{2R+\frac{2\pi}{2k+1}(k+1)R}}{(2R + \frac{2\pi}{2k+1}kR)^{2R+\frac{2\pi}{2k+1}kR}}\Big)^{2k+1}\Big\}. \tag{5.21}$$

In such cases, $(\partial|\Delta S_{\text{topo}}|/\partial k) > 0$ for regions with boundary much larger than the correlation length. which renders higher k definitions of the topological entropy S_{topo} more sensitive to local corrections to entanglement entropy. In principle, for some realistic condensed matter system with non-trivial topological order, the generalized definition (5.16) offers a wider range of selection where one can choose the optimal k for purposes of studying both the topological entanglement entropy and local deviations from area-law scaling.

5.4 All entropy inequalities for systems with an exact area law

We will now derive the full set of constraints satisfied by the entanglement entropy in systems with an exact area law, $S(A) \sim \partial A$. We begin with a useful construction from [171] that allows us to reduce from continuous geometries to a combinatorial problem. For simplicity, we shall assume that the system lives on a manifold without boundary.

Let $A_1, \ldots, A_n$ be disjoint (apart from their boundaries) regions in a system with an exact area law. We introduce the purifying region A_{n+1} as the closure of $(A_1 \cup \cdots \cup A_n)^c$. The entropy of an arbitrary composite region $A_I = \bigcup_{i \in I} A_i$ for $I \subseteq [n+1] := \{1, \ldots, n+1\}$ can then be evaluated in the following way,

$$S(A_I) \sim \partial A_I = \sum_{i \in I, j \in I^c} \partial A_i \cap \partial A_j,$$

where I^c denotes the complement of I in $[n+1]$.

We now consider the undirected complete graph on $n+1$ vertices, equipped with the edge weights $w(i,j) = \partial A_i \cap \partial A_j$. Let $w(I,J) = \sum_{i \in I, j \in J} w(i,j)$ denote the total weight of all edges between two disjoint subsets I and J, and $\delta(I) = w(I, I^c)$ the *cut function*. Then it follows from the above that

$$S(A_I) \sim \partial A_I = \delta(I).$$

Conversely, for any given undirected graph with non-negative edge weights we can always construct a geometry and associated regions $A_1, \ldots, A_{n+1}$ such that $\partial A_I = \delta(I)$ (cf. [171]). Therefore, proving entropy inequalities for systems with an exact area law is completely equivalent to proving linear inequalities for the cut function.

To determine if a linear inequality

$$\sum_I c_I \, \delta(I) \geq 0 \tag{5.22}$$

holds for the cut function in an arbitrary undirected weighted graph, we expand:

$$\sum_I c_I \, \delta(I) = \sum_I c_I \, w(I, I^c) = \sum_I c_I \sum_{i \in I, j \in I^c} w(i,j) = \sum_{i \neq j} w(i,j) \sum_{I : i \in I, j \notin I} c_I = \sum_{\{i,j\}} w(i,j) \sum_{I : i \in I \text{ xor } j \in I} c_I.$$

In the last step, the outer sum is over edges of the undirected graph. Since the edge weights $w(i,j)$ are arbitrary non-negative numbers, this immediately implies that the inequality (5.22) is valid if and only if

$$\sum_{I : i \in I \text{ xor } j \in I} c_I \geq 0 \tag{5.23}$$

for any edge $\{i,j\}$. Note that (5.23) asserts simply that the inequality (5.22) holds for the graph with a single edge $\{i,j\}$ of edge weight 1, since the cut function in this case is given by

$$(\beta_{ij})_I := \delta(I) = \begin{cases} 1 & i \in I \text{ xor } j \in I \\ 0 & \text{otherwise} \end{cases}. \tag{5.24}$$

But note that β_{ij} are precisely the entropies of a Bell pair shared between subsystems i and j in an $(n+1)$-partite pure state. In view of our reduction from systems with an exact area law to graphs, we thus obtain the following result:

Lemma 5.4.1. *An entropy inequality $\sum_{I\subseteq[n]} c_I\, S(A_I) \geq 0$ is valid for all systems with an exact area law if and only if it is valid for the entropies of Bell pairs shared between any two subsystems A_i and A_j of the purified $(n+1)$-partite system.*

In section 5.2, we had proved that the cyclic inequalities (5.7) hold with *equality* for system that satisfy an exact area law. It follows immediately from lemma 5.4.1 that we can test the validity of an arbitrary entropy equality by verifying that they hold with equality when evaluated for Bell pairs. In [171], it was observed that this is the case for the cyclic inequalities (5.7) as well as four other holographic entropy inequalities established therein. It follows that all these inequalities hold with equality for systems satisfying an exact area law. In particular, this confirms our explicit derivation for the cyclic inequalities in section 5.2.

In principle, lemma 5.4.1 solves completely the problem of characterizing the entanglement entropy in systems with an exact area law. We will now describe the set of all possible entanglement entropies more concretely. For this, it is useful to observe that, for any fixed number of regions n, the collection of valid entropy inequalities $\sum_I c_I S(A_I) \geq 0$ cuts out a convex cone. This cone consists of all vectors $s = (S(A_I))_{\emptyset\neq I\subseteq[n]} \in \mathbb{R}^{2^n-1}$ formed from the entanglement entropies obtained by varying over arbitrary regions $A_1, \dots, A_n$ and all systems satisfying an exact area law. Following [182, 183, 173, 171], we shall call it the *area-law entropy cone*. Like any convex cone, it can be dually described in terms of its extreme rays, which we obtain immediately from lemma 5.4.1:

Lemma 5.4.2. *The extreme rays of the area-law entropy cone for n regions are given by the entropy vectors β_{ij} of Bell pairs shared between any two subsystems in the purified $(n+1)$-partite system.*

Since the entropies of Bell pairs can be realized holographically, we may think of the area-law entropy cone as a degeneration of the holographic entropy cone defined in [171]. It is arguably the smallest entropy cone that can capture bipartite entanglement.

The following theorem then gives a complete characterization of the entanglement entropy in systems with an exact area law:

Theorem 5.4.3. *A minimal and complete set of entropy (in)equalities for systems with an exact area law is given by (1) the subadditivity inequality $S(A_1) + S(A_2) \geq S(A_1 A_2)$ and its permutations, (2) the Araki-Lieb inequality $S(A_1) + S(A_1 \ldots A_n) \geq S(A_2 \ldots A_n)$ and its permutations, and (3) the multivariate information* equalities $\sum_{I \subseteq V} (-1)^{|I|} S(A_I) = 0$ *induced by any subset $V \subseteq [n]$ of cardinality at least three.*

Proof. We first argue that the entropy equalities in (3) are correct and linearly independent. Their correctness can be verified by evaluating them on the rays β_{ij} for $i < j \in [n+1]$:

$$\sum_{I \subseteq V} (-1)^{|I|} (\beta_{ij})_I = \sum_{I : i \in I \subseteq V \setminus \{j\}} (-1)^{|I|} + \sum_{I : j \in I \subseteq V \setminus \{i\}} (-1)^{|I|}.$$

By symmetry, it suffices to consider the first sum. If $i \notin V$ then it is zero. Otherwise,

$$\sum_{I : i \in I \subseteq V \setminus \{j\}} (-1)^{|I|} = -\sum_{J : J \subseteq V \setminus \{i,j\}} (-1)^{|J|} = -\sum_{k=0}^{|V \setminus \{i,j\}|} (-1)^k \binom{|V \setminus \{i,j\}|}{k} = 0$$

by the standard identity for an alternating sum of binomial coefficients, which is applicable since $|V \setminus \{i,j\}| \geq 3 - 2 = 1$. The fact that the equalities in (3) are all linearly independent can easily be seen by induction on $|V|$.

It follows from the above that the area-law cone is contained in a linear subspace of dimension $2^n - 1 - \sum_{k=3}^{n} \binom{n}{k} = n + \binom{n}{2} = \binom{n+1}{2}$. We will now show that this is indeed the dimension of the area-law cone. For this, it suffices to observe that $(\beta_{ij})_k + (\beta_{ij})_l - (\beta_{ij})_{\{k,l\}} = 2$ if $\{i,j\} = \{k,l\}$, and otherwise zero. This not only implies that the $\binom{n+1}{2}$ many extreme rays β_{ij} are all linearly independent, but also that the area-law entropy cone is cut out by the inequalities

$$S(A_k) + S(A_l) \geq S(A_{kl})$$

on the subspace defined by the multivariate information equalities (3). For $l \leq n$, these are just the inequalities in (1), while for $l = n+1$ we obtain the inequalities in (2) by using the relation $S(A_I) = S(A_{I^c})$. It is clear from the above that the entropy (in)equalities (1)–(3) form a minimal set. □

Geometrically, the area-law entropy cone is an "orthant" of dimension $\binom{n+1}{2}$, as follows from the proof of the theorem, where we have shown that the extreme rays are linearly independent. We note that the set of defining (in)equalities is in general not unique as the entropy cone has positive codimension for $n > 2$.

5.4.1 Generating entropy equalities from graphs

Our method can be easily adapted to include information about the spatial connectivity of the regions $A_1, \ldots, A_n$ that enter an (in)equality: If we can guarantee that $A_i \cap A_j = \emptyset$ then we do not need to consider the corresponding Bell pair β_{ij} when verifying an entropy (in)equality by using lemma 5.4.1. For a concrete example, consider the conditional mutual information $I(A : C|B) = S(AB) + S(BC) - S(ABC) - S(B)$, which is equal to zero for all Bell pairs except for β_{AC}. If we choose A, B, and C as in the figure 5.4 below then $I(A : C|B) = 0$ for systems with an exact area law, since $A \cap C = \emptyset$. This cancellation has been used in [178] to extract the topological entanglement entropy.

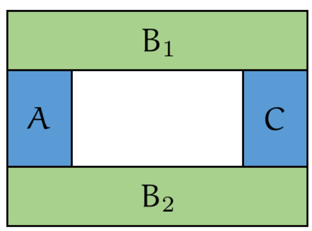

Figure 5.4: In systems with an exact area law, the conditional information $I(A : C|B)$ vanishes for this configuration of regions [178].

This example has the following pleasant generalization:

Lemma 5.4.4. *Let (V, E) be an undirected graph on the vertex set $V = [n]$, $n \geq 3$, and let $A_1, \ldots, A_n$ be regions such that $\partial A_i \cap \partial A_j \neq \emptyset$ only if $\{i, j\} \in E$. Then we have the following entropy equality,*

$$\sum_{I \subseteq V} (-1)^{|I|} \sum_{J \in \pi_0(I)} S(J) = 0, \tag{5.25}$$

where $\pi_0(I)$ denotes the connected components of the induced subgraph with vertex set I.

For a complete graph (V, E), (5.25) is precisely one of the multivariate information equalities proved in theorem 5.4.3 for arbitrary regions.

Proof. It suffices to argue that the difference to the multivariate information vanishes given our assumption on the spatial connectivity of the regions $A_1, \ldots, A_n$. For this, note that, for any $I \subseteq V$,

$$\left(\sum_{J \in \pi_0(I)} S(J)\right) - S(I) = \sum_{J \neq K \in \pi_0(I)} \sum_{j \in J, k \in K} \partial A_j \cap \partial A_k = 0,$$

since j and k are in different connected components so that $(j, k) \notin E$ and therefore $\partial A_j \cap \partial A_k = \emptyset$ by our assumption. □

For the graph displayed in figure 5.5 below we recover the statement derived above that $I(A : C|B) = 0$ for systems with $A \cap C = \emptyset$.

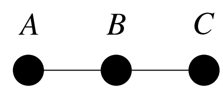

Figure 5.5: Graph corresponding to $I(A : C|B) = 0$ for regions with $A \cap C = \emptyset$.

We note that the connectivity assumption in lemma 5.4.4 is equivalent to requiring that $I(A_i : A_j) = 0$ for all $\{i, j\} \notin E$. We may therefore think of 5.25 as a *constrained entropy equality* in the sense of [184]. Below we list all non-trivial constrained entropy equalities obtained by lemma 5.4.4 from graphs with four vertices:

$$\begin{aligned}
(\text{e.g., } K_{1,3})\text{:} \quad & S(A_1A_2A_3A_4) - S(A_2A_3A_4) - S(A_1A_2A_4) - S(A_1A_3A_4) \\
& + S(A_1A_4) + S(A_2A_4) + S(A_3A_4) - S(A_4) = 0 \\
(C_4 = K_{2,2})\text{:} \quad & S(A_1A_2A_3A_4) - \sum_{i=1}^{4} S(A_i|A_{i+1}A_{i+2}) = 0 \\
(\text{Diamond})\text{:} \quad & S(A_1A_2A_3A_4) - S(A_1A_2A_3) - S(A_2A_3A_4) - S(A_3A_4A_1) \\
& - S(A_1A_2A_4) + S(A_1A_2) + S(A_1A_4) + S(A_2A_3) \\
& + S(A_2A_4) + S(A_3A_4) - S(A_2) - S(A_4) = 0 \\
(K_4 = W_4)\text{:} \quad & S(A_1A_2A_3A_4) - S(A_1A_2A_3) - S(A_1A_2A_4) - S(A_1A_3A_4) - S(A_2A_3A_4) \\
& + S(A_1A_2) + S(A_1A_3) + S(A_1A_4) + S(A_2A_3) + S(A_2A_4) + S(A_3A_4) \\
& - S(A_1) - S(A_2) - S(A_3) - S(A_4) = 0.
\end{aligned}$$

The last equality is in fact unconditionally true for systems with an exact area law; it is the fourpartite information equality from theorem 5.4.3.

5.4.2 The search for general quantum entropy inequalities

The simplistic method of graph combinatorics has thus far managed to reproduce the forms of many familiar entropic inequalities. In light of the observation, one may suspect that it could also be useful in generating other generic n-party quantum inequalities. In light of the above speculation, we attempt a simple search for 4-party linear quantum inequalities beyond the *von Neumann entropy inequalities* (5.1)–(5.4).

To search for the 4-party non-von Neumann inequality candidates, we employ again the notion of an entropy cone [182, 183]. Let $K = \{A, B, C, D\}$ be the labels of the 4 systems and E be the purifying system. Given a density operator ρ_{ABCD}, we obtain the entropy vector $\mathbf{v} = (v_I) \in \mathbb{R}^{15}$ where $\emptyset \neq I \subseteq K$ and $v_I = S(I)_\rho$ denotes the von Neumann entropy of the reduced density matrix ρ_I obtained by tracing out all but the systems in I. Consider the set $\Gamma_4^* \subset \mathbb{R}^{15}$ of all entropy vectors $\mathbf{v}$ produced by physical 4-party quantum states, we define the 4-party *quantum entropy cone* as the closure $\overline{\Gamma_4^*}$, which is shown to be a a convex cone in the entropy vector space $\mathbb{R}^{15}$. Similarly, the *von Neumann cone* Γ_4 can be defined as the set of vectors that satisfy the von Neumann entropy inequalities for 4-party systems, i.e., positivity, strong subadditivity, and weak monotonicity. Because these inequalities hold for an arbitrary quantum system, it necessarily follows that $\overline{\Gamma_4^*} \subset \Gamma_4$. It was proven that $\overline{\Gamma_n^*} = \Gamma_n$ for $n \leq 3$. Therefore von Neumann inequalities completely characterize the quantum entropy cone for 3 or fewer parties.

Due to the convexity of the cones, we know that all points inside an entropy cone can be written as a linear combination of its extremal rays. The entropy cone Γ_4 produced by all von Neumann entropy inequalities is known and is characterized by the extremal rays listed in table 5.1 [185].

It is shown in [184], however, that families 7 and 8 are not physically constructible. Therefore, it is suspected that $\overline{\Gamma_4^*}$ should be a proper subset of Γ_4 for $n \geq 4$ [184, 185],[1] so that additional 4-party entropy inequalities may be needed to complete the entropy cone.[2] By searching through the integral linear combinations of the constrained entropy equalities constructed from graphs as described in section 5.4.1 above, we have generated a set of inequalities that satisfy families 1 through 6 but can violate families 7 and 8 for certain permutations. After a cursory search, we

[1] In fact, studies in the classical Shannon entropy reveal that additional entropy inequalities, such as Zhang-Yeung Inequality, are needed in addition to the Shannon-type entropies.

[2] There is also the possibility of a characterization in terms of non-linear inequalities. However, that is beyond the scope of this work.

	A	B	C	D	E	AB	AC	AD	AE	BC	BD	BE	CD	CE	DE
Family 1	1	1	0	0	0	0	1	1	1	1	1	1	0	0	0
Family 2	1	1	1	1	0	1	1	1	1	1	1	1	1	1	1
Family 3	1	1	1	1	0	2	2	2	1	2	2	1	2	1	1
Family 4	1	1	1	1	1	1	1	1	1	1	1	1	1	1	1
Family 5	2	1	1	1	1	3	3	3	3	2	2	2	2	2	2
Family 6	1	1	2	2	2	2	3	3	3	3	3	3	2	2	2
Family 7	3	3	2	2	2	4	3	3	3	3	3	3	3	4	4
Family 8	3	3	3	3	2	4	4	4	5	4	4	5	6	5	5

Table 5.1: Families of extremal rays of the 4-party von Neumann cone constructed using known quantum inequalties. For a (mixed) state with subregions A, B, C and D, the region E is the corresponding purifying region.

A	B	C	D	E	AB	AC	AD	AE	BC	BD	BE	CD	CE	DE
1	1	2	2	2	2	2	2	2	2	2	2	2	2	2

Table 5.2: A candidate extremal ray for the 4-party quantum entropy cone proposed by [185].

found two such candidate inequalities (up to permutations):

$$\begin{aligned} &S(ABD) + S(ABC) + S(CD) - S(BC) - S(AB) - S(BD) - S(AC) \\ &- S(AD) + S(B) + S(A) \leq 0 \end{aligned} \tag{5.26}$$

$$\begin{aligned} &S(ABD) + S(ABC) + S(BCD) - 2S(BD) - 2S(BC) + S(CD) - S(AD) \\ &- S(AC) - S(AB) + 2S(B) + S(A) \leq 0. \end{aligned} \tag{5.27}$$

Both inequalities, as well as the quantum analogue of the Zhang-Yeung inequality [186, 187],

$$I(A:B) + I(A:CD) + 3I(C:D|A) + I(C:D|B) - 2I(C:D) \geq 0,$$

also satisfy the candidate extremal ray in table 5.2 for the 4-party quantum entropy cone $\overline{\Gamma^*_4}$. We note that the graph construction, as currently formulated, cannot produce the Zhang-Yeung inequality.

Inequality (5.26) is known as the *Ingleton inequality*. It can also be written as

$$I(A:B|C) + I(A:B|D) + I(C:D) - I(A:B) \geq 0.$$

It is known that the Ingleton inequality does not hold for general quantum states (not even for classical probability distributions), but that it is a valid inequality for the subclass of stabilizer states [172, 173].

Inequality (5.27) on the other hand seems to be independent of the other 4-party linear candidates, and to the best of our knowledge has not been tested to a greater extent. All tests we've conducted so far on this inequality return the same result as the quantum analogue of Zhang-Yeung inequality. It will be worthwhile to generate random 5-partite quantum pure states and numerically check if the inequality can be violated. Note that such checks do not constitute a proof. However, it can be useful in finding a counterexample.

5.5 Conclusion and future directions

We here restate our findings:

1. We have completely characterized the entropy (in)equalities obeyed by systems in which the entanglement entropy satisfies an exact area law. We find that such an entropy inequality is valid if and only if it is valid for the entropies of Bell pairs shared between arbitrary subsystems. In particular, all holographic entropy inequalities, such as the cyclic inequalities established recently in [171], are satisfied by systems with an exact area law. These (in)equalities may provide constraining tests to determine whether certain condensed matter systems satisfy an area law.

2. The cyclic (in)equalities in two-dimensional systems with non-trivial topological order can be seen as a generalization of [177] which extracts the topological entanglement entropy using higher number of partitions. These higher k generalizations of S_{topo} are sensitive (or insensitive) to different types of deviations from area-law scaling.

3. A graph representation for constrained entropy equalities for systems with an exact area-law scaling is found. As this construction recovers a wide class of entropy equalities including strong subadditivity, it may be suspected that further quantum inequalities may also be found in the set of graph-generated equalities. Following this approach, we have found a candidate linear entropy inequality for general 4-party quantum states.

As we have seen, the graph representation of entropies in area-law systems used in section 5.4 offers surprisingly powerful insights. In the absence of the minimization that appears in holography, several holographic inequalities now hold exactly as equalities for systems satisfying an exact area law, and we may understand the entropy cone spanned by the area law systems as a particular degeneration of the holographic entropy cone [171]. The method may also provide useful insight for the long-standing problem of finding linear inequalities for the entropies of general multipartite quantum states. In this regard, we also note that generalizations of the graph-theoretical approach is much desirable. One such generalization will involve constructing different graphs for a quantum state with holographic dual. We suspect that the geometry of AdS or its dual kinematic space can be effectively captured by analyzing generalized graph representations for these states. In particular, machineries developed in spectral graph drawing may be used to recover the emergent geometry for more general states.

Chapter 6

SPACE FROM HILBERT SPACE

We examine how to construct a spatial manifold and its geometry from the entanglement structure of an abstract quantum state in Hilbert space. Given a decomposition of Hilbert space $\mathcal{H}$ into a tensor product of factors, we consider a class of "redundancy-constrained states" in $\mathcal{H}$ that generalize the area-law behavior for entanglement entropy usually found in condensed-matter systems with gapped local Hamiltonians. Using mutual information to define a distance measure on the graph, we employ classical multidimensional scaling to extract the best-fit spatial dimensionality of the emergent geometry. We then show that entanglement perturbations on such emergent geometries naturally give rise to local modifications of spatial curvature which obey a (spatial) analog of Einstein's equation. The Hilbert space corresponding to a region of flat space is finite-dimensional and scales as the volume, though the entropy (and the maximum change thereof) scales like the area of the boundary. A version of the ER=EPR conjecture is recovered, in that perturbations that entangle distant parts of the emergent geometry generate a configuration that may be considered as a highly quantum wormhole.

This chapter is based on the Ref:

ChunJun Cao, Sean M. Carroll, and Spyridon Michalakis. "Space from Hilbert Space: Recovering Geometry from Bulk Entanglement". In: Phys. Rev. *D95.2 (2017), p. 024031. DOI:* `10.1103/PhysRevD.95.024031`*. arXiv:* `1606.08444 [hep-th]`*.*

6.1 Introduction

Quantum-mechanical theories are generally thought of as theories *of* something. Quantum states are square-integrable complex-valued functions of the configuration of some particular kind of "stuff," where that stuff may be a simple harmonic oscillator, a set of interacting spins, or a collection of relativistic fields.

But quantum states live in Hilbert space, a complete complex vector space of specified dimension with an inner product. The same quantum states, even with the same dynamics, might be thought of as describing very different kinds of stuff. Coleman long ago showed that the quantum theory of the sine-Gordon boson in 1+1 dimensions was equivalent to that of a massive Thirring fermion [188]. AdS/CFT posits an equivalence (in a certain limit) between a conformal field theory in a fixed d-dimensional Minkowski background and a gravitational theory in a dynamical $(d + 1)$-dimensional spacetime with asymptotically anti-de Sitter boundary conditions [21]. The wave functions of a single quantum theory can be represented in very different-looking ways. It is therefore interesting to consider the inverse problem to "quantizing" a theory: starting with a quantum theory defined in Hilbert space, and asking what it is a theory of. In this paper we take steps toward deriving the existence and properties of space itself from an intrinsically quantum description using entanglement.

A good deal of recent work has addressed the relationship between quantum entanglement and spacetime geometry. Much of the attention has focused on holographic models, especially in an AdS/CFT context. Entanglement in the boundary theory has been directly related to bulk geometry, including deriving the bulk Einstein equation from the entanglement first law (EFL) [189, 28, 190, 191]. (The EFL relates a perturbative change in the entropy of a density matrix to the change in the expectation value of its modular Hamiltonian, as discussed below.) Tensor networks have provided a connection between emergent geometry, quantum information, and many-body systems [71, 37, 57, 48, 41, 80, 79, 49, 76].

It is also possible to investigate the entanglement/geometry connection directly in a spacetime bulk. The ER=EPR conjecture relates entanglement between individual particles to spacetime wormholes [192, 143, 193, 194, 195, 196]. Consider two entangled particles, separated by a long distance, compared to the same particles but unentangled. If sufficient entanglement gives rise to a wormhole geometry, some weak gravitational effects should arise from small amounts of entanglement, and evidence for this phenomenon can be found in the context of AdS/CFT [197, 193, 143]. From a different perspective, Jacobson has argued that Einstein's equation can be derived from bulk entanglement under an assumption of local thermodynamic equilibrium between infrared and ultraviolet degrees of freedom [40, 198, 199].

While the current paper is inspired by the idea of emerging space from entanglement, our approach of bulk emergent gravity differs from the aforementioned papers in that our starting point is directly in Hilbert space, rather than perturbations around a boundary theory or a semiclassical spacetime. We will first try to construct a generic framework by which an approximate sense of geometry can be defined purely from the entanglement structure of some special states. We conjecture that mutual information (See [128, 127] for a review), similar to suggestions by [143, 48], can be used to associate spatial manifolds with certain kinds of quantum states. More tentatively, we explore the possibility that perturbations of the state lead to relations between the modular Hamiltonian and the emergent geometry that can be interpreted as Einstein's equation, as has been suggested in a holographic AdS/CFT context. In doing so we will follow some of the logic in [190] and [40]. In particular, we show that "nonlocal" perturbations that entangle distant parts of the emergent geometry, similar to the case in ER=EPR, will give rise to what might be understood as a highly quantum wormhole, where spatial curvature generated by (modular) energy, in a manner similar to Einstein's equation, is localized at the wormhole "mouths".

Our basic strategy is as follows:

- Decompose Hilbert space into a large number of factors, $\mathcal{H} = \bigotimes_p^N \mathcal{H}_p$. Each factor is finite-dimensional.
- Consider states $|\psi_0\rangle \in \mathcal{H}$ that are "redundancy-constrained," a generalization of states in which the entropy of a region obeys an area law.
- Use the mutual information between factors A and B, $I(A:B) = S(A)+S(B)-S(AB)$, to define a metric on the graph connecting the factors $\mathcal{H}_p$.
- Show how to reconstruct smooth, flat geometries from such a graph metric (when it exists).
- Consider perturbations $|\psi_0\rangle \to |\psi_0\rangle + |\delta\psi\rangle$, and show these produce local curvature proportional to the local change in entropy.
- Relate the change in entropy to that in an effective IR field theory, and show how the entanglement first law $\delta S = \delta\langle K\rangle$ (where K is the modular Hamiltonian) implies a geometry/energy relation reminiscent of Einstein's equation.

We do not assume any particular Hamiltonian for the quantum dynamics of our state, nor do we explore the emergence of Lorentz invariance or other features necessary to claim we truly have an effective quantum theory of gravity, leaving that for future work.

We begin the paper by reviewing entropy bounds and properties of entanglement for area-law systems in section 6.2. In section 7.3 we introduce the notion of redundancy constraint for entanglement structure and show how an approximate sense of geometry for can emerge in such states. In particular, we give a generic outline of the procedure, followed by an example using an area-law state from a gapped system where it is possible to approximately reconstruct space with Euclidean geometry. Then in section 6.4 we discuss the effects of entanglement perturbations in terms of the approximate emergent geometry, and in 6.5 show that an analog of the Einstein's equations can be derived. Finally, in 6.6 we conclude with a few remarks.

As this work was being completed we became aware of a paper with related goals [200]. There are also potential connections with a number of approaches to quantum gravity, including loop quantum gravity [10], quantum graphity [14], holographic space-time[201, 120], and random dynamics [202]; we do not investigate these directly here.

Throughout this paper, we will use d to denote spacetime dimension and $D = d - 1$ for spatial dimensionality.

6.2 Area-Law Entanglement

6.2.1 Gravity and Entropy Bounds

The Bekenstein-Hawking entropy of a black hole in 3+1 dimensions is proportional to the area $\mathcal{A}$ of its event horizon,

$$S_{\mathrm{BH}} = \frac{\mathcal{A}}{4G} = 2\pi\frac{\mathcal{A}}{\ell_p^2}, \tag{6.1}$$

where we use $\hbar = c = 1$ and the reduced Planck length is $\ell_p = \sqrt{8\pi G}$. At a quick glance this might seem like a surprising result, as the entropy of a classical thermodynamic system is an extensive quantity that scales with volume rather than area. What does this imply about the Hilbert space describing the quantum system that is a black hole, or spatial regions more generally?

Consider a fixed lattice of qubits, with a spacing ℓ_0 and a linear size r. The total number of qubits is $n \sim (r/\ell_0)^D$, where D is the dimensionality of space, and the associated dimension of Hilbert space is $N = 2^n$. If the system is in a (potentially mixed) state with density matrix ρ, the von Neumann entropy is $S = -\operatorname{Tr}\rho\log\rho$. The maximum entropy of such a system is then $S_{\max} = \log_2(N) = n$, proportional to the system volume. We might guess that gravity provides an ultraviolet cutoff that acts similarly to a lattice with $\ell_0 = \ell_p$. However, Bekenstein argued that the vast majority of the states included in such a calculation are physically unattainable, and that the entropy of a system with mass M and linear size R is bounded by $S \leq 2\pi RM$ [203, 204]. Since a system with $GM > R/2$ undergoes gravitational collapse to a black hole, this suggests that (6.1) represents an upper bound on the entropy of any system in spacetime, a constraint known as the holographic bound. If we were able to construct a higher-entropy state with less energy than a black hole, we could add energy to it and make it collapse into a black hole; but that would represent a decrease in entropy, apparently violating the Second Law. The Bousso bound [19] provides a covariant version of the holographic bound. 't Hooft and Susskind built on this argument to suggest the holographic principle: in theories with gravity, the total number of true degrees of freedom inside *any* region is proportional to the area of the boundary of that region [43, 42], and such a system can be described by a Hilbert space with dimension of approximately

$$\dim \mathcal{H} \sim e^{S} \sim e^{(r/\ell_p)^{D-1}}. \tag{6.2}$$

Meanwhile, it is now appreciated that area-law behavior for entanglement entropy occurs in a variety of quantum systems, including many non-gravitational condensed-matter examples [205]. Divide space into a region A and its complement $\overline{A}$. A quantum state $|\psi\rangle$ is said to obey an area law if the entropy S_A of the reduced density matrix $\rho_A = \mathrm{Tr}_{\overline{A}}\,|\psi\rangle\langle\psi|$ satisfies

$$S_A = \eta\mathcal{A} + \cdots, \tag{6.3}$$

where $\mathcal{A}$ is the area of the surface bounding A, and η is a constant independent of $\mathcal{A}$. (Here and elsewhere in this paper, entropy equalities should be interpreted as approximations valid in the limit of large system size.) This behavior is generally expected in low-energy states of quantum field theories with an ultraviolet cutoff [206, 70] and those of discrete condensed-matter systems with gapped local Hamiltonians (*i.e.*, short-range interactions) [167]. In conformal field theories, Ryu and Takayanagi showed that the entanglement entropy of a region was related to area, not of the region itself, but of an extremal surface in a dual bulk geometry [23, 207, 208].

The existence of an area law does not by itself imply holographic behavior; holography is a statement about the number of degrees of freedom in a region, which is related to the maximum possible entropy, but not directly to the entropy of some specific state as in (6.3). (The AdS/CFT correspondence is of course holographic on the dual gravity side, but the CFT by itself is not.) In either a gapped condensed-matter system or a QFT with an ultraviolet cutoff ℓ_0, we would still expect degrees of freedom to fill the enclosed volume, and the subsystem in A to have $\dim \mathcal{H}_A \sim e^{(r/\ell_0)^D}$.

As the UV cutoff length is taken to zero, we find an infinite-dimensional Hilbert space in any QFT, and the entropy of a region of space will generically diverge. Nevertheless, QFT reasoning can be used to derive a quantum version of the Bousso bound [209, 18, 20], by positing that the relevant entropy is not the full entanglement entropy, but the vacuum-subtracted or "Casini" entropy [210]. Given the reduced density matrix ρ_A in some region A, and the reduced density matrix σ_A that we would obtain had the system been in its vacuum state, the Casini entropy is given by

$$\Delta S = S(\rho_A) - S(\sigma_A) = -\operatorname{Tr}\rho_A \log\rho_A + \operatorname{Tr}\sigma_A \log\sigma_A. \tag{6.4}$$

This can be finite even when Hilbert space is infinite-dimensional and the individual entropies $S(\rho_A)$ and $S(\sigma_A)$ are infinite. This procedure sidesteps the question of whether the true physical Hilbert space is infinite-dimensional (and the holographic entropy bounds refer to entanglement entropy over and above that of the vacuum) or finite-dimensional (and the Casini regularization is just a convenient mathematical trick).

One might imagine being bold and conjecturing not only that there are a finite number of degrees of freedom in any finite region, as holography implies, but also that the holographic bound is not merely an upper limit, but an actual *equality* [157, 211, 212]. That is, for any region of spacetime, its associated entanglement entropy obeys an area law (6.3). Evidence for this kind of area law, and its relationship to gravity, comes from different considerations. Jacobson [213] has argued that if UV physics renders entropy finite, then a thermodynamic argument implies the existence of gravity, and also vice-versa. Lloyd [214] has suggested that if each quantum event is associated with a Planck-scale area removed from two-dimensional surfaces in the volume in which the event takes place, then Einstein's equation must hold.

In this paper, we examine quantum states in a finite-dimensional Hilbert space and look for emergent spatial geometries, under the assumptions that distances are determined by mutual information and that "redundancy constraint," which reduces to the usual area-law relationship of the basic form (6.3), holds when there exists an emergent geometric interpretation of the state. The conjecture that arbitrary regions of space are described in quantum gravity by finite-dimensional Hilbert spaces represents a significant departure from our intuition derived from quantum field theory.

We suggest that the emergence of geometry from the entanglement structure of the state can reconcile $\dim\mathcal{H}_A \sim e^{(r/\ell_0)^D}$ (degrees of freedom proportional to enclosed volume) with the holographic principle in a simple way: if we were to "excite" states in the interior by entangling them with exterior degrees of freedom, the emergent geometry would be dramatically altered so that the system would no longer resemble a smooth background manifold. In other words, those degrees of freedom are only "in the interior" in a geometric sense when they are entangled with their neighbors but not with distant regions, in a way reminiscent of ER=EPR.

6.2.2 Area Laws and Graphs

Simply being given a state $|\psi_0\rangle$ in a Hilbert space $\mathcal{H}$ is almost being given no information at all. Hilbert space has very little structure, and we can always find a basis $\{|\phi_n\rangle\}$ for $\mathcal{H}$ such that $\langle\psi_0|\phi_1\rangle = 1$ and $\langle\psi_0|\phi_{n>1}\rangle = 0$. To make progress we need some additional data, such as the Hamiltonian or a decomposition of $\mathcal{H}$ into a tensor product of factors. In this paper we don't assume any particular Hamiltonian, but begin by looking at states and decompositions that give us a generalization of area-law behavior for entropy.

To get our bearings, we start by considering systems for which we have an assumed notion of space and locality, and states that obey an area law of the form (6.3), and ask how such behavior can be recovered in a more general context. Typically such a state $|\psi_0\rangle$ is a low-lying energy state of a gapped local system. Its entanglement structure above a certain scale seems to capture the space on which the Hamiltonian is defined [71]. The entanglement structure of such states is highly constrained.

A remarkable feature of these states is that the entanglement structure above the said scale can be fully characterized once all the mutual information between certain subsystems are known. Divide the system into a set of sufficiently large non-overlapping regions A_p. We can calculate the entropy $S(A_p)$ of each region, as well as the mutual information $I(A_p : A_q)$ between any two regions. The system therefore naturally defines a weighted graph $G = (V, E)$, on which vertices V are the regions A_p, and the edges E between them are weighted by the mutual information (which is manifestly symmetric). .

The mutual information between regions is a measure of how correlated they are. It provides a useful way of characterizing the "distance" between such regions because of its relation to correlation functions between operators. We expect that in the ground state of a field theory, correlators of field operators will decay as exponentials (for massive fields) or power laws (for massless ones). The mutual information may reflect this behavior, as it provides an upper bound on the correlation function between two operators. For the mutual information between regions A and B, we have:

$$
\begin{aligned}
I(A:B) &= S(\rho_{AB}||\rho_A \otimes \rho_B) && (6.5)\\
&\geq \frac{1}{2}|\rho_{AB} - \rho_A \otimes \rho_B|^2 && (6.6)\\
&\geq \frac{\{\mathrm{Tr}[(\rho_{AB} - \rho_A \otimes \rho_B)(O_A O_B)]\}^2}{2\|O_A\| \, \|O_B\|^2} && (6.7)\\
&= \frac{(\langle O_A O_B\rangle - \langle O_A\rangle\langle O_B\rangle)^2}{2\|O_A\|^2 \, \|O_B\|^2}. && (6.8)
\end{aligned}
$$

We therefore choose to concentrate on mutual information as a way of characterizing emergent distance without picking out any preferred set of operators.

Consider grouping a set of non-overlapping subregions A_p into a larger region $\mathbf{B}$, dividing space into $\mathbf{B}$ and its complement $\bar{\mathbf{B}}$. Taking advantage of the short-ranged entanglement in such states, the approximate entanglement entropy of $\mathbf{B}$ can be calculated using the cut function,

$$
S(\mathbf{B}) = \frac{1}{2} \sum_{p \in \mathbf{B}, q \in \bar{\mathbf{B}}} I(A_p : A_q). \tag{6.9}
$$

To find the approximate entanglement of region $\mathbf{B}$, one simply cuts all edges connecting $\mathbf{B}$ and its complement $\bar{\mathbf{B}}$. The entanglement entropy is the sum over all the weights assigned to the cut edges. This is similar to counting the entanglement entropy by the bond cutting in tensor networks, except in this special case where we are content with approximate entanglement entropy for large regions, a simple graph representation is sufficient. Comparatively, a tensor network that characterizes this state contains far more entanglement information than the simple connectivity captured by the graphs considered here.

Our conjecture is that this graph information is enough to capture the coarse geometry of this area-law state. If we restrict ourselves to work at scales for which $S \propto \mathcal{A}$, all information encoded in the form of larger-scale entanglement is highly redundant. In a generic state, the mutual information between all disjoint regions A_p, A_q would not be enough to characterize entanglement entropy of $S(A_r A_s A_t A_u)$ for $r, s, t, u \in V$. Naively, to specify the entanglement entropy of all larger regions $\mathbf{B}$, one needs on the order of $O(2^N)$ data points, where N is the number of vertices (Hilbert-space factors). However, in the special case of area-law entanglement, it suffices to specify all the mutual information between N factors. The amount of

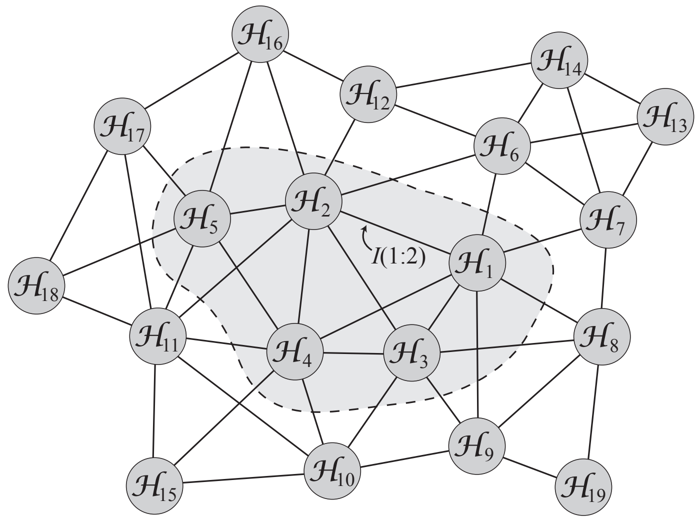

Figure 6.1: An "information graph" in which vertices represent factors in a decomposition of Hilbert space, and edges are weighted by the mutual information between the factors. In redundancy-constrained states, the entropy of a group of factors (such as the shaded region **B** containing $\mathcal{H}_1 \otimes \mathcal{H}_2 \otimes \mathcal{H}_3 \otimes \mathcal{H}_4 \otimes \mathcal{H}_5$.) can be calculated by summing over the mutual information of the cut edges, as in (6.9). In the following section we put a metric on graphs of this form by relating the distance between vertices to the mutual information, in (6.13) and (6.14).

classical bits needed to store this is only of order $O(N^2)$. Therefore, all larger partition entanglement entropy data are "redundant" as they are captured by the mutual information of smaller parts. Because all subsequent higher-partition entanglement information is encoded in the mutual information between all suitably chosen partitions, the approximate geometric information above the chosen scale of partitioning can be characterized by the graph representation.

One may worry that the subleading terms in the area-law function can scale as volume and therefore ruin the estimate for higher-partition entropies at some level of coarse-graining. This is, however, an over-estimation. The entropy of a region with approximate radius r computed by the cut function assumes a strict area law, which scales as r^{D-1} for a D-spatial-dimensional area-law system. This is off from the actual entropy by amount $r^{D-2} + \ldots$, where missing terms have even lower power in r. The relative error, which scales as r^{-1}, vanishes in the large-region limit.

On the other hand, if one keeps all sub-leading terms, the correct edge weights one should assign are given by the intersecting area plus an error term,

$$I(A_p : A_q) = \alpha \mathcal{A}(A_p \cap A_q) + \beta \mathcal{E}. \tag{6.10}$$

Therefore one may worry that in our subsequent estimate of entropy for a bigger region, the error term may accumulate as r^D. But since the system is dominated by short-range entanglement, the number of edge cuts only scales as r^{D-1}. So in the worst case scenario, the subleading terms will contribute a term that scales as area. Therefore, the error in using the cut function as an estimate for the entropy of a region A in an area-law system is upper bounded by a term $\beta\mathcal{A}$ for some β, which one may absorb by redefining $\alpha' = \alpha + \beta$. In this discussion, we are not concerning ourselves with the specific value of α, so the sub-leading terms only minimally change the results.

6.3 Emergent Space

6.3.1 Redundancy-Constrained States

Having established the above properties for area-law states in systems for which space and locality are defined, we now turn to a more general context. For area-law states, the entanglement information between different factors of Hilbert space is sufficiently redundant that it can be effectively characterized by only limited knowledge of mutual information [215]. In the rest of this work, we restrict ourselves to the study of quantum states that are approximately "redundancy-constrained," defined by slight generalizations of the observations we made for area-law states using purely entanglement information.

Consider a quantum state $|\psi_0\rangle \in \mathcal{H} = \bigotimes_p^N \mathcal{H}_p$. We say that the state is *redundancy-constrained* (RC) if, for any subsystem $\mathbf{B}$ constructed as a tensor product of some subset of the $\{\mathcal{H}_p\}$, its entanglement entropy is given by a cut function of the form (6.9), where A_p denotes the subsystem that lives in the Hilbert subspace $\mathcal{H}_p$. Note that there is no geometric meaning associated with the Hilbert space at this point.

Due to the redundancy of the entanglement entropy information, the entanglement structure for more coarse-grained partitions can be sufficiently captured by quantum mutual information, and hence admit a graph description as in the previous section. The vertices of the graph label subregions, and edge weights are given by their mutual information. By (6.9), it immediately follows that the degree of each vertex A_p (the number of edges emerging from it) is bounded from above by

$$\deg(A_p) = \sum_q I(A_p : A_q) \leq 2S_{max}(A_p) \leq 2\ln D_p, \tag{6.11}$$

where $\dim \mathcal{H}_{A_p} = D_p$.

RC states admit the same graph construction as area-law states, $G = (V, E)$, where vertices are Hilbert-space factors and edges are weighted by the mutual information between them. Such states can be seen as a straightforward generalization of states with area-law scaling that also lie in the area-law entropy cone [215]. As such, they form a superset of area-law states which also satisfy the holographic inequalities [165]. This doesn't imply, however, that such states have holographic duals. It is easy to check that satisfaction of all holographic inequalities is not a sufficient condition to indicate if a state has a holographic dual. (As a simple example, we know that area-law states from a gapped system don't have holographic duals, yet they still satisfy the holographic inequalities.)

The individual Hilbert-space factors $\mathcal{H}_p$ are not necessarily qubits or some other irreducible building blocks of the space. In particular, they may be further factorizable, and are required to be sufficiently large that redundancy-constraint becomes a good approximation, even if it would not hold at finer scales. In a phenomenologically relevant model, we would expect each factor to describe not only the geometry but the field content of a region of space somewhat larger than the Planck volume, though we will not discuss those details here. Note that the RC property is preserved under a coarse-graining operation in which we decompose Hilbert space into factors $\mathcal{H}_P$ that are products of several of the original factors $\mathcal{H}_p$. We discuss coarse-graining more in Appendix 6.A.

RC states are highly non-generic; they represent situations where entanglement is dominated by short-range effects. For example, a CFT ground state in D dimensions with a holographic dual is not RC, although its entanglement data is still somewhat redundant in that one only needs the entanglement entropy for balls of all radii to reconstruct the AdS geometry [28, 191]. However, additional data encoded in the larger partitions cannot be characterized by mere mutual information between the partitions A_p for any coarse-graining. In this case, the attempt to define entanglement entropy as area or mutual information doesn't quite work in d spatial dimensions any more because there is no simple additive expression for $S(B_X)$ from $I(A_p : A_q)$. This extra data for larger partitions is essential in constructing the emergent dimension with AdS geometry.

At the same time, if we have some dual bulk fields living in AdS whose ground state is presumably also short range entangled [48], then it may in turn be described by a RC state in AdS with proper coarse-graining. Therefore, if one has the complete holographic dictionary, an experiment of entangling two copies of CFT to create a thermofield double state has its dual experiment with certain constraints in the bulk, where the entanglement now is directly created in the bulk and two copies of AdS are turned into a wormhole. Our general program, however, does not rely on the existence of a dual CFT.

Although most states in Hilbert space given a certain decomposition are not redundancy-constrained, RC states seem like an appropriate starting point for investigating theories of quantum gravity, especially if area-law behavior for entropy is universal. For the remainder of the program, we are going to focus on simple RC states that correspond to flat space in D spatial dimensions.

6.3.2 Metric from Information

Consider a state $|\psi_0\rangle$ for which there exist a decomposition of the Hilbert space such that $|\psi_0\rangle \in \mathcal{H} = \bigotimes_p^N \mathcal{H}_p$ is redundancy-constrained. Such a state naturally defines a graph $G = (V, E)$, with N vertices labelled by p and each edge $\{p, q\}$ is weighted by the mutual information $I(A_p : A_q)$. Without loss of generality, assume G is connected. In the case when G has multiple large disconnected components, one can simply perform the procedure separately for each connected component.

Our conjecture is that this graph contains sufficient information to define another weighted graph, $\widetilde{G}(\widetilde{V}, \widetilde{E})$, on which the edge weights can be interpreted as distances, thereby defining a metric space. In general, passing from the "information graph" G to the "distance graph" $\widetilde{G}$ might be a nontrivial transformation,

$$G(V, E) \to \widetilde{G}(\widetilde{V}, \widetilde{E}), \tag{6.12}$$

with a different set of vertices and edges as well as weights. However, we will make the simplifying assumptions that the vertices and edges remain fixed, so that the graph is merely re-weighted, and furthermore that the distance weight for any edge $w(p, q)$ is determined solely by the corresponding mutual information, $I(A_p : A_q)$ (where it is nonzero), rather than depending on the rest of the graph.

Our expectation is that nearby parts of space have higher mutual information, while faraway ones have lower. We therefore take as our ansatz that the distance between entangled factors is some function Φ of the mutual information, and express this as a new weight $w(p, q)$ on the edges of our graph. That is, for any $p, q \in V$ where $I(A_p : A_q) \neq 0$, define the edge weights to be

$$w(p, q) = \begin{cases} \ell_{\mathrm{RC}} \Phi\Big(I(A_p : A_q)/I_0\Big) & (p \neq q) \\ 0 & (p = q) \end{cases} \tag{6.13}$$

for some length scale $\ell_{\rm RC}$, the "redundancy-constraint scale". No edges are drawn if $I(A_p : A_q) = 0$. Here we define the "normalized" mutual information $i(p : q) \equiv I(A_p : A_q)/I_0$, where normalization I_0 is chosen such that $I(A_p : A_q)/I_0 = 1$ when two regions A_p, A_q are maximally entangled. In the case when the Hilbert space dimension is constant for all subregions, we have $I_0 = 2S(A_p)_{\rm max} = 2\log(\dim \mathcal{H}_D)$.

The specific form of the scaling function Φ will presumably be determined by the kind of system we are describing (*e.g.* by the matter content); only some of its basic properties will be crucial to our considerations. To be consistent with our intuition, we require $\Phi(1) = 0$ and $\lim_{x\to 0}\Phi(x) = \infty$, namely, the distance is zero when two states are maximally entangled and far apart when they are unentangled. Similar notions were found in [48, 143]. In addition, we choose $\Phi(x)$ to be a non-negative monotonically decreasing function in the interval $[0, 1]$, where a smaller mutual information indicates a larger distance. For definiteness it may be helpful to imagine that $\Phi(x) = -\log(x)$, as might be expected in the ground state of a gapped system [167, 216].

We can now construct a metric space in the usual way, treating weights $w(p, q)$ as distances $\tilde{d}(p, q)$. For vertices connected by more than one edge, the metric $\tilde{d}(p, q)$ is given by the shortest distance connecting p and q. Let P be a connected path between p and q, denoted by the sequence of vertices $P = (p = p_0, p_1, p_2, \ldots p_k = q)$. The metric $\tilde{d}(p, q)$ is then

$$\tilde{d}(p, q) = \min_P \{\sum_{n=0}^{k-1} w(p_n, p_{n+1})\} \tag{6.14}$$

for all connected paths P. It is clear from the definition that for a connected component, $\tilde{d}(p, q) = \tilde{d}(q, p)$, $\tilde{d}(p, q) = 0 \Leftrightarrow p = q$, and the triangle inequality is satisfied.

Given a graph with N vertices with a metric defined on it, we would like to ask whether it approximates a smooth manifold of dimension $D \ll N$. Clearly that will be true for some graphs, but not all. One approach is to consider an r-ball centered at p using the metric $\tilde{d}$, and compute the entropy of the reduced density matrix obtained by tracing out all regions outside the ball. The fractal dimension near some vertex p can be recovered if

$$S(r, p) \sim r^{D_f}. \tag{6.15}$$

In general this expression may not converge to an integer D_f. In the case of integer dimension, one can then proceed to find a $D = D_f + 1$ dimensional manifold on which G can be embedded that comes closest to preserving the metric $\tilde{d}(p,q)$. We also assign the *interface area* between two subregions A_p, A_q as

$$\mathcal{A} := I(A_p : A_q)/2\alpha, \tag{6.16}$$

for some constant α. Note that this implies the area that encloses the region A_p in a redundancy-constrained state is given by $\mathcal{A}(A_p) = S(A_p)/\alpha$. We define this to be the emergent spatial geometry of the state and assign geometric labels to the Hilbert space factors based on the embedding. For simple geometries, we will show in section 6.3.3 that one can use the so-called dimensionality reduction techniques in manifold learning.

6.3.3 Classical Multidimensional Scaling

We now turn to the problem of going from a graph with a metric to a smooth manifold. One approach is to use Regge calculus, which we investigate in appendix 6.B. Here we look at an alternative procedure, multidimensional scaling (MDS). For a more detailed review, see e.g. [217].

This procedure defines an embedding of the graph into a symmetric manifold; for simplicity, we restrict our attention to cases where the manifold is Euclidean. The embedding is an isometry when the graph itself is exactly flat, but also works to find approximate embeddings for spaces with some small distortion. In our current program, one expects that there exists some natural number $D \ll N$ where the corresponding embedding in D-Euclidean space is (approximately) isometric, but there can be distortion since there is some arbitrariness in our choice of the distance function Φ appearing in (6.13).

Consider the distance graph $\widetilde{G} = (V, E)$, with edges weighted by the metric distance $\tilde{d}(p,q)$. These vertices and distances now define a metric space $(V, \tilde{d})$. The first thing we can do is define the emergent dimension of this discrete space. Consider a subset of vertices, $X = \{v_0, v_1, \ldots, v_r\} \subseteq G$, equipped with its induced metric. X is a metric subspace and a r-simplex of V. Now construct the matrix

$$R_{ij} = \frac{1}{2}(\tilde{d}(v_i, v_0)^2 + \tilde{d}(v_j, v_0)^2 - \tilde{d}(v_i, v_j)^2). \tag{6.17}$$

Since the determinant $det(R) = R(v_0, v_1, \ldots, v_r)$ is a symmetric function, define simplicial volume

$$vol_r(X) = \frac{1}{r!}\sqrt{det(R)}, \tag{6.18}$$

which is nothing but the spatial volume of the r-simplex if X is a subset of Euclidean space equipped with the induced Euclidean metric. The dimension of a metric space, if it exists, is the largest natural number k for which there exists a D-simplex with positive volume. As demonstrated by [218], the metric space can be isometrically embedded into Euclidean space with dimension d if and only if the metric space is flat and has dimension $\leq D$.

The output of MDS applied to N vertices with distances $\tilde{d}(p, q)$ embedded into a D-dimensional space is an $N \times D$ matrix $\mathbf{X}$, which can be thought of as the embedded coordinates of all the vertices: the nth row contains the D coordinate values of the nth vertex, up to isometric transformations.

To see how this might work, imagine for the moment working backwards: given some coordinate matrix $\mathbf{X}$, how is it related to the distances $\tilde{d}(p, q)$? First define an $n \times n$ matrix $\mathbf{B} = \mathbf{X}\mathbf{X}^t = (\mathbf{XO})(\mathbf{XO})^t$, which is equivalent for coordinate matrix $\mathbf{X}$ up to some arbitrary orthonormal transformation $\mathbf{O}$. Then we notice that the Euclidean distances between two rows of $\mathbf{X}$ can be written as

$$\begin{aligned}
\tilde{d}(p, q)^2 &= \sum_{r=1}^{d} (X_{pr} - X_{qr})^2 && (6.19)\\
&= \sum_{r=1}^{d} [X_{pr}X_{pr} + X_{qr}X_{qr} - 2X_{pr}X_{qr}] && (6.20)\\
&= B_{pp} + B_{qq} - 2B_{pq}. && (6.21)
\end{aligned}$$

Therefore, if $\mathbf{B}$ can be recovered only from the Euclidean distances $\tilde{d}(p, q)$, a solution for $\mathbf{X}$ can be obtained.

The solution $\mathbf{X}$ for the embedding coordinates is non-unique up to isometric transformations. To get a unique solution, we first impose the following constraints such that the embedding is centered at the origin,

$$\sum_{p=1}^{N} X_{pr} = 0, \quad \forall r. \tag{6.22}$$

Then it follows that $\sum_{q=1}^{N} B_{pq} = 0$ and

$$B_{pq} = -\frac{1}{2}\Big(\tilde{d}(p, q)^2 - \frac{1}{N}\sum_{l=1}^{N} \tilde{d}(p, l)^2 - \frac{1}{N}\sum_{l=1}^{N} \tilde{d}(l, q)^2 + \frac{1}{N^2}\sum_{l,m=1}^{N} \tilde{d}(l, m)^2\Big). \tag{6.23}$$

This defines the components B_{pq} in terms of the graph distances.

We diagonalize $\mathbf{B}$ via

$$\mathbf{B} = \mathbf{V}\boldsymbol{\Lambda}\mathbf{V}^t. \tag{6.24}$$

Here $\mathbf{\Lambda}$ is a diagonal matrix with diagonal eigenvalues $\lambda_1 \geq \lambda_2 \geq \ldots \lambda_N$ arranged in descending order. In addition, because $\mathbf{B}$ has rank D, we choose the D eigenvectors corresponding to the D non-zero eigenvalues. A solution for $\mathbf{X}$ is then

$$\tilde{\mathbf{X}} = (\sqrt{\lambda_1}\mathbf{v_1}, \ldots, \sqrt{\lambda_d}\mathbf{v_d}), \tag{6.25}$$

which is an isometric embedding of N points into a D-dimensional Euclidean space.

For the case where exact embedding is not possible, *i.e.*, the distance function is Euclidean but with some small deviations, there will be D dominant positive eigenvalues followed by smaller non-zero eigenvalues. We consider the D-dimensional embedding to be approximately valid if $\epsilon_D = 1 - \sum_{i=1}^{D} |\lambda_i| / \sum_{i=1}^{N} |\lambda_i|$ is sufficiently small. One can quantify the distortion from exact embedding in various ways. For instance, for the classical MDS algorithm we use here, a so-called stress function is used as a measure of distortion

$$Stress = \sqrt{1 - \frac{(\sum_{p,q} \tilde{d}(p,q) d_E(x_p, x_q))^2}{\sum_{p,q} \tilde{d}(p,q)^2 \sum_{p,q} d_E(x_p, x_q)^2}}, \tag{6.26}$$

where $d_E(x_p, x_q)$ is the Euclidean distance between the two corresponding vertices p, q in the embedded space. Essentially, MDS analytically generates a set of embedding coordinates in a lower dimensional Euclidean space [219, 217], where the algorithm seeks an optimal Euclidean embedding such that the inter-vertex distances are best preserved in sense that $Stress$ is minimized. Although it also works well for graph embedding in highly symmetric surfaces (hyperbolic and spherical as well as flat) [219, 220, 221], it is considered a difficult problem to find an embedding for generic curved manifolds. The matching problem, although non-trivial, can be significantly simplified if the embedding manifold is known [222].

6.3.4 Examples with Area-Law States

Let's see how MDS works in practice for our redundancy-constrained quantum states. To do this, we will examine states whose geometric interpretation is known, and show that our procedure can recover that geometry.

We start by imagining that an unsuspecting group of theorists have been handed the state $|\psi_0\rangle \in \mathcal{H} = \bigotimes_p^N \mathcal{H}_p$, which is actually the ground state of a d-dimensional gapped local Hamiltonian that also satisfies an area law. Although the theorists are only given $|\psi_0\rangle$ and its Hilbert space decomposition, they are tasked with finding an approximate geometry for the state.

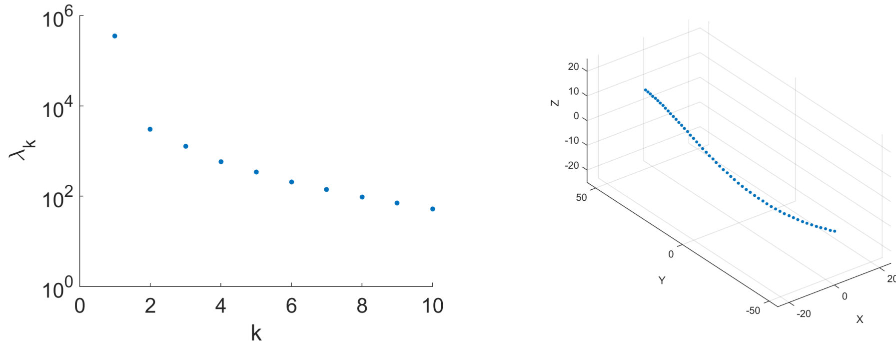

(a) (b)

Figure 6.2: Multidimensional scaling results for the 1-d antiferromagnetic Heisenberg chain. On the left we plot the eigenvalues of the matrix (6.24). The fact that the first eigenvalue is much greater than the others indicates that we have a 1-d embedding. On the right we show the reconstructed geometry by plotting the first three coordinates of the graph vertices.

We start by constructing the graph $\widetilde{G} = (V, E)$, where the vertices are labelled by subregions A_p, and edge weights are given by the distance function $w(p, q) = \ell_{\text{RC}}\Phi[I(A_p : A_q)/I_0]$, as in (6.13). For convenience we choose $\Phi(x) = -\ln(x)$. This function is chosen as most finitely correlated states have fast decaying correlation which, in the limit of large distances, is exponentially suppressed [167]. In particular, this is satisfied for any system with a spectral gap whose observables commute at large distances [216]. The correlation of any state that is locally entangled (finitely correlated states), *e.g.*, ones that can be expressed in terms of MPS or PEPS tensor networks, are expected to take this form.

Two examples are illustrated here, corresponding to a state living on a one-dimensional line and one living on a two-dimensional plane. In both cases we start with a known vacuum state of a gapped local system, where correlations are expected be short-ranged. Computing the mutual information for a quantum state of such systems is in general not an easy task. Consequently, we did not calculate directly the mutual information from density matrices in the 1-d case and instead used the correlation function as a proxy.

Our one-dimensional example is the ground state of an (S=1) 1-dimensional anti-ferromagnetic Heisenberg chain [223, 224]. Recalling (6.8), we use the magnitude squared of the correlation function as an estimate for the mutual information. The ground state correlation function $|\langle S_i^a S_j^a \rangle|$ is approximately proportional to the modified Bessel function $K_0(r/\xi)$, where $a = x, y, z$. This is a fast-decaying correlation,

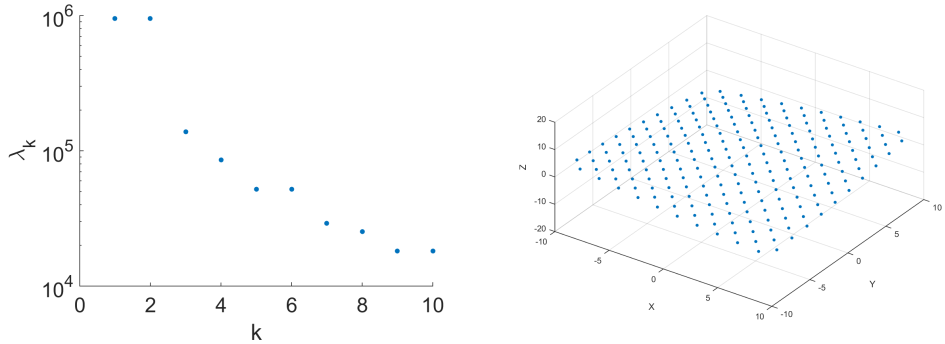

(a) (b)

Figure 6.3: Multidimensional scaling results for a coarse-grained 2-d toric code ground state. Again, the left shows the eigenvalues of (6.24) and the right shows the reconstructed geometry. The two dominant eigenvalues show that the geometry is two-dimensional, though the fit is not as close as it was in the 1-d example. Similarly, the reconstructed geometry shows a bit more distortion.

scaling as as $\exp(-r/\xi)/\sqrt{r/\xi}$ in the asymptotical limit when $r \gg \xi$. (For $a = z$ the correlator is supplemented with an extra term of the same order, given by $\sim 2\xi K_0(r/2\xi)K_1(r/2\xi)/r$. The distortion is still minimal, and in fact yields a slightly better isometric embedding.)

We constructed a graph of 100 vertices and assigned edge weights given by the square of correlator. No coarse-graining is performed. Applying MDS to this graph returns a vector of embedding coordinates in Euclidean space. As expected, there is distortion in the embedding and the coordinate matrix $\tilde{\mathbf{X}}$ has rank greater than one. However, the distortion, as measured using eigenvalues, has $\epsilon_1 = 0.0167$, from which we determine that it only slightly deviates from an embedding in 1d. In figure 6.2, a patch of approximately 50 points is plotted. The one-dimensional nature of the reconstructed geometry is evident.

Our second example reconstructs a patch of the 2-d toric code [225], where it is possible to exactly calculate the entropy for different subregions [226]. In a coarse-graining where each region is homeomorphic to a plaquette, the exact entropy is $S = \Sigma_{AB} - 1 = L_{\partial A} - n_2 - 2n_3 - 1 = n_1 + n_2 + n_3 - 1$, where $L_{\partial A}$ is the length of the boundary that separates bipartitions A and B. Here, n_i denotes the number of sites/star operators that have i nearest neighbors in A. The mutual information used for the network is again given by the length of overlapping boundary, up to a constant correction term. As neighboring spins are uncorrelated, the constant entanglement entropy offset only changes the overall definition of length scale by a constant factor for a near-uniform coarse-graining. As a result, the geometric reconstruction of a 2-d patch is given by (6.3), up to coordinate rescaling. The distortion now is visibly higher because $-\ln(x)$ is no longer an ideal ansatz for $\Phi(x)$. The distortion factor as measured by eigenvalues for an embedding in 2-d has $\epsilon_2 = 0.41$, but the 2-d nature of the emergent space is evident from figure 6.3.

6.4 Curvature and Entanglement Perturbations

In this section we examine the effects on our reconstructed spatial geometries of perturbing the entanglement structure of our states. As we are only considering space rather than spacetime, we cannot directly make contact with general relativity; in particular, we can say nothing about the emergence of dynamical fields obeying local Lorentz invariance. Nevertheless, we will see that the induced geometry responds to perturbations in a way reminiscent of Einstein's equation, suggesting that an emergent spacetime geometry could naturally recover gravity in the infrared.

6.4.1 Entanglement Perturbations

Consider some unperturbed "vacuum" density operator $\sigma = |\psi_0\rangle\langle\psi_0| \in L(\mathcal{H})$, for which there exists a D-dimensional geometric reconstruction as discussed in the last section. (Here $L(\mathcal{H})$ denotes the space of complex-valued linear operators on $\mathcal{H}$, of which the density operator is an element.) We choose a vertex p on the distance-weighted graph $\widetilde{G}$ that is associated with some subregion A_p of the emergent geometry. The reduced density matrix associated with the region is defined in the usual way: $\sigma_{A_p} = \mathrm{Tr}_{\overline{A}_p}[\sigma]$, where $\overline{A}_p$ is the complement of A_p. The entropy of such a region is again $S_{A_p}(\sigma_{A_p}) = -\mathrm{Tr}[\sigma_{A_p} \log \sigma_{A_p}] = 1/2 \sum I(A_p : \overline{A}_p)$. The interface area between regions A_p and A_q is defined as $\alpha\mathcal{A} = I(A_p : A_q)/2$, and the distance between vertices p, q is defined by $\tilde{d}(p,q) = l_p \Phi(i(A_p : A_q))$. Recall that the normalized mutual information is $i(p:q) = I(A_p : A_q)/I_0(p:q)$, where $i(p:q) = 1$ when subsystems A_p, A_q are maximally entangled.

There are a variety of entanglement perturbations one can consider. We can separately investigate "local" perturbations that change the entanglement between A_p and nearby degrees of freedom, and "nonlocal" ones that introduce entanglement between A_p and degrees of freedom far away; the latter can be modeled by nonunitary transformations on $\mathcal{H}_{A_p}$.

A local perturbation is generated by some unitary operator $U_{A_p\overline{A}_p}$ acting on the original system $\mathcal{H} = \mathcal{H}_{A_p} \otimes \mathcal{H}_{\overline{A}_p}$. The perturbed state is $\rho = U^\dagger_{A_p\overline{A}_p} \sigma U_{A_p\overline{A}_p}$. From the definition of mutual information, we know that

$$\begin{aligned}\delta I(A_p:\overline{A}_p) &= \delta S_{A_p} + \delta S_{\overline{A}_p} - \delta S_{A_p\overline{A}_p} \\ &= 2\delta S_{A_p}, \qquad \text{(local)}\end{aligned} \tag{6.27}$$

where $\delta S_i = S_i(\rho) - S_i(\sigma)$ denotes the infinitesimal change of entanglement entropy for region i. (This relation also holds for finite changes in entropy.) The second equality follows because $\delta S_{A_p} = \delta S_{\overline{A}_p}$ and $\delta S_{A_p\overline{A}_p} = 0$, since $U_{A_p\overline{A}_p}$ does not change the total entropy of the system. By construction, the definitions of area and length are related to mutual information of the quantum state; as we will soon discover, the entanglement perturbation here is tantamount to a local curvature perturbation at A_p.

Nonlocal entanglement perturbations correspond to applying a lossy quantum channel Λ, which can equivalently be treated as a completely positive and trace preserving (CPTP) map, to the system. To that end we introduce an extended Hilbert space

$$\mathcal{H}^* = \mathcal{H}_{A_p} \otimes \mathcal{H}_{\overline{A}_p} \otimes \mathcal{H}_B, \tag{6.28}$$

where B represents some ancillary degrees of freedom that are initially unentangled with those in A_p. One can think of B, described by state $\sigma_B \in L(\mathcal{H}_B)$, as a different patch of emergent space, or simply some degrees of freedom that the system has not yet encountered. A nonlocal perturbation is enacted by a unitary $U_{A_p\overline{A}_pB} = U_{A_pB} \otimes I_{\overline{A}_p}$ that acts only on the degrees of freedom in A_p and B. The perturbed state is $\rho = \Lambda(\sigma) = \mathrm{Tr}_B[U^\dagger_{A_p\overline{A}_pB}\sigma \otimes \sigma_B U_{A_p\overline{A}_pB}]$. In this case, the change in mutual information between A_p and $\overline{A}_p$ is non-positive, and will depend on the local entanglement structure as well as the entangling unitary.

Let $F_\Lambda(\Delta S_{A_p}; A_p, \overline{A}_p)$ be a function that describes the finite change in mutual information between A_p and its complement. The specific implementation of this function will depend on Λ and the entanglement structures related to the regions of interest, A_p and $\overline{A}_p$. The total change in mutual information in this case is given by

$$\Delta I(A_p : \overline{A}_p) = F_\Lambda(\Delta S_{A_p}; A_p, \overline{A}_p). \tag{6.29}$$

Because the change in mutual information has to be zero when no unitary is applied, we must have $F_\Lambda(0; A_p, \overline{A}_p) = 0$. For infinitesimal perturbations, we can write

$$\delta I(A_p:\overline{A}_p) = \delta S_{A_p} \frac{dF_\Lambda(\Delta S_{A_p}; A_p, \overline{A}_p)}{d(\Delta S_{A_p})}\Big|_{\Delta S_{A_p}=0} \tag{6.30}$$

$$= \delta S_{A_p} F'_\Lambda(0; A_p, \overline{A}_p). \qquad \text{(nonlocal)} \tag{6.31}$$

We have written the change in mutual information as if it is proportional to the change in entropy, but note that (in contrast with the case of local perturbations) here the proportionality is not a universal constant, but rather a factor that depends on the channel Λ. In general, for mixed states σ, σ_B which are not maximally entangled, we can easily find unitary operations where $F'_\Lambda(0; A_p, \overline{A}_p) \neq 0$. Note that this relation differs from the local perturbation by an F'_Λ-dependent constant factor.

6.4.2 Geometric Implications

We now consider the effect of an entanglement perturbation on the emergent spatial geometry. In this section we imagine mapping our graph to a Riemannian embedding manifold, as we did for the vacuum case using MDS in the previous section. In appendix 6.B we study the problem using Regge calculus.

Although it is operationally difficult to find for the graph an embedding manifold with variable curvature, it is considerably more tractable if we only wish to quantify a perturbation around a known manifold that corresponds to the density matrix σ. Namely, in order for the manifold to be a good embedding, its perturbed form should at least be consistent with the deviations in area and geodesic lengths. Since we have outlined explicit algorithms for flat space configurations, here we assume that a D-dimensional flat configuration $\mathcal{M}$ has been obtained using the above framework.

6.4.2.1 Effects of Local Entanglement Perturbations

We begin by considering a local perturbation that decreases the entropy of our region,

$$\delta S_{A_p} < 0, \tag{6.32}$$

which as we will see induces positive spatial curvature. Thus we are considering a local operation that decreases the entanglement between A_p and the rest of Hilbert space. Without altering the dimension, the minimal change to $\mathcal{M}$ that can be imposed is some perturbation to spatial curvature at p. For the simplest case, let A_p be a region that contains a single graph vertex p whose entanglement with the adjacent vertices q (regions A_q) is gradually decreased.

Following Jacobson [40], we proceed by defining Riemann normal coordinates in the vicinity of A_p,

$$h_{ij} = \delta_{ij} - \frac{1}{3}r^2 R_{ijkl}x^k x^l + O(r^3). \tag{6.33}$$

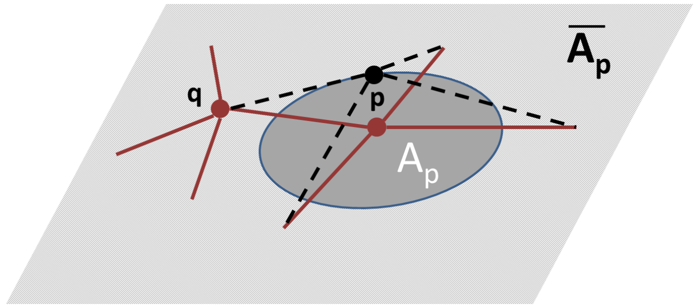

Figure 6.4: For a graph $\widetilde{G}$ embedded in some manifold, we assign subregion A_p (dark blue region) to the vertex p, which is connected to adjacent vertices q (Black solid line). An entanglement perturbation that decreases the mutual information between A_p with its neighbors elongates the connected edges (dashed red lines), creating an angular deficit which is related to the curvature perturbation at p.

Consider the perturbed subregion fixed at some constant volume V, of characteristic linear size $r = V^{1/D}$. The decrease in area under the perturbation is given by

$$\delta\mathcal{A} = -\frac{\Omega_{D-1} r^{D+1}}{2D(D+2)}\mathcal{R}_p, \tag{6.34}$$

where $\mathcal{R}_p = R_{ij}{}^{ij}(p)$ is the spatial curvature scalar and Ω_{D-1} is the volume of a unit $(D-1)$-sphere. We know that the boundary area is defined by local mutual information, namely,

$$\delta\mathcal{A} = \frac{1}{2\alpha}\sum_{A_q \in \overline{A}_p} \delta I(A_p : A_q) \approx \frac{1}{2\alpha}\delta I(A_p : \overline{A}_p). \tag{6.35}$$

Because the system is only short-range entangled, the local mutual information is well-approximated by the mutual information between the region and its complement. For instance, if the graph that captures entanglement structure for the toric code ground state above the RC scale is used, then the two quantities will be exactly equal. In general for systems with exponentially decaying mutual information, the error with this estimation is also upper-bounded by a quantity of order $\exp(-r/\ell_{\mathrm{RC}})$, which vanishes as long as the vertices correspond to sufficiently coarse-grained regions.

Plugging (6.27) for the change in mutual information due to an infinitesimal local perturbation into (6.34) and (6.35), we can relate the curvature scalar to the entropy perturbation by

$$\mathcal{R}_p = -\frac{2D(D+2)}{\alpha\Omega_{D-1}(\gamma\ell_{\mathrm{RC}})^{D+1}}\delta S_{A_p}. \tag{6.36}$$

Here we have set r equal to $\gamma\ell_{\mathrm{RC}}$, a characteristic size of the region for some constant γ. Such an approximation is most accurate when the symmetry is also approximately reflected by the graph. Because $\delta S_{A_p} < 0$, the induced curvature is positive.

The relation between curvature and the entropy perturbation can alternatively be derived by using (6.35) to estimate the decrease in mutual information for each individual edge, and relate that to a length excess. Since the edge weights sum to the total change in entropy, for each edge we can write

$$\delta I(A_p : A_q) = 2\eta_q \delta S_{A_p}, \tag{6.37}$$

for some constants η_q such that $\sum_q \eta_q = 1$. The values of η_q are determined by the graph structure near p, as well as the unitary $U_{A_p\bar{A}_p}$. For a unitary that symmetrically disentangles all the edges on a regular lattice, $\eta_q = 1/\deg(p)$.

Alternatively, we can also relate the change in entropy to the curvature perturbation by considering the change in linear size. The radius excess for the same perturbation at some fixed area is

$$\delta d = \frac{r^3 \mathcal{R}_p}{6D(D+2)}. \tag{6.38}$$

Recall that distance is related to mutual information by $\tilde{d}(p,q) = \ell_{\mathrm{RC}}\Phi(i(p:q))$, where the normalized mutual information is $i(p:q) = I(A_p : A_q)/I_0(p:q)$. Assuming an approximately symmetric configuration, to leading order we have

$$\begin{aligned} \delta\tilde{d}(p,q) &= \ell_{\mathrm{RC}}\Phi'(i(p:q))\delta i(p:q) + O(\delta i^2) \\ &= -2\eta_q \ell_{\mathrm{RC}} |\Phi'(i(p:q))| \delta S_A / I_0(p:q) + O(\delta i^2), \end{aligned} \tag{6.39}$$

where for the last line we used (6.27) to relate the linear change in entropy to the change in the distance function. Note that $\Phi' = d\Phi/di$ is negative by construction.

Comparing (6.38) to (6.39) yields an alternative relation between curvature and entanglement entropy,

$$\mathcal{R}_p = -\frac{12\eta_q |\Phi'(i(p:q))| D(D+2)}{I_0(p:q)\ell_{\mathrm{RC}}^2 \gamma^3} \delta S_{A_p}, \tag{6.40}$$

where again we have set $r = \gamma\ell_{\mathrm{RC}}$. One can check that for $1/\alpha \propto \ell_{\mathrm{RC}}^{D-1}$, the two results (6.36) and (6.40) are equivalent up to some dimension-dependent choice of η_q, the inverse function Φ, and constant factor α. Both imply positive curvature for local disentangling perturbations. Similarly, entangling perturbations with $\delta S_{A_p} > 0$ yields negative spatial curvature.

6.4.2.2 Effects of Nonlocal Entanglement Perturbations

The derivation with nonlocal entanglement perturbation is similar, where we simply replace the constant proportionality factors with the channel-dependent factor $F'_\Lambda(0)$. Repeating the above steps, analogously to the area deficit condition (6.36) we have

$$\mathcal{R}_p = -\frac{D(D+2)F'_\Lambda(0; A_p, \overline{A}_p)}{\alpha \Omega_{D-1}(\gamma \ell_{\mathrm{RC}})^{D+1}} \delta S_{A_p}, \tag{6.41}$$

while analogously to the radius deficit (6.40) we obtain

$$\mathcal{R}_p = -\frac{6F'_\Lambda(0; A_p, A_q)|\Phi'(i(p:q))|D(D+2)}{I_0(p:q)\ell_{\mathrm{RC}}^2 \gamma^3} \delta S_{A_p}. \tag{6.42}$$

Interestingly, we find that nonlocal entanglement perturbations are only able to generate positive curvature perturbations. Because $\delta I(A_p : \overline{A}_p) \leq 0$ under any operations acting on A_p and B, from (6.31) we must have

$$F'_\Lambda(0; A_p, \overline{A}_p) < 0 \tag{6.43}$$

for a generic entangling unitary when $\delta S_A > 0$. If $\delta S_{A_p} < 0$, then it must follow that $F'_\Lambda(0; A_p, \overline{A}_p) > 0$ for the same reason.

The nonlocal case is also interesting due to its connection with the ER=EPR conjecture. In this case, some spatial region A_p, described by some mixed state σ_{A_p}, is far separated from some other spatial region B, with corresponding mixed state σ_B. An entangling unitary then creates some weak entanglement between the regions, similar to having an EPR pair shared between them. Such entanglement, as we have seen, decreases the mutual information between A_p (B) and their respective neighboring regions. This, we claim, can be interpreted as a quantum proto-wormhole. No smooth classical geometry is present to form the usual ER bridge; nevertheless, the entanglement backreacts on the emergent geometry in a way such that positive modular energy “curves” the spatial regions near the “wormhole mouths."

A large entanglement modification beyond the perturbative limit does not create disconnected regions. Heuristically, because the entanglement of $\overline{A}_p$ is always constant under such a unitary, it must become more entangled with region B. From the point of view of emergent geometry from entanglement, it implies that the region $\overline{A}_p$ should also be connected to the distant region B in some way. When such a connection between the two regions becomes manifestly geometric, the process may then be interpreted as the formation of a classical wormhole.

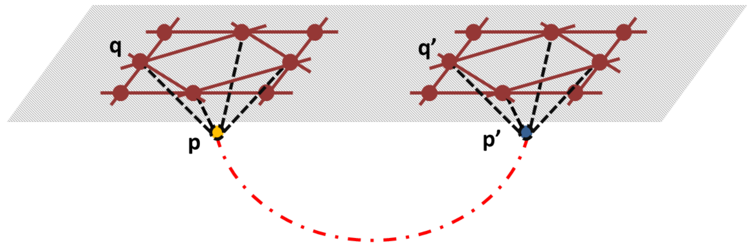

Figure 6.5: For perturbations that slightly entangle two regions of the emergent space, as represented by the vertices, a positive curvature perturbation is induced locally near each perturbed site. We may interpret this as a highly "quantum wormhole." The dotted red line joining p and p' denotes some trace amount of entanglement between the two subsystems.

However, because the function F_Λ depends on the entanglement structure of $\rho_{A\bar{A}}$ and Λ in addition to ΔS_A, the entropy-curvature relation does not seem to be universal as in the local case. Interpreting nonlocal effects as "gravitational" in this model may be in tension with our expectations for a theory of gravity, although further assumptions on symmetries in entanglement structure may resolve this issue.

6.5 Energy and Einstein's equation

We have seen how spatial geometry can emerge from the entanglement structure of a quantum state, and how that geometry changes under perturbations. This is a long way from completely recovering the curved spacetime of general relativity, both because we don't have a covariant theory with dynamics, and because we haven't related features of the state to an effective stress-energy. We can address the second of these points by considering general features of a map from our original theory to that of an effective field theory on a fixed spacetime background, then appealing to the entanglement first law (EFL); we leave the issue of dynamics to future work. Our approach here is similar in spirit to previous work in AdS/CFT [189, 28, 190, 191] and bulk entropic gravity [40, 198, 199].

6.5.1 Renormalization and the Low Energy Effective Theory

To make contact with semiclassical gravitation, we need to understand how an effective field theory, and in particular a local energy density, can emerge from our Hilbert-space formalism. This is a nontrivial problem, and here we simply sketch some steps toward a solution, by integrating out ultraviolet (gravitational) degrees of freedom to obtain an infrared field theory propagating on a background. We argue that, for local entanglement perturbations, a perturbation that decreases the entropy of a quantum-gravity state in a region A will correspond to increased entropy density in the effective IR field theory, which lives in a lower-dimensional (coarse-grained) Hilbert space.

Our construction posits an RC scale ℓ_{RC} at distances greater than which the state obeys the redundancy-constraint condition. Intuitively we expect ℓ_{RC} to be close to the reduced Planck length ℓ_p, at which the spatial geometry has barely emerged. Let the corresponding UV energy scale be $\lambda_{\mathrm{RC}} = 1/\ell_{\mathrm{RC}}$. We imagine an "emergence" map

$$\mathcal{E} : \mathcal{H} \to \mathcal{H}^{\mathrm{EFT}(\lambda_{\mathrm{RC}})}, \tag{6.44}$$

which maps states in the Hilbert space of our original theory to those of an effective field theory with cutoff λ_{RC} in a semiclassical spacetime background.

To study the relationship of entropy and energy in this emergent low-energy effective description, we consider the RG flow of the theory, defined by a parameterized map that takes the theory at λ_{RC} and flows it to a lower scale λ by integrating out UV degrees of freedom:

$$\mathcal{F}_\lambda : \mathcal{H}^{\mathrm{EFT}(\lambda_{\mathrm{RC}})} \to \mathcal{H}^{\mathrm{EFT}(\lambda)}. \tag{6.45}$$

This flow is defined purely in the context of QFT in curved spacetime, so that the background geometry remains fixed. Note that we could also discuss RG flow directly in the entanglement language, where it would be enacted by a tensor network similar to MERA [39]. There, the equivalent of $\mathcal{F}_\lambda$ would be a quantum channel that could be defined by a unitary circuit if we include ancillae representing UV degrees of freedom that are integrated out. In this case, λ depends on the number of layers of the MERA tensor network.

Given that (6.36) relates a spatial curvature perturbation in the emergent geometry to a change in entropy in the full theory, we would like to know how this entropy change relates to that of the vacuum-subtracted entropy $S^{\mathrm{EFT}(\lambda)}$ in the effective field theory with cutoff λ defined on a background (and ultimately to the emergent mass/energy in that theory). We posit that they are related by a positive constant κ_λ that depends on the cutoff but is otherwise universal:

$$\delta S = -\kappa_\lambda \delta S^{\mathrm{EFT}(\lambda)}. \tag{6.46}$$

The minus sign deserves some comment. A perturbation that disentangles a Hilbert space factor A_p decreases its entropy, $\delta S_{A_p} < 0$, while inducing positive spatial curvature in the emergent geometry and a decrease in the area $\mathcal{A}_p$ of the boundary of the corresponding region. Naively, a decrease in boundary area results in the decrease of the entropy of a region in a cutoff effective field theory. However, that expectation comes from changing the area of a near-vacuum state in a fixed background geometry. Here we have a different situation, where the perturbation affects both the geometry and the EFT state defined on it.

In that context, as Jacobson has argued [40], we expect an equilibrium condition for entanglement in small regions of spacetime. Consider a perturbation of the EFT defined on a semiclassical background, which changes both the background geometry and the quantum state of the fields. Fix a region in which we keep the spatial volume constant. In the spirit of holography and the Generalized Second Law, the total entropy in the region can be considered as the sum of an area term representing UV quantum gravity modes plus a term for the IR effective field theory,

$$\delta_V S_{\mathrm{total}} = \eta \delta_V \mathcal{A} + \delta_V S^{\mathrm{EFT}(\lambda)}. \tag{6.47}$$

Here, the subscript V reminds us that we are considering a variation at fixed volume (in contrast with the original perturbation in our underlying quantum theory). The unperturbed state is taken to be an equilibrium vacuum state. The total entropy is therefore at an extremal point, $\delta_V S_{\mathrm{total}} = 0$. A decrease in the geometric entropy (represented by the boundary area) is thus compensated by an increase in the entropy of the EFT state. Since our original perturbation δS decreases the boundary area of our region, we expect the field-theory entropy to increase. This accounts for the minus sign in (6.46).

Plugging (6.46) into (6.36) produces a relation between the local scalar curvature of a region around p and the change in the entropy of the EFT state on the background:

$$\mathcal{R}_p = \frac{2D(D+2)\kappa_\lambda}{\alpha \Omega_{D-1} (\gamma \ell_{\mathrm{RC}})^{D+1}} \delta S_{A_p}^{\mathrm{EFT}(\lambda)}. \tag{6.48}$$

Here, $\delta S_{A_p}^{\mathrm{EFT}(\lambda)}$ is interpreted as the change in the entropy of the EFT state in the region defined by A_p, due to shifts in both the background geometry and the fields themselves. Considering nonlocal rather than local perturbations results in multiplying the right-hand side by $F'_\Lambda(0)/2$.

6.5.2 Energy and Gravity

We can now use the Entanglement First Law to relate the change in entropy to an energy density. The EFL, which relates changes in entropy under small perturbations to the system's modular Hamiltonian, holds true for general quantum systems. Given a density matrix σ, we define its associated modular Hamiltonian $K(\sigma)$ through the relation

$$\sigma = \frac{e^{-K}}{\mathrm{Tr}(e^{-K})}. \tag{6.49}$$

The Kullback-Leibler divergence, or relative entropy, between two density matrices ρ and σ is given by

$$\begin{aligned} D(\rho||\sigma) &\equiv \mathrm{Tr}(\rho \ln \rho) - \mathrm{Tr}(\rho \ln \sigma) \\ &= -\Delta S + \Delta\langle K(\sigma)\rangle, \end{aligned} \tag{6.50}$$

where

$$\Delta S = S(\rho) - S(\sigma), \quad \Delta\langle K(\sigma)\rangle = \mathrm{Tr}[\rho K(\sigma)] - \mathrm{Tr}[\sigma K(\sigma)]. \tag{6.51}$$

The relative entropy is nonnegative, and is only zero when the states are identical. Hence, for infinitesimal perturbations $\sigma = \rho + \delta\rho$, we have $D(\sigma||\rho) = 0$ to linear order, and we arrive at the EFL [189],

$$\delta S = \delta\langle K\rangle. \tag{6.52}$$

This equation allows us to establish a relationship between (modular) energy and the change in entropy, and thereby geometry, of our emergent space.

Comparing to the curvature-entropy relations for local perturbations (6.36), we see that the (positive) induced local curvature $\mathcal{R}_p$ is proportional to $-\delta\langle K_{A_p}\rangle$. We therefore define an effective modular energy density,

$$\varepsilon_p = -\delta\langle K_{A_p}\rangle. \tag{6.53}$$

The curvature is then related to the effective modular energy via

$$\mathcal{R}_p = -\zeta \delta S_{A_p} = \zeta \varepsilon_p, \tag{6.54}$$

where

$$\zeta \equiv \frac{2D(D+2)}{\alpha \Omega_{D-1} (\gamma \ell_{RC})^{D+1}} \tag{6.55}$$

is a positive constant. On the other hand, an entangling operation in the vicinity of A_p would give rise to a negative "energy" in the region, adding negative spatial curvature to the emergent geometry. Having a large amount of negative energy seems unphysical; if our model for emergent space is to be consistent with gravity as we know it, there must be conditions limiting such effects, such as instabilities or other dynamical processes rendering them unattainable.

For nonlocal perturbations, we saw from (6.43) that only positive curvature is generated, regardless of the precise form of the perturbation. The curvature-modular-energy relation for nonlocal perturbations is therefore

$$\mathcal{R}_p = \tilde{\zeta}|\varepsilon_p|, \tag{6.56}$$

where $\tilde{\zeta} = |F'_\Lambda(0)|\zeta/2$.

Thus, once we define an emergent geometry using mutual information, we see that perturbing the modular energy induces scalar curvature in the surrounding space. This is manifestly reminiscent of the presence of mass-energy in the region for the usual case in Einstein gravity. This relationship between energy and curvature did not come about by "quantizing gravity"; rather, it is a natural consequence of defining the emergent geometry in terms of entanglement.

However, the effective modular energy is only an analogous expression for the actual mass/energy. To connect with our familiar notion of energy, we need to find the explicit expression of the modular Hamiltonian in terms of a stress tensor. Such expression will generally be highly nonlocal, and is not known explicitly except for a few cases [227]. One exception, however, is for a conformal field theory, where K can be directly related to the stress-energy tensor $T^{\mathrm{CFT}}_{\mu\nu}$ [28, 189]. Consider a small region centered at p of size $\gamma\ell_{\mathrm{RC}}$, in which T^{CFT}_{00} is approximately constant. Then we have

$$\delta\langle K^{\mathrm{CFT}}_{A_p}\rangle = \frac{2\pi\Omega_{D-1}(\gamma\ell_{\mathrm{RC}})^{D+1}}{D(D+2)}\delta\langle T^{\mathrm{CFT}}_{00}(p)\rangle. \tag{6.57}$$

Here $\delta\langle T^{\mathrm{CFT}}_{00}\rangle = \mathrm{Tr}[\delta\rho^{(IR)}_\lambda T^{\mathrm{CFT}}_{00}]$ is the expectation with respect to the perturbed state of the IR effective theory. Of course the 00 component of the stress tensor is simply the energy density of the theory.

Suppose that the RG flow $\mathcal{F}_\lambda$ for our EFT passes through an IR fixed point at a scale λ_*. At that scale, the entanglement structure of the IR state can be approximated by the ground state of a conformal field theory, and (6.57) applies. Combining (6.52) and (6.57) with (6.48) in the context of of the low-energy effective field theory, we find that the spatial curvature is related to the EFT stress tensor by

$$\mathcal{R} = \frac{4\pi\kappa_{\lambda_*}}{\alpha}\delta\langle T^{\mathrm{CFT}}_{00}\rangle, \tag{6.58}$$

where α is the constant in the entanglement/area relation (6.16) and κ_{λ_*} relates the full entropy perturbation to that of the EFT as in (6.46). For nonlocal perturbations, we saw from (6.43) that only positive curvature is generated, regardless of the precise form of the perturbation. The curvature-modular-energy relation for nonlocal perturbations is therefore

$$\mathcal{R} = \frac{2\pi |F'_\Lambda(0)| \kappa_{\lambda_*}}{\alpha} \delta \langle T_{00}^{\mathrm{CFT}} \rangle. \tag{6.59}$$

All of our work thus far has been purely in the context of space, rather than spacetime. We have not posited any form of Hamiltonian or time evolution. Let us (somewhat optimistically) assume that the present framework can be adapted to a situation with conventional time evolution, and furthermore that the dynamics are such that an approximate notion of local Lorentz invariance holds. (Such an assumption is highly nontrivial; see *e.g.* [228].) Thinking of our emergent space as some spatial slice of a Lorentzian spacetime manifold, the spatial curvature can be related to the usual quantities in the Einstein tensor. In particular, for slices with vanishing extrinsic curvature we have

$$\mathcal{R}_p = 2G_{00}(p). \tag{6.60}$$

Comparing to (6.58), we therefore find

$$G_{00} = \frac{2\pi \kappa_{\lambda_*}}{\alpha} \delta \langle T_{00}^{\mathrm{CFT}} \rangle. \tag{6.61}$$

If we make the identification $2\pi\kappa_{\lambda_*}/\alpha \rightarrow 8\pi G$, this is nothing but the 00-component of the semiclassical Einstein equation. The interaction strength is determined in part by the dimensionful constant α that relates entropy to area, similar to [40]. If this reasoning is approximately true for all time-like observers traveling along u^μ, then one can covariantize and arrive at the full equation

$$G_{\mu\nu} = \frac{2\pi \kappa_{\lambda_*}}{\alpha} \delta \langle T_{\mu\nu}^{\mathrm{CFT}} \rangle. \tag{6.62}$$

This is the result for local perturbations using the smooth-manifold approach to the emergent geometry. An additional factor of $F'_\Lambda(0)/2$ would accompany nonlocal perturbations using the lossy channel on A_p, and an analogous equation can be derived from the Regge calculus approach using (6.71).

An immediate consequence of our bulk emergent gravity program is that there is a bound on the change in entropy within a region, reminiscent of the Bekenstein and holographic bounds. We have argued that positive energy corresponds to a decrease in the (full, UV) entropy, so we expect there to be an upper limit on the amount by which the entropy can decrease. This is of course automatic, as the entropy is a nonnegative number. Once the region A_p is fixed, the maximum possible decrease in entropy that corresponds to positive "mass-energy" has to be bounded by the total entanglement entropy of S_{A_p}, which is proportional to the area $\mathcal{A}_p$ of the region. More explicitly,

$$|\Delta S_{A_p}| \leq \alpha \mathcal{A}_p. \tag{6.63}$$

This resembles the holographic entropy bound. For an entropy change that saturates the bound, the vertices in regions A_p and $\overline{A}_p$ become disconnected from the graph point of view. An embedding space for $\overline{A}_p$ that reflects this change now has a hole around region A_p. Perturbations that increase the entropy are also bounded, but the bound scales with the volume of the region; we believe that configurations that saturate such a bound do not have a simple geometric interpretation.

6.6 Discussion

We have examined how space can emerge from an abstract quantum state in Hilbert space, and how something like Einstein's equation (in the form of a relationship between curvature and energy) is a natural consequence of this bulk emergent gravity program.

We considered a particular family of quantum states, those that are "redundancy-constrained" in a given decomposition of Hilbert space. For such states, a weighted graph that captures the entanglement structure can be constructed from the mutual information between different factors, and a manifold on which the graph can be (approximately) isometrically embedded is defined to be its emergent geometry. We presented specific implementations of the reconstruction framework using the classical multidimensional scaling algorithm for certain known area-law states. Both the dimension and the embedding coordinates for flat geometries can be found through the procedure. At leading order, entanglement perturbations backreact on the emergent geometry, and allow modular energy to be associated with the spatial curvature. This relation is analogous to the semiclassical Einstein equation.

A crucial feature of this approach is that we work directly with quantum states, rather than by quantizing classical degrees of freedom. No semiclassical background or asymptotic boundary conditions are assumed, and the theory is manifestly finite (since regions of space are associated with finite-dimensional factors of Hilbert space). There is clearly a relation with approaches that derive geometry from the entanglement structure of a boundary dual theory, but the entanglement we examine is directly related to degrees of freedom in the emergent bulk spacetime. Because lengths and other geometric quantities are determined by entanglement, a connection between perturbations of the quantum state and perturbations of the geometry appears automatically; in this sense, gravity appears to arise from quantum mechanics in a natural way.

Clearly, the framework is still very incomplete, and leaves much for future investigation. An important step in our procedure was assuming that we were given a preferred Hilbert-space decomposition $\mathcal{H} = \bigotimes \mathcal{H}_p$; ultimately we would like to be able to derive that decomposition rather than posit it. Perhaps most importantly, our definition of distance in terms of mutual information is compatible with the behavior of field theories at low energies, but we would like to verify that this really is the "distance" we conventionally refer to in quantum field theory. Ultimately that will require an investigation of the dynamics of these states. An obvious next step is to define time evolution, either through the choice of an explicit Hamiltonian or by letting time itself emerge from the quantum state. One important challenge will be to see whether approximately Lorentz-invariant dynamics can be recovered at low energies, and whether or not the finite nature of Hilbert space predicts testable deviations from exact Lorentz symmetry. We might imagine that, given a state $|\psi\rangle$ whose geometry is constructed using entanglement, one can generate all time-slices using a known local Hamiltonian such that $|\psi\rangle$ is a low energy state. Alternatively, by working with mixed states one could adopt the thermal time hypothesis [229] and generate state-dependent time flow purely from the modular Hamiltonian, which is in principle attainable from just the density operator.

To analyze the emergent geometries of states beyond redundancy-constraint, deeper understandings of the entropy data for subregions of different sizes will be important. One such case is manifest in the context of AdS/CFT correspondence, where entanglement entropy of different-sized balls in the CFT are needed to obtain bulk geometric information through a radon transform. One such approach may be to introduce additional structures on the graph and extend it to a tensor network. The program of geometry from tensor networks has mostly been based on states with a high degree of symmetry, such that notions of length and curvature can be assigned through simple geodesic matching and tessellation of space. The results obtained here suggest that for tensor networks with small perturbations, one can also modify the geometric assignment accordingly, matching the change in correlation or entanglement to perturbation in geodesic lengths. A notion of (coarse) local curvature can also be defined on triangulated spaces using entanglement and Regge calculus, which seems more natural for programs that relate network geometries to those of spacetime.

The emergence of time evolution will also be useful for the study of more complex behaviors related to entanglement perturbations. For instance, one can examine the interactions among multiple perturbations created in some local region. If the model is truly gravitational, the time evolution experiment should be consistent with our knowledge of gravitational dynamics. It will also be interesting to study the redundancy-constrained deformations of states beyond perturbative limit. Intuitively, we expect the emergence of a classical wormhole geometry by nonlocally entangling large number of degrees of freedom in a coherent manner. One can also examine purely quantum phenomena outside the context of classical Einstein gravity, including black-hole entropy and evaporation, using mutual information rather than classical spacetime geometry.

6.A Redundancy-Constraint and Coarse-graining

In this appendix we consider how to construct a coarse-grained decomposition of Hilbert space that is redundancy-constrained (RC), as defined in Section 6.3.1, when an initial fine-grained one is not.

Given some state $|\psi_0\rangle \in \mathcal{H}$ and some fixed Hilbert space decomposition $\mathcal{H} = \bigotimes_i^M \mathcal{H}_i$ for M sufficiently large, we first create a network represented by a graph $G_0 = (V_0, E_0)$. The graph has N vertices labelled by i, and each edge $\{i, j\}$ is weighted by $I(i:j)$, where $I(i:j)$ is the mutual information of partitions i and j. If the resulting graph is RC to the desired degree of accuracy, no further coarse-graining is needed.

If not, consider the set of all partitioning schemes C for a coarse-grained decomposition of the Hilbert space such that $\mathcal{H} = \bigotimes_p^N \mathcal{H}_p$. For each scheme $\mathcal{S} \in C$, we require that $N \leq M$ for some sufficiently large N so that non-trivial entanglement structure is still allowed. Each partition $\mathcal{S} = \{\{i_1, i_2, \ldots\}, \{i_k, i_{k+1}, \ldots\}, \ldots\}$ corresponds to constructing a more coarse-grained decomposition of the Hilbert space by taking the union of original subfactors; that is, for each $s_p \in \mathcal{S}$, $\mathcal{H}_p = \bigotimes_{i \in s_p} \mathcal{H}_i$.

A partition is RC-valid if the mutual-information-weighted-network $G = (V, E)$ based on the coarse-grained decomposition is redundancy-constrained. While there is no obvious way to choose the best coarse-graining scheme at this point, it is natural to consider the most uniform partitioning, so that all Hilbert-space subfactors have approximately equal dimensions.

If no such coarse-graining can be found for N reasonably large, then the procedure fails and we are forced to conclude that the given state cannot be cast in RC form in a simple way. We do not claim, however, that it doesn't admit a simple geometric description, as this is clearly false from our knowledge of AdS/CFT. Reconstructing the geometry from such states are interesting problems.

A more specific method for coarse-graining can also be constructed using network renormalization. While the algorithm is less computationally intensive, it fails for certain states if the original decomposition yields little useful information. For instance, it fails for the ground state of Toric code on a square lattice where the given Hilbert space decomposition is the usual tensor product of spin-1/2 degree of freedom on each link. It is, however, useful for certain finitely correlated states and/or those of typical condensed matter system at scales larger than the correlation length. It also works for the toric code if the decomposition is more coarse-grained.

For such states and decompositions, we follow network renormalization procedure by again constructing the mutual-information-weighted-network $G_0 = (V_0, E_0)$. Assume G_0 is connected; in the case when G_0 has multiple large disconnected components, one can simply perform the procedure separately for each connected component.

Then proceed to define a metric $\tilde{d}_0(i,j)$ on G_0 in the same manner as (6.14), with $\ell_{\text{RC}} \to \ell_0$. Then, for any vertex v on the graph, we consider an ϵ-ball $B_\epsilon(v)$ such that

$$B_\epsilon(v) = \{v' \in V | \tilde{d}(v, v') \leq \epsilon\}, \tag{6.64}$$

where $\tilde{d}(v, v')$ is a metric defined on the set of vertices V. Seed the entire graph with points like v until the whole graph is covered by ϵ-balls. Choose a minimum cover and compute the entanglement entropy for each the union of subregions in each ball to generate a coarse-grained graph G_1, where each vertex now is labeled by the union of the original subregions and the edge weights are given by the mutual informations of the coarse-grained subregions. Repeating the coarse-graining procedure until all higher subregions B_X can be well approximated by the cut function (6.9), we then label the coarse-grained subregion at this scale to be A_p for $p \in \mathcal{S}$, and label the corresponding coarse-grained network with A_p also. The resulting state will be, to a good approximation, redundancy-constrained.

6.B Entanglement Perturbations and Coarse Curvature

In this appendix we consider an alternative approach to calculating the curvature induced by an entanglement perturbation, working directly with the discrete graph rather than finding an embedding Riemannian manifold. Here we use the techniques in Regge calculus [230], in which the sense of spatial curvature is determined by deficit angles.

For a space of fixed integral Hausdorff dimension D obtained from (6.15), consider a vertex p and construct a local triangulation, if one exists. We say the space is r-locally triangulable at p if one can construct a abstract simplicial complex $\mathcal{K}$, where the simplices are sets of vertices in the metric subspace near p, by imposing a distance cutoff r, and if there exists an isometry (with respect to the metric distance) that maps $\mathcal{K}$ to a geometric simplicial complex K where inter-vertex distances of the metric subspace are preserved. If K is also a simplicial manifold we can proceed to define Regge curvature.

Select a codimension-2 simplex $X \ni p$ as a hinge, its volume given by (6.18). As the simplices in K are equipped with the usual Euclidean inner product, angles can be defined and deficit angle at the hinge $\delta(X) = 2\pi - \theta(X)$ can computed using the inner product structure in Euclidean space. Here we define

$$\theta(X) = \sum_i \phi_i(X), \tag{6.65}$$

where $\phi_i(X)$ is the angle between the unique two faces of a simplex containing the hinge X. In the case of a D-dimensional area-law system where $I(p:q) \neq 0$, construct a simplex by considering the n shortest distances. The curvature is then related to the deficit angles δ_i in the region by

$$R_T = \sum_i \delta_i L_i, \tag{6.66}$$

where L_i are the volumes of the codimension-2 hinges at which the curvature is concentrated. For $D = 2$, the hinge is a point, and the curvature is given by the deficit angle, where we set $L_i = 1$. In the continuum limit, (6.66) becomes $\int d^D x \sqrt{g} \mathcal{R}$, where $\mathcal{R}$ is the scalar curvature. In the case of emergent Euclidean (flat) space, we require $R_T = 0$.

Let us consider the effect of an entanglement perturbation on the geometry of a distance-function graph $\widetilde{G}$, using this technique. Again, the forms for both local and nonlocal perturbations are similar up to an overall factor.

Since the original deficit angle $\delta_p = 0$ in flat space, for p lying on the hinge, we may consider the angular deficit produced by varying each elongated edge connected to p. For each such simplex S connected to the hinge, the deficit at p induced by varying the length l_j of each edge in the simplex assumes, at leading order, the form

$$\delta_p^{(S)} = \frac{\delta l_j}{\ell_j^{(S)}(l_1, l_2, \dots)} + O((\delta l_j / l_j^{(S)})^2), \tag{6.67}$$

where l_j denotes the jth edge length of the D-simplex S. $\ell_j^{(S)}(l_1, l_2, \dots)$ is a function that has dimension of length and depends on the edge that is varied, as well as all the edge lengths that connect the vertices of S.

The overall deficit in a triangulation where all edges have roughly the same (unperturbed) length ℓ is

$$\Delta_p = \sum_{j,S} \frac{\delta l_j}{\ell_j^{(S)}} + O((\delta l_j / l_j^{(S)})^2) \tag{6.68}$$

$$= \mathcal{N}_p(D) \frac{\delta \ell}{\ell} + O((\delta \ell / \ell)^2), \tag{6.69}$$

where $\mathcal{N}_p(D)$ depends on the simplices in the triangulation. For example, if equilateral triangles with sides ℓ are used to triangulate the 2-dimensional flat space around p, then $\mathcal{N}_p(D = 2) = 12/\sqrt{3}$ in the case where all edges emanating from p vary by the same amount $\delta\ell$ under the entanglement perturbation. Note that in dimension greater than 2, there is no uniform tiling such that all edges are equal, hence the approximation in some average sense.

To estimate the coarse curvature at p, take $L_p \sim \ell^{D-2}$ as the volume of the codimension-2 hinge. $\delta\ell$ is identified with $\delta\tilde{d}(p, q)$ for the change in distance between adjacent vertices, and $\ell \approx \tilde{d}(p, q)$ for all q immediately adjacent to p in the triangulation. The total coarse curvature is given by

$$R_c = \Delta_p L_p \sim \mathcal{N}_p(D) \ell^{D-3} \delta\ell. \tag{6.70}$$

On the other hand, we know from [230] that in the continuum limit, if the metric g is approximately constant in the small region, $R_c \to \ell^D \mathcal{R}$, where $\mathcal{R}$ is the average coarse scalar curvature of the space contained in the small region with approximate volume ℓ^D. Applying (6.39) and the EFL, the average coarse curvature in the region is

$$\mathcal{R} = Z \delta \langle H \rangle. \tag{6.71}$$

Here, for a perturbation induced by a unitary $U_{A_p \overline{A}_p}$, the constant $Z = \ell_{\mathrm{RC}}^{-2} \xi(p, q, D)$ depends on the triangulation, strength of entanglement, and choice of coarse-graining. The factor $\xi(p, q, D) \propto |\mathcal{N}_p(D) \Phi'(i(p:q))| / I_0(p:q)$, which parametrizes all the order-one constants that enter into the process of averaging, can be explicitly computed once the triangulation and the inverse function Φ are known. We have taken $\ell = \gamma\ell_{\mathrm{RC}}$ to denote the average radius of the region, as before. Note that this is consistent with (6.40) up to the dimension- and triangulation-dependent factors.

For a nonlocal perturbation through a channel Λ, because the unitary only acts on A_p and the ancilla, the mutual information $\delta i(s:q) = 0$, and hence the distance functions $\tilde{d}(s, q)$ are invariant for all $s, q \neq p$. Only legs emanating from the vertex p in the triangulation are varied. The unitary perturbing map has a wider range of possible consequences, as its form is unspecified. Although the values of Z may be different depending on the specific map used, the formalism remain the same. As a result, for nonlocal perturbations with channel Λ, we have an equation of the same form, with $Z \to ZF'_{\Lambda}(0)/2$. In particular, if we restrict $U_{A_p\overline{A}_p}$ to only remove entanglement symmetrically near the boundary of the region A_p as before, the values of Z will be the same.

Chapter 7

BULK ENTANGLEMENT GRAVITY

We consider the emergence from quantum entanglement of spacetime geometry in a bulk region. For certain classes of quantum states in an appropriately factorized Hilbert space, a spatial geometry can be defined by associating areas along codimension-one surfaces with the entanglement entropy between either side. We show how Radon transforms can be used to convert this data into a spatial metric. Under a particular set of assumptions, the time evolution of such a state traces out a four-dimensional spacetime geometry, and we argue using a modified version of Jacobson's "entanglement equilibrium" that the geometry should obey Einstein's equation in the weak-field limit. We also discuss how entanglement equilibrium is related to a generalization of the Ryu-Takayanagi formula in more general settings, and how quantum error correction can help specify the emergence map between the full quantum-gravity Hilbert space and the semiclassical limit of quantum fields propagating on a classical spacetime.

This chapter is based on the Ref:
ChunJun Cao and Sean M. Carroll. "Bulk Entanglement Gravity without a Boundary: Towards Finding Einstein's Equation in Hilbert Space". In: (2017). arXiv: `1712.02803 [hep-th]`.

7.1 Introduction

There has been considerable recent interest in the idea of deriving an emergent spacetime geometry from the entanglement properties of a quantum state [37, 143, 71, 28, 29, 79]. Much of this work has taken place within the context of the Anti-de Sitter/Conformal Field Theory (AdS/CFT) correspondence [21]. In particular, various results related to emergent gravity [28, 232, 29] have yielded not only confidence in the program, but also helpful insights in understanding quantum gravity itself [233, 234]. Moreover, the idea need not be restricted to the context of holographic duality. Indeed, as it was originally proposed [143], it can in principle be generalized to derive other geometries closer to our own physical universe [235, 82, 86, 75, 236]. Entanglement also plays a role in entropic/thermodynamic gravity [65, 237, 238, 239, 199, 163] and the holographic-spacetime approaches of Banks and Fishler [201, 120, 121] and of Nomura et al. [240, 241].

The real world, needless to say, does not seem to have anti-de Sitter boundary conditions. It is therefore interesting to ask whether we can derive spacetime and gravitational field equations directly in the bulk from the entanglement properties of quantum states. The emergence of a semiclassical spacetime description from a quantum state, thought of as an abstract vector in Hilbert space, is essentially inevitable if we think that such an evolving quantum state provides a sufficient and complete description of physical reality. Our approach is to take the quantum state as fundamental and search for an appropriate classical limit, rather than quantizing any particular classical model.

In this work we tackle this problem, building on previous work on deriving emergent spatial geometry from entanglement of a quantum state [82]. There we investigated how a spatial metric (distance along curves) could be derived from a quantum state using the mutual information between different factors in Hilbert space. Our interest here is dynamical rather than static: to model the universe as a quantum state evolving in Hilbert space, show how the geometry of spacetime can emerge from the entanglement features of such a state in an appropriate factorization, and derive Einstein's equation in the semiclassical limit, an approach we label Bulk Entanglement Gravity (BEG). This requires us to consider a somewhat generic quantum system (or operator algebra), and examine which properties of a complex quantum system may be important in emerging spacetime geometry and gravity.

To concretely implement aspects of BEG, we will restrict ourselves in this paper to quantum states corresponding to emergent spacetimes in the weak-field regime, small perturbations of Minkowski space. (Since boundary conditions play no role in our analysis, the results will apply equally well to spacetimes with a nonzero cosmological constant, as long as we consider regions much smaller than the background curvature scale.) This represents a significant departure from the AdS/CFT version of the geometry-from-entanglement program. That approach may be thought of as "maximally holographic," with all of the bulk data encoded directly on the conformal boundary, and in particular the entanglement from which geometry emerges is that of the CFT state. Our regime is "anti-holographic", considering a small region that is a weak perturbation of flat spacetime. We are therefore interested in the entanglement of quantum states in Hilbert spaces that can be decomposed directly into factors corresponding to local regions of bulk spacetime (or equivalent ways of encoding entanglement data).

We will consider three different aspects of the BEG program. The first involves deriving emergent spatial geometry from entanglement data. Using assumptions (A1), (A2), and (A3) below, one may start from an appropriate quantum state and obtain an emergent geometry and its best-fit dimensionality. Rather than deriving *distances* from mutual information, it is more natural to derive *areas* of surfaces using the entanglement entropy across them. We will show in section 7.3 that for some class of geometries, the metric tensor can be obtained from these data using the tensor Radon transform [242]. In the case of AdS/CFT, a procedure like this would correspond to directly recovering the bulk geometry (plus matter) from a state of the fundamental theory, such as that of a CFT, but without relying on the knowledge that it has a flat geometry or that it can be interpreted to reside on the asymptotic boundary of the emergent geometry. In general, we still refer to this emergent spatial geometry as the "bulk" geometry, even when no boundary theory is available.

The second aspect is the emergence of gravitational dynamics. In section 7.4, we show that the linearized Einstein's equation can be derived from a background-free approach using quantum entanglement when a set of assumptions outlined in the next section are satisfied. In particular, one can derive the Hamiltonian constraint 7.4.1 from assumptions (A1) through (A5). Our approach is closely related to the entanglement-equilibrium proposal of [239]. It differs from [239] in that the analogous entanglement condition is valid across global cuts, instead of small local spherical surfaces. In addition, it is valid for all matter fields and does not rely on CFT modular Hamiltonians, which require matter fields to have UV fixed points. The main difference is that we derive our results directly from an abstract quantum state, rather than starting with quantum fields on an existing classical spacetime.

The third aspect deals with the "emergence map": the map from abstract quantum states in Hilbert space to quantum fields on a semiclassical background geometry. Part of this task can be thought of as determining which quantum degrees of freedom are responsible for emergent geometry as opposed to matter fields. This is important for the emergence of Einstein's equation with sources. To this end, we elaborate the relations with entanglement equilibrium and the Ryu-Takayanagi (RT) formula in section 7.5. In particular, we will discuss how one can distinguish the semiclassical geometry from quantum fields on that geometry solely from the features in a general background-free setting. Following Harlow [243], we argue that this can be done purely from the entanglement structure of the state or from the properties of a quantum error-correction code (QECC). It seems that quantum error correction properties can naturally provide a separation between geometric and matter degrees of freedom.

Our framework, partly inspired by [27], uses the Radon transform to tie together previous work on the thermodynamics of spacetime [65, 239], AdS/CFT approaches to emergent gravity [28], and kinematic space [50]. The Radon transform can also be used to construct emergent geometries for quantum error correction codes or tensor networks in general.

For the sake of concreteness, we will use the specific language of entanglement as computed from a quantum state in a Hilbert space. However, this work only relies on a configuration that defines subsystems and entanglement entropy data. Consequently, it also applies to more general formulations.

7.2 The Road to Bulk Entanglement Gravity

Our derivation of Einstein's equation from entanglement in the bulk of spacetime can be considered axiomatically: we can specify a list of explicit assumptions allowing us to start with an abstract quantum state and derive a semiclassical spacetime geometry with the appropriate dynamics. Here we briefly list the assumptions, before discussing them in detail in subsequent sections. Some of these assumptions will seem *prima facie* reasonable, while others are more conjectural. We will present arguments for their validity where available, and sketch a roadmap for the future work to complete this kind of program.

Our assumptions are as follows:

(A1) *Factorization.* Hilbert space $\mathcal{H}$ comes equipped with a preferred tensor product decomposition into individual factors,

$$\mathcal{H} = \bigotimes_i \mathcal{H}_i . \tag{7.1}$$

The individual factors $\mathcal{H}_i$ will correspond roughly to local points or small regions of space. See also [244]. The decomposition may be defined by the dynamics of the theory, as in [245].

(A2) *Redundancy constraint.* We are given a state $|\Psi\rangle$ in this decomposition with a very specific behavior of the entanglement entropy: the entanglement entropies of individual factors (or groups thereof) are approximately "redundancy constrained" (RC). Given a collection $\mathbf{B}$ of factors of $\mathcal{H}$ and its complement $\bar{\mathbf{B}}$, a state is RC if its entropy can be written as a sum over the mutual informations of the individual factors,

$$S(\mathbf{B}) := \frac{1}{2} \sum_{i \in \mathbf{B}, j \in \bar{\mathbf{B}}} I(i : j). \tag{7.2}$$

(Details of our notation are given in Section 7.3.1.) Thus, RC states generalize the notion of area-law states. In an approximately RC state, the entanglement entropy of a subsystem $\mathbf{B}$ can be written as

$$S(\mathbf{B}) = S_{\mathrm{RC}} + S_{\mathrm{sub}}, \tag{7.3}$$

where S_{RC} is the leading order contribution that satisfies the RC condition, and S_{sub} is a subleading correction.

(A3) *Area from mutual information.* For states that define an emergent geometry, the mutual information I between subsystems is proportional to the interface area $\mathcal{A}$ between corresponding subregions in that geometry,

$$\mathcal{A}(\mathbf{B}, \bar{\mathbf{B}}) = \frac{1}{2\alpha} I(\mathbf{B} : \bar{\mathbf{B}}). \tag{7.4}$$

(A4) *Entanglement equilibrium.* Entanglement perturbations of this configuration satisfy a modified entanglement equilibrium condition (MEEC), following Jacobson [239]. That is, under small perturbations, the total entropy perturbation $\delta S(R)$ of certain subsystems vanish, so that

$$0 = \delta S_{\mathrm{RC}} + \delta S_{\mathrm{sub}}. \tag{7.5}$$

(A5) *Emergent field theory.* The variation of the subleading correction can be generated by the entanglement variation of a state in some emergent effective field theory (EFT),

$$\delta S_{\mathrm{sub}} = \delta S_{\mathrm{EFT}}. \tag{7.6}$$

Here by S_{EFT} we mean the vacuum-subtracted or Casini entropy, representing entanglement over and above the divergent contribution of the QFT vacuum [210, 18, 20].

(A6) *Dynamics.* There exists a consistent dynamical theory, e.g., a Hamiltonian or a quantum circuit, that generates a sequence of such configurations, each admitting an emergent spatial geometry. Furthermore, there is a way to organize these emergent geometries to create a consistent Lorentzian spacetime geometry via time evolution.

(A7) *Lorentz invariance*. The above assumptions hold for any constant-time slice of the emergent Minkowski space, and the overall theory is Lorentz-invariant in an appropriate limit.

In the sections that follow we will show how to weave together these assumptions to derive geometry and Einstein's equation in the weak-field regime.

7.3 Emergent Spatial Geometries and Radon Transforms

In our earlier work on emergent space [82] we derived a spatial metric by using the quantum mutual information of two factors of Hilbert space to define a distance measure, based on our intuition from quantum field theory that the entanglement of low-energy states decreases monotonically with distance. If entanglement is our main quantity of interest, however, it is more natural to directly derive areas from the entanglement across a boundary separating two regions, rather than to derive distances between any two small regions. We expect the entropy across such a boundary to be proportional to the geometric area, plus some subdominant correction. In this section we explore the Radon transform as a natural tool for characterizing this data, and converting the entanglement of a quantum state into the metric tensor of a spatial slice.

7.3.1 Space from Hilbert Space

Here we briefly review the emergence of spatial geometry from appropriate quantum states [82]. Following assumption (A1), we are given a quantum state and a tensor product decomposition of the Hilbert space, $|\psi\rangle \in \mathcal{H} = \bigotimes_i \mathcal{H}_i$. The individual factors $\mathcal{H}_i$ correspond roughly to the degrees of freedom (geometric and field-theoretic) associated with a small local region of space. In the back of our minds we are thinking of these factors as finite-dimensional vector spaces [246], though this doesn't play a crucial role in our analysis. While this local picture of degrees of freedom runs against the spirit of holography, our interest here is in the weak-gravity regime, where it should be sufficient to think of gravity as a theory of local degrees of freedom.

One can generate an "information graph" $G = (V, E)$ based on this structure. The graph vertices in $V = \{i\}$ label each individual Hilbert space factors in $\{\mathcal{H}_i\}$, and the edges E between any two vertices i, j are weighted by the quantum mutual information between those factors,

$$I(i:j) = S(i) + S(j) - S(i \cup j). \tag{7.7}$$

An example graph is shown in Figure 7.1. For convenience, when we talk about quantities associated with the quantum state or the Hilbert space, we will use graph vertices and sets of vertices to denote tensor factors of the Hilbert space and products of the tensor factors, respectively. Note that we are not given the graph as a fundamental piece of information; it is derived from the quantum state in this particular factorization. The factorization itself could be derived, for example, from the requirement that the Hamiltonian look approximately local [245].

We say that the state $|\psi\rangle$ (or more generally, the entanglement data) is "redundancy constrained" (RC) if the entanglement entropy of any subsystem $\mathbf{B} \subset V$ can be computed by summing over the weights of all edges that connect vertices in $\mathbf{B}$ with those in its complement $\bar{\mathbf{B}}$, as in assumption (A2). More precisely, the entanglement entropy of a subsystem $\mathbf{B}$ in a redundancy-constrained state is given by the cut function [166],

$$S(\mathbf{B}) = S_{\mathrm{RC}}(\mathbf{B}) := \frac{1}{2} \sum_{i \in \mathbf{B}, j \in \bar{\mathbf{B}}} I(i:j). \tag{7.8}$$

Other than the familiar examples, such as area-law states [180] in certain condensed matter systems, a wider class of states such as Projected Entangled-Pair states [47], holographic quantum error correction code [49], and (bulk) random tensor network states [76] are also (approximately) redundancy constrained. Note that a *generic* state in Hilbert space will be very far from RC, and the information graph will be highly connected rather than taking the sparse form suggested by locality; the states we have in mind resemble low-energy states of approximately-local Hamiltonians.

In states that are only approximately RC, (7.8) holds to leading order, and the exact entanglement entropy takes on a subleading correction

$$S(\mathbf{B}) = S_{\mathrm{RC}}(\mathbf{B}) + S_{\mathrm{sub}}(\mathbf{B}), \tag{7.9}$$

where $S_{\mathrm{sub}} \ll S_{\mathrm{RC}}$. There are two natural sources for such corrections. One is long-range entanglement even in the vacuum, which we expect to be present but subdominant. The other is entanglement between excited degrees of freedom over and above the vacuum. An EPR pair, for example, can have an entanglement that is independent of the distance between the two particles; however in a quantum field theory such entanglement is a very small correction to the huge entanglement between the vacuum modes. (For discussions of vacuum-subtracted entropy in quantum field theory, see [210, 18, 20].)

In order to obtain an emergent space, one has to make certain assumptions about the connection between entanglement and geometry. A natural identification can be

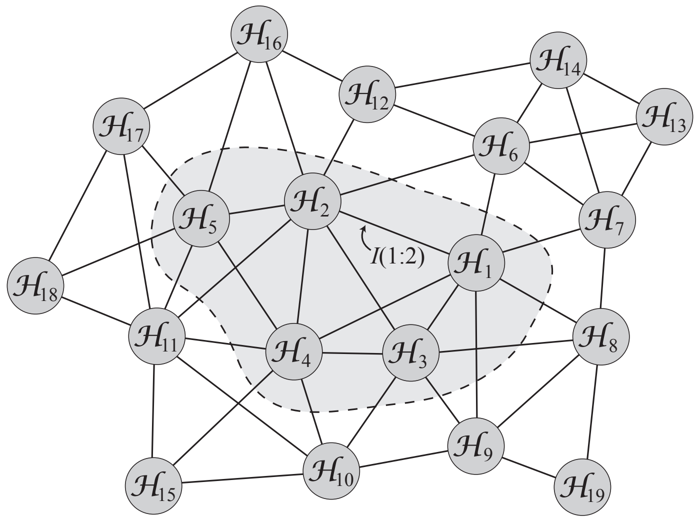

Figure 7.1: This shows an example of the information graph in which vertices represent factors in a decomposition of Hilbert space, and edges are weighted by the mutual information between the factors. In redundancy-constrained states, the entropy of a group of factors (such as the shaded region **B** containing $\mathcal{H}_1 \otimes \mathcal{H}_2 \otimes \mathcal{H}_3 \otimes \mathcal{H}_4 \otimes \mathcal{H}_5$.) can be calculated by summing over the mutual information of the cut edges, as in (7.8).

motivated by area-law systems, where the entanglement entropy of a region scales as the interface area that separates the region and its complement. To leading order, this implies that the interface area is proportional to the mutual information between the region and its complement. Because RC states generalize area-law states, a natural definition is to define the "interface area" of an emergent geometry as the mutual information between a system and its complement, as in assumption (A3). That is,

$$\mathcal{A}(\mathbf{B}, \bar{\mathbf{B}}) := \frac{1}{2\alpha} I(\mathbf{B} : \bar{\mathbf{B}}). \tag{7.10}$$

See also [157, 212]. At this level α serves as an undetermined constant of proportionality; we will later relate it to Newton's gravitational constant via $\alpha = 1/4G_N$.

Given the information graph, however, it is more convenient to work with the length measure between factors, instead of their mutual interface areas. To derive the approximate geometry that may be encoded by the graph, [82] defines an *ad hoc* distance function between vertices from the edge weights. This, together with the set V, generate a metric space, which is isometrically embedded in to a manifold. We define the embedding manifold as the emergent geometry of the graph. The technique of classical multi-dimensional scaling (MDS) [219, 220, 221, 222, 217] can be used for this purpose to determine the best-fit dimensionality of the geometry, as well as the embedding coordinates for the elements of V.

7.3.2 Metric tensor from the inverse tensor Radon transform

While straightforward in an approximate recovery of geometry, the correct "transform" function from an area quantity to distances can, in principle, be non-local. A simple local function from area to distance is expected to yield a distortion unless we operate in the case with a high degree of symmetry. To address this deficiency, we seek an improved method to directly transform (dualize) the area quantity, which is proportional to mutual information, to a measure of distances via a global transformation. In this section, we reconstruct the spatial metric tensor directly from entanglement data.

In cases of interest where the emergent geometry is not highly symmetric, we can imagine a two-part procedure, in which we use MDS to emerge a symmetric "background" geometry, and then recover the metric perturbation from an inverse tensor Radon transform. (In fact the background geometries of interest to us will generally be flat Euclidean spaces.) The recovery procedure is valid as long as the tensor Radon transform has a unique inverse. Such is the case for simple manifolds in 2 dimensions [247], which have been extensively studied in the context of the boundary-rigidity problem. In higher dimensions, similar inversions are also possible in Riemannian geometries that are close to flat space or hyperbolic space [248].

Intuitively, the Radon transform maps a function on a space to a function on a set of surfaces embedded in that space, by integrating the function over the surface [**helgason1999Radon**, 242, 27]. More formally, consider an n-dimensional Riemannian manifold $\mathcal{M}$ and a totally-geodesic codimension-1 submanifold $\mathcal{S}$, where "totally geodesic" means that the geodesics of the submanifold with respect to its induced metric are also geodesics of the original manifold.[1] Most geometries will not admit any totally-geodesic submanifolds, but they are plentiful in the highly-symmetric backgrounds of interest to us here, *e.g.* hyperplanes in Euclidean spaces. The Radon transform of a function f on $\mathcal{M}$ at $\mathcal{S}$ is defined as the integral

$$\mathscr{R}[f](\mathcal{S}) = \int_{\mathcal{S}} f \, d\sigma \tag{7.11}$$

over $\mathcal{S}$ with area element $d\sigma$. Clearly, a well-defined transform requires the function to be regularized in some way, *e.g.,* by setting $f = 0$ outside some domain. If the

[1] Analogous transforms along $n-k$ dimensional submanifolds can also be defined. Here we only discuss the case when $k = 1$.

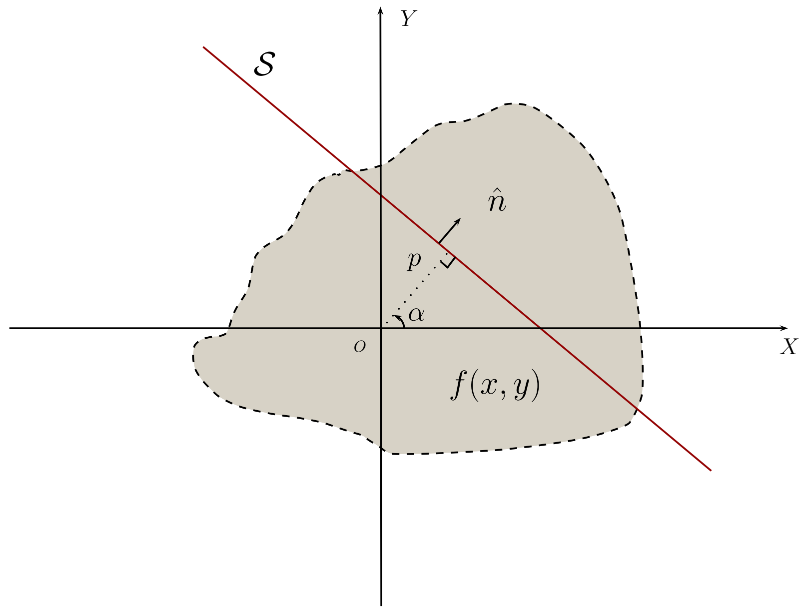

Figure 7.2: The Radon transform of a scalar function $f(x, y)$ defined on some compact domain (shaded area) is done by integrating the function over the submanifold $\mathcal{S}$, which is a line in 2-dimensional flat space. The transformed data $\mathscr{R}[f](p, \alpha)$ corresponds to the value at a point in the space of $\mathcal{S}$ (the space of lines in this case). p is the perpendicular distance between the plane and the origin and α parametrizes the direction of the unit normal $\hat{n}$.

geometry on $\mathcal{M}$ is Euclidean (in the sense of flat), an appropriate set of surfaces $\mathcal{S}$ is given by planes specified by a distance and angle from the origin, as shown in Figure 7.2.

We can also perform the Radon transform of a tensor field. Such tensor Radon transforms were used in [27] to derive the linearized Einstein's equation in the context AdS/CFT. We will employ analogous techniques, but directly in the bulk, without reference to kinematic space or holography.

Let g_{ij} be the metric tensor on $\mathcal{M}$ and let w_{ij} be the induced metric of the submanifold $\mathcal{S}$. (Our notation follows [27], and differs from the more common notation in the mathematical literature.) The longitudinal tensor Radon transform of s_{ij} on $\mathcal{M}$ is defined as

$$\mathscr{R}_{\parallel}[s_{ij}] = \int_{\mathcal{S}} w^{ij} s_{ij} \, d\sigma. \tag{7.12}$$

(Henceforth we will drop the explicit appearance of the submanifold $\mathcal{S}$ on the right-hand side.) Similarly, the transverse tensor Radon transform is

$$\mathscr{R}_{\perp}[s_{ij}] = \int_{\mathcal{S}} (g^{ij} - w^{ij}) s_{ij} \, d\sigma. \tag{7.13}$$

Indices are raised and lowered with the spatial metric. Since at this point we are only considering spatial geometry and related tensors, we do not discuss metrics with Lorentzian signatures. A process to invert the above transform and obtain the tensor s_{ij} is referred to as inverse tensor Radon transform.

The inversion problem in $n = 2$ has been mostly studied in the context of the boundary-rigidity problem [249, 250], which examines if the bulk geometry of a manifold can be recovered knowing only the pair-wise geodesic distances between all its boundary points. A manifold for which this is possible is called boundary-rigid. This problem has been shown [242] to be equivalent to the tensor geodesic X-ray transform problem [251, 242, 250], which coincides with the tensor Radon transform in 2 dimensions. An earlier classification of boundary-rigid manifolds is now known as the Michel's conjecture [252], where so-called simple manifolds are boundary-rigid. (A Riemannian manifold $\mathcal{M}$ is simple if, given any two points, there exists a unique geodesic joining the points, and if the second fundamental form is positive definite at every point on $\partial\mathcal{M}$.) A proof has been given in $n = 2$ [247], although some other higher-dimensional results are also known [253]. See [250, 254, 255] and references therein. Results related to applying the inverse were explored both analytically [256, 257] and numerically [258]. The inverse problem of the higher-dimensional tensor Radon transform has remained largely unexplored until recently, where a proof on invertibility was produced [248], but an explicit inversion formula and numerical results are still unknown, to the best of our knowledge. Henceforth we will simply assume that the appropriate tensor-transform inversion can be performed.

7.3.3 Spatial metric from entanglement

We now describe how to use the Radon transform to obtain an emergent spatial geometry from the quantum state. Suppose we begin with a quantum state $|\psi\rangle$ from which, following [82], we may use MDS to find a best-fit maximally-symmetric geometry g_{ij} on a spatial manifold $\{\mathcal{M}\}$, which we will refer to as the background. We now would like to consider a perturbed state,

$$|\Psi\rangle = |\psi\rangle + \delta|\psi\rangle. \tag{7.14}$$

The perturbed entanglement entropy δS associated with each subsystem also changes the associated emergent geometry. Using these perturbed data δS for different subsystems, we will show that the inverse tensor Radon transform allows us to recover a perturbed metric δh_{ij} on the background.[2]

We are thus considering a situation in which we attempt to recover δh_{ij} when we are given a background metric g_{ij} and an entanglement perturbation δS that can be computed from the state itself. For discrete finite-dimensional quantum systems, such as some condensed matter models [259, 260, 225] or the ones we considered in [82], we will also assume a continuum limit or a smoothing process over the data δS such that the usual Radon transform is well-defined and can be performed. Alternatively, a discrete version may also be applied [261].

We illustrate the reconstruction of δh_{ij} with an example in flat space, although the procedure can be easily generalized to other backgrounds, as long as an inverse transform exists. Consider the case where one determined the exact geometry encoded in the state $|\psi\rangle$ to be an n-dimensional flat space with metric $g_{ij} = \delta_{ij}$. For any codimension-1 hyperplane $C(p, \hat{n})$ that separates the space into two adjacent regions $\Sigma, \bar{\Sigma}$, one can compute the interface area $\mathcal{A}(C)$ using the flat metric of the embedding space. This follows from assumption (A3), that area is proportional to mutual information,[3]

$$\mathcal{A}(C) = \frac{1}{2\alpha} I(\Sigma_C : \bar{\Sigma}_C). \tag{7.15}$$

Given the RC assumption (A2), $I(\Sigma_C : \bar{\Sigma}_C)$ is determined by the sum of mutual informations along all edges that are cut by C [166]. Adding a perturbation $\delta|\psi\rangle$ in general also perturbs the mutual information across different bipartitions. For the same bipartition along the cut, the perturbed area is now given by perturbed mutual information $\mathcal{A}' = (1/2\alpha) I'(\Sigma_C : \bar{\Sigma}_C)$, and one can define the area perturbation

$$\delta\mathcal{A} = \mathcal{A}' - \mathcal{A} = \frac{1}{2\alpha}\delta I = \frac{1}{2\alpha}(I' - I)(\Sigma_C : \bar{\Sigma}_C), \tag{7.16}$$

so that

$$\delta I(C) = 2\alpha\delta\mathcal{A}(C). \tag{7.17}$$

Let $\tilde{w}_{ij}$ be the induced metric of C in the perturbed geometry, where w_{ij} is the induced metric in the background,

$$\tilde{w}_{ij} = w_{ij} + \delta w_{ij}. \tag{7.18}$$

[2]A similar procedure may be used when MDS itself gives an imperfect embedding of the background geometry.

[3]With MDS, we are considering only a geometry that is finite in extent. In the case where the space is infinite, we restrict ourselves to a particular finite region for analysis.

The area is then

$$\mathcal{A}'(C) = \int_C \sqrt{\det \tilde{w}_{ij}}\, d\sigma, \tag{7.19}$$

and the area perturbation is

$$\delta\mathcal{A} = \int_C \left(\sqrt{\det \tilde{w}_{ij}} - \sqrt{\det w_{ij}} \right) d\sigma. \tag{7.20}$$

Using $\det(\mathbb{I} + \epsilon M) = 1 + \epsilon \operatorname{Tr}[M] + O(\epsilon^2)$ for any symmetric matrix M, this becomes

$$\delta\mathcal{A} = \frac{1}{2} \int_C \operatorname{Tr}(\delta w)\, d\sigma, \tag{7.21}$$

where $\operatorname{Tr}(\delta w) = w^{ij}\delta w_{ij}$. Comparing to (7.12), we see that the area perturbation is directly related to the longitudinal Radon transform of the induced metric perturbation,

$$\delta\mathcal{A} = \frac{1}{2}\mathscr{R}_{\parallel}[\delta w_{ij}]. \tag{7.22}$$

It is straightforward to show, for example by choosing an appropriate coordinate system, that $\mathscr{R}_{\parallel}[\delta w_{ij}] = \mathscr{R}_{\parallel}[\delta h_{ij}]$. We therefore see that the mutual information across the bipartition is proportional to the Radon transform of the metric perturbation,

$$\delta I(C) = \alpha \mathscr{R}_{\parallel}[\delta h_{ij}]. \tag{7.23}$$

Given the entanglement data $\delta I(C) = 2\alpha\delta\mathcal{A}(C)$ over all such cuts $C(p, \hat{n})$, we can perform the inverse tensor Radon transform of $\mathscr{R}_{\parallel}[\delta h_{ij}]$, thus completing the metric reconstruction procedure, so that the full spatial metric $g_{ij} + \delta h_{ij}$ is obtained from entanglement data of a quantum state in a background-free approach.

We therefore need assurance that the tensor Radon transform of interest is indeed invertible. At first sight, this requirement of invertibility to recover a tensor from a scalar function seem unlikely, simply from counting degrees of freedom; there are several components of the metric, and only one value each of $\mathscr{R}_{\perp}$ and $\mathscr{R}_{\parallel}$. However, this is indeed uniquely invertible for a certain set of manifolds, up to natural obstructions that are not simply fixed by the data. In this case, the degrees of freedom that are undetermined by entanglement are manifested as gauge transformations of the δh_{ij} field by an arbitrary vector field ξ,

$$\delta h_{ij} \to \delta h_{ij} + \partial_i \xi_j + \partial_j \xi_i, \tag{7.24}$$

for the simple reason that the longitudinal tensor Radon transform vanishes for tensors of the form $\partial_{(j}\xi_{i)}$.

From the existing mathematical literature, we conclude that for $n = 2$, an inverse transform can be explicitly implemented to obtain δh_{ij} from an entanglement perturbation as long as the background manifold $\mathcal{M}$ is boundary-rigid. Current knowledge classifies simple manifolds and certain quotients [262] as boundary-rigid, although other particulate examples such as tori have also been given [255, 263, 264]. For $n > 2$, an inverse, if it exists, can also be uniquely obtained near flat or hyperbolic geometries. Recently, [25] also proposes a recovery of the metric for certain types of Riemannian manifolds at $n = 3$. However, an explicit reconstruction algorithm for general dimensions is still contingent on further progress in the mathematical community.[4]

7.4 Emergent Gravity from Quantum Entanglement

We now turn to the gravitational dynamics of our emergent geometries, and explain how assumptions (A1) through (A7) allow us to derive the linearized Einstein equation in the weak-field limit. In the first subsection we look at classical spacetime, using the Radon transform to write the terms appearing in Einstein's equation in a convenient form. In the following subsection we use the results to derive a modified entanglement equilibrium condition, and in the final subsection we derive Einstein's equation for an emergent Lorentzian spacetime geometry from the quantum state.

7.4.1 The Hamiltonian Constraint and its Radon transform

Let us momentarily set aside spacetime emerging from quantum mechanics and instead consider the conventional classical Einstein's equation linearized around a Minkowski background.

Given a spacetime with a parameterized set of time slices $\mathcal{M}_t$ with timelike unit normal vectors t^μ, the classical Hamiltonian constraint of general relativity corresponds to the condition

$$G_{\mu\nu}t^\mu t^\nu = 8\pi G_N T_{\mu\nu}t^\mu t^\nu. \tag{7.25}$$

In the following derivation, we work in the linearized regime where we consider metric perturbations on a Minkowski background: $g_{\mu\nu} = \eta_{\mu\nu} + \delta h_{\mu\nu}$. As such, we can consider the constant-time slices of Minkowski space. The (background)

[4]The boundary-rigidity problem is intimately related to that of reconstructing bulk geometry from boundary data in the context of AdS/CFT. The existence of a manifold that is not boundary-rigid may be indicative of the limitations of the Ryu-Takayanagi formula in AdS_3/CFT_2 for constructing bulk geometries. Similar conclusions also apply to certain reconstruction schemes in higher dimensions, which use correlation functions to estimate geodesic lengths [265]. For instance, consider the back-reacted geometry of a single massive particle in AdS. The spatial geometry of a time slice is not boundary-rigid.

extrinsic curvature vanishes on each of these time slices. At the linearized level we can then relate the Einstein tensor to the *spatial* curvature scalar via $\mathcal{R} = 2G_{tt}$ [266]. Therefore, for linearized equations, the Hamiltonian constraint reads

$$\delta\mathcal{R} = 16\pi G_N \delta T_{tt}. \tag{7.26}$$

Because we are specializing to flat backgrounds, for each such constant time slice, let the background spatial metric be δ_{ij} and the perturbation be δh_{ij}, which is a tensor-valued function on flat space. To linear order we can expand

$$\delta\mathcal{R} = \delta^{ij}\frac{1}{2}(\partial_i\partial_r\delta h_{jr} + \partial_j\partial_r\delta h_{ir} - \partial_i\partial_j\delta h - \nabla^2\delta h_{ij}), \tag{7.27}$$

where ∇^2 is the Laplacian in n-dimensional flat space, with n being the dimension of the constant-time slice. Now consider taking the Radon transform of both sides of equation (7.27) along $(n-1)$-dimensional hyperplanes. We can derive[5]

$$\mathscr{R}[\delta\mathcal{R}] = -\mathscr{R}_{\|}[\nabla^2\delta h_{ij}]. \tag{7.28}$$

Radon transforms obey an intertwinement relation [**helgason1999Radon**],

$$\mathscr{R}[\nabla^2 f] = \frac{\partial^2}{\partial p^2}\mathscr{R}[f], \tag{7.29}$$

where p is the distance from the origin to the hyperplane. From this and the fact that $\mathscr{R}_{\|}[\delta h_{ij}] = 2\delta\mathcal{A}$, we find a relation between the spatial curvature and the area perturbation,

$$\mathscr{R}[\delta\mathcal{R}] = -2\frac{\partial^2}{\partial p^2}\delta\mathcal{A}. \tag{7.30}$$

Comparing to (7.26), we end up with

$$-\frac{\partial^2}{\partial p^2}\delta\mathcal{A} = 8\pi G_N \mathscr{R}[\delta T_{tt}]. \tag{7.31}$$

To solve (7.31) for $\delta\mathcal{A}$, we convolve the source with the Green function,[6]

$$G(p,q) = (q-p)\theta(q-p). \tag{7.32}$$

[5]The derivation is simpler by writing the metric in the Gaussian normal coordinate.

[6]The full Green function has additional terms $c_1 p + c_2$. However, since the boundary condition is unknown, unlike the case in AdS/CFT, we fix the coefficients by requiring the solution $\delta\mathcal{A}$ matches to the Rindler Hamiltonian of the bulk matter fields, by choosing $c_1 = c_2 = 0$.

This yields

$$\delta\mathcal{A} = -\int (q-p)\theta(q-p)\mathscr{R}[8\pi G\delta T_{tt}]\,dq \tag{7.33}$$

$$= -8\pi G_N \int_C \int_{q>p} (q-p)\delta T_{tt}\,dq\,d^{n-1}\sigma. \tag{7.34}$$

Recall that each surface C is specified by a distance parameter p from the origin and its unit normal $\hat{n}$. Then the integral is over the half space up to a surface with unit normal $\hat{n}$ and distance p from the origin.

7.4.2 Emergent entanglement equilibrium

We can now connect these classical GR concepts to entanglement data of an underlying quantum state in an abstract Hilbert space. Although the physical meaning of equation (7.34) is unambiguous in the classical theory, these quantities should ultimately be derived from the quantum state if space is emergent from entanglement. On the left-hand side, as we know from previous constructions [82], the area perturbation δA can be identified with the sum of mutual information $\delta I/2\alpha$ along the cut C in an RC state. In the case where the overall state is pure,

$$\delta I(\Sigma_C : \bar{\Sigma}_C) = 2\delta S(\Sigma_C). \tag{7.35}$$

On the right-hand side of (7.34), in a semiclassical theory we interpret the classical quantity δT_{tt} as the expectation value of a quantum operator $\widehat{T}_{tt}$ in some particular state of a quantum field theory on curved spacetime. We then recognize that the integral in (7.34) is related to the modular Hamiltonian of the right Rindler wedge for a quantum field theory, translated spatially by p. More explicitly, take $p = 0$ and identify the normal of C with the direction in which the Rindler observer accelerates, which we take to be the x-axis. We then have the QFT expression for the Rindler modular Hamiltonian,

$$\widehat{H}_{\text{mod}} = 2\pi \int \int_{x>0} x\widehat{T}_{tt}\,d^n x. \tag{7.36}$$

We therefore consider the right-hand side of (7.34) to represent the expectation value of the modular Hamiltonian of some effective field theory on a flat background, evaluated with respect to some linearized perturbation of a quantum state $\delta\rho_{\text{EFT}}$, such that

$$\delta T_{tt} = \text{Tr}[\delta\rho_{\text{EFT}}\widehat{T}_{tt}]. \tag{7.37}$$

In the linearized regime, it must also be proportional to the entanglement entropy perturbation $\delta S_{\text{EFT}}(C)$ of the same half-space demarcated by C, via the entanglement first law [267],

$$\delta\langle \widehat{H}_{\mathrm{mod}}\rangle = \delta S_{\mathrm{EFT}}(C). \tag{7.38}$$

Substituting these new variables and using (7.15), (7.34) becomes

$$\frac{1}{2}\delta I(\Sigma_C : \bar{\Sigma}_C) + 4G\alpha\delta S_{\mathrm{EFT}}(C) = 0 \ \ \text{(pure state)}, \tag{7.39}$$

or using the RC relation (7.2),

$$\delta S(\Sigma_C) + 4G_N\alpha\delta S_{\mathrm{EFT}}(C) = 0. \tag{7.40}$$

Let us try to understand this relation in the context of deriving geometry from a quantum state. By construction, $\delta S(\Sigma_C)$, which is proportional to the area perturbation, is the contribution that we have consistently identified with the RC part of the entanglement. The more difficult question is how δS_{EFT} should be identified. Recall that from assumption (A2), in ground states of systems satisfying an area law [180] or other approximately-redundancy-constrained states, one can write the total entanglement entropy associated with a subsystem Σ as

$$S_{\mathrm{total}}(\Sigma) = S_{\mathrm{RC}}(\Sigma) + S_{\mathrm{sub}}(\Sigma), \tag{7.41}$$

where the RC contribution S_{RC}, or the area-scaling contribution when there is a well-defined geometry, dominates over the subleading correction S_{sub}. Motivated by the RT formula with subleading corrections, we claim in assumption (A5) that S_{EFT} can be interpreted as originating from the subleading corrections S_{sub} to the RC entropy contribution. We will further discuss this claim and its similarities with a generalized form of the RT formula in section 7.5.

Jacobson [239] derived Einstein's equation in a semiclassical bulk spacetime from the concept of entanglement equilibrium. This is the assumption that the total entanglement entropy of a small ball in some maximally-symmetric background spacetime is extremal, i.e., $\delta S_{\mathrm{total}} = 0$ when a small perturbation is added. To complete the derivation, one has to separate the entanglement into UV and IR contributions, such that $\delta S_{\mathrm{total}} = \delta S_{\mathrm{UV}} + \delta S_{\mathrm{IR}}$. In [239], $\delta S_{\mathrm{UV}} \sim \delta A$ is assumed to be the area variation in some background geometry and δS_{IR} is identified with the entanglement entropy of a field theory regulated in some way.

Our equation (7.40) relating geometric entropy to the entropy perturbation of an emergent EFT can be thought of as a version of the modified entanglement equilibrium condition (MEEC) from assumption (A4). The geometric term corresponds to the UV contribution, while the EFT (matter) term corresponds to the infrared,

$$\delta S(\Sigma_C) \leftrightarrow \delta S_{\text{UV}} \leftrightarrow \delta S_{\text{RC}}, \tag{7.42}$$

$$4G_N \alpha \delta S_{\text{EFT}}(C) \leftrightarrow \delta S_{\text{IR}} \leftrightarrow \delta S_{\text{sub}}, \tag{7.43}$$

and the condition (7.40) states that these sum to zero near the background. A crucial difference, however, is instead of entanglement across some small ball centered at a point, the condition now has to hold across all cuts C made by $(n-1)$-dimensional totally-geodesic submanifolds in the background space. This also differs from [239] in that one no longer has to rely on CFT modular Hamiltonians by assuming the special property of the matter field theory having an UV fixed point. The result holds for a generic QFT with the corresponding Rindler Hamiltonian.

For now, we will proceed with the identification $\delta S_{\text{sub}} = \delta S_{\text{EFT}}$. This fixes the constant $\alpha = 1/4G_N$, the value required for the consistency of Einstein's equation and the holographic bound. Consequently, MEEC translates into a more general relation, whereby UV and IR portions of the entropy are identified not based on assumptions in semiclassical physics, but rather on the properties of quantum entanglement,

$$\begin{aligned} 0 &= \delta S_{\text{total}} \\ &= \delta S_{\text{RC}} + \delta S_{\text{sub}} \\ &= \alpha \delta A + \delta S_{\text{EFT}}. \end{aligned} \tag{7.44}$$

With this identification, the above relation is a necessary condition for a state to have emergent properties consistent with general relativity at low energies.

Therefore, by making the identification that the subleading entropy to RC with matter field entropy, similar to the vacuum-subtracted (Casini) entropy [210, 18, 20], we establish an equivalence between the modified entanglement equilibrium condition (7.44) and the Radon transform of the linearized Hamiltonian constraint (7.31). This argument can also be used to generalize the result of [28] in AdS/CFT to other (non-flat) geometries, as long as the function is invertible under Radon transform in the background Riemannian manifold.

7.4.3 Linearized Einstein Equation from entanglement

We can now put the picture together to derive dynamics for the emergent spacetime geometry, in a way similar to [239]. For the sake of convenience, let's assume that from our previous results one has already emerged a flat background geometry from MDS or tensor Radon transform techniques. Similar to the AdS/CFT case considered in [28], we now wish to determine if the geometric deformation from entanglement perturbations responds in a way consistent with Einstein gravity. A similar conclusion can also be generalized to hyperbolic spaces using MDS with a best fit curvature parameter following the procedure of [27], but we will not consider that case here.

Consider the quantum system from which flat space is emergent. For concreteness, the total system could be described by a quantum state $|\psi\rangle \in \mathcal{H} = \bigotimes_i \mathcal{H}_i$, as in assumption (A1). A subsystem is thus described by the reduced density operator associated with some Hilbert subspace. Any cut C that corresponds to a codimension-1 hyperplane in the emergent geometry will bipartition the system into two adjacent non-overlapping regions. One can compute the entanglement entropy for either region Σ, which reads $S(\Sigma) = S_{\text{RC}}(\Sigma) + S_{\text{sub}}(\Sigma)$, as in (A2). Now we add a perturbation to obtain $|\Psi\rangle = |\psi\rangle + \delta|\psi\rangle$. The perturbation will modify the entanglement, which in turn changes the emergent geometry, following the area perturbation defined by (A3).

The MEEC assumption (A4) relates perturbations in the RC and subdominant contributions to the entropy across C,

$$0 = \delta S_{\text{RC}} + \delta S_{\text{sub}}. \tag{7.45}$$

Using assumption (A5) to relate the subdominant term to the vacuum-subtracted entropy of an effective field theory, the MEEC is equivalent to the (scalar) Radon transform of the classical Hamiltonian constraint linearized against a flat background,

$$\mathscr{R}[\delta\mathcal{R}] = 16\pi G_N \mathscr{R}[\delta T_{tt}], \tag{7.46}$$

as argued in the previous subsection. Here $\delta\mathcal{R}$ is the spatial curvature perturbation and δT_{tt} is the linear perturbation of the stress-energy associated with an effective field theory living on the background. Because this relation holds for all such cuts in the flat background space, equation (7.46) uniquely determines the linearized Hamiltonian constraint,

$$\delta\mathcal{R} = 16\pi G_N \delta T_{tt}, \tag{7.47}$$

provided the inverse is well-defined.

Following assumption (A6) about dynamics, we consider a sequence of states $|\Psi(t)\rangle$ labeled by a single parameter t, which together describe a Lorentzian spacetime. The corresponding emergent spatial geometries can be thought of as embedded spacelike slices in a spacetime with coordinates in synchronous gauge. In terms of a unit timelike vector field t^μ normal to these slices, the Hamiltonian constraint (7.47) can be written as

$$\delta G_{\mu\nu} t^\mu t^\nu = 8\pi G_N \delta T_{\mu\nu} t^\mu t^\nu. \tag{7.48}$$

Under the Lorentz-invariance assumption (A7), this must be valid for arbitrary normal t^μ. We therefore have the full linearized Einstein's equation,

$$\delta G_{\mu\nu} = 8\pi G_N \delta T_{\mu\nu}. \tag{7.49}$$

While the number of conjectural assumptions needed to reach the result is admittedly considerable, we find the path we've outlined to be a promising route to deriving bulk gravitational dynamics directly from the evolution of an abstract wave function in Hilbert space.

7.5 Entanglement RT Formula and Quantum Error Correction

It would be useful to have a more systematic approach to decomposing an abstract quantum state into geometric (UV) and matter (IR) degrees of freedom. In the previous section we proposed one such procedure, identifying $S_{\rm RC} = \alpha\mathcal{A}$ and $S_{\rm sub} = S_{\rm EFT}$ when the state is approximately RC and admits an emergent geometry. This identification also proposes a background-free way of understanding these "UV" and "IR" entropies purely from the characteristics of entanglement, which can be done for arbitrary quantum states.

In this section, we will connect these observations with the Ryu-Takayanagi (RT) formula from AdS/CFT. We will also argue that more general emergent geometries can be assigned to quantum error correction codes, where the code subspace naturally separates the geometric and matter contributions to entanglement entropy. Our considerations here are tentative (even by the standards of the rest of the paper), and would require more elaboration to make precise.

Let's first recall the RT entropy relation in the case of AdS/CFT with a subleading N^0 correction [208],

$$S_{\rm CFT}(A) = \frac{\mathcal{A}_{\rm ext}(A)}{4G_N} + S_{\rm bulk}. \tag{7.50}$$

Here, $S_{\rm CFT}(A)$ is the entanglement entropy of a subregion A in the boundary field theory, $\mathcal{A}_{\rm ext}(A)$ denotes the area of a bulk extremal surface homologous to A, and $S_{\rm bulk}$ is a correction representing contributions from bulk matter fields.

The RT formula relates boundary quantities to bulk quantities in a holographic setting. But there is an obvious analogy to the BEG relation

$$S_{\mathrm{total}} = S_{\mathrm{RC}} + S_{\mathrm{sub}} \tag{7.51}$$

$$= \frac{\mathcal{A}(C)}{4G} + S_{\mathrm{EFT}}(C) \tag{7.52}$$

for a cut C by a totally geodesic codimension-1 submanifold of an emergent space-time. In this case, the MEEC is an infinitesimal version of (7.52), and can be interpreted as a perturbative version of an RT-like relation for which $\delta S_{\mathrm{CFT}} = 0$. It may be possible to understand this relation from a more general perspective, in which AdS/CFT is a special case manifested as a duality.

If we interpret the bulk AdS as an emergent entity from the boundary conformal field theory, we can think of the CFT to be the fundamental theory, from which we reconstruct a theory in the IR that describes bulk gravity. In this emergent limit, different parts of the entanglement entropy of the supposed fundamental theory take on other physical meanings related to geometry and matter. In [268], Lin proposed that such a separation of entanglement may also be understood in a more general setting, where the "fundamental" theory, whose Hilbert space factorizes and does not have a gauge symmetry, has an emergent gauge theory in the IR.[7] As such, the entanglement entropy S_{fund} of a subregion in the fundamental theory can be written in a form $S_{\mathrm{fund}} = S_{\mathrm{edge}} + S_{\mathrm{IR}}$. Here S_{edge}, which depends on the UV regulator such as a lattice cutoff, takes on the meaning of the analogous area-law term in RT. The IR entropy S_{IR} corresponds to the entanglement of the emergent gauge theory[8].

Therefore, we may also speculate that a geometry other than AdS emerges from a fundamental theory that is amorphous, in the sense that there are no pre-determined geometric elements. In this case, a generalization of the RT formula (7.50) should still provide a natural separation between UV and IR and identification of the geometric and matter parts of the entanglement without something like a $1/N$ expansion. It's worth investigating the prospect that this can be done directly from the state and its associated Hilbert space.

Here we point out another possible construction proposed by Harlow [243] making use of quantum error correction codes (QECC), or more specifically, the erasure

[7] A gauge theory is emergent if the low energy behavior of the fundamental theory can be identified with that of a gauge theory. We refer the readers to the original reference for the precise definition used in the derivations.

[8] Similar ideas appear in the study of emergent gravity in condensed matter models [269] with emergent gauge theories [270].

correction codes. A similar RT-like formula is derived in the context of quantum error correction, without having to rely on a background geometry. For the sake of clarity we briefly review some findings of [243].

A typical way to protect states against quantum errors is to encode the information non-locally, such that local errors will not easily contaminate the protected information. For instance, let $|\phi\rangle \in \mathcal{H}_\phi$ be a qudit worth of quantum information. One can encode it in a larger Hilbert space

$$\mathcal{H} = (\mathcal{H}_\phi)^{\otimes N}. \tag{7.53}$$

A basis for $\mathcal{H}$ can be formed from the tensor product of basis vectors $|i_j\rangle$ of each copy j of $\mathcal{H}_\phi$. To encode the original state

$$|\phi\rangle = \sum_i C_i |i\rangle \in \mathcal{H}_\phi \tag{7.54}$$

by mapping it to $\mathcal{H}$, we first map each basis element by some fixed rule,

$$|i\rangle \to |\tilde{i}\rangle = \sum_{i_1, i_2 \ldots i_N} \mu^{\tilde{i}}_{i_1 i_2 \ldots i_N} |i_1, i_2 \ldots i_N\rangle \tag{7.55}$$

for some coefficients $\mu^{\tilde{i}}_{i_1 i_2 \ldots i_N}$. The encoding then takes the form

$$|\phi\rangle \to |\tilde{\phi}\rangle = \sum_{\tilde{i}} C_{\tilde{i}} |\tilde{i}\rangle \in \mathcal{H}. \tag{7.56}$$

The vector subspace of $\mathcal{H}$ spanned by $\{|\tilde{i}\rangle\}$ is the code subspace, $\mathcal{H}_{\text{code}}$.

To be consistent with the notation in the literature, we will refer to the N qudits making up $\mathcal{H}$ as the physical qudits. Let A be a subsystem consisting of a subset of the physical qudits, and $\bar{A}$ its complement, so that

$$\mathcal{H} = \mathcal{H}_A \otimes \mathcal{H}_{\bar{A}}. \tag{7.57}$$

The encoded information is said to be protected against erasure on $\bar{A}$ if for all

$$|\tilde{\phi}\rangle \in \mathcal{H}_{\text{code}} \subset \mathcal{H}, \tag{7.58}$$

there exists an operator $U_A \otimes I_{\bar{A}}$ such that

$$U_A \otimes I_{\bar{A}} |\tilde{\phi}\rangle_{A \cup \bar{A}} = |\phi\rangle_{j \in A} \otimes |\chi\rangle_{A \cup \bar{A} \setminus \{j\}} \tag{7.59}$$

for some state $|\chi\rangle \in \otimes_{i \neq j} \mathcal{H}_\phi$. Intuitively, this property allows one to recover the encoded quantum information even though degrees of freedom in $\mathcal{H}_{\bar{A}}$ are inaccessible.

Now consider the scenario in which the code subspace can encode many qudits. One construction is to consider a QECC in which the code subspace factorizes

$$\mathcal{H}_{\text{code}} = \mathcal{H}_a \otimes \mathcal{H}_{\bar{a}}. \tag{7.60}$$

We want the subset a of these code-subspace qudits to be recoverable from the subsystem A of the larger Hilbert space, and similarly the complementary set $\bar{a}$ to be recoverable from $\bar{A}$. Assume each of $\mathcal{H}_A, \mathcal{H}_{\bar{A}}$ is further factorizable:

$$\mathcal{H}_A = \mathcal{H}_{A_1} \otimes \mathcal{H}_{A_2}, \quad \mathcal{H}_{\bar{A}} = \mathcal{H}_{\bar{A}_1} \otimes \mathcal{H}_{\bar{A}_2}, \tag{7.61}$$

where $\dim \mathcal{H}_{A_1} = \dim \mathcal{H}_{\bar{A}_1} = \dim \mathcal{H}_{\text{code}}$. As demonstrated by Harlow, a QECC that performs the desired complementary recovery, which satisfies

$$|\tilde{i}\rangle|\tilde{j}\rangle = U_A U_{\bar{A}}(|i\rangle_{A_1}|j\rangle_{\bar{A}_1}|\chi\rangle_{A_2\bar{A}_2}) \tag{7.62}$$

for some entangled state $|\chi\rangle_{A_2\bar{A}_2}$ and unitaries $U_A \otimes \mathbb{I}_{\bar{A}}, \mathbb{I}_A \otimes U_{\bar{A}}$, will also satisfy an analogous RT relation. Here, $|\tilde{i}\rangle$, $|\tilde{j}\rangle$,$|i\rangle_{A_1}$, $|j\rangle_{\bar{A}_1}$ are orthonormal basis vectors for the Hilbert spaces $\mathcal{H}_a$, $\mathcal{H}_{\bar{a}}$, $\mathcal{H}_{A_1}$ and $\mathcal{H}_{\bar{A}_1}$ respectively.

Given a density operator in the code subspace

$$\tilde{\rho} = |\tilde{\phi}\rangle\langle\tilde{\phi}| \in L(\mathcal{H}_{\text{code}}) \subset L(\mathcal{H}), \tag{7.63}$$

define reduced density matrices

$$\tilde{\rho}_A = \operatorname{Tr}_{\bar{A}} \tilde{\rho} \tag{7.64}$$

$$\tilde{\rho}_a = \operatorname{Tr}_{\bar{a}} \tilde{\rho} \tag{7.65}$$

$$\rho_\chi = \operatorname{Tr}_{\bar{A}_2} |\chi\rangle\langle\chi|. \tag{7.66}$$

The resulting RT-like relation for the entropies then takes the form,

$$\begin{aligned} S(\tilde{\rho}_A) &= S(\rho_\chi) + S(\tilde{\rho}_a) \\ S(\tilde{\rho}_{\bar{A}}) &= S(\rho_\chi) + S(\tilde{\rho}_{\bar{a}}). \end{aligned} \tag{7.67}$$

In the familiar examples of holographic tensor networks and quantum error correction codes [49, 76], the term $S(\rho_\chi)$ is proportional to the area of the minimal RT surface anchored at the boundary of A.[9] Consequently, the term $S(\rho_\chi)$ can be understood as the geometric entanglement contribution, while $S(\tilde{\rho}_a)$ is naturally identified

[9]For example, the entropy $S(\chi)$ is computed by a distillation process and counting the Bell pairs in Sec 4 of [49]. The cut along the Bell pairs is precisely the bulk minimal surface $\gamma_{A\bar{A}}$ anchored at the boundary of A and $\bar{A}$.

with the “matter” contribution to bulk entropy. The sum of these two quantities is equal to $S(\tilde{\rho}_A)$, which is the entanglement entropy of the boundary subregion A.

This generalized RT-like formula can be compared to our equation for the entanglement entropy of a subsystem (7.41) as the sum of an RC contribution and a subdominant correction. In particular, the emergent entanglement equilibrium relation (7.40) can be thought of as the first-order variation of this formula, with the first term representing an area and the second the contribution from the emergent EFT. In this sense, the entropy formulae underlying BEG can be found more generally in the context of quantum error-correcting codes. This relation helps shed light on the decomposition of the entanglement entropy into UV geometric contributions and IR contributions from matter fields.

The derivation leading to (7.67) makes no reference to a pre-existing geometry or holography. Indeed, it is reasonable to expect such properties to apply to contexts more general than AdS/CFT. In particular, conventional QECC as well as the operator-algebra quantum error correction seem directly applicable to bulk entanglement gravity. In fact, they can be used to reconstruct a geometry as long as a notion of entanglement entropy can be consistently defined and computed.

In the case we are currently interested in, the overall finite-dimensional Hilbert spaces $\mathcal{H}$ in BEG can be identified with the physical Hilbert space in QECC. A state $|\psi\rangle$ that encodes geometric information corresponds to the code state $|\tilde{\phi}\rangle \in \mathcal{H}$ above. The subsystem A in the form of physical qudits can be identified with some collection of Hilbert space factors (graph vertices) in BEG. In addition, the code comes equipped with a code subspace $\mathcal{H}_{\text{code}} \subset \mathcal{H}$ which is now identified with the IR subspace of the emergent matter fields. Thus, a natural separation of UV (geometric) and IR (matter) degrees of freedom is simply provided by the subspace or subalgebra associated with a QECC.

Hence, a spatial geometry can be obtained and assigned to quantum error correction codes that do not presume a geometrical interpretation *a priori*. BEG can be particularly useful in the case when one considers deviations from maximally symmetric spaces. For a dynamical theory that preserves the code subspace and Lorentz invariance, the linearized Einstein’s equation may emerge as a more generic property, rather than coming from a special theory.

7.6 Discussion

In this work, we have extended the "space from Hilbert space" program of [82], which posits that spatial geometry can emerge from the entanglement features of appropriate quantum states, to consider the gravitational dynamics of spacetime. By suggesting a modified entanglement equilibrium condition as well as other assumptions, we are able to sketch how the spacetime metric can be reconstructed from entanglement using the Radon transform, and it how it naturally obeys Einstein's equation at the linearized level. Our analysis was carried out entirely in (what emerges as) the bulk of spacetime; the entanglement we consider is between Hilbert-space factors representing local degrees of freedom, without reference to AdS/CFT or any other holographic boundary construction. Colloquially, this bulk entanglement gravity approach can be thought of as finding gravity within quantum mechanics, as opposed to the more conventional approach of quantizing a particular model of spacetime structure. It also seems to indicate the plausibility of discovering gravitational features from more generic complex quantum systems.

Further work will clearly be required to flesh out this program and put the necessary assumptions on a firmer footing. We can list a few of the biggest looming questions.

- One is to explore the feasibility of developing a specific theory of quantum gravity using quantum information beyond the context of AdS/CFT, for example by specifying an explicit Hamiltonian, but perhaps by less direct means. For instance, a set of constraints on the quantum dynamics could be derived by requiring the emergence of classical general relativity.
- Geometry from entanglement is an interesting program all by itself, even without the emergence of gravity. It is important to understand how and if more general emergent geometries, possibly along with their metric tensors, can be reconstructed from entanglement data.
- It is also important to address the hope that Lorentz symmetry can be emergent. While there have been discussions mostly in the loop quantum gravity and condensed matter communities, a clear understanding of its feasibility is still lacking.
- Given the recent interest in emergent gauge theories in condensed matter models, it may be possible to understand if certain condensed matter models can be "gravitized" by emerging the geometry through entanglement of a state,

instead of using the pre-existing geometry provided by the lattice structure or Hamiltonian. This may yield interesting toy models that exhibit (analogous) features of gravity.

- It would be useful to contemplate the emergence of holography from this perspective, going beyond the weak-field gravity context considered here.

In addition, one can point to a few more circumscribed and well-defined challenges.

- The BEG framework is natural for assigning emergent geometries to tensor networks directly from entanglement. It is also useful for deriving emergent geometry for conventional QECCs as well as their generalizations in the form of operator-algebras. It may be interesting to construct toy models using these concrete tool sets to improve our intuition for the program.

- Generalizing the tensor Radon transform approach to other Riemannian backgrounds. One particular direction is to make contact with AdS/CFT by considering asymptotically hyperbolic spaces.

- Another task is to further understand the UV/IR separation. Since QECC provides a natural separation and a concrete testing ground, specific toy models may be constructed that have non-trivial dynamical properties [271]. Efforts in this direction would also improve our understanding in adding backreaction and incorporating general geometries in a tensor network model. On the other hand, geometric characterizations may also help categorize entanglement and code properties.

- It would be useful to understand how general the MEEC is in quantum systems near equilibrium, and what physical interpretation can be attached to the two terms.

This work has been guided by the conviction that quantum mechanics is the most fundamental theory we have, and implicitly by the Everettian formulation of the theory (the wave function is the only physical variable, and it evolves smoothly and deterministically over time). In that context, one can argue informally that quantum gravity *must* emerge in roughly the way outlined here. We human beings generally construct quantum theories by starting with classical theories and quantizing them, but presumably nature doesn't work that way. There simply is a quantum state, represented by a vector in Hilbert space, evolving according to the Schrödinger equation with some particular Hamiltonian. (For these purposes we take time as fundamental, but it is also conceivable that time itself is emergent, arising through the entanglement of "system" and "clock" factors of Hilbert space.) Familiar classical concepts such as "locations in space" and "fields" are necessarily emergent from this basic structure. Here we have sketched how space and its geometry may plausibly emerge from the entanglement between discrete Hilbert-space factors, and how gravitational dynamics obeying Einstein's equation can be related to entanglement equilibrium. The is a promising route to a perspective on quantum gravity that puts "quantum" first.

BIBLIOGRAPHY

[1] Albert Einstein. "The Foundation of the General Theory of Relativity". In: *Annalen Phys.* 49.7 (1916). [,65(1916)], pp. 769–822. DOI: 10.1002/andp.200590044,10.1002/andp.19163540702.

[2] Charles W. Misner, Kip S. Thorne, and John Archibald Wheeler. *Gravitation / Charles W. Misner, Kip S. Thorne, John Archibald Wheeler*. English. W. H. Freeman San Francisco, 1973, xxvi, 1279 p. : ISBN: 0716703343 0716703440.

[3] Sean M. Carroll. *Spacetime and geometry: An introduction to general relativity*. 2004. ISBN: 0805387323, 9780805387322. URL: http://www.slac.stanford.edu/spires/find/books/www?cl=QC6:C37:2004.

[4] Ramamurti Shankar. *Principles of quantum mechanics*. New York, NY: Plenum, 1980. URL: https://cds.cern.ch/record/102017.

[5] David J. Griffiths. *Introduction to quantum mechanics*. 2nd ed. London: Pearson / Prentice Hall, 2005.

[6] Michael E. Peskin and Daniel V. Schroeder. *An Introduction to quantum field theory*. Reading, USA: Addison-Wesley, 1995. ISBN: 9780201503975, 0201503972. URL: http://www.slac.stanford.edu/~mpeskin/QFT.html.

[7] M. Srednicki. *Quantum field theory*. Cambridge University Press, 2007. ISBN: 9780521864497, 9780511267208.

[8] J. Polchinski. *String theory. Vol. 1: An introduction to the bosonic string*. Cambridge University Press, 2007. ISBN: 9780511252273, 9780521672276, 9780521633031.

[9] J. Polchinski. *String theory. Vol. 2: Superstring theory and beyond*. Cambridge University Press, 2007. ISBN: 9780511252280, 9780521633048, 9780521672283.

[10] Carlo Rovelli. "Zakopane lectures on loop gravity". In: *PoS* QGQGS2011 (2011), p. 003. arXiv: 1102.3660 [gr-qc].

[11] David D. Reid. "Introduction to causal sets: An Alternate view of space-time structure". In: *Can. J. Phys.* 79 (2001), pp. 1–16. DOI: 10.1139/cjp-79-1-1,10.1139/p01-032. arXiv: gr-qc/9909075 [gr-qc].

[12] Bryce S. DeWitt. "Quantum Theory of Gravity. I. The Canonical Theory". In: *Phys. Rev.* 160 (5 Aug. 1967), pp. 1113–1148. DOI: 10.1103/PhysRev.160.1113. URL: https://link.aps.org/doi/10.1103/PhysRev.160.1113.

[13] Bryce S. DeWitt. “Quantum Theory of Gravity. II. The Manifestly Covariant Theory”. In: *Phys. Rev.* 162 (5 Oct. 1967), pp. 1195–1239. DOI: 10.1103/PhysRev.162.1195. URL: https://link.aps.org/doi/10.1103/PhysRev.162.1195.

[14] Tomasz Konopka, Fotini Markopoulou, and Lee Smolin. “Quantum Graphity”. In: (2006). arXiv: hep-th/0611197 [hep-th].

[15] S. W. Hawking. “Black holes and thermodynamics”. In: *Phys. Rev. D* 13 (2 Jan. 1976), pp. 191–197. DOI: 10.1103/PhysRevD.13.191. URL: https://link.aps.org/doi/10.1103/PhysRevD.13.191.

[16] Jacob D. Bekenstein. “Black Holes and Entropy”. In: *Phys. Rev. D* 7 (8 Apr. 1973), pp. 2333–2346. DOI: 10.1103/PhysRevD.7.2333. URL: https://link.aps.org/doi/10.1103/PhysRevD.7.2333.

[17] Jacob D. Bekenstein. “Generalized second law of thermodynamics in black-hole physics”. In: *Phys. Rev. D* 9 (12 June 1974), pp. 3292–3300. DOI: 10.1103/PhysRevD.9.3292. URL: https://link.aps.org/doi/10.1103/PhysRevD.9.3292.

[18] Raphael Bousso, Horacio Casini, Zachary Fisher, and Juan Maldacena. “Proof of a Quantum Bousso Bound”. In: *Phys. Rev.* D90.4 (2014), p. 044002. DOI: 10.1103/PhysRevD.90.044002. arXiv: 1404.5635 [hep-th].

[19] Raphael Bousso. “A Covariant entropy conjecture”. In: *JHEP* 07 (1999), p. 004. DOI: 10.1088/1126-6708/1999/07/004. arXiv: hep-th/9905177 [hep-th].

[20] Raphael Bousso, Horacio Casini, Zachary Fisher, and Juan Maldacena. “Entropy on a null surface for interacting quantum field theories and the Bousso bound”. In: *Phys. Rev.* D91.8 (2015), p. 084030. DOI: 10.1103/PhysRevD.91.084030. arXiv: 1406.4545 [hep-th].

[21] Juan Martin Maldacena. “The Large N limit of superconformal field theories and supergravity”. In: *Int. J. Theor. Phys.* 38 (1999). [Adv. Theor. Math. Phys.2,231(1998)], pp. 1113–1133. DOI: 10.1023/A:1026654312961. arXiv: hep-th/9711200 [hep-th].

[22] J.D. Brown and Marc Henneaux. “Central charges in the canonical realization of asymptotic symmetries: An example from three dimensional gravity”. English. In: *Commun.Math.Phys.* 104 (1986), pp. 207–226. ISSN: 0010-3616. DOI: 10.1007/BF01211590. URL: http://dx.doi.org/10.1007/BF01211590.

[23] Shinsei Ryu and Tadashi Takayanagi. “Holographic derivation of entanglement entropy from AdS/CFT”. In: *Phys. Rev. Lett.* 96 (2006), p. 181602. DOI: 10.1103/PhysRevLett.96.181602. arXiv: hep-th/0603001 [hep-th].

[24] Matthew Headrick, Robert C. Myers, and Jason Wien. “Holographic Holes and Differential Entropy”. In: *JHEP* 10 (2014), p. 149. DOI: 10.1007/JHEP10(2014)149. arXiv: 1408.4770 [hep-th].

[25] S. Alexakis, T. Balehowsky, and A. Nachman. “Determining a Riemannian Metric from Minimal Areas”. In: *ArXiv e-prints* (Nov. 2017). arXiv: 1711.09379 [math.DG].

[26] Bartlomiej Czech, Lampros Lamprou, Samuel McCandlish, Benjamin Mosk, and James Sully. “A Stereoscopic Look into the Bulk”. In: *JHEP* 07 (2016), p. 129. DOI: 10.1007/JHEP07(2016)129. arXiv: 1604.03110 [hep-th].

[27] Bartlomiej Czech, Lampros Lamprou, Samuel McCandlish, Benjamin Mosk, and James Sully. “Equivalent Equations of Motion for Gravity and Entropy”. In: *JHEP* 02 (2017), p. 004. DOI: 10.1007/JHEP02(2017)004. arXiv: 1608.06282 [hep-th].

[28] Thomas Faulkner, Monica Guica, Thomas Hartman, Robert C. Myers, and Mark Van Raamsdonk. “Gravitation from Entanglement in Holographic CFTs”. In: *JHEP* 03 (2014), p. 051. DOI: 10.1007/JHEP03(2014)051. arXiv: 1312.7856 [hep-th].

[29] Thomas Faulkner, Felix M. Haehl, Eliot Hijano, Onkar Parrikar, Charles Rabideau, and Mark Van Raamsdonk. “Nonlinear Gravity from Entanglement in Conformal Field Theories”. In: *JHEP* 08 (2017), p. 057. DOI: 10.1007/JHEP08(2017)057. arXiv: 1705.03026 [hep-th].

[30] J. Maldacena and L. Susskind. “Cool horizons for entangled black holes”. In: *Fortschritte der Physik* 61 (Sept. 2013), pp. 781–811. DOI: 10.1002/prop.201300020. arXiv: 1306.0533 [hep-th].

[31] Thomas Hartman and Juan Maldacena. “Time Evolution of Entanglement Entropy from Black Hole Interiors”. In: *JHEP* 05 (2013), p. 014. DOI: 10.1007/JHEP05(2013)014. arXiv: 1303.1080 [hep-th].

[32] Adam R. Brown, Daniel A. Roberts, Leonard Susskind, Brian Swingle, and Ying Zhao. “Holographic Complexity Equals Bulk Action?” In: *Phys. Rev. Lett.* 116.19 (2016), p. 191301. DOI: 10.1103/PhysRevLett.116.191301. arXiv: 1509.07876 [hep-th].

[33] Adam R. Brown, Daniel A. Roberts, Leonard Susskind, Brian Swingle, and Ying Zhao. “Complexity, action, and black holes”. In: *Phys. Rev.* D93.8 (2016), p. 086006. DOI: 10.1103/PhysRevD.93.086006. arXiv: 1512.04993 [hep-th].

[34] Robert A. Jefferson and Robert C. Myers. “Circuit complexity in quantum field theory”. In: (2017). arXiv: 1707.08570 [hep-th].

[35] Shira Chapman, Michal P. Heller, Hugo Marrochio, and Fernando Pastawski. “Towards Complexity for Quantum Field Theory States”. In: (2017). arXiv: 1707.08582 [hep-th].

[36] Masafumi Fukuma, So Matsuura, and Tadakatsu Sakai. "Holographic renormalization group". In: *Prog. Theor. Phys.* 109 (2003), pp. 489–562. DOI: 10.1143/PTP.109.489. arXiv: hep-th/0212314 [hep-th].

[37] Brian Swingle. "Entanglement Renormalization and Holography". In: *Phys. Rev.* D86 (2012), p. 065007. DOI: 10.1103/PhysRevD.86.065007. arXiv: 0905.1317 [cond-mat.str-el].

[38] Koji Hashimoto, Sotaro Sugishita, Akinori Tanaka, and Akio Tomiya. "Deep Learning and AdS/CFT". In: (2018). arXiv: 1802.08313 [hep-th].

[39] G. Vidal. "Class of Quantum Many-Body States That Can Be Efficiently Simulated". In: *Physical Review Letters* 101.11, 110501 (Sept. 2008), p. 110501. DOI: 10.1103/PhysRevLett.101.110501. eprint: quant-ph/0610099.

[40] T. Jacobson. "Entanglement equilibrium and the Einstein equation". In: *ArXiv e-prints* (May 2015). arXiv: 1505.04753 [gr-qc].

[41] Ning Bao, ChunJun Cao, Sean M. Carroll, Aidan Chatwin-Davies, Nicholas Hunter-Jones, Jason Pollack, and Grant N. Remmen. "Consistency conditions for an AdS multiscale entanglement renormalization ansatz correspondence". In: *Phys. Rev.* D91.12 (2015), p. 125036. DOI: 10.1103/PhysRevD.91.125036. arXiv: 1504.06632 [hep-th].

[42] Leonard Susskind. "The World as a hologram". In: *J. Math. Phys.* 36 (1995), pp. 6377–6396. DOI: 10.1063/1.531249. arXiv: hep-th/9409089 [hep-th].

[43] Gerard 't Hooft. "Dimensional reduction in quantum gravity". In: *Salamfest 1993:0284-296*. 1993, pp. 0284–296. arXiv: gr-qc/9310026 [gr-qc].

[44] Edward Witten. "Anti-de Sitter space and holography". In: *Adv.Theor.Math.Phys.* 2 (1998), pp. 253–291. arXiv: hep-th/9802150 [hep-th].

[45] Ofer Aharony, Steven S. Gubser, Juan Martin Maldacena, Hirosi Ooguri, and Yaron Oz. "Large N field theories, string theory and gravity". In: *Phys.Rept.* 323 (2000), pp. 183–386. DOI: 10.1016/S0370-1573(99)00083-6. arXiv: hep-th/9905111 [hep-th].

[46] Aitor Lewkowycz and Juan Maldacena. "Generalized gravitational entropy". In: *JHEP* 1308 (2013), p. 090. DOI: 10.1007/JHEP08(2013)090. arXiv: 1304.4926 [hep-th].

[47] Roman Orus. "A Practical Introduction to Tensor Networks: Matrix Product States and Projected Entangled Pair States". In: *Annals Phys.* 349 (2014), pp. 117–158. DOI: 10.1016/j.aop.2014.06.013. arXiv: 1306.2164 [cond-mat.str-el].

[48] Xiao-Liang Qi. "Exact holographic mapping and emergent space-time geometry". In: (2013). arXiv: 1309.6282 [hep-th].

[49] Fernando Pastawski, Beni Yoshida, Daniel Harlow, and John Preskill. “Holographic quantum error-correcting codes: Toy models for the bulk/boundary correspondence”. In: *JHEP* 06 (2015), p. 149. DOI: 10.1007/JHEP06(2015)149. arXiv: 1503.06237 [hep-th].

[50] Bartlomiej Czech, Lampros Lamprou, Samuel McCandlish, and James Sully. “Integral Geometry and Holography”. In: *JHEP* 10 (2015), p. 175. DOI: 10.1007/JHEP10(2015)175. arXiv: 1505.05515 [hep-th].

[51] C. Bény. “Causal structure of the entanglement renormalization ansatz”. In: *New Journal of Physics* 15.2, 023020 (Feb. 2013), p. 023020. DOI: 10.1088/1367-2630/15/2/023020. arXiv: 1110.4872 [quant-ph].

[52] G. Evenbly and G. Vidal. “Algorithms for entanglement renormalization”. In: *Phys. Rev.* B79.14 (2009), p. 144108. DOI: 10.1103/PhysRevB.79.144108. arXiv: 0707.1454 [cond-mat.str-el].

[53] Robert N. C. Pfeifer, Glen Evenbly, and Guifré Vidal. “Entanglement renormalization, scale invariance, and quantum criticality”. In: *Phys. Rev. A* 79 (4 Apr. 2009), p. 040301. DOI: 10.1103/PhysRevA.79.040301. URL: https://link.aps.org/doi/10.1103/PhysRevA.79.040301.

[54] G. Evenbly, P. Corboz, and G. Vidal. “Nonlocal scaling operators with entanglement renormalization”. In: *Phys. Rev. B* 82 (13 Oct. 2010), p. 132411. DOI: 10.1103/PhysRevB.82.132411. URL: https://link.aps.org/doi/10.1103/PhysRevB.82.132411.

[55] Y.-Y. Shi, L.-M. Duan, and G. Vidal. “Classical simulation of quantum many-body systems with a tree tensor network”. In: *Phys.Rev.* A74, 022320 (2006), p. 022320. DOI: 10.1103/PhysRevA.74.022320. eprint: quant-ph/0511070.

[56] Pierre Pfeuty. “The one-dimensional Ising model with a transverse field”. In: *Ann.Phys.* 57 (1970), pp. 79–90. ISSN: 0003-4916. DOI: http://dx.doi.org/10.1016/0003-4916(70)90270-8. URL: http://www.sciencedirect.com/science/article/pii/0003491670902708.

[57] Brian Swingle. “Constructing holographic spacetimes using entanglement renormalization”. In: (2012). arXiv: 1209.3304 [hep-th].

[58] G. Evenbly and G. Vidal. “Scaling of entanglement entropy in the (branching) multiscale entanglement renormalization ansatz”. In: *Phys.Rev.* B89, 235113 (2014), p. 235113. DOI: 10.1103/PhysRevB.89.235113. arXiv: 1310.8372 [quant-ph].

[59] Jutho Haegeman, Tobias J. Osborne, Henri Verschelde, and Frank Verstraete. “Entanglement Renormalization for Quantum Fields in Real Space”. In: *Phys. Rev. Lett.* 110.10 (2013), p. 100402. DOI: 10.1103/PhysRevLett.110.100402. arXiv: 1102.5524 [hep-th].

[60] Masahiro Nozaki, Shinsei Ryu, and Tadashi Takayanagi. "Holographic Geometry of Entanglement Renormalization in Quantum Field Theories". In: *JHEP* 10 (2012), p. 193. DOI: 10.1007/JHEP10(2012)193. arXiv: 1208.3469 [hep-th].

[61] Ali Mollabashi, Masahiro Nozaki, Shinsei Ryu, and Tadashi Takayanagi. "Holographic Geometry of cMERA for Quantum Quenches and Finite Temperature". In: *JHEP* 1403 (2014), p. 098. DOI: 10.1007/JHEP03(2014)098. arXiv: 1311.6095 [hep-th].

[62] Christoph Holzhey, Finn Larsen, and Frank Wilczek. "Geometric and renormalized entropy in conformal field theory". In: *Nucl.Phys.* B424 (1994), pp. 443–467. DOI: 10.1016/0550-3213(94)90402-2. arXiv: hep-th/9403108 [hep-th].

[63] Pasquale Calabrese and John L. Cardy. "Entanglement entropy and quantum field theory". In: *J.Stat.Mech.* 0406 (2004), P06002. DOI: 10.1088/1742-5468/2004/06/P06002. arXiv: hep-th/0405152 [hep-th].

[64] S. Ryu and T. Takayanagi. "Aspects of holographic entanglement entropy". In: *Journal of High Energy Physics* 8, 045 (Aug. 2006), p. 45. DOI: 10.1088/1126-6708/2006/08/045. eprint: hep-th/0605073.

[65] Ted Jacobson. "Thermodynamics of space-time: The Einstein equation of state". In: *Phys. Rev. Lett.* 75 (1995), pp. 1260–1263. DOI: 10.1103/PhysRevLett.75.1260. arXiv: gr-qc/9504004 [gr-qc].

[66] J.D. Bekenstein. "Black holes and the second law". English. In: *Lett.Nuovo Cim.* 4 (1972), pp. 737–740. ISSN: 0375-930X. DOI: 10.1007/BF02757029. URL: http://dx.doi.org/10.1007/BF02757029.

[67] Raphael Bousso. "The Holographic principle". In: *Rev. Mod. Phys.* 74 (2002), pp. 825–874. DOI: 10.1103/RevModPhys.74.825. arXiv: hep-th/0203101 [hep-th].

[68] Maximo Bañados, Claudio Teitelboim, and Jorge Zanelli. "Black hole in three-dimensional space-time". In: *Phys.Rev.Lett.* 69 (1992), pp. 1849–1851. DOI: 10.1103/PhysRevLett.69.1849. arXiv: hep-th/9204099 [hep-th].

[69] Cristian Martinez, Claudio Teitelboim, and Jorge Zanelli. "Charged rotating black hole in three space-time dimensions". In: *Phys.Rev.* D61 (2000), p. 104013. DOI: 10.1103/PhysRevD.61.104013. arXiv: hep-th/9912259 [hep-th].

[70] Mark Srednicki. "Entropy and area". In: *Phys. Rev. Lett.* 71 (1993), pp. 666–669. DOI: 10.1103/PhysRevLett.71.666. arXiv: hep-th/9303048 [hep-th].

[71] G. Evenbly and G. Vidal. “Tensor Network States and Geometry”. In: *J.Stat.Phys.* 145 (2011), pp. 891–918. DOI: 10.1007/s10955-011-0237-4. arXiv: 1106.1082 [quant-ph].

[72] Ahmed Almheiri, Xi Dong, and Daniel Harlow. “Bulk Locality and Quantum Error Correction in AdS/CFT”. In: (2014). arXiv: 1411.7041 [hep-th].

[73] G. Evenbly and G. Vidal. “Tensor network renormalization yields the multiscale entanglement renormalization ansatz”. In: (2015). eprint: 1502.05385 (cond-mat.str-el).

[74] Javier Molina-Vilaplana and Javier Prior. “Entanglement, Tensor Networks and Black Hole Horizons”. In: *Gen.Rel.Grav.* 46 (2014), p. 1823. DOI: 10.1007/s10714-014-1823-y. arXiv: 1403.5395 [hep-th].

[75] Ning Bao, ChunJun Cao, Sean M. Carroll, and Aidan Chatwin-Davies. “De Sitter Space as a Tensor Network: Cosmic No-Hair, Complementarity, and Complexity”. In: *Phys. Rev.* D96.12 (2017), p. 123536. DOI: 10.1103/PhysRevD.96.123536. arXiv: 1709.03513 [hep-th].

[76] Patrick Hayden, Sepehr Nezami, Xiao-Liang Qi, Nathaniel Thomas, Michael Walter, and Zhao Yang. “Holographic duality from random tensor networks”. In: *JHEP* 11 (2016), p. 009. DOI: 10.1007/JHEP11(2016)009. arXiv: 1601.01694 [hep-th].

[77] Matthew Heydeman, Matilde Marcolli, Ingmar Saberi, and Bogdan Stoica. “Tensor networks, *p*-adic fields, and algebraic curves: arithmetic and the AdS_3/CFT_2 correspondence”. In: (2016). arXiv: 1605.07639 [hep-th].

[78] Steven S. Gubser, Matthew Heydeman, Christian Jepsen, Matilde Marcolli, Sarthak Parikh, Ingmar Saberi, Bogdan Stoica, and Brian Trundy. “Edge length dynamics on graphs with applications to *p*-adic AdS/CFT”. In: (2016). arXiv: 1612.09580 [hep-th].

[79] Bartlomiej Czech, Lampros Lamprou, Samuel McCandlish, and James Sully. “Tensor Networks from Kinematic Space”. In: *JHEP* 07 (2016), p. 100. DOI: 10.1007/JHEP07(2016)100. arXiv: 1512.01548 [hep-th].

[80] Bartlomiej Czech, Glen Evenbly, Lampros Lamprou, Samuel McCandlish, Xiao-Liang Qi, James Sully, and Guifre Vidal. “Tensor network quotient takes the vacuum to the thermal state”. In: *Phys. Rev.* B94.8 (2016), p. 085101. DOI: 10.1103/PhysRevB.94.085101. arXiv: 1510.07637 [cond-mat.str-el].

[81] G. Evenbly. “Hyper-invariant tensor networks and holography”. In: *ArXiv e-prints* (Apr. 2017). arXiv: 1704.04229 [quant-ph].

[82] ChunJun Cao, Sean M. Carroll, and Spyridon Michalakis. “Space from Hilbert Space: Recovering Geometry from Bulk Entanglement”. In: *Phys. Rev.* D95.2 (2017), p. 024031. DOI: 10.1103/PhysRevD.95.024031. arXiv: 1606.08444 [hep-th].

[83] Andrew Strominger. "The dS / CFT correspondence". In: *JHEP* 10 (2001), p. 034. DOI: 10.1088/1126-6708/2001/10/034. arXiv: hep-th/0106113 [hep-th].

[84] Yasuhiro Sekino and Leonard Susskind. "Census Taking in the Hat: FRW/CFT Duality". In: *Phys. Rev.* D80 (2009), p. 083531. DOI: 10.1103/PhysRevD.80.083531. arXiv: 0908.3844 [hep-th].

[85] Raj Sinai Kunkolienkar and Kinjal Banerjee. "Towards a dS/MERA correspondence". In: (2016). arXiv: 1611.08581 [hep-th].

[86] Ning Bao, ChunJun Cao, Sean M. Carroll, and Liam McAllister. "Quantum Circuit Cosmology: The Expansion of the Universe Since the First Qubit". In: (2017). arXiv: 1702.06959 [hep-th].

[87] Yasunori Nomura. "Physical Theories, Eternal Inflation, and Quantum Universe". In: *JHEP* 11 (2011), p. 063. DOI: 10.1007/JHEP11(2011)063. arXiv: 1104.2324 [hep-th].

[88] Yasunori Nomura. "Quantum Mechanics, Spacetime Locality, and Gravity". In: *Found. Phys.* 43 (2013), pp. 978–1007. DOI: 10.1007/s10701-013-9729-1. arXiv: 1110.4630 [hep-th].

[89] G. W. Gibbons and S. W. Hawking. "Action integrals and partition functions in quantum gravity". In: *Phys. Rev. D* 15 (10 May 1977), pp. 2752–2756. DOI: 10.1103/PhysRevD.15.2752. URL: https://link.aps.org/doi/10.1103/PhysRevD.15.2752.

[90] Masamichi Miyaji, Tadashi Takayanagi, and Kento Watanabe. "From path integrals to tensor networks for the AdS/CFT correspondence". In: *Phys. Rev.* D95.6 (2017), p. 066004. DOI: 10.1103/PhysRevD.95.066004. arXiv: 1609.04645 [hep-th].

[91] Robert M. Wald. "Asymptotic behavior of homogeneous cosmological models in the presence of a positive cosmological constant". In: *Phys. Rev.* D28 (1983), pp. 2118–2120. DOI: 10.1103/PhysRevD.28.2118.

[92] Alexei A. Starobinsky. "Isotropization of arbitrary cosmological expansion given an effective cosmological constant". In: *JETP Lett.* 37 (1983), pp. 66–69.

[93] John D Barrow. "Cosmic no-hair theorems and inflation". In: *Phys. Lett. B* 187.1 (1987). DOI: 10.1016/0370-2693(87)90063-3.

[94] John D Barrow and Günter Götz. "The asymptotic approach to de Sitter space-time". In: *Phys. Lett. B* 231.3 (1989), pp. 228–230. DOI: 10.1016/0370-2693(89)90204-9.

[95] Yuichi Kitada and Kei-ichi Maeda. "Cosmic no hair theorem in power law inflation". In: *Phys. Rev.* D45 (1992), pp. 1416–1419. DOI: 10.1103/PhysRevD.45.1416.

[96] Yuichi Kitada and Kei-ichi Maeda. "Cosmic no hair theorem in homogeneous space-times. 1. Bianchi models". In: *Class. Quant. Grav.* 10 (1993), pp. 703–734. DOI: 10.1088/0264-9381/10/4/008.

[97] Marco Bruni, Sabino Matarrese, and Ornella Pantano. "A local view of the observable universe". In: *Phys. Rev. Lett.* 74 (11 1995), pp. 1916–1919. DOI: 10.1103/PhysRevLett.74.1916. arXiv: astro-ph/9407054.

[98] Marco Bruni, Filipe C Mena, and Reza Tavakol. "Cosmic no-hair: non-linear asymptotic stability of de Sitter universe". In: *Class. Quant. Grav.* 19.L23 (2002), pp. 1–8. ISSN: 02649381. DOI: 10.1088/0264-9381/19/5/101. arXiv: gr-qc/0107069.

[99] W Boucher and G W Gibbons. "Cosmic baldness". In: 1.4 (2011), pp. 1–5. arXiv: 1109.3535.

[100] A. Maleknejad and M. M. Sheikh-Jabbari. "Revisiting cosmic no-hair theorem for inflationary settings". In: *Phys. Rev. D* 85 (12 2012), p. 123508. DOI: 10.1103/PhysRevD.85.123508. arXiv: 1203.0219.

[101] Sean M. Carroll and Aidan Chatwin-Davies. "Cosmic Equilibration: A Holographic No-Hair Theorem from the Generalized Second Law". In: (2017). arXiv: 1703.09241 [hep-th].

[102] Stefan Hollands. *Correlators, Feynman diagrams, and quantum no-hair in de Sitter spacetime*. Vol. 68. 2010, p. 57. ISBN: 0022001216532. arXiv: 1010.5367.

[103] Donald Marolf and Ian A. Morrison. "Infrared stability of de Sitter space: Loop corrections to scalar propagators". In: *Phys. Rev. D* 82.10 (2010), pp. 1–20. ISSN: 15507998. DOI: 10.1103/PhysRevD.82.105032. arXiv: 1006.0035.

[104] Donald Marolf and Ian A. Morrison. "Infrared stability of de Sitter QFT: Results at all orders". In: *Phys. Rev. D* 84.4 (2011), pp. 1–15. ISSN: 15507998. DOI: 10.1103/PhysRevD.84.044040.

[105] Maxim Raginsky. "Strictly contractive quantum channels and physically realizable quantum computers". In: *Phys. Rev. A* 65 (3 Feb. 2002), p. 032306. DOI: 10.1103/PhysRevA.65.032306. URL: https://link.aps.org/doi/10.1103/PhysRevA.65.032306.

[106] Leonard Susskind, Larus Thorlacius, and John Uglum. "The Stretched horizon and black hole complementarity". In: *Phys. Rev.* D48 (1993), pp. 3743–3761. DOI: 10.1103/PhysRevD.48.3743. arXiv: hep-th/9306069 [hep-th].

[107] Kip S. Thorne, R. H. Price, and D. A. Macdonald, eds. *Black Holes: The Membrane Paradigm*. New Haven: Yale Univ. Press, 1986. ISBN: 9780300037708.

[108] Ahmed Almheiri, Donald Marolf, Joseph Polchinski, and James Sully. "Black Holes: Complementarity or Firewalls?" In: *JHEP* 02 (2013), p. 062. DOI: 10.1007/JHEP02(2013)062. arXiv: 1207.3123 [hep-th].

[109] Willy Fischler. "Taking de Sitter Seriously". Talk given at Role of Scaling Laws in Physics and Biology (Celebrating the 60th Birthday of Geoffrey West), Santa Fe, Dec. 2000.

[110] Tom Banks. "QuantuMechanics and CosMology". Talk given at the festschrift for L. Susskind, Stanford University, May 2000. 2000.

[111] Raphael Bousso. "Positive vacuum energy and the N-bound". In: *Journal of High Energy Physics* 2000.11 (2000), p. 038. eprint: https://arxiv.org/abs/hep-th/0010252. URL: http://stacks.iop.org/1126-6708/2000/i=11/a=038.

[112] Tom Banks. "Cosmological breaking of supersymmetry?" In: *Int. J. Mod. Phys.* A16 (2001), pp. 910–921. DOI: 10.1142/S0217751X01003998. arXiv: hep-th/0007146 [hep-th].

[113] Edward Witten. "Quantum gravity in de Sitter space". In: *Strings 2001: International Conference Mumbai, India, January 5-10, 2001*. 2001. arXiv: hep-th/0106109 [hep-th]. URL: http://alice.cern.ch/format/showfull?sysnb=2259607.

[114] Lisa Dyson, Matthew Kleban, and Leonard Susskind. "Disturbing implications of a cosmological constant". In: *JHEP* 10 (2002), p. 011. DOI: 10.1088/1126-6708/2002/10/011. arXiv: hep-th/0208013 [hep-th].

[115] Maulik K. Parikh and Erik P. Verlinde. "De Sitter holography with a finite number of states". In: *JHEP* 01 (2005), p. 054. DOI: 10.1088/1126-6708/2005/01/054. arXiv: hep-th/0410227 [hep-th].

[116] Andreas Albrecht and Lorenzo Sorbo. "Can the universe afford inflation?" In: *Phys. Rev.* D70 (2004), p. 063528. DOI: 10.1103/PhysRevD.70.063528. arXiv: hep-th/0405270 [hep-th].

[117] Sean M. Carroll. "Why Boltzmann Brains Are Bad". In: (2017). arXiv: 1702.00850 [hep-th].

[118] Kimberly K. Boddy, Sean M. Carroll, and Jason Pollack. "De Sitter Space Without Dynamical Quantum Fluctuations". In: *Found. Phys.* 46.6 (2016), pp. 702–735. DOI: 10.1007/s10701-016-9996-8. arXiv: 1405.0298 [hep-th].

[119] T. Banks and W. Fischler. "Holographic cosmology 3.0". In: *Phys. Scripta* T117 (2005), pp. 56–63. DOI: 10.1238/Physica.Topical.117a00056. arXiv: hep-th/0310288 [hep-th].

[120] Tom Banks. "Holographic Space-Time: The Takeaway". In: (2011). arXiv: 1109.2435 [hep-th].

[121] Tom Banks and Willy Fischler. "Holographic Inflation Revised". In: (2015). arXiv: 1501.01686 [hep-th].

[122] Dénes Petz. "Sufficient subalgebras and the relative entropy of states of a von Neumann algebra". In: *Communications in Mathematical Physics* 105.1 (Mar. 1986), pp. 123–131. ISSN: 1432-0916. DOI: 10.1007/BF01212345. URL: https://doi.org/10.1007/BF01212345.

[123] Dénes Petz. "Sufficiency of channels over Von Neumann algebras". In: *Quarterly Journal of Mathematics* 39.1 (Mar. 1988), pp. 97–108. ISSN: 0033-5606. DOI: 10.1093/qmath/39.1.97.

[124] Denes Petz. "MONOTONICITY OF QUANTUM RELATIVE ENTROPY REVISITED". In: *Reviews in Mathematical Physics* 15.01 (2003), pp. 79–91. DOI: 10.1142/S0129055X03001576. eprint: http://www.worldscientific.com/doi/pdf/10.1142/S0129055X03001576. URL: http://www.worldscientific.com/doi/abs/10.1142/S0129055X03001576.

[125] M. Junge, R. Renner, D. Sutter, M. M. Wilde, and A. Winter. "Universal recovery from a decrease of quantum relative entropy". In: *ArXiv e-prints* (Sept. 2015). arXiv: 1509.07127 [quant-ph].

[126] Á. Rivas and S. F. Huelga. *Open Quantum Systems*. 2012. DOI: 10.1007/978-3-642-23354-8.

[127] Michael A. Nielsen and Isaac L. Chuang. *Quantum Computation and Quantum Information: 10th Anniversary Edition*. 10th. New York, NY, USA: Cambridge University Press, 2011. ISBN: 1107002176, 9781107002173.

[128] John Preskill. "Lecture Notes on Quantum Computation". University Lecture. 2004.

[129] Alan Reynolds and Simon F. Ross. "Complexity in de Sitter Space". In: *Class. Quant. Grav.* 34.17 (2017), p. 175013. DOI: 10.1088/1361-6382/aa8122. arXiv: 1706.03788 [hep-th].

[130] Daniel Harlow, Stephen H. Shenker, Douglas Stanford, and Leonard Susskind. "Tree-like structure of eternal inflation: A solvable model". In: *Phys. Rev.* D85 (2012), p. 063516. DOI: 10.1103/PhysRevD.85.063516. arXiv: 1110.0496 [hep-th].

[131] G. Evenbly and G. Vidal. "Entanglement Renormalization in Two Spatial Dimensions". In: *Physical Review Letters* 102.18, 180406 (May 2009), p. 180406. DOI: 10.1103/PhysRevLett.102.180406. arXiv: 0811.0879 [cond-mat.str-el].

[132] Alan H. Guth. "The Inflationary Universe: A Possible Solution to the Horizon and Flatness Problems". In: *Phys. Rev.* D23 (1981), pp. 347–356. DOI: 10.1103/PhysRevD.23.347.

[133] Andrei D. Linde. “A New Inflationary Universe Scenario: A Possible Solution of the Horizon, Flatness, Homogeneity, Isotropy and Primordial Monopole Problems”. In: *Phys. Lett.* B108 (1982), pp. 389–393. DOI: 10.1016/0370-2693(82)91219-9.

[134] Andreas Albrecht and Paul J. Steinhardt. “Cosmology for Grand Unified Theories with Radiatively Induced Symmetry Breaking”. In: *Phys. Rev. Lett.* 48 (1982), pp. 1220–1223. DOI: 10.1103/PhysRevLett.48.1220.

[135] Jérôme Martin and Robert H. Brandenberger. “Trans-Planckian problem of inflationary cosmology”. In: *Phys. Rev. D* 63 (12 May 2001), p. 123501. DOI: 10.1103/PhysRevD.63.123501. URL: https://link.aps.org/doi/10.1103/PhysRevD.63.123501.

[136] Craig J. Hogan. “Holographic discreteness of inflationary perturbations”. In: *Phys. Rev.* D66 (2002), p. 023521. DOI: 10.1103/PhysRevD.66.023521. arXiv: astro-ph/0201020 [astro-ph].

[137] Richard Easther, Brian R. Greene, William H. Kinney, and Gary Shiu. “A Generic estimate of transPlanckian modifications to the primordial power spectrum in inflation”. In: *Phys. Rev.* D66 (2002), p. 023518. DOI: 10.1103/PhysRevD.66.023518. arXiv: hep-th/0204129 [hep-th].

[138] Nemanja Kaloper, Matthew Kleban, Albion E. Lawrence, and Stephen Shenker. “Signatures of short distance physics in the cosmic microwave background”. In: *Phys. Rev.* D66 (2002), p. 123510. DOI: 10.1103/PhysRevD.66.123510. arXiv: hep-th/0201158 [hep-th].

[139] Samir D. Mathur. “How does the universe expand?” In: *Int. J. Mod. Phys.* D12 (2003), pp. 1681–1686. DOI: 10.1142/S0218271803004031. arXiv: hep-th/0305204 [hep-th].

[140] Hael Collins and R. Holman. “Renormalization of initial conditions and the trans-Planckian problem of inflation”. In: *Phys. Rev.* D71 (2005), p. 085009. DOI: 10.1103/PhysRevD.71.085009. arXiv: hep-th/0501158 [hep-th].

[141] R. H. Brandenberger and J. Martin. “Trans-Planckian issues for inflationary cosmology”. In: *Classical and Quantum Gravity* 30.11, 113001 (June 2013), p. 113001. DOI: 10.1088/0264-9381/30/11/113001. arXiv: 1211.6753.

[142] T. S. Bunch and P. C. W. Davies. “Quantum field theory in de Sitter space - Renormalization by point-splitting”. In: *Proceedings of the Royal Society of London Series A* 360 (Mar. 1978), pp. 117–134. DOI: 10.1098/rspa.1978.0060.

[143] Mark Van Raamsdonk. “Building up spacetime with quantum entanglement”. In: *Gen. Rel. Grav.* 42 (2010). [Int. J. Mod. Phys.D19,2429(2010)], pp. 2323–2329. DOI: 10.1007/s10714-010-1034-0, 10.1142/S0218271810018529. arXiv: 1005.3035 [hep-th].

[144] T. Jacobson. "Entanglement Equilibrium and the Einstein Equation". In: *Physical Review Letters* 116.20, 201101 (May 2016), p. 201101. DOI: 10.1103/PhysRevLett.116.201101. arXiv: 1505.04753 [gr-qc].

[145] Seth Lloyd. "The Computational universe: Quantum gravity from quantum computation". In: *Submitted to: Science* (2005). arXiv: quant-ph/0501135 [quant-ph].

[146] Fotini Markopoulou. "The Computing Spacetime". In: *Lect. Notes Comput. Sci.* 7318 (2012), p. 472. arXiv: 1201.3398 [gr-qc].

[147] Alexei A. Starobinsky. "A New Type of Isotropic Cosmological Models Without Singularity". In: *Phys. Lett.* B91 (1980), pp. 99–102. DOI: 10.1016/0370-2693(80)90670-X.

[148] R. Brout, F. Englert, and E. Gunzig. "The Creation of the Universe as a Quantum Phenomenon". In: *Annals Phys.* 115 (1978), p. 78. DOI: 10.1016/0003-4916(78)90176-8.

[149] K. Sato. "First Order Phase Transition of a Vacuum and Expansion of the Universe". In: *Mon. Not. Roy. Astron. Soc.* 195 (1981), pp. 467–479.

[150] T. Banks and Willy Fischler. "An Upper bound on the number of e-foldings". In: (2003). arXiv: astro-ph/0307459 [astro-ph].

[151] Nemanja Kaloper, Matthew Kleban, and Lorenzo Sorbo. "Observational implications of cosmological event horizons". In: *Phys. Lett.* B600 (2004), pp. 7–14. DOI: 10.1016/j.physletb.2004.08.068. arXiv: astro-ph/0406099 [astro-ph].

[152] David A. Lowe and Donald Marolf. "Holography and eternal inflation". In: *Phys. Rev.* D70 (2004), p. 026001. DOI: 10.1103/PhysRevD.70.026001. arXiv: hep-th/0402162 [hep-th].

[153] Nima Arkani-Hamed, Sergei Dubovsky, Alberto Nicolis, Enrico Trincherini, and Giovanni Villadoro. "A Measure of de Sitter entropy and eternal inflation". In: *JHEP* 05 (2007), p. 055. DOI: 10.1088/1126-6708/2007/05/055. arXiv: 0704.1814 [hep-th].

[154] Daniel Phillips, Andrew Scacco, and Andreas Albrecht. "Holographic bounds and finite inflation". In: *Phys. Rev.* D91.4 (2015), p. 043513. DOI: 10.1103/PhysRevD.91.043513. arXiv: 1410.6065 [gr-qc].

[155] A. Yu. Kitaev, A. H. Shen, and M. N. Vyalyi. *Classical and Quantum Computation*. Boston, MA, USA: American Mathematical Society, 2002. ISBN: 0821832298.

[156] Jacob D. Bekenstein. "Black Holes and Entropy". In: *Phys. Rev. D* 7 (8 Apr. 1973), pp. 2333–2346. DOI: 10.1103/PhysRevD.7.2333. URL: http://link.aps.org/doi/10.1103/PhysRevD.7.2333.

[157] Eugenio Bianchi and Robert C. Myers. “On the Architecture of Spacetime Geometry”. In: *Class. Quant. Grav.* 31 (2014), p. 214002. DOI: 10.1088/0264-9381/31/21/214002. arXiv: 1212.5183 [hep-th].

[158] M. Van Raamsdonk. “Lectures on Gravity and Entanglement”. In: *ArXiv e-prints* (Aug. 2016). arXiv: 1609.00026 [hep-th].

[159] G. W. Gibbons and S. W. Hawking. “Cosmological event horizons, thermodynamics, and particle creation”. In: *Phys. Rev. D* 15 (10 May 1977), pp. 2738–2751. DOI: 10.1103/PhysRevD.15.2738. URL: http://link.aps.org/doi/10.1103/PhysRevD.15.2738.

[160] Sean M. Carroll. “In What Sense Is the Early Universe Fine-Tuned?” In: (2014). arXiv: 1406.3057 [astro-ph.CO]. URL: http://inspirehep.net/record/1300332/files/arXiv:1406.3057.pdf.

[161] Andreas Albrecht. “Cosmic curvature from de Sitter equilibrium cosmology”. In: *Phys. Rev. Lett.* 107 (2011), p. 151102. DOI: 10.1103/PhysRevLett.107.151102. arXiv: 1104.3315 [astro-ph.CO].

[162] Sergei Dubovsky, Leonardo Senatore, and Giovanni Villadoro. “Universality of the Volume Bound in Slow-Roll Eternal Inflation”. In: *JHEP* 05 (2012), p. 035. DOI: 10.1007/JHEP05(2012)035. arXiv: 1111.1725 [hep-th].

[163] Erik P. Verlinde. “Emergent Gravity and the Dark Universe”. In: *SciPost Phys.* 2.3 (2017), p. 016. DOI: 10.21468/SciPostPhys.2.3.016. arXiv: 1611.02269 [hep-th].

[164] P. A. R. Ade et al. “Improved Constraints on Cosmology and Foregrounds from BICEP2 and Keck Array Cosmic Microwave Background Data with Inclusion of 95 GHz Band”. In: *Phys. Rev. Lett.* 116 (2016), p. 031302. DOI: 10.1103/PhysRevLett.116.031302. arXiv: 1510.09217 [astro-ph.CO].

[165] N. Bao, S. Nezami, H. Ooguri, B. Stoica, J. Sully, and M. Walter. “The Holographic Entropy Cone”. In: *ArXiv e-prints* (May 2015). arXiv: 1505.07839 [hep-th].

[166] Ning Bao, ChunJun Cao, Michael Walter, and Zitao Wang. “Holographic entropy inequalities and gapped phases of matter”. In: *JHEP* 09 (2015), p. 203. DOI: 10.1007/JHEP09(2015)203. arXiv: 1507.05650 [hep-th].

[167] M. M. Wolf, F. Verstraete, M. B. Hastings, and J. I. Cirac. “Area Laws in Quantum Systems: Mutual Information and Correlations”. In: *Physical Review Letters* 100.7, 070502 (Feb. 2008), p. 070502. DOI: 10.1103/PhysRevLett.100.070502. arXiv: 0704.3906 [quant-ph].

[168] M. B. Hastings. “An area law for one-dimensional quantum systems”. In: *Journal of Statistical Mechanics: Theory and Experiment* 8 (Aug. 2007), p. 24. DOI: 10.1088/1742-5468/2007/08/P08024. arXiv: 0705.2024 [quant-ph].

[169] J. Eisert, M. Cramer, and M. B. Plenio. "Colloquium: Area laws for the entanglement entropy". In: *Reviews of Modern Physics* 82 (Jan. 2010), pp. 277–306. DOI: 10.1103/RevModPhys.82.277. arXiv: 0808.3773 [quant-ph].

[170] P. Hayden, M. Headrick, and A. Maloney. "Holographic mutual information is monogamous". In: *Phys.Rev.D.* 87.4, 046003 (Feb. 2013), p. 046003. DOI: 10.1103/PhysRevD.87.046003. arXiv: 1107.2940 [hep-th].

[171] N. Bao, S. Nezami, H. Ooguri, B. Stoica, J. Sully, and M. Walter. "The Holographic Entropy Cone". In: *ArXiv e-prints* (May 2015). arXiv: 1505.07839 [hep-th].

[172] N. Linden, F. Matúš, M. B. Ruskai, and A. Winter. "The Quantum Entropy Cone of Stabiliser States". In: *ArXiv e-prints* (Feb. 2013). arXiv: 1302.5453 [quant-ph].

[173] D. Gross and M. Walter. "Stabilizer information inequalities from phase space distributions". In: *Journal of Mathematical Physics* 54.8 (2013), p. 082201.

[174] M. Walter. "Multipartite Quantum States and their Marginals". PhD thesis. ETH Zurich, 2014. eprint: 1410.6820.

[175] S. A. Hartnoll. "Lectures on holographic methods for condensed matter physics". In: *Classical and Quantum Gravity* 26.22, 224002 (Nov. 2009), p. 224002. DOI: 10.1088/0264-9381/26/22/224002. arXiv: 0903.3246 [hep-th].

[176] J. McGreevy. "Holographic duality with a view toward many-body physics". In: *ArXiv e-prints* (Sept. 2009). arXiv: 0909.0518 [hep-th].

[177] A. Kitaev and J. Preskill. "Topological Entanglement Entropy". In: *Physical Review Letters* 96.11, 110404 (Mar. 2006), p. 110404. DOI: 10.1103/PhysRevLett.96.110404. eprint: hep-th/0510092.

[178] M. Levin and X.-G. Wen. "Detecting Topological Order in a Ground State Wave Function". In: *Physical Review Letters* 96.11, 110405 (Mar. 2006), p. 110405. DOI: 10.1103/PhysRevLett.96.110405. eprint: cond-mat/0510613.

[179] T. Grover, A. M. Turner, and A. Vishwanath. "Entanglement entropy of gapped phases and topological order in three dimensions". In: *Phys.Rev.B.* 84.19, 195120 (Nov. 2011), p. 195120. DOI: 10.1103/PhysRevB.84.195120. arXiv: 1108.4038 [cond-mat.str-el].

[180] J. Eisert, M. Cramer, and M. B. Plenio. "Colloquium: Area laws for the entanglement entropy". In: *Reviews of Modern Physics* 82 (Jan. 2010), pp. 277–306. DOI: 10.1103/RevModPhys.82.277. arXiv: 0808.3773 [quant-ph].

[181] D. Gioev and I. Klich. "Entanglement Entropy of Fermions in Any Dimension and the Widom Conjecture". In: *Physical Review Letters* 96.10, 100503 (Mar. 2006), p. 100503. DOI: 10.1103/PhysRevLett.96.100503. eprint: quant-ph/0504151.

[182] Zhen Zhang and R.W. Yeung. "A non-Shannon-type conditional inequality of information quantities". In: *Information Theory, IEEE Transactions on* 43.6 (Nov. 1997), pp. 1982–1986. ISSN: 0018-9448. DOI: 10.1109/18.641561.

[183] Nicholas Pippenger. *The Inequalities of Quantum Information Theory*. Tech. rep. Vancouver, BC, Canada, 2002.

[184] N. Linden and A. Winter. "A New Inequality for the von Neumann Entropy". In: *Communications in Mathematical Physics* 259 (Oct. 2005), pp. 129–138. DOI: 10.1007/s00220-005-1361-2. eprint: quant-ph/0406162.

[185] B. Ibinson. "Quantum Information and Entropy". PhD thesis. University of Bristol, 2006.

[186] Z. Zhang and R.W. Yeung. "On characterization of entropy function via information inequalities". In: *Information Theory, IEEE Transactions on* 44.4 (July 1998), pp. 1440–1452. ISSN: 0018-9448. DOI: 10.1109/18.681320.

[187] R. Dougherty, C. Freiling, and K. Zeger. "Six New Non-Shannon Information Inequalities". In: *Information Theory, 2006 IEEE International Symposium on*. July 2006, pp. 233–236. DOI: 10.1109/ISIT.2006.261840.

[188] Sidney Coleman. "Quantum sine-Gordon equation as the massive Thirring model". In: *Phys. Rev. D* 11 (8 Apr. 1975), pp. 2088–2097. DOI: 10.1103/PhysRevD.11.2088. URL: http://link.aps.org/doi/10.1103/PhysRevD.11.2088.

[189] D. D. Blanco, H. Casini, L.-Y. Hung, and R. C. Myers. "Relative entropy and holography". In: *Journal of High Energy Physics* 8, 60 (Aug. 2013), p. 60. DOI: 10.1007/JHEP08(2013)060. arXiv: 1305.3182 [hep-th].

[190] B. Swingle and M. Van Raamsdonk. "Universality of Gravity from Entanglement". In: *ArXiv e-prints* (May 2014). arXiv: 1405.2933 [hep-th].

[191] J. Lin, M. Marcolli, H. Ooguri, and B. Stoica. "Tomography from Entanglement". In: *ArXiv e-prints* (Dec. 2014). arXiv: 1412.1879 [hep-th].

[192] J. Maldacena and L. Susskind. "Cool horizons for entangled black holes". In: *Fortschritte der Physik* 61 (Sept. 2013), pp. 781–811. DOI: 10.1002/prop.201300020. arXiv: 1306.0533 [hep-th].

[193] K. Jensen and A. Karch. "The holographic dual of an EPR pair has a wormhole". In: *ArXiv e-prints* (July 2013). arXiv: 1307.1132 [hep-th].

[194] N. Bao, J. Pollack, and G. N. Remmen. "Splitting spacetime and cloning qubits: linking no-go theorems across the ER=EPR duality". In: *Fortschritte der Physik* 63 (Nov. 2015), pp. 705–710. DOI: 10.1002/prop.201500053. arXiv: 1506.08203 [hep-th].

[195] N. Bao, J. Pollack, and G. N. Remmen. "Wormhole and entanglement (non-)detection in the ER=EPR correspondence". In: *Journal of High Energy Physics* 11, 126 (Nov. 2015), p. 126. DOI: 10.1007/JHEP11(2015)126. arXiv: 1509.05426 [hep-th].

[196] G. N. Remmen, N. Bao, and J. Pollack. "Entanglement Conservation, ER=EPR, and a New Classical Area Theorem for Wormholes". In: *ArXiv e-prints* (Apr. 2016). arXiv: 1604.08217 [hep-th].

[197] D. E. Bruschi. "On the weight of entanglement". In: *ArXiv e-prints* (Dec. 2014). arXiv: 1412.4007 [quant-ph].

[198] Horacio Casini, Damian A. Galante, and Robert C. Myers. "Comments on Jacobson's "entanglement equilibrium and the Einstein equation"". In: *JHEP* 03 (2016), p. 194. DOI: 10.1007/JHEP03(2016)194. arXiv: 1601.00528 [hep-th].

[199] Sean M. Carroll and Grant N. Remmen. "What is the Entropy in Entropic Gravity?" In: (2016). arXiv: 1601.07558 [hep-th].

[200] Matti Raasakka. "Spacetime-free Approach to Quantum Theory and Effective Spacetime Structure". In: (2016). arXiv: 1605.03942 [gr-qc].

[201] Tom Banks. "TASI Lectures on Holographic Space-Time, SUSY and Gravitational Effective Field Theory". In: *Proceedings, Theoretical Advanced Study Institute in Elementary Particle Physics (TASI 2010). String Theory and Its Applications: From meV to the Planck Scale: Boulder, Colorado, USA, June 1-25, 2010*. 2010. arXiv: 1007.4001 [hep-th]. URL: http://inspirehep.net/record/862426/files/arXiv:1007.4001.pdf.

[202] H. B. Nielsen and Astri Kleppe. "Towards a Derivation of Space". In: *Bled Workshops Phys.* 14.2 (2013), pp. 171–196. arXiv: 1403.1410 [hep-th].

[203] Jacob D. Bekenstein. "A Universal Upper Bound on the Entropy to Energy Ratio for Bounded Systems". In: *Phys. Rev.* D23 (1981), p. 287. DOI: 10.1103/PhysRevD.23.287.

[204] Jacob D. Bekenstein. "Entropy bounds and black hole remnants". In: *Phys. Rev.* D49 (1994), pp. 1912–1921. DOI: 10.1103/PhysRevD.49.1912. arXiv: gr-qc/9307035 [gr-qc].

[205] J. Eisert, M. Cramer, and M. B. Plenio. "Area laws for the entanglement entropy - a review". In: *Rev. Mod. Phys.* 82 (2010), pp. 277–306. DOI: 10.1103/RevModPhys.82.277. arXiv: 0808.3773 [quant-ph].

[206] Luca Bombelli, Rabinder K. Koul, Joohan Lee, and Rafael D. Sorkin. "A Quantum Source of Entropy for Black Holes". In: *Phys. Rev.* D34 (1986), pp. 373–383. DOI: 10.1103/PhysRevD.34.373.

[207] Veronika E. Hubeny, Mukund Rangamani, and Tadashi Takayanagi. "A Covariant holographic entanglement entropy proposal". In: *JHEP* 07 (2007), p. 062. DOI: 10.1088/1126-6708/2007/07/062. arXiv: 0705.0016 [hep-th].

[208] Thomas Faulkner, Aitor Lewkowycz, and Juan Maldacena. "Quantum corrections to holographic entanglement entropy". In: *JHEP* 11 (2013), p. 074. DOI: 10.1007/JHEP11(2013)074. arXiv: 1307.2892 [hep-th].

[209] Andrew Strominger and David Mattoon Thompson. "A Quantum Bousso bound". In: *Phys. Rev.* D70 (2004), p. 044007. DOI: 10.1103/PhysRevD.70.044007. arXiv: hep-th/0303067 [hep-th].

[210] H. Casini. "Relative entropy and the Bekenstein bound". In: *Class. Quant. Grav.* 25 (2008), p. 205021. DOI: 10.1088/0264-9381/25/20/205021. arXiv: 0804.2182 [hep-th].

[211] Joshua H. Cooperman and Markus A. Luty. "Renormalization of Entanglement Entropy and the Gravitational Effective Action". In: *JHEP* 12 (2014), p. 045. DOI: 10.1007/JHEP12(2014)045. arXiv: 1302.1878 [hep-th].

[212] Robert C. Myers, Razieh Pourhasan, and Michael Smolkin. "On Spacetime Entanglement". In: *JHEP* 06 (2013), p. 013. DOI: 10.1007/JHEP06(2013)013. arXiv: 1304.2030 [hep-th].

[213] Ted Jacobson. "Gravitation and vacuum entanglement entropy". In: *Int. J. Mod. Phys.* D21 (2012), p. 1242006. DOI: 10.1142/S0218271812420060. arXiv: 1204.6349 [gr-qc].

[214] Seth Lloyd. "The quantum geometric limit". In: (2012). arXiv: 1206.6559 [gr-qc].

[215] Ning Bao, ChunJun Cao, Michael Walter, and Zitao Wang. "Holographic entropy inequalities and gapped phases of matter". In: *JHEP* 09 (2015), p. 203. DOI: 10.1007/JHEP09(2015)203. arXiv: 1507.05650 [hep-th].

[216] M. B. Hastings and T. Koma. "Spectral Gap and Exponential Decay of Correlations". In: *Communications in Mathematical Physics* 265 (Aug. 2006), pp. 781–804. DOI: 10.1007/s00220-006-0030-4. eprint: math-ph/0507008.

[217] I. Borg and P.J.F. Groenen. *Modern Multidimensional Scaling: Theory and Applications*. Springer, 2005.

[218] C.L. Morgan. "Embedding metric spaces in Euclidean space". English. In: *Journal of Geometry* 5.1 (1974), pp. 101–107. ISSN: 0047-2468. DOI: 10.1007/BF01954540. URL: http://dx.doi.org/10.1007/BF01954540.

[219] J.B. Kruscal and M. Wish. “Multidimensional Scaling”. In: *Sage University Paper series on Quantitative Application in the Social Sciences* 07 (1978), p. 011.

[220] J.A. Walter and H. Ritter. “On Interactive Visualization of High-dimensional Data Using the Hyperbolic Plane”. In: *Proceedings of the Eighth ACM SIGKDD International Conference on Knowledge Discovery and Data Mining*. KDD ’02. Edmonton, Alberta, Canada: ACM, 2002, pp. 123–132. ISBN: 1-58113-567-X. DOI: 10.1145/775047.775065. URL: http://doi.acm.org/10.1145/775047.775065.

[221] A. Elad and R. Kimmel. “Spherical Flattening of the Cortex Surface”. English. In: *Geometric Methods in Bio-Medical Image Processing*. Ed. by Ravikanth Malladi. Mathematics and Visualization. Springer Berlin Heidelberg, 2002, pp. 77–89. ISBN: 978-3-642-62784-2. DOI: 10.1007/978-3-642-55987-7_5. URL: http://dx.doi.org/10.1007/978-3-642-55987-7_5.

[222] Alexander M. Bronstein, Michael M. Bronstein, and Ron Kimmel. “Generalized multidimensional scaling: A framework for isometry-invariant partial surface matching”. In: *Proceedings of the National Academy of Science* (2006), pp. 1168–1172. URL: http://www.pubmedcentral.nih.gov/articlerender.fcgi?artid=1360551.

[223] Erik S. So/rensen and Ian Affleck. “Equal-time correlations in Haldane-gap antiferromagnets”. In: *Phys. Rev. B* 49 (22 June 1994), pp. 15771–15788. DOI: 10.1103/PhysRevB.49.15771. URL: http://link.aps.org/doi/10.1103/PhysRevB.49.15771.

[224] Y. J. Kim, M. Greven, U. J. Wiese, and R. J. Birgeneau. “Monte-Carlo study of correlations in quantum spin chains at non-zero temperature”. In: *European Physical Journal B* 4.3 (1998), pp. 291–297. ISSN: 1434-6028.

[225] A. Y. Kitaev. “Fault-tolerant quantum computation by anyons”. In: *Annals of Physics* 303 (Jan. 2003), pp. 2–30. DOI: 10.1016/S0003-4916(02)00018-0. eprint: quant-ph/9707021.

[226] Alioscia Hamma, Radu Ionicioiu, and Paolo Zanardi. “Bipartite entanglement and entropic boundary law in lattice spin systems”. In: *Phys. Rev. A* 71 (2 Feb. 2005), p. 022315. DOI: 10.1103/PhysRevA.71.022315. URL: https://link.aps.org/doi/10.1103/PhysRevA.71.022315.

[227] Klaus Fredenhagen. “On the modular structure of local algebras of observables”. In: *Comm. Math. Phys.* 97.1-2 (1985), pp. 79–89. URL: http://projecteuclid.org/euclid.cmp/1103941979.

[228] John Collins, Alejandro Perez, Daniel Sudarsky, Luis Urrutia, and Hector Vucetich. “Lorentz invariance and quantum gravity: an additional fine-tuning problem?” In: *Phys. Rev. Lett.* 93 (2004), p. 191301. DOI: 10.1103/PhysRevLett.93.191301. arXiv: gr-qc/0403053 [gr-qc].

[229] A. Connes and C. Rovelli. "Von Neumann algebra automorphisms and time-thermodynamics relation in generally covariant quantum theories". In: *Classical and Quantum Gravity* 11 (Dec. 1994), pp. 2899–2917. DOI: 10.1088/0264-9381/11/12/007. eprint: gr-qc/9406019.

[230] T. Regge. "General relativity without coordinates". English. In: *Il Nuovo Cimento (1955-1965)* 19.3 (1961), pp. 558–571. DOI: 10.1007/BF02733251. URL: http://dx.doi.org/10.1007/BF02733251.

[231] ChunJun Cao and Sean M. Carroll. "Bulk Entanglement Gravity without a Boundary: Towards Finding Einstein's Equation in Hilbert Space". In: (2017). arXiv: 1712.02803 [hep-th].

[232] Brian Swingle and Mark Van Raamsdonk. "Universality of Gravity from Entanglement". In: (2014). arXiv: 1405.2933 [hep-th].

[233] Juan Maldacena and Leonard Susskind. "Cool horizons for entangled black holes". In: *Fortsch. Phys.* 61 (2013), pp. 781–811. DOI: 10.1002/prop.201300020. arXiv: 1306.0533 [hep-th].

[234] Fabio Sanches and Sean J. Weinberg. "Holographic entanglement entropy conjecture for general spacetimes". In: *Phys. Rev.* D94.8 (2016), p. 084034. DOI: 10.1103/PhysRevD.94.084034. arXiv: 1603.05250 [hep-th].

[235] Leonard Susskind. "Entanglement is not enough". In: *Fortsch. Phys.* 64 (2016), pp. 49–71. DOI: 10.1002/prop.201500095. arXiv: 1411.0690 [hep-th].

[236] Leonard Susskind. "Dear Qubitzers, GR=QM". In: (2017). arXiv: 1708.03040 [hep-th].

[237] T. Padmanabhan. "Thermodynamical Aspects of Gravity: New insights". In: *Rept. Prog. Phys.* 73 (2010), p. 046901. DOI: 10.1088/0034-4885/73/4/046901. arXiv: 0911.5004 [gr-qc].

[238] Erik P. Verlinde. "On the Origin of Gravity and the Laws of Newton". In: *JHEP* 04 (2011), p. 029. DOI: 10.1007/JHEP04(2011)029. arXiv: 1001.0785 [hep-th].

[239] Ted Jacobson. "Entanglement Equilibrium and the Einstein Equation". In: *Phys. Rev. Lett.* 116.20 (2016), p. 201101. DOI: 10.1103/PhysRevLett.116.201101. arXiv: 1505.04753 [gr-qc].

[240] Yasunori Nomura, Nico Salzetta, Fabio Sanches, and Sean J. Weinberg. "Spacetime Equals Entanglement". In: *Phys. Lett.* B763 (2016), pp. 370–374. DOI: 10.1016/j.physletb.2016.10.045. arXiv: 1607.02508 [hep-th].

[241] Yasunori Nomura, Nico Salzetta, Fabio Sanches, and Sean J. Weinberg. "Toward a Holographic Theory for General Spacetimes". In: *Phys. Rev.* D95.8 (2017), p. 086002. DOI: 10.1103/PhysRevD.95.086002. arXiv: 1611.02702 [hep-th].

[242] V.A. Sharafutdinov. *Integral Geometry of Tensor Fields*. Inverse and ill-posed problems series. VSP, 1994. ISBN: 9789067641654. URL: https://books.google.com/books?id=gj6Sq6nZZAEC.

[243] Daniel Harlow. "The Ryu–Takayanagi Formula from Quantum Error Correction". In: *Commun. Math. Phys.* 354.3 (2017), pp. 865–912. DOI: 10.1007/s00220-017-2904-z. arXiv: 1607.03901 [hep-th].

[244] Federico Piazza. "Glimmers of a pre-geometric perspective". In: *Found. Phys.* 40 (2010), pp. 239–266. DOI: 10.1007/s10701-009-9387-5. arXiv: hep-th/0506124 [hep-th].

[245] Jordan S. Cotler, Geoffrey R. Penington, and Daniel H. Ranard. "Locality from the Spectrum". In: (2017). arXiv: 1702.06142 [quant-ph].

[246] Ning Bao, Sean M. Carroll, and Ashmeet Singh. "The Hilbert Space of Quantum Gravity Is Locally Finite-Dimensional". In: (2017). arXiv: 1704.00066 [hep-th].

[247] L. Pestov and G. Uhlmann. "Two dimensional compact simple Riemannian manifolds are boundary distance rigid". In: *ArXiv Mathematics e-prints* (May 2003). eprint: math/0305280.

[248] Gunther Uhlmann. in prep.

[249] P. Stefanov and G. Uhlmann. "Recent progress on the boundary rigidity problem". In: *Electron. Res. Announc. Amer. Math. Soc.* 11 (June 2005), pp. 64–70. ISSN: 1079-6762.

[250] Plamen Stefanov and Gunther Uhlmann. "Boundary and lens rigidity, tensor tomography and analytic microlocal analysis". In: *Algebraic Analysis of Differential Equations: from Microlocal Analysis to Exponential Asymptotics Festschrift in Honor of Takahiro Kawai*. Ed. by Takashi Aoki, Hideyuki Majima, Yoshitsugu Takei, and Nobuyuki Tose. Tokyo: Springer Japan, 2008, pp. 275–293. ISBN: 978-4-431-73240-2. DOI: 10.1007/978-4-431-73240-2_23. URL: https://doi.org/10.1007/978-4-431-73240-2_23.

[251] Fritz John. "The ultrahyperbolic differential equation with four independent variables". In: *Duke Math. J.* 4.2 (June 1938), pp. 300–322. DOI: 10.1215/S0012-7094-38-00423-5. URL: http://dx.doi.org/10.1215/S0012-7094-38-00423-5.

[252] R. Michel. "Sur la rigidité imposée par la longueur des géodésiques". In: *Invent. Math.* 65 (1981), pp. 71–83.

[253] Dmitri Burago and Sergei Ivanov. "Boundary rigidity and filling volume minimality of metrics close to a flat one". In: *Annals of Mathematics* 171.2 (2010), pp. 1183–1211. ISSN: 0003486X. URL: http://www.jstor.org/stable/20752236.

[254] G. P. Paternain, M. Salo, and G. Uhlmann. “Tensor tomography: progress and challenges”. In: *ArXiv e-prints* (Mar. 2013). arXiv: 1303.6114 [math.DG].

[255] Christopher B. Croke. “Rigidity Theorems in Riemannian Geometry”. In: *Geometric Methods in Inverse Problems and PDE Control*. Ed. by Christopher B. Croke, Michael S. Vogelius, Gunther Uhlmann, and Irena Lasiecka. New York, NY: Springer New York, 2004, pp. 47–72. ISBN: 978-1-4684-9375-7. DOI: 10.1007/978-1-4684-9375-7_4. URL: https://doi.org/10.1007/978-1-4684-9375-7_4.

[256] Vladimir Sharafutdinov. “Variations of Dirichlet-to-Neumann map and deformation boundary rigidity of simple 2-manifolds”. In: *The Journal of Geometric Analysis* 17.1 (Mar. 2007), p. 147. ISSN: 1559-002X. DOI: 10.1007/BF02922087. URL: https://doi.org/10.1007/BF02922087.

[257] P. Stefanov, G. Uhlmann, and A. Vasy. “Inverting the local geodesic X-ray transform on tensors”. In: *ArXiv e-prints* (Oct. 2014). arXiv: 1410.5145 [math.DG].

[258] François Monard. “Numerical Implementation of Geodesic X-Ray Transforms and Their Inversion”. In: *SIAM Journal on Imaging Sciences* 7.2 (2014), pp. 1335–1357. DOI: 10.1137/130938657. eprint: https://doi.org/10.1137/130938657. URL: https://doi.org/10.1137/130938657.

[259] R J Elliott and C Wood. “The Ising model with a transverse field. I. High temperature expansion”. In: *Journal of Physics C: Solid State Physics* 4.15 (1971), p. 2359. URL: http://stacks.iop.org/0022-3719/4/i=15/a=023.

[260] P Pfeuty and R J Elliott. “The Ising model with a transverse field. II. Ground state properties”. In: *Journal of Physics C: Solid State Physics* 4.15 (1971), p. 2370. URL: http://stacks.iop.org/0022-3719/4/i=15/a=024.

[261] G. Beylkin. “Discrete radon transform”. In: *IEEE Transactions on Acoustics, Speech, and Signal Processing* 35.2 (Feb. 1987), pp. 162–172. ISSN: 0096-3518. DOI: 10.1109/TASSP.1987.1165108.

[262] Christopher Croke. “Boundary and Lens Rigidity of Finite Quotients”. In: *Proceedings of the American Mathematical Society* 133.12 (2005), pp. 3663–3668. ISSN: 00029939, 10886826. URL: http://www.jstor.org/stable/4097512.

[263] Christopher B. Croke. “Volumes of Balls in Manifolds without Conjugate Points”. In: *International Journal of Mathematics* 03.04 (1992), pp. 455–467. DOI: 10.1142/S0129167X92000205. eprint: http://www.worldscientific.com/doi/pdf/10.1142/S0129167X92000205. URL: http://www.worldscientific.com/doi/abs/10.1142/S0129167X92000205.

[264] Christopher B. Croke. “Rigidity and the distance between boundary points”. In: *J. Differential Geom.* 33.2 (1991), pp. 445–464. DOI: 10.4310/jdg/1214446326. URL: http://dx.doi.org/10.4310/jdg/1214446326.

[265] M. Porrati and R. Rabadan. “Boundary rigidity and holography”. In: *JHEP* 01 (2004), p. 034. DOI: 10.1088/1126-6708/2004/01/034. arXiv: hep-th/0312039 [hep-th].

[266] Eric Gourgoulhon. “3+1 formalism and bases of numerical relativity”. In: (2007). arXiv: gr-qc/0703035 [GR-QC].

[267] David D. Blanco, Horacio Casini, Ling-Yan Hung, and Robert C. Myers. “Relative Entropy and Holography”. In: *JHEP* 08 (2013), p. 060. DOI: 10.1007/JHEP08(2013)060. arXiv: 1305.3182 [hep-th].

[268] Jennifer Lin. “Ryu-Takayanagi Area as an Entanglement Edge Term”. In: (2017). arXiv: 1704.07763 [hep-th].

[269] Michael Pretko. “Emergent gravity of fractons: Mach’s principle revisited”. In: *Phys. Rev.* D96.2 (2017), p. 024051. DOI: 10.1103/PhysRevD.96.024051. arXiv: 1702.07613 [cond-mat.str-el].

[270] Zheng-Cheng Gu and Xiao-Gang Wen. “Emergence of helicity +- 2 modes (gravitons) from qbit models”. In: *Nucl. Phys.* B863 (2012), pp. 90–129. DOI: 10.1016/j.nuclphysb.2012.05.010. arXiv: 0907.1203 [gr-qc].

[271] Tobias J. Osborne and Deniz E. Stiegemann. “Dynamics for holographic codes”. In: (2017). arXiv: 1706.08823 [quant-ph].